UNCLASSIFIED

AD NUMBER

AD873844

LIMITATION CHANGES

TO:

Approved for public release; distribution is unlimited.

FROM:

**Distribution authorized to U.S. Gov't. agencies and their contractors;
Administrative/Operational Use; MAY 1970. Other requests shall be referred to Army Aviation Materiel Labs., Fort Eustis, VA.**

AUTHORITY

USAAVLABS ltr 28 Jun 1971

THIS PAGE IS UNCLASSIFIED

AD 738844

AD No. ____
DDC FILE COPY

OK per 4 Sep. 70

2 cys

AD

USAAVLABS TECHNICAL REPORT 70-20

SMALL AXIAL-CENTRIFUGAL COMPRESSOR MATCHING STUDY

By

Laurence E. Brown

DDC
RECEIVED
SEP 4 1970
A

May 1970

U. S. ARMY AVIATION MATERIEL LABORATORIES
FORT EUSTIS, VIRGINIA

CONTRACT DAAJ02-69-C-0075
CURTISS-WRIGHT CORPORATION
WOOD-RIDGE, NEW JERSEY

This document is subject to special export controls, and each transmittal to foreign governments or foreign nationals may be made only with prior approval of U.S. Army Aviation Materiel Laboratories, Fort Eustis, Virginia 23604.

324

Disclaimers

The findings in this report are not to be construed as an official Department of the Army position unless so designated by other authorized documents.

When Government drawings, specifications, or other data are used for any purpose other than in connection with a definitely related Government procurement operation, the United States Government thereby incurs no responsibility nor any obligation whatsoever; and the fact that the Government may have formulated, furnished, or in any way supplied the said drawings, specifications, or other data is not to be regarded by implication or otherwise as in any manner licensing the holder or any other person or corporation, or conveying any rights or permission, to manufacture, use, or sell any patented invention that may in any way be related thereto.

Disposition Instructions

Destroy this report when no longer needed. Do not return it to the originator.

DEPARTMENT OF THE ARMY
HEADQUARTERS US ARMY AVIATION MATERIEL LABORATORIES
FORT EUSTIS, VIRGINIA 23604

The research described herein was conducted by the Curtiss-Wright Corporation, Wood-Ridge, New Jersey, under U. S. Army Contract DAAJ02-69-C-0075. The work was performed under the technical management of David B. Cale, Propulsion Division, U. S. Army Aviation Materiel Laboratories.

Appropriate technical personnel of this Command have reviewed this report and concur with the conclusions and recommendations contained herein.

The findings and recommendations outlined herein will be considered in planning subsequent axial/centrifugal research efforts.

Task 1G162203D14413
Contract DAAJ02-69-C-0075
USAAVLABS Technical Report 70-20
May 1970

SMALL AXIAL-CENTRIFUGAL COMPRESSOR MATCHING STUDY

Final Report

By

Laurence E. Brown

Prepared by

Curtiss-Wright Corporation
Wood-Ridge, New Jersey

for

U. S. ARMY AVIATION MATERIEL LABORATORIES
FORT EUSTIS, VIRGINIA

This document is subject to special export controls, and each transmittal to foreign governments or foreign nationals may be made only with prior approval of U. S. Army Aviation Materiel Laboratories, Fort Eustis, Virginia 23604.

SUMMARY

The prime objective of this program is to define the preliminary design and matching of an axial-centrifugal compressor for minimum engine specific fuel consumption at 60 percent power and 30 percent power, with secondary importance attached to SFC at 100 percent power.

Analytical procedures were employed to investigate effects of engine cycle parameters, stage-matching characteristics of several axial and centrifugal compressors, variable compressor geometry (two-spools and stator variable setting angles), and power turbine variable area, upon minimum fuel consumption. Design studies were employed in the consideration of shafting and component arrangements. Comparative engine complexity of one-spool and two-spool compressors in front drive engines was evaluated in the selection of an optimum compressor configuration.

The selected compressor preliminary design is based closely on stage pressure ratio levels that have been attained in previous developments; new requirements are an axial compressor with improved efficiency and demonstrated flow variability and a centrifugal compressor with modified configuration for close coupling behind axial stages. The selected compressor can be developed in a three-year program.

The compressor preliminary design has a single spool with two variable stator transonic axial stages close coupled to a centrifugal compressor. At 60 percent of military rated power, a pressure ratio of 14.6 results in an engine specific fuel consumption of 0.45 lb/hp/hr at 60 percent power. The need for performance range in such high pressure ratio compressors is found to be satisfied by two-spool compressors as well as by single-spool variable stator compressors. Compared to the latter, two-spool compressors were judged to hold potential performance advantages which, for front-drive turboshaft engines, are outweighed by development risks due to the associated mechanical complexity. In addition, a preliminary design was developed for a single-spool fixed-geometry compressor, which has two transonic axial stages close coupled to a centrifugal compressor with inter-stage bleed required for low-speed operation. At 60 percent of military rated power a pressure ratio of 9.1 results in an engine specific fuel consumption of 0.5 lb/hp/hr. A hypothetical engine incorporating this compressor was found to yield no lower part-power specific fuel consumption values with power turbine area variable than with power turbine area fixed. The fixed-geometry power turbine can provide both minimum SFC and mechanical simplicity.

Attainment of minimum part-load fuel consumption can be facilitated by further work on the axial and centrifugal compressor elements. The development of axial compressors should include investigation of flow modulation by varying stator setting angles so as to keep the axial stages operating out of stall and at high efficiency over the engine operating range. The development of centrifugal compressors should include investigation of configurations with high inlet hub radii suitable for close coupling to axial boost stages.

FOREWORD

A study has been performed under United States Army Contract DAAJ02-69-C-0075 Task 1G162203D14413, by Curtiss-Wright Corporation to investigate the matching and design of axial-centrifugal compressors for small turboshaft engines. The objective was to minimize engine specific fuel consumption at part load, specifically 60 percent of military rated power. The complete study is reported herein. This contract was administered by the Propulsion Division of the U.S. Army Aviation Materiel Laboratories.

The manager of the Small Gas Turbine Engine Program was Thomas Schober, and the manager of this contract was Laurence E. Brown. Principal contributing engineers were A. G. Sievers, Richard P. Beverly, and Wallace Van Heemst. The direction and guidance of Jesse O. Wiggins, David W. Wagner, C. H. Muller, H. Watts, and Erold F. Pierce are gratefully acknowledged. The guidance of David B. Cale of the U.S. Army Aviation Materiel Laboratories is also gratefully acknowledged.

BLANK PAGE

TABLE OF CONTENTS

	Page
SUMMARY	iii
FOREWORD	v
LIST OF ILLUSTRATIONS	viii
LIST OF TABLES	xv
LIST OF SYMBOLS	xvii
INTRODUCTION	1
DISCUSSION	5
Engine Cycle Analysis	5
Preliminary Design	34
Compressor Performance Prediction	137
Engine Performance Prediction	145
CONCLUSIONS	156
RECOMMENDATIONS	157
LITERATURE CITED	158
GLOSSARY	160
APPENDIXES	162
I. LP/HP Compressor Matching Procedures	162
II. Compressor/Engine Preliminary Matching Procedures	174
III. Computation Procedures	179
DISTRIBUTION	205

LIST OF ILLUSTRATIONS

Figure		Page
1	Turboshaft Engine Parametric Cycle Data for 1900°F Turbine Inlet Temperature and 75% Turbine Adiabatic Efficiency	7
2	Turboshaft Engine Parametric Cycle Data for 1900°F Turbine Inlet Temperature and 80% Turbine Adiabatic Efficiency	8
3	Turboshaft Engine Parametric Cycle Data for 1900°F Turbine Inlet Temperature and 85% Turbine Adiabatic Efficiency	9
4	Turboshaft Engine Parametric Cycle Data for 1900°F Turbine Inlet Temperature and 90% Turbine Adiabatic Efficiency	10
5	Turboshaft Engine Parametric Cycle Data for 2100°F Turbine Inlet Temperature and 85% Turbine Adiabatic Efficiency	11
6	Turboshaft Engine Parametric Cycle Data for 2200°F Turbine Inlet Temperature and 75% Turbine Adiabatic Efficiency	12
7	Turboshaft Engine Parametric Cycle Data for 2200°F Turbine Inlet Temperature and 80% Turbine Adiabatic Efficiency	13
8	Turboshaft Engine Parametric Cycle Data for 2200°F Turbine Inlet Temperature and 85% Turbine Adiabatic Efficiency	14
9	Turboshaft Engine Parametric Cycle Data for 2200°F Turbine Inlet Temperature and 90% Turbine Adiabatic Efficiency	15
10	Turboshaft Engine Parametric Cycle Data for 2500°F Turbine Inlet Temperature and 75% Turbine Adiabatic Efficiency	16
11	Turboshaft Engine Parametric Cycle Data for 2500°F Turbine Inlet Temperature and 80% Turbine Adiabatic Efficiency	17

Figure		Page
12	Turboshaft Engine Parametric Cycle Data for 2500°F Turbine Inlet Temperature and 85% Turbine Adiabatic Efficiency	18
13	Turboshaft Engine Parametric Cycle Data for 2500°F Turbine Inlet Temperature and 90% Turbine Adiabatic Efficiency	19
14	Turboshaft Engine Parametric Cycle Data for Adiabatic Efficiency of 85% at Turbine and 80% at Compressor	20
15	Attainable Efficiency for Subsonic and Transonic Axial Compressor Stages	22
16	Attainable Efficiency for Supersonic Axial Compressor Stages	23
17	Attainable Efficiency for Centrifugal Compressor Stages	25
18	Attainable Efficiency for a Two-Stage Compressor, Incorporating a Supersonic Stage Followed by a Transonic Stage	26
19	Attainable Efficiency for a Two-Stage Compressor, Incorporating a Supersonic Stage Followed by a Centrifugal Stage	28
20	Attainable Efficiency for Two- and Three-Stage Compressors, Incorporating an Axial Compressor Feeding a Centrifugal Stage	29
21	Effect of Compressor Off-Design Efficiency for Compressor Design Point at 60% Power With 8:1 Pressure Ratio	30
22	Effect of Compressor Off-Design Efficiency for Compressor Design Point at 60% Power With 12:1 Pressure Ratio	31
23	Two-Spool Front Shaft Compressor Design	35
24	Comparison of Boeing RF-2 and Proposed Centrifugal Impeller Configurations	38
25	Centrifugal Compressor Disc Stresses Based on Scaling Boeing RF-2 Stresses for Inconel 718 Material	39

Figure		Page
26	Centrifugal Compressor Disc Stresses Based on Scaling Boeing RF-2 Stresses, for Titanium 6AL-4V Material .	40
27	Centrifugal Compressor Disc Average Tangential Stresses in Proposed Disc Configuration for Titanium 7Al-4M Material at 600°F	42
28	Centrifugal Compressor Disc Average Tangential Stresses in Proposed Disc Configuration for Inconel 718 Material at 600°F	43
29	Compressor/Engine Matching Map Mean-Line Mapping Case 1B, U_t = 1700 ft/sec	47
30	Compressor/Engine Matching Map Mean-Line Mapping Case 2A, U_t = 1530 ft/sec	48
31	Compressor/Engine Matching Map Mean-Line Mapping Case 3A, U_t = 1360 ft/sec	49
32	Compressor Test Performance, Modified, 2.8 Supersonic Compressor (F1)	57
33	Compressor Test Performance, Modified Two-Stage Transonic Compressor (F1)	58
34	Compressor Base Performance, 2.8 Supersonic (F1) Plus Hypothetical Transonic Stage	59
35	Compressor Test Performance, Modified, 405 Centrifugal Compressor (F1)	60
36	Compressor Test Performance, PW-G Centrifugal Compressor	61
37	Compressor Test Performance, Modified, Boeing RF-2 Centrifugal Compressor (F1)	62
38	LP/HP Compressor Aerodynamic Match, Supersonic Axial Plus PW-G Centrifugal, Case 2,2	63
39	LP/HP Compressor Aerodynamic Match, Supersonic Axial Plus PW-G Centrifugal, Case 2,3	64
40	LP/HP Compressor Aerodynamic Match, Supersonic Axial Plus PW-G Centrifugal, Two-Spools, Case 3	65
41	LP/HP Compressor Aerodynamic Match, Two-Stage Transonic Axial Plus PW-G Centrifugal, Case 4,1	66

Figure		Page
42	LP/HP Compressor Aerodynamic Match, Two-Stage Transonic Axial Plus PW-G Centrifugal, Variable Stators, Case 4,1-VS	67
43	LP/HP Compressor Aerodynamic Match Two-Stage Transonic Axial Plus PW-G Centrifugal, Case 4,3	68
44	LP/HP Compressor Aerodynamic Match Two-Stage Transonic Axial Plus PW-G Centrifugal, Variable Stators, Case 4,4-VS	69
45	LP/HP Compressor Aerodynamic Match, Supersonic Plus Transonic Axial Plus 405 Centrifugal, Case 7,2	70
46	LP/HP Compressor Aerodynamic Match, Two-Stage Transonic Axial Plus PW-G Centrifugal, Two-Spool, Case 11,1	71
47	LP/HP Compressor Aerodynamic Match, Supersonic Plus Transonic Axial Plus PW-G Centrifugal, Case 13,3	72
48	Compressor/Engine Matching Map, Supersonic Axial Plus PW-G Centrifugal, Case 2,2	73
49	Compressor/Engine Matching Map, Supersonic Axial Plus PW-G Centrifugal, Case 2,3	74
50	Compressor/Engine Matching Map, Supersonic Axial Plus PW-G Centrifugal, Two-Spool, Case 3	75
51	Compressor/Engine Matching Map, Two-Stage Transonic Axial Plus PW-G Centrifugal, Case 4,1	76
52	Compressor/Engine Matching Map, Two-Stage Transonic Axial Plus PW-G Centrifugal, Case 4,1-AAA	77
53	Compressor/Engine Matching Map, Two-Stage Transonic Axial Plus PW-G Centrifugal, Variable Stators, Case 4,1-VS	78
54	Compressor/Engine Matching Map, Two-Stage Transonic Axial Plus PW-G Centrifugal, Case 4,3	79
55	Compressor/Engine Matching Map, Two-Stage Transonic Plus PW-G Centrifugal, Variable Stators, Case 4,4-VS	80
56	Compressor/Engine Matching Map, Supersonic and Transonic Axial Plus 405 Centrifugal, Case 7,2	81

Figure		Page
57	Compressor/Engine Matching Map, Two-Stage Transonic Plus PW-G Centrifugal, Two-Spools, Case 11,1	82
58	Compressor/Engine Matching Map, RF-2 Centrifugal, Case 12	83
59	Compressor/Engine Matching Map, Supersonic and Transonic Axial Plus PW-G Centrifugal, Case 13,3 . . .	84
60	Loci of Stage Pressure Ratio Peak Values on the Performance Map of a 5-Stage Axial Compressor	87
61	Compressor Stage Speed/Flow-Efficiency Match Relationships, 2.8 Supersonic (F1) Axial LP Compressor	88
62	Compressor Stage Speed/Flow-Efficiency Match Relationships, Two-Stage Transonic (F1) Axial LP Compressor . . .	89
63	Compressor Stage Speed/Flow-Efficiency Match Relationships, 2.8 Supersonic (F1) Plus Transonic Axial LP Compressor	90
64	Compressor Stage Speed/Flow-Efficiency Relationships, 405 Centrifugal Stage HP Compressor	91
65	Compressor Stage Speed/Flow-Efficiency Relationships, PW-G Centrifugal HP Compressor	92
66	Estimated Performance Variation With Stator Setting Angle Variation at Design Speed	94
67	Estimated Performance Variation With Stator Setting Single Variation at 80% Design Speed	95
68	Estimated Performance Variation With Stator Setting Angle Variation at 60% Design Speed	96
69	Effects of Centrifugal Compressor Tip Speed on 60% Power Performance of One-Spool Compressor Engines . . .	102
70	Effects of Centrifugal Compressor Tip Speed on 60% Power Performance of Two-Spool Compressor Engines . . .	104
71	Effects of Compressor Peak Efficiency Location, Efficiency Variation Assumptions	106
72	Effects of Compressor Peak Efficiency Location 60% Power Performance vs. Percent Military Airflow for Military Pressure Ratios of 10, 15, and 20 at Turbine Inlet Temperature 2500°F	107

Figure		Page
73	Effects of Compressor Peak Efficiency Location, 60 Percent Power Performance vs. Airflow for Military Ratio Pressure Ratio of 12:1 and Turbine Inlet Temperature of 2500°F	109
74	Effect of Variable Power Turbine Area on Part-Load Fuel Consumption, Efficiency Based on Compressor Performance Map, Case 4,1-AAA	111
75	Effect of Variable Power Turbine Area on Part-Load Fuel Consumption With Compressor Efficiency Constant . .	112
76	Fixed-Geometry Compressor Velocity Diagrams at 100 Percent Military Rated Power Design Point	123
77	Fixed-Geometry Compressor Design	124
78	Variable-Stator Compressor and Engine Design	127
79	Variable-Stator Compressor Velocity Diagrams at 100 Percent Military Rated Power Design Points	131
80	Fixed-Geometry Compressor Performance Map With Engine Operating Line Superimposed	138
81	Variable-Stator Compressor Performance Map With Engine Operating Line Superimposed	139
82	Variable-Stator Compressor Off-Design Performance Prediction Based on Mean-Line Mapping Program Compared With Overall Performance	140
83	Variable Geometry Compressor Velocity Diagrams at 60% of Military Power Operating Point	142
84	Variable Geometry Compressor Velocity Diagrams at 30% of Military Power Operating Point	143
85	Variable-Stator Compressor Turboshaft Engine Part-Load Brake Specific Fuel Consumption at Sea Level Standard Day With Military Rated Power Point at P/P = 19.3/1, TIT = 2500°F, Wa = 4.47 lbs/sec	147
86	Fixed-Geometry Turboshaft Engine Part-Load Brake Specific Fuel Consumption at Sea Level Standard Day With Military Rated Power Point at P/P = 11.8/1, TIT = 2500°F, Wa = 4.416 lbs/sec	148

Figure		Page
87	Comparison of Fixed-Geometry Compressor With Variable-Stator Compressor for Gas Generator Airflow and Speed Characteristics at Power Turbine 100% Speed and Sea Level Static Conditions	150
88	Variable-Stator Compressor Turboshaft Engine Part-Load Performance Characteristics at 100% Power Turbine Speed at Sea Level Standard Day	152
89	Fixed-Geometry Compressor Turboshaft Engine Part-Load Performance Characteristics at 100% Power Turbine Speed at Sea Level Standard Day	153
90	Power Turbine Performance Characteristics With Superimposed Engine Operating Lines for Variable-Stator Compressor Turboshaft Engine	154
91	Typical LP Compressor Matching Base Data, Two-Stage Transonic Compressor (F1), Corrected Speed	163
92	Typical HP Compressor Matching Base Data, PW-G Centrifugal Stage, Corrected Speed	164
93	Typical LP Compressor Matching Base Data, Two-Stage Transonic Compressor (F1), Corrected Enthalpy Rise .	166
94	Typical LP Compressor Matching Base Data, Two-Stage Transonic Compressor (F1), Corrected Isentropic Enthalpy Rise	167
95	Typical HP Compressor Matching Base Data, PW-G Centrifugal Stage, Corrected Enthalpy Rise	168
96	Typical HP Compressor Matching Base Data: PW-G Centrifugal Stage, Corrected Isentropic Enthalpy Rise	169
97	Sketch of Compressor Performance Map for Compressor/Engine Matching	175
98	Compressor/Engine Matching Performance, Power and Brake Specific Fuel Consumption as a Function of Pressure Ratio for Temperatures of 1900°, 2100°, 2200°, and 2500°F, 2.8 Supersonic Plus PW-G Centrifugal, Case 2,3	177

LIST OF TABLES

Table		Page
I	Summary of Preliminary Cycle Performance	51
II	One-Spool Compressor Axial Stage Type Rating Data	115
III	One-Spool Compressor Axial Stage Type Merit Ratings	116
IV	One-Spool Compressor Axial Stage Type Merit Rating Summary	117
V	Fixed-Geometry Compressor Flow Path and Military Rated Design Point Performance	120
VI	Fixed-Geometry Compressor Preliminary Design - Velocity Diagram Data	122
VII	Variable-Stator Compressor Flow Path and Military Rated Design Point Performance	125
VIII	Variable-Stator Compressor Preliminary Design Mean Radius Velocity Diagram Data at Three Power Levels	130
IX	Variable-Stator Compressor Preliminary Design Blade Geometry at Mean Radius Sections	132
X	Variable-Stator Compressor Blade Incidence Angles, Inlet Mach Number, and Pressure Recoveries at Three Power Levels	144
XI	Single-Spool Turboshaft Engine Performance Comparison	145
XII	Adder Input List	181
XIII	Adder Sample Output	182
XIV	Adder FORTRAN Listing	183
XV	Fixer and Blah Input List	184
XVI	Fixer FORTRAN Listing	185
XVII	Blah Sample Output	186
XVIII	Blah FORTRAN Listings	183
XIX	One-Spool Compressor Match Input List	196

LIST OF TABLES - Continued

Table		Page
XX	One-Spool Match Sample Output	197
XXI	One-Spool Match FORTRAN Listing	198
XXII	Two-Spool Compressor Match Input List	201
XXIII	Two-Spool Match Sample Output	202
XXIV	Two-Spool Match FORTRAN Listing	203

LIST OF SYMBOLS

BSFC	brake specific fuel consumption, lb/hr/hp
D	diameter, ft
H	enthalpy rise (as Δ H), Btu/lb
HCO	actual corrected enthalpy rise (HCOI/η_{ad}), Btu/lb
HCOI	ideal corrected enthalpy rise isentropic $\Delta H/(N/N_D)^2$, Btu/lb
IGV	inlet guide vane
J	work constant, 778 foot-pounds per Btu
k,K	equation constants
N	rotational speed, RPM
P/P	total pressure ratio
r	radius, ft
SHP/Wa	specific horsepower output, hp/lb of air
T	total temperature, °F
TIT	turbine inlet temperature, °F
U	rotor blade section speed, ft/sec
V	air velocity, ft/sec
Wa	airflow, lb/sec
δ	P/2116, pressure correction (P in lb/sq. ft), dimensionless
η	efficiency, dimensionless
θ	T/518.69, temperature correction (T in degrees Rankine), dimensionless

Subscripts

ad	adiabatic
ax	axial component of velocity
c	compressor
D	design
GG	gas generator
p	polytropic
PT	power turbine
t	turbine
tan	component in plane of rotation
1	velocity at stator exit
2	compressor inlet
2	velocity at rotor inlet
3	compressor (or stage) exit
3	velocity at rotor exit
4	velocity at stator inlet
6	turbine inlet

INTRODUCTION

BACKGROUND

For a number of years, the Army has sponsored research on small (2-5 lb/sec airflow) gas turbine engine components. Prior to this program, the major effort had been devoted to individual components, i.e., axial compressor, centrifugal compressor, combustor, radial turbine, axial turbine, regenerator, etc. In addition, engine studies primarily directed toward optimization at military power operation had been conducted, although part-power operation had also been investigated.

Under this contract, the contractor has conducted the preliminary design and matching of two axial-centrifugal compressors having one centrifugal stage and two (transonic) axial stages. Primary emphasis in the selection and design of these compressors has been placed on obtaining minimum specific fuel consumption at 60 percent and 30 percent power points, with the 100 percent power point being of secondary importance. The turbine performance was considered only to the extent necessary to permit the computation of engine performance.

APPROACH

Engine Cycle Analysis

The merit of compressors was evaluated by making a preliminary estimate of engine performance by use of the parametric cycle data described below. Compressor performance curves show the efficiencies attainable in a three-year development program by various stage combinations at various pressure ratios, thus permitting a preliminary estimate of the optimum performance and parametric match point data. The parametric cycle data presented in this section provide working tools for later stages of the program.

Parametric Cycle Data

Engine cycle studies were conducted for a family of front-drive turboshaft engines for the following range of parameters:

Pressure Ratio: 3, 5, 10, 15, 20
Turbine Efficiency: 75, 80, 85, 90 percent
Compressor Efficiency: 70, 75, 80, 85, 90 percent
Turbine Inlet Temperature: 1900°, 2200°, 2500°F

An additional set of data was computed for a turbine inlet temperature of 2100°F, for a turbine efficiency of 85 percent, and for the ranges of pressure ratio and compressor efficiency given above.

Compressor Performance Curves

The variations of attainable (in a three-year development program) compressor efficiency with pressure ratio were defined by reference to literature for subsonic-transonic axial stages, supersonic axial stages, and centrifugal stages. The stage performances were combined to determine the corresponding attainable efficiencies, as functions of pressure ratio, for various composite compressors. In the course of this combining of stages, the best stage combinations for high efficiency were defined, and the principles for the best division of work between stages were set forth.

Optimum Performance and Parametric Match Point Data

The data of the preceding work were examined in an attempt to establish combinations of cycle parameters which produce the minimum specific fuel consumption and to define goals for 60 and 30 percent of military rated power points. Parametric match curves were determined for a range of compressor efficiencies at two pressure ratios. An evaluation of the effects of turbine area was necessarily deferred until the compressor characteristics could be defined and considered in greater detail.

Preliminary Design

Numerous compressor preliminary designs were investigated for which each compressor and engine match was optimized for 60 percent power specific fuel consumption. Investigations of front drive-shaft locations, compressor stage combinations, optimum location of peak efficiency, and turbine area variation preceded the final selection of the compressor type and the definition of compressor design and performance.

Component Configuration

1. Two-spool compressors were investigated to determine the added complexity associated with front or rear drive-shaft location.

2. Centrifugal compressor blade path was configured to be coupled close behind the axial compressor.

Compressor Characteristics (Related to Engine Performance)

Compressor performance was defined in terms of conventional performance maps. The compressor maps were then matched to engines, and the engine performance criteria, particularly BSFC at 60 percent power, were used as indicators of merit for comparing the various compressor configurations.

1. A mean-line mapping program was used to predict performance for a family of three compressors with designs optimized at various fractions of a maximum speed. An optimum design speed for 60 percent power minimum specific fuel consumption was sought.

2. A stage matching procedure was used to determine the combined performance of two compressors, called LP (low pressure) and HP (high pressure). More than 25 various combinations of 3 LP axial and 2 HP centrifugal compressors were investigated, including fixed-stator, two-spool, and variable-stator configurations. One- and two-stage LP's were used.

3. The location of peak efficiency on the compressor map was selected as a parameter affecting 60 percent power fuel consumption. Location of the peak at 50 percent, 75 percent, and 100 percent of the military power flow rate was investigated for pressure ratios of 10, 15, and 20 to determine effects on minimum 60 percent power fuel consumption.

Power Turbine Flow Area

Power turbine flow area affects the temperature, pressure ratio, and airflow at which the gas generator operates at a given fraction of military power. For the fixed-stator compressor design (discussed below), the effect of flow area on part-load specific fuel consumption was investigated.

Select Configuration

Several types and numbers of axial stages were rated relative to 60 percent power specific fuel consumption, 30 percent power specific fuel consumption, size of compressor and engine, mechanical complexity, development status, cost, durability, and maintainability; and an optimum compressor was selected for the definition of a preliminary design.

Preliminary Design of Selected Configurations

Two preliminary designs were produced, a fixed-stator compressor and a variable-stator compressor. The variable-stator compressor was the selected design and received more comprehensive definition than the fixed-stator design.

The fixed-stator compressor design has a 60 percent power pressure ratio of about 9:1. The compressor arrangement, the flow path, and the mechanical and vibratory criteria and limits were defined and investigated. A preliminary design layout of the compressor was produced.

The variable-stator compressor design has a 60-percent power pressure ratio of about 14:1. The compressor arrangement, the airflow path, the airfoil shapes and solidity, the compressor shafting arrangement, the variable geometry, and the mechanical and vibratory design criteria and limitations were defined. A preliminary design layout of the compressor and engine was produced.

Compressor Performance Prediction

Performance was predicted for two compressors: the fixed-stator compressor, and the final variable-stator compressor for which the prediction was more comprehensive.

The fixed-stator compressor off-design performance was predicted for eight speed lines using stage-matching procedures.

The variable-stator compressor off-design performance was predicted for nine speed lines using matching procedures. In addition, the mean-line mapping procedures were used to define speed lines near 60 percent and 30 percent of military rated power operating conditions. At points near these operating conditions, and at the military-rated condition, details of the internal flow were defined, and velocity triangles were defined.

Engine Performance Prediction

Engine performance was predicted for two engines, one incorporating the fixed-stator compressor, and the other the variable-stator compressor. For both engines, performance was defined over a range from 20 to 100 percent power, giving values over this range for the following parameters: pressure ratio, compressor efficiency, turbine inlet temperature, compressor turbine efficiency, power turbine efficiency, and specific fuel consumption.

DISCUSSION

ENGINE CYCLE ANALYSIS

The gas turbine engine cycle, consisting of the compression, combustion, and expansion of gases with firmly established thermodynamic properties, is readily adaptable to investigation. The effects of the performance characteristics of the major components on the overall performance are predictable with a high degree of assurance. With this knowledge, it was considered reasonable to initiate this compressor matching study with an investigation of the effects of the principal cycle variables.

Parametric Cycle Data

Nonregenerative turboshaft cycle output performance, in terms of specific brake horsepower, BHP/W_a, and brake specific fuel consumption (BSFC) was generated using a high-speed digital computer program. The cycle variables investigated and the range of variation are as follows:

Compressor Pressure Ratio: 3, 5, 10, 15, 20
Compressor Adiabatic Efficiency: 70, 75, 80, 85, 90 percent
Power and Compressor Turbine Adiabatic Efficiency: 75, 80, 85, 90 percent
Turbine Inlet Temperature: 1900°, 2200°, 2500°F

Supplementary data were computed for a turbine inlet temperature of 2100°F, for a turbine efficiency of 85 percent, and for the same range of compressor pressure ratios and efficiencies given above.

Additional Performance Assumptions

1. Ambient Conditions: Sea Level, static, standard day
2. Inlet Duct Pressure Recovery: 100 percent
3. Combustion Efficiency: 99 percent
4. Lower Heating Value of Fuel: 18,400 Btu/lb
5. Combustor Total Pressure Recovery: 96.5 percent
6. Mechanical Efficiencies: Compressor Shaft 99 percent
   Output Shaft 99 percent
6. Power Extraction (other than output): None
7. Internal Leakage and Bleed Overboard: None

8. Turbine Cooling Air Quantity:

	Percent Inlet Air	Turb. Inlet Temp.
(Cooling air was bled at compressor discharge conditions, was returned to first turbine stator and mixed. Effect was to reduce Turb. Inlet Temp from values listed.)	1.0	1900°F
	3.0	2100°F
	4.0	2200°F
	7.0	2500°F

9. Exhaust Total Pressure: 1.03
(From power turbine exit to ambient)

Performance Assumption Considerations

A conventional practice was followed by using a certain amount of optimism in making the additional performance assumptions stated above. The reasoning behind such a practice considers that cycle investigation results are target performance values achievable from a conscientious long-term design and development effort. By establishing this high level for the performance of the other cycle components, a meaningful delineation for the component under study will be obtained.

Cycle Analysis Results

The turboshaft engine parametric cycle performance results are presented in Figures 1 through 13, with the output performance of specific power and specific fuel consumption plotted versus compressor pressure ratio with lines of compressor adiabatic efficiency. This form of presentation of results was selected to provide the compressor designer with a convenient form for a quick assessment of the trade-off between pressure ratio and efficiency on engine output performance. An important association made at this initial phase of the study was between turbine inlet temperature (TIT) and percent of military rated power. In general,

TIT = 2500°F	100 percent military rated power
TIT = 2200°F 2100°F	60 percent military rated power
TIT = 1900°F	30 percent military rated power

This association is evident from a review of Figure 14. In this figure, specific fuel consumption and specific power variations with compressor pressure ratio and turbine inlet temperature are presented for constant compressor and turbine adiabatic efficiencies. Consider a representative cycle with minimum specific fuel consumption at 60 percent power at a P/P = 12 and TIT = 2100°F. The specific power of 180 is already 74 percent of the potential military value at 2500°F, lessening the flow variation requirements and the accompanying efficiency and pressure ratio variations necessary for absolute power

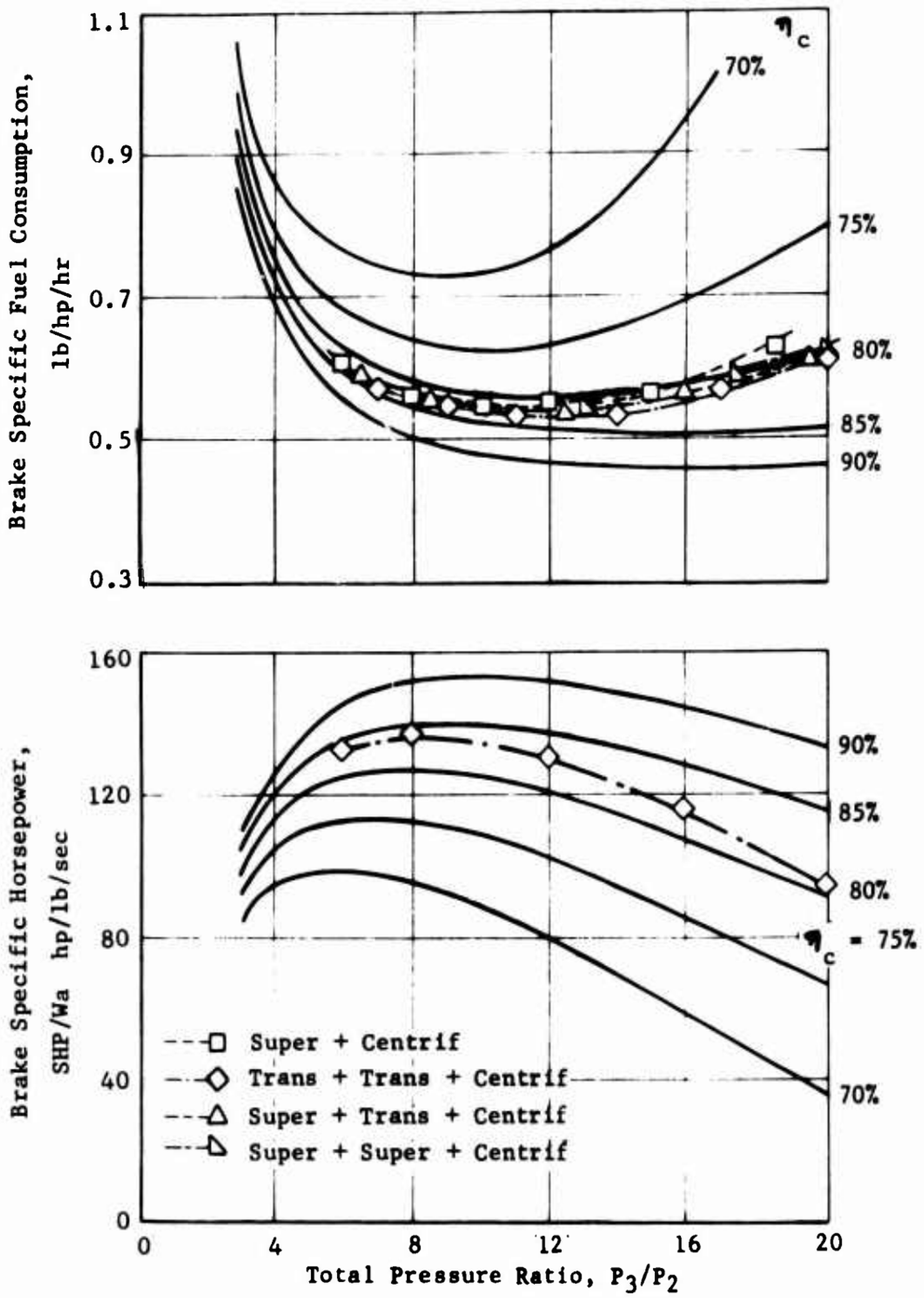

Figure 1. Turboshaft Engine Parametric Cycle Data for 1900°F Turbine Inlet Temperature and 75% Turbine Adiabatic Efficiency.

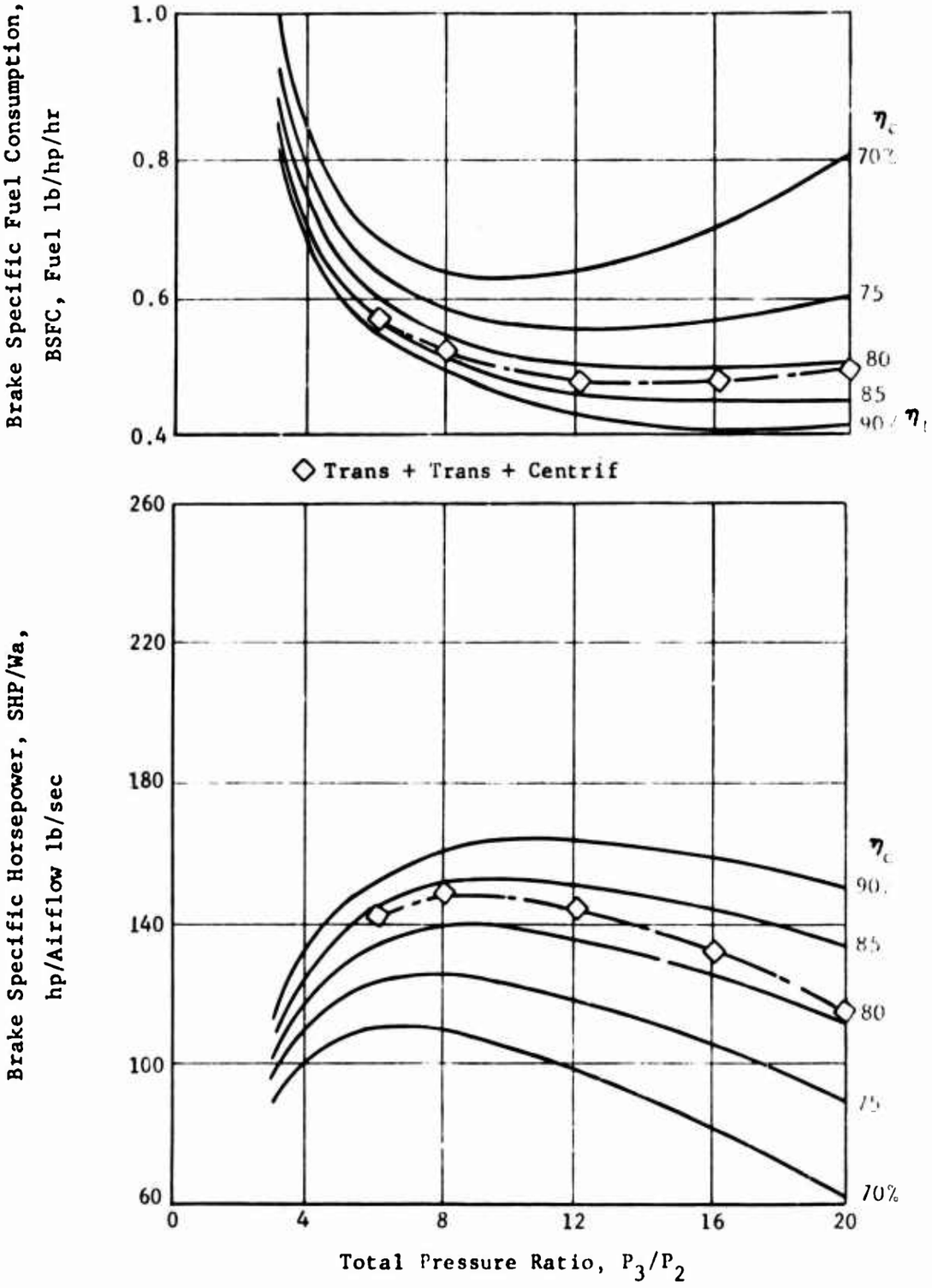

Figure 2. Turboshaft Engine Parametric Cycle Data for 1900°F Turbine Inlet Temperature and 80% Turbine Adiabatic Efficiency.

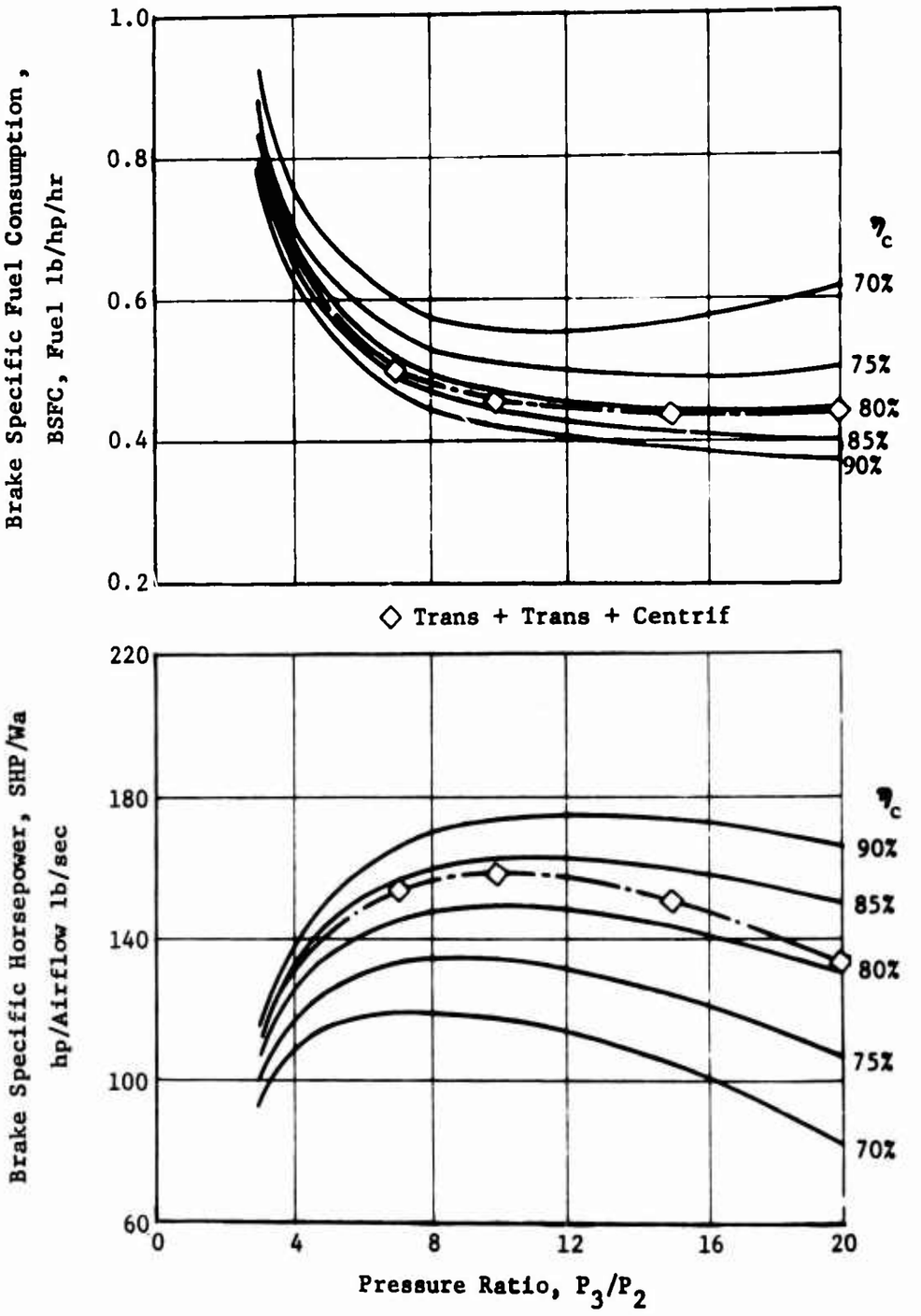

Figure 3. Turboshaft Engine Parametric Cycle Data for 1900°F Turbine Inlet Temperature and 85% Turbine Adiabatic Efficiency.

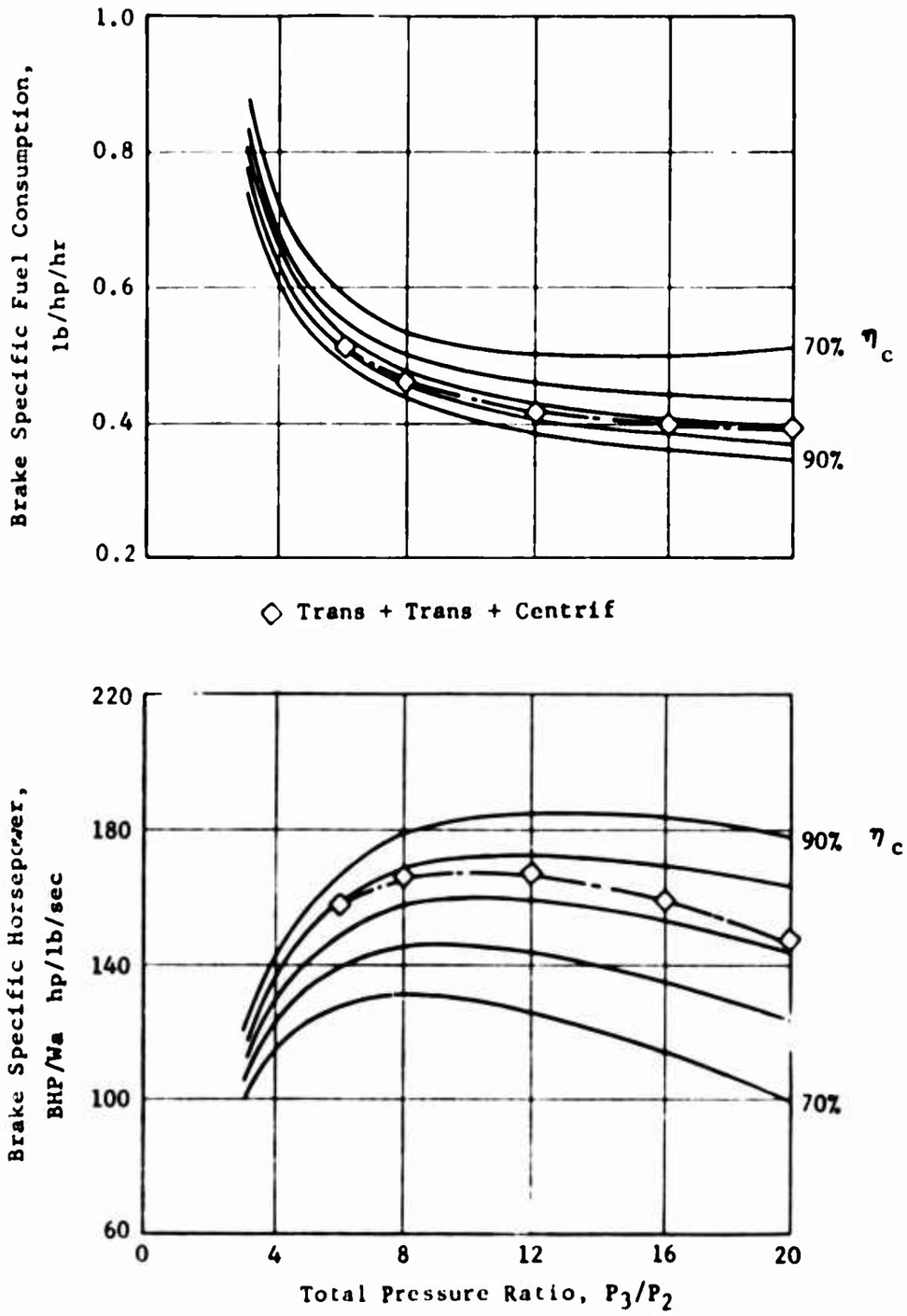

Figure 4. Turboshaft Engine Parametric Cycle Data for 1900°F Turbine Inlet Temperature and 90% Turbine Adiabatic Efficiency.

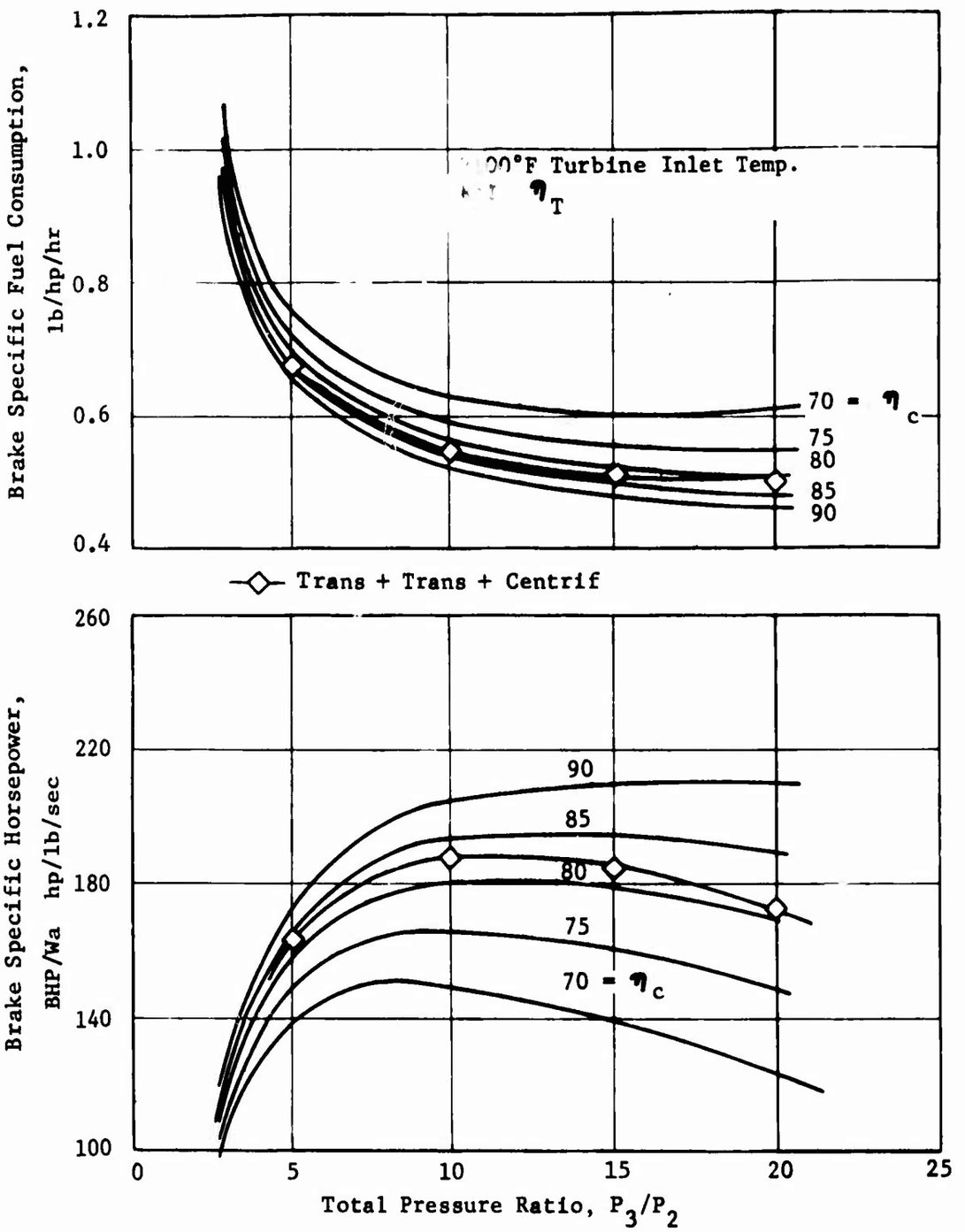

Figure 5. Turboshaft Engine Parametric Cycle Data for 2100°F Turbine Inlet Temperature and 85% Turbine Adiabatic Efficiency.

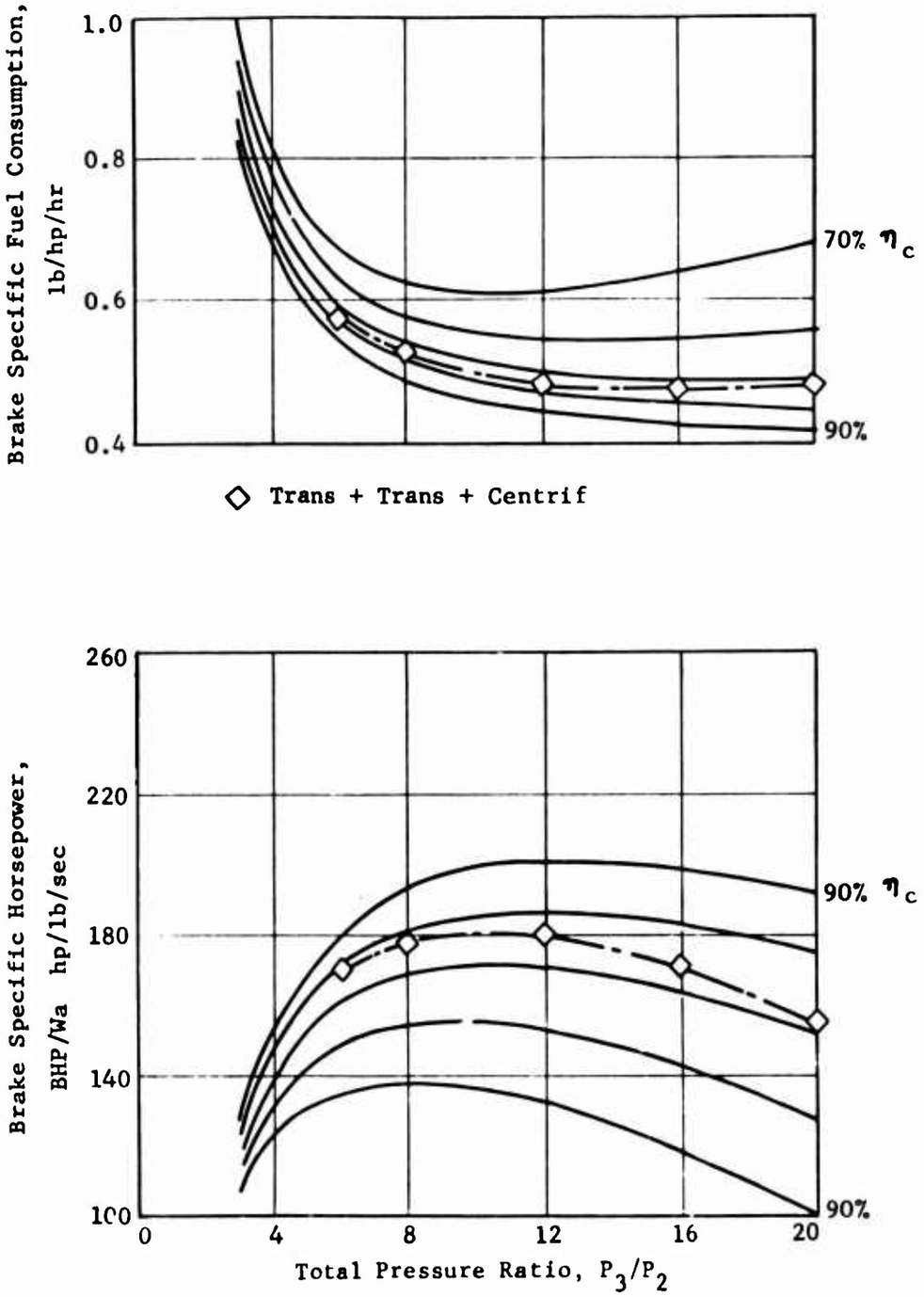

Figure 6. Turboshaft Engine Parametric Cycle Data for 2200°F Turbine Inlet Temperature and 75% Turbine Adiabatic Efficiency.

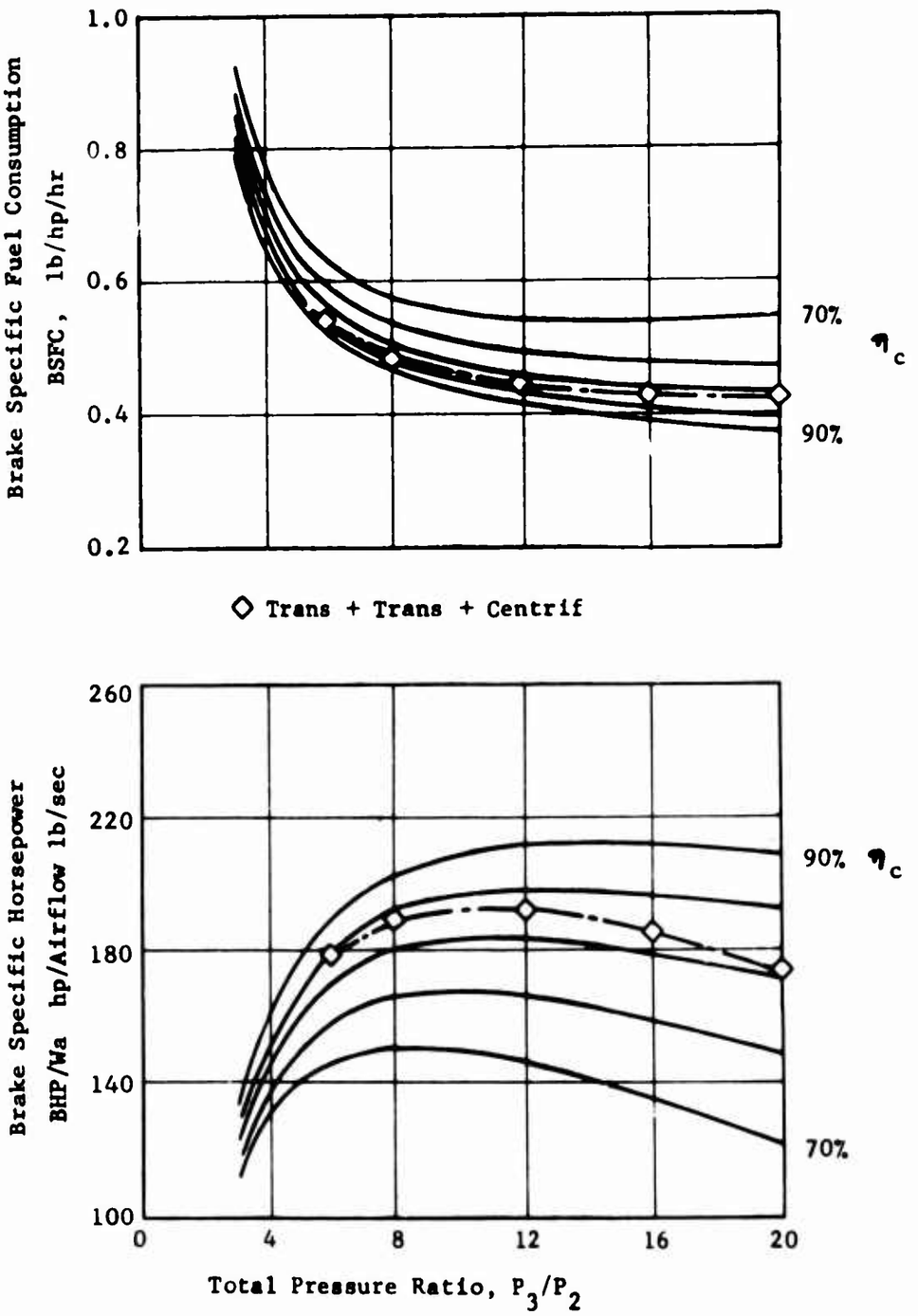

Figure 7. Turboshaft Engine Parametric Cycle Data for 2200°F Turbine Inlet Temperature and 80% Turbine Adiabatic Efficiency.

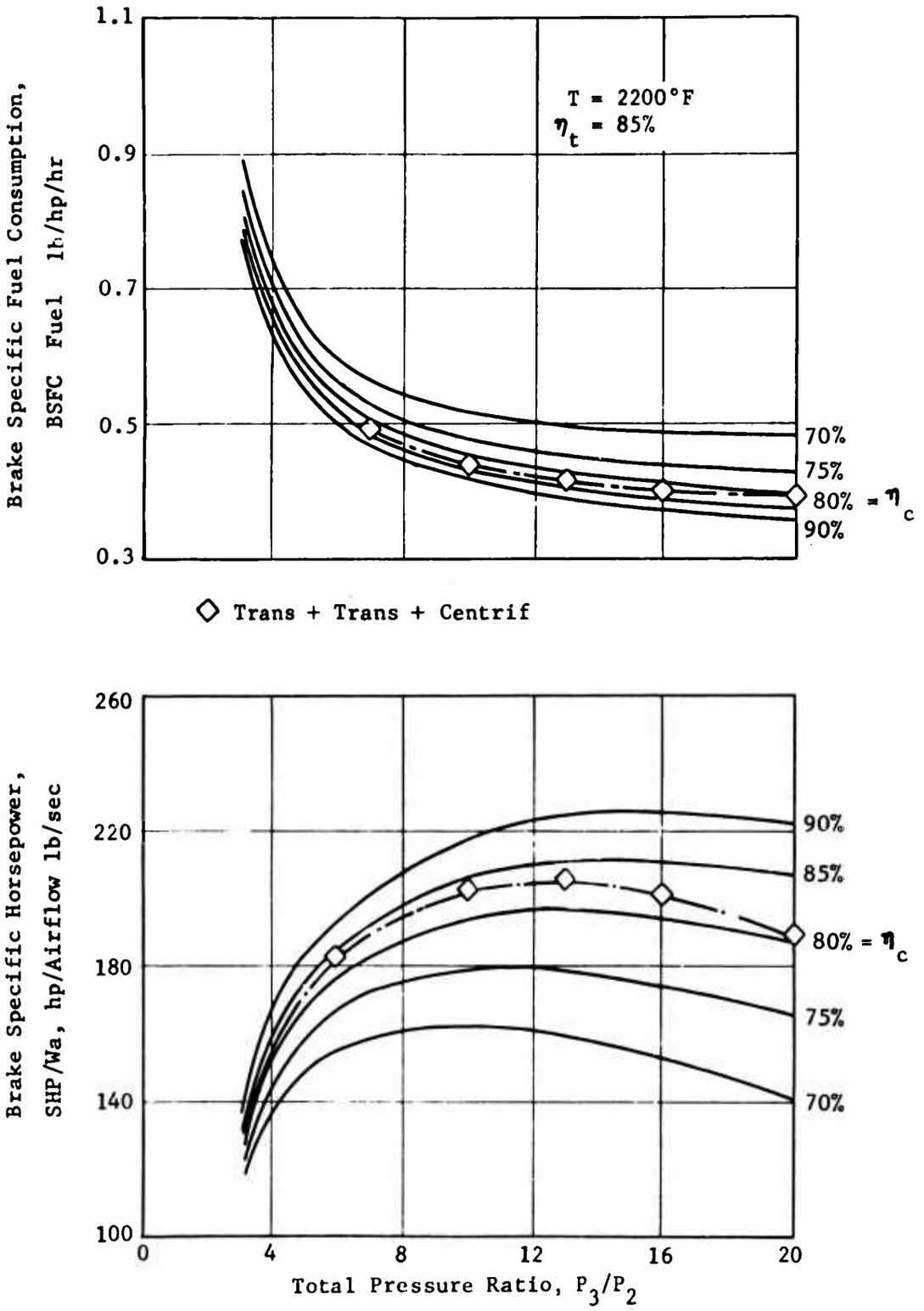

Figure 8. Turboshaft Engine Parametric Cycle Data for 2200°F Turbine Inlet Temperature and 85% Turbine Adiabatic Efficiency.

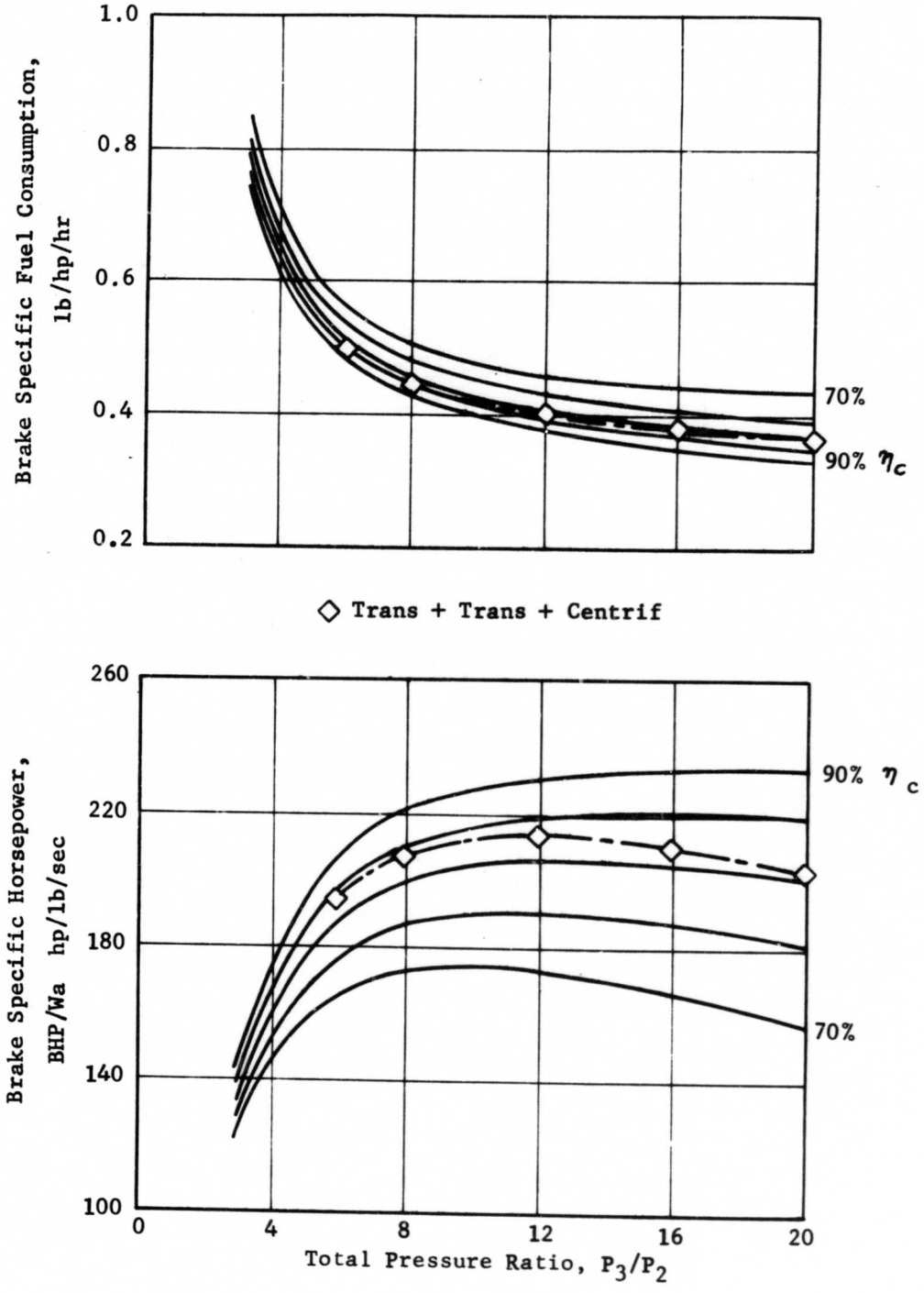

Figure 9. Turboshaft Engine Parametric Cycle Data for 2200°F Turbine Inlet Temperature and 90% Turbine Adiabatic Efficiency.

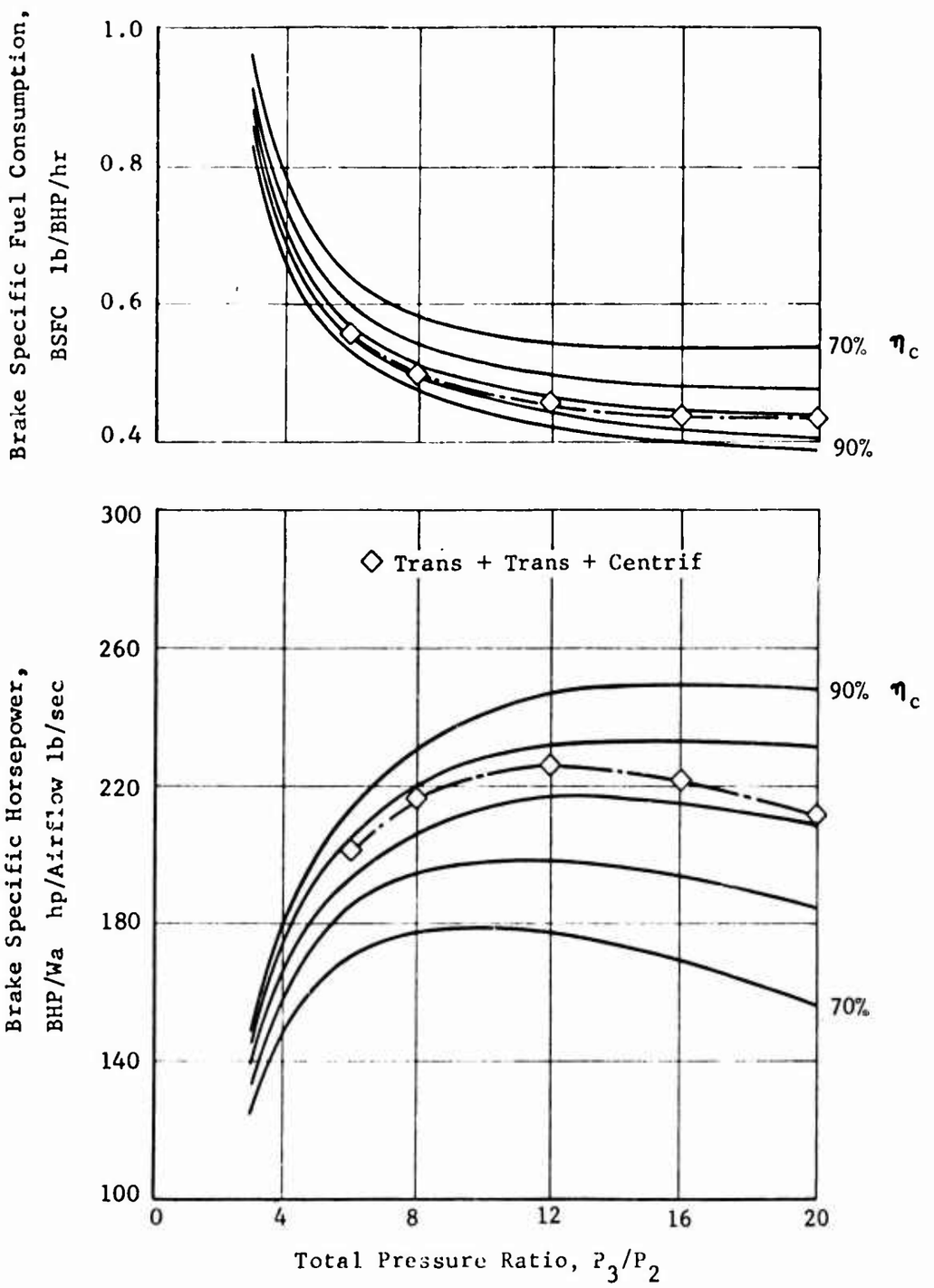

Figure 10. Turboshaft Engine Parametric Cycle Data for 2500°F Turbine Inlet Temperature and 75% Turbine Adiabatic Efficiency.

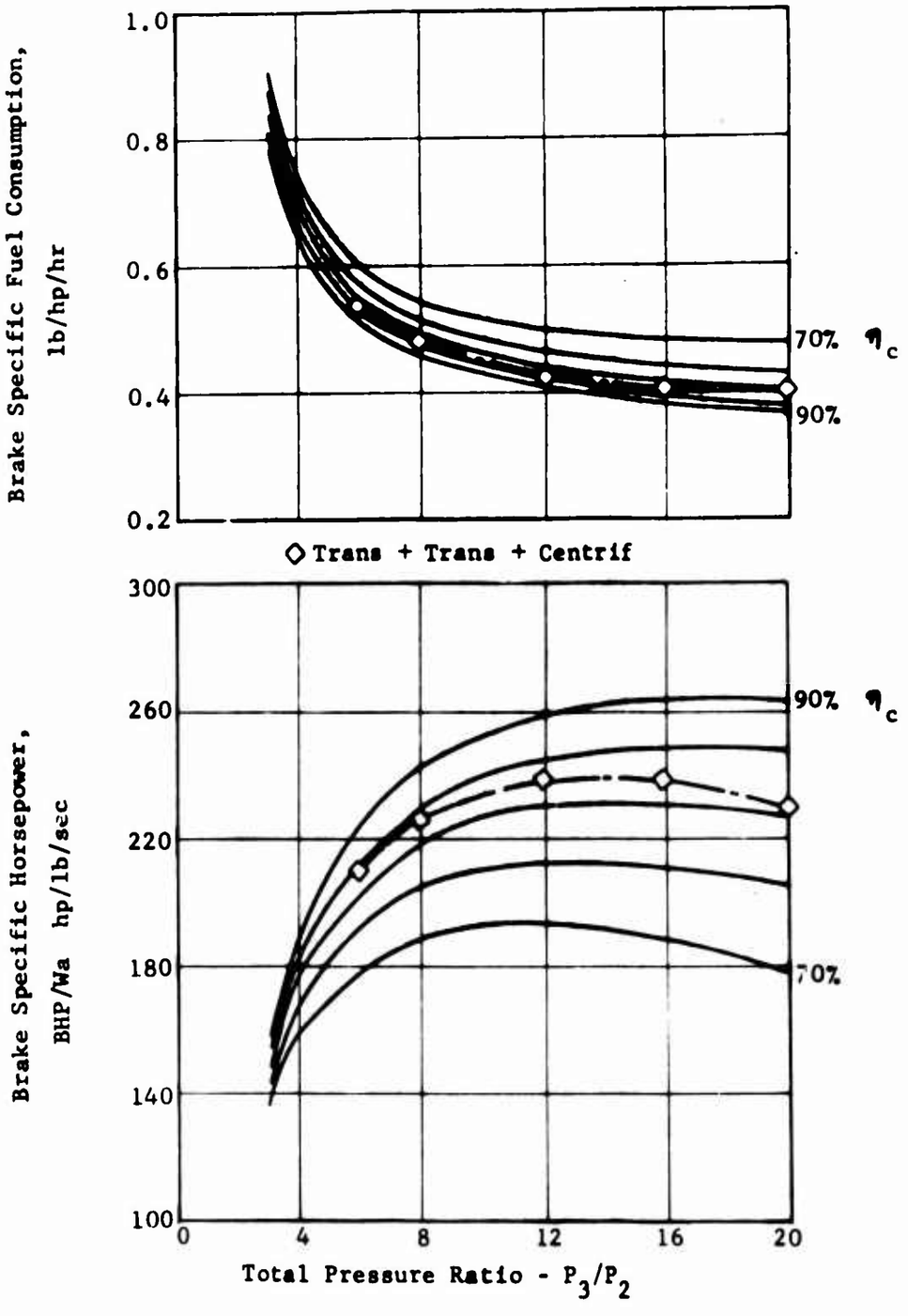

Figure 11. Turboshaft Engine Parametric Cycle Data for 2500°F Turbine Inlet Temperature and 80% Turbine Adiabatic Efficiency.

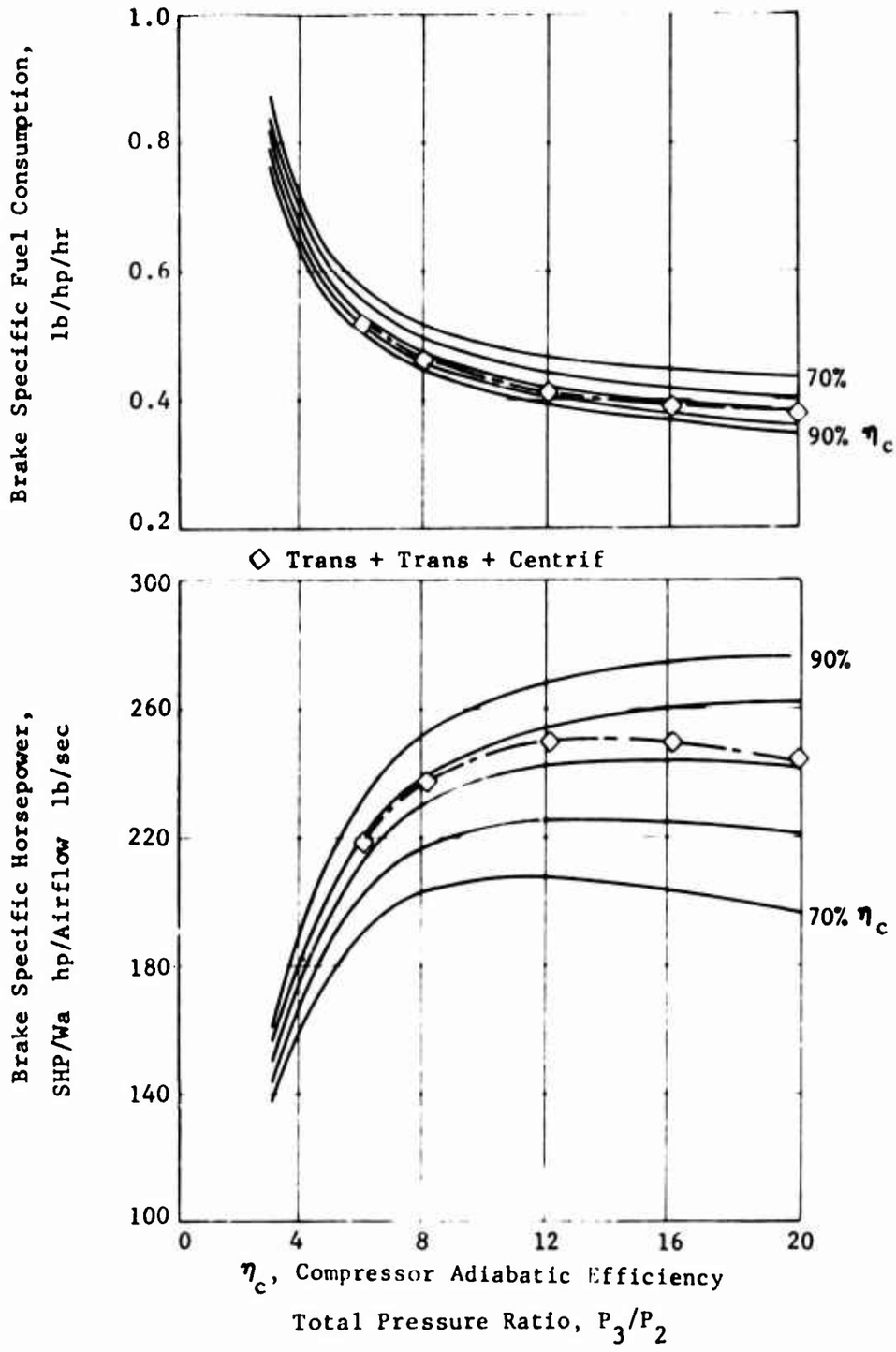

Figure 12. Turboshaft Engine Parametric Cycle Data for 2500°F Turbine Inlet Temperature and 85% Turbine Adiabatic Efficiency.

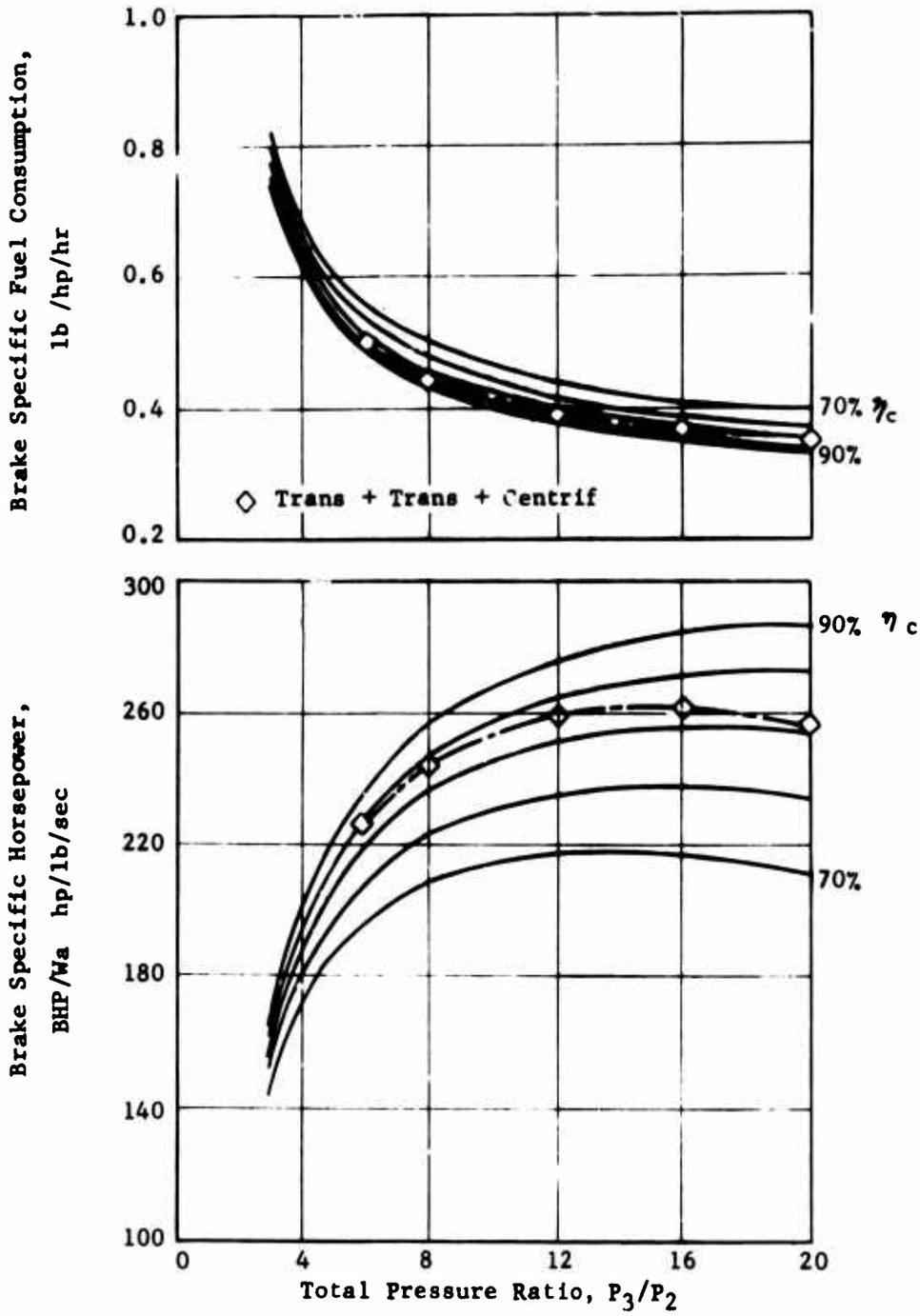

Figure 13. Turboshaft Engine Parametric Cycle Data for 2500°F Turbine Inlet Temperature and 90% Turbine Adiabatic Efficiency.

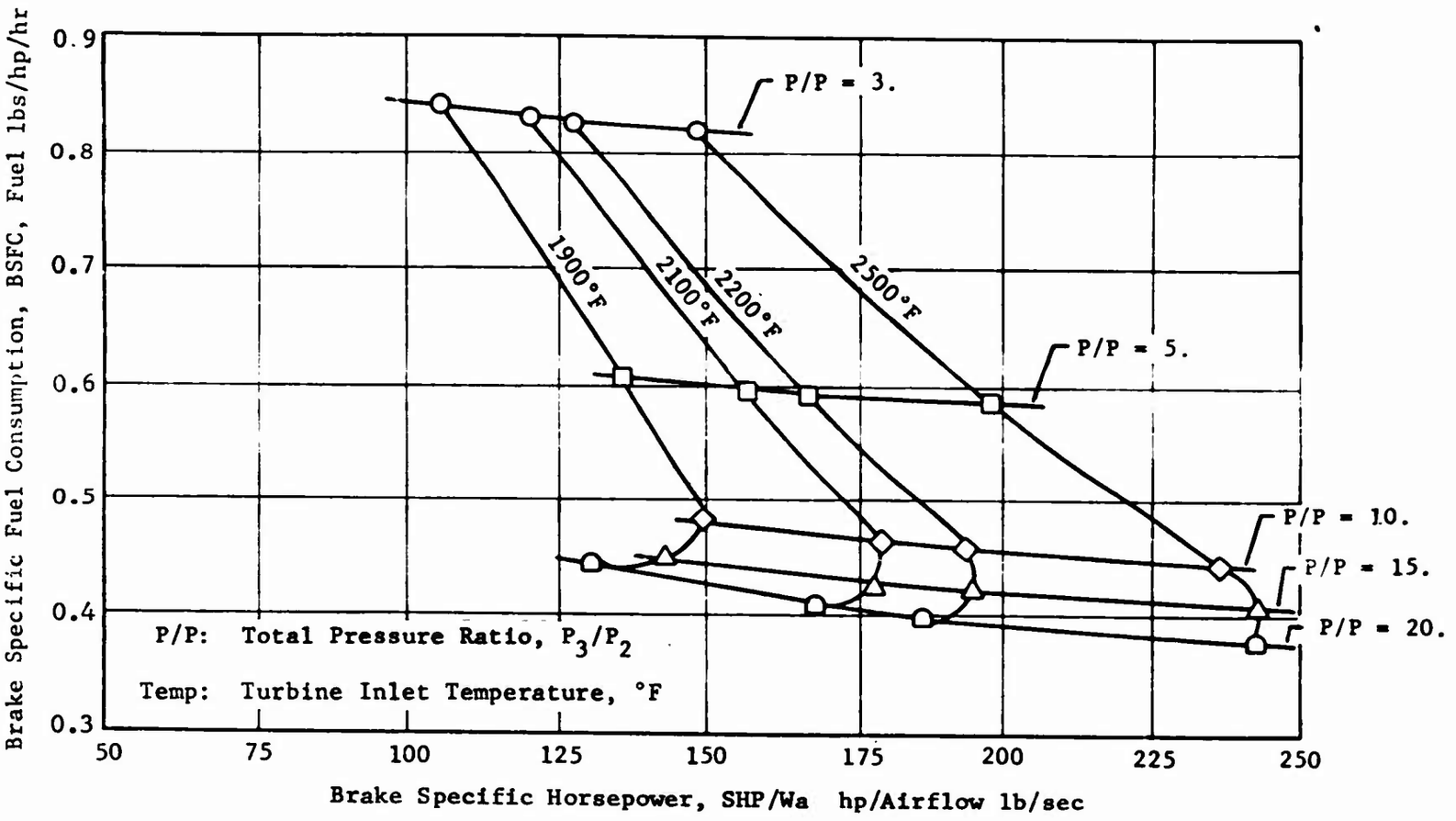

Figure 14. Turboshaft Engine Parametric Cycle Data for Adiabatic Efficiency of 85% at Turbine and 80% at Compressor

level attainment. Further evidence of this association was developed as the study progressed.

Compressor Performance Curves

The program was directed toward an advanced compressor which could be expected, with a high level of confidence, to be developed in a three-year development program. Efficiency is a major determinant of compressor performance, most clearly reflecting the state of the art. A survey of the literature was made to determine the efficiency as a function of pressure ratio for the following compressor types: subsonic-transonic axial stages, supersonic axial stages, and centrifugal stages. Subsequently, the optimum-efficiency distribution of work between stages of various types was investigated.

Performance data for subsonic and transonic axial stages are shown in Figure 15, as a plot of adiabatic efficiency versus stage total pressure ratio. The efficiencies shown on the graph are for large machines: the Jones and Oscarson data are for a 43-inch-diameter machine (Reference 1), the Kovach-Sandercock data for a 20-inch-diameter machine (Reference 2), and the Wright-Novak data for a 48-inch-machine (Reference 3). The literature indicates that it is possible to obtain good efficiency in smaller size compressors. In Reference 4, Groh and Robb report rotor efficiency above 90 percent at a pressure ratio of 1.38 and a tip diameter of 4.8 inches.

In Reference 5, Lieblein and Johnsen gave the performance of the NACA 8-stage compressor, on which the designs of several other compressors have been based. Performance data reported for two of the derivatives are compared with the prototype as follows.

Flow lbs/sec	Efficiency percent	Pressure Ratio	Authors	Reference No.
53	87+	6.6	Lieblein and Johnsen	5
43	84	6.6	Knowles	6
14	86	6.6	Mills and Pitt	7

The last compressor of the three is the smallest in flow and therefore in size, yet its efficiency, static-to-total, is only about one point less than the efficiency, total-to-total, of the original compressor. The attainable efficiency line drawn on Figure 15 represents an average of reported data for efficient large compressors and a reasonable advancement for small compressors.

Performance data for supersonic axial compressor stages are shown in Figure 16 as a plot of adiabatic efficiency versus stage total pressure ratio. Data from Cox and Muller, in Reference 8, were obtained from two supersonic stages; for one of these, the 2.8:1 stage, work was still in

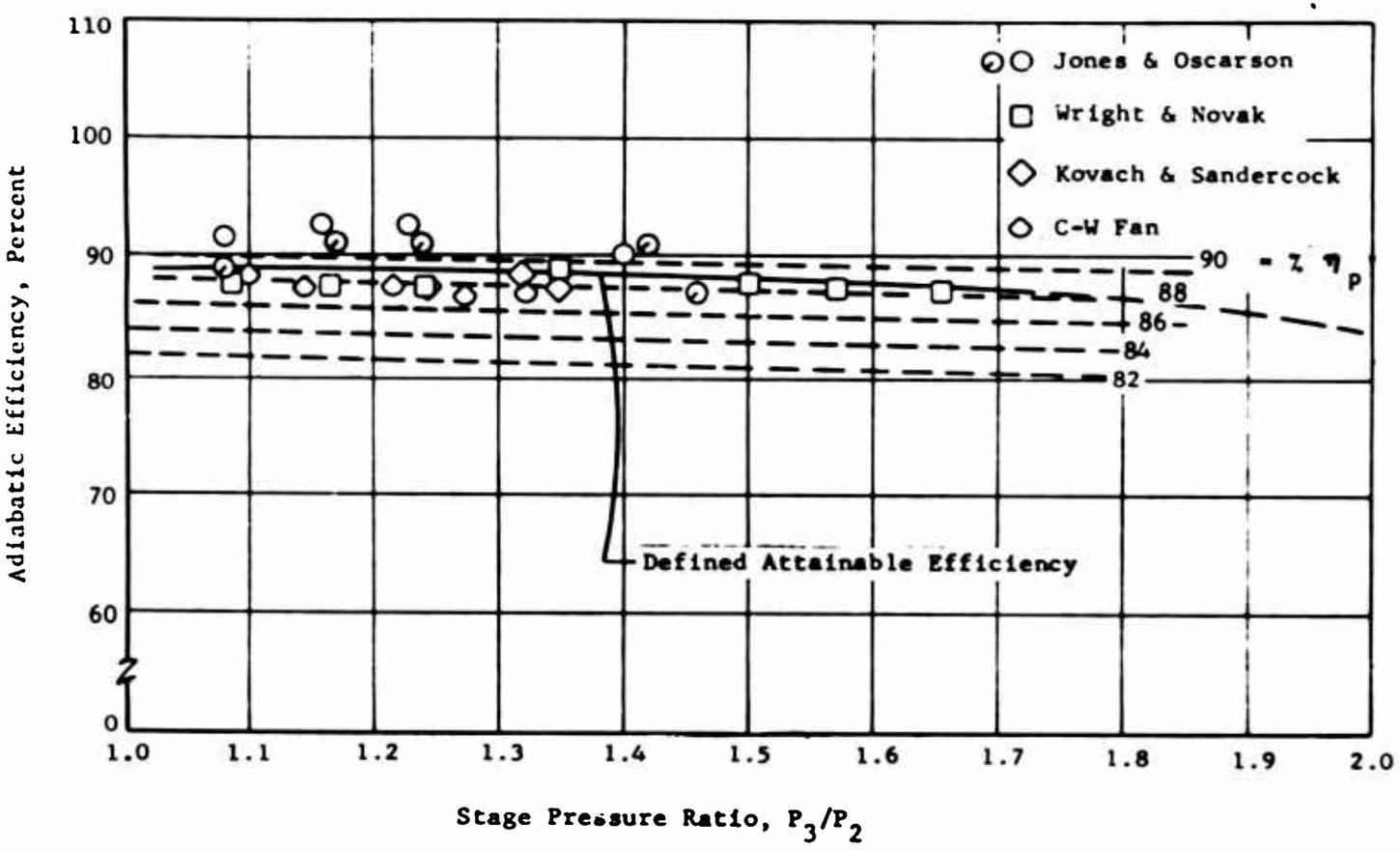

Figure 15. Attainable Efficiency for Subsonic and Transonic Axial Compressor Stages.

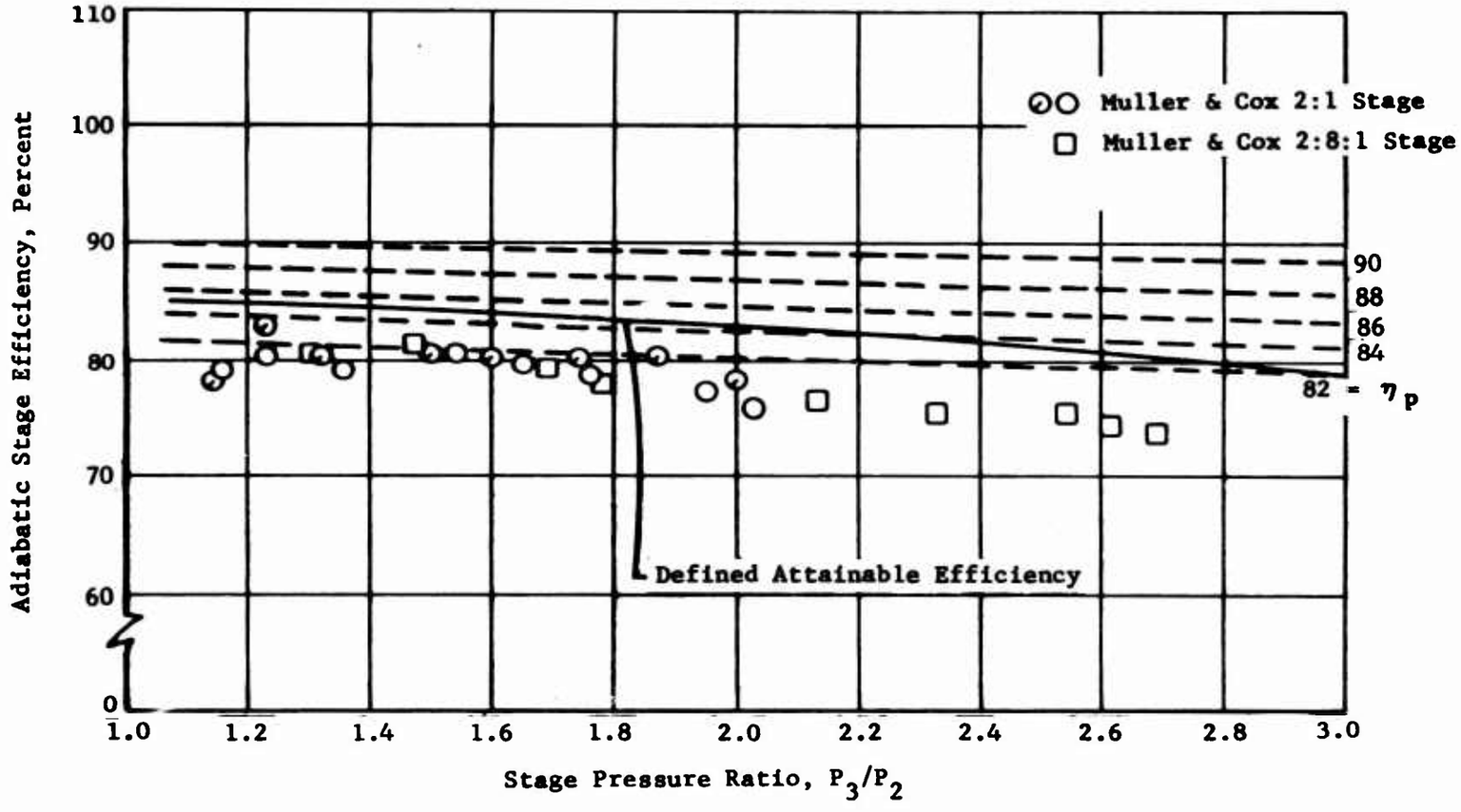

Figure 16. Attainable Efficiency for Supersonic Axial Compressor Stages.

progress at reporting time. The attainable efficiency curve is raised above reported values to reflect expectations of the current stator research program.

Performance data for centrifugal compressor stages are shown in Figure 17. Schwartz, in Reference 9, reported the performance of a number of centrifugal compressors for automotive applications. The static-to-total pressure ratio performance data of an aircraft reciprocating engine supercharger were taken from unpublished Curtiss-Wright data. Welliver and Acurio, in Reference 10, reported the performance of a 6:1 workhorse compressor and a 10:1 RF-2 research compressor, both based on exit static-to-inlet total pressure measurements. Morris and Kenny, in Reference 11, reported the performance of a 6:1 G-rotor stage and a 12:1 H-rotor stage, both based on total-to-total pressure measurements. In private communication with the author, Welliver estimated the efficiency difference between values based on exit total and on exit static to be two points for the workhorse and RF-2 compressors. The curve for centrifugal stage attainable efficiency conforms to the best reported data at pressure ratios near 6:1 and anticipates modest increases at higher and lower pressure ratios. At low pressure ratios, the increases should come more easily but are not likely to be sought because of the advantages of high pressure ratio.

The task definition required the matching of a centrifugal compressor with a one- or two-stage axial compressor, raising a question of the proper distribution of work between stages of different types. The following combinations of axial stages were investigated and later combined with centrifugal stages:

a supersonic stage alone
a supersonic stage plus a transonic stage
two transonic stages
two supersonic stages

The stage efficiency characteristics were defined by the attainable efficiency curves given in Figures 15 through 17, and the overall performance data were obtained using a small FORTRAN calculation procedure called Adder, which is presented in Appendix III.

An example of combining two stages is shown graphically in Figure 18. The curve shows the attainable efficiency for various LP compressors composed of a supersonic stage plus a transonic stage. This curve illustrates the principle of best work distribution between stages, namely, that highest overall efficiency is obtained for a given pressure ratio by assigning as much work as possible to the more efficient stage. Each of the short curves represents a fixed pressure ratio for the first stage, which in this case is a supersonic stage. On each curve the second-stage pressure ratio is varied, causing overall pressure ratio to vary. Although pressure ratios above 1.8 were considered elsewhere in the study, based on Reference 12 data acquired subsequently, the maximum stage pressure ratio considered in this instance was 1.6. Examination of the curve shows that

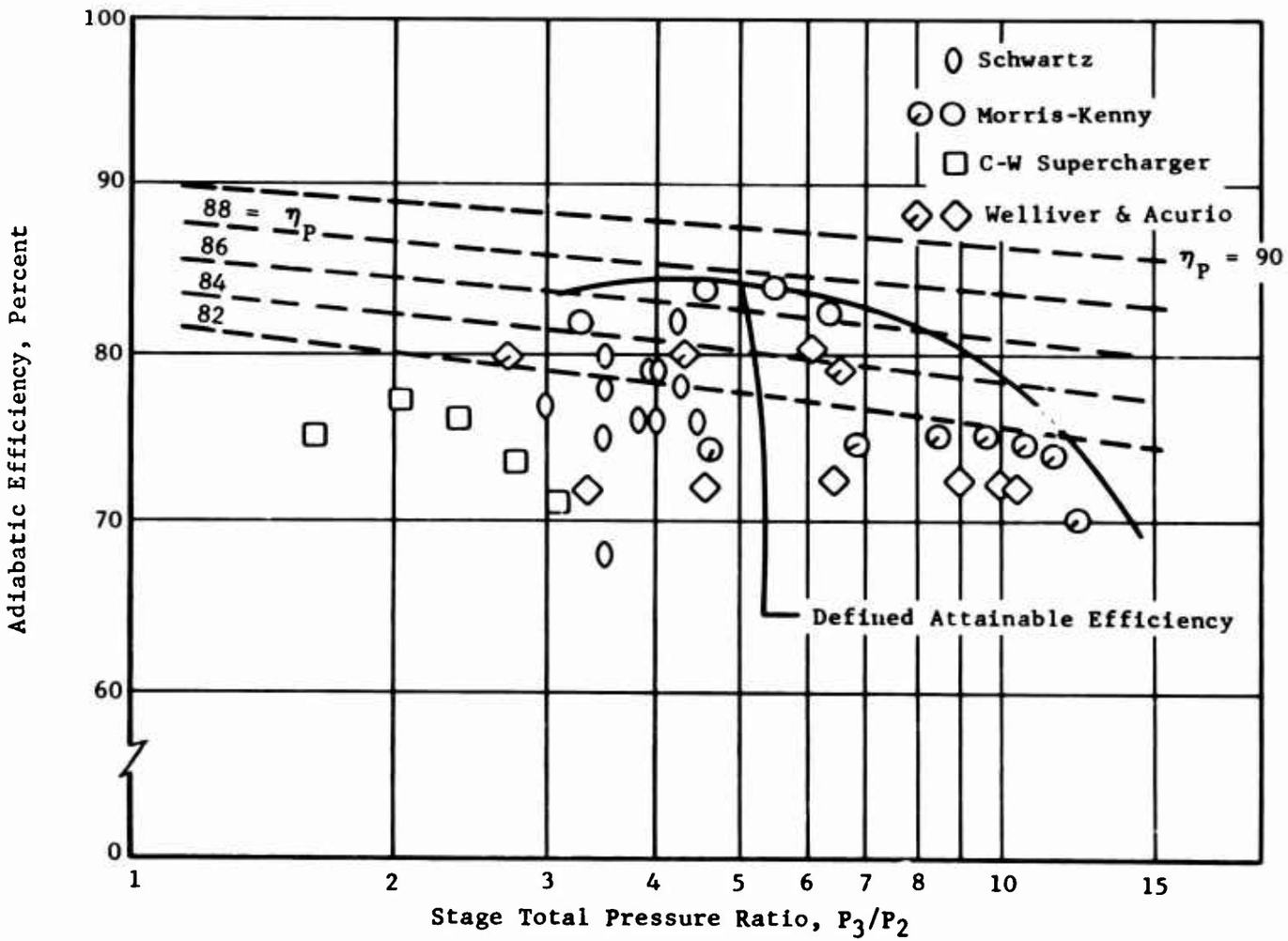

Figure 17. Attainable Efficiency for Centrifugal Compressor Stages.

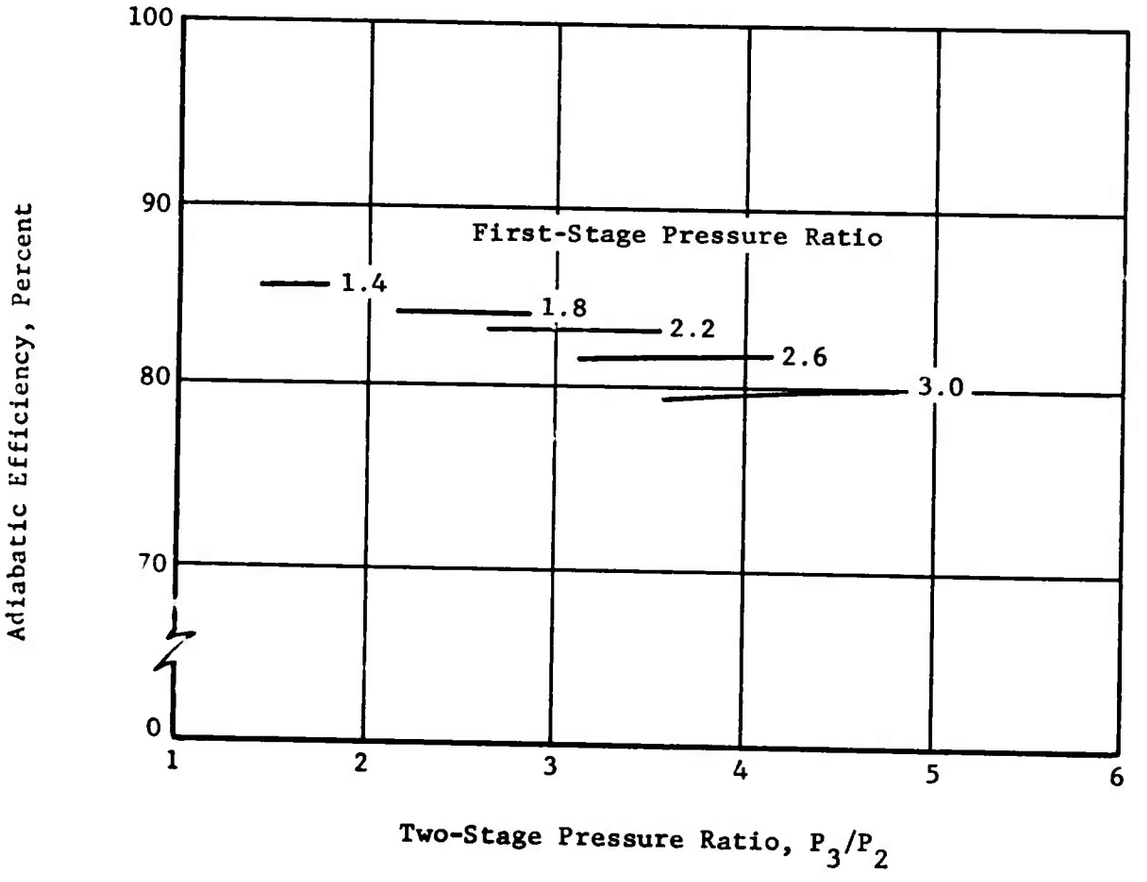

Figure 18. Attainable Efficiency for a Two-Stage Compressor, Incorporating a Supersonic Stage Followed by a Transonic Stage.

an envelope line can be drawn through the right-hand ends of the curves to define maximum attainable efficiencies for this particular combination of axial stages. This LP compressor envelope line was then used in combination with attainable centrifugal compressor performance to define overall compressor performance.

The combination of an axial and a centrifugal compressor is illustrated in Figure 19, for a supersonic stage plus a centrifugal stage. The best distribution of work between axial and centrifugal stages is again represented by an envelope line. There, the line at constant LP pressure ratio has a peaking form, which is due to the peaking form of the centrifugal compressor attainable efficiency curve. The data show that as overall pressure ratio increases, it is desirable to allocate enough work to the axial stage to keep the centrifugal stage working near its efficiency peak.

The attainable efficiencies of various axial compressors combined with centrifugal stages are shown in Figure 20. Each of these lines represents an envelope of the type described above. These efficiency values are obtainable at design point conditions, based on optimum matching of compressor elements; off-design efficiencies will of course vary. The highest efficiency at pressure ratios below 20:1 is obtained from the two-transonic plus centrifugal combination of stages; at higher pressure ratios the best combination substitutes a supersonic stage for the first transonic stage. The efficiency difference between these two combinations is only about one point at lower pressure ratios.

The performance of the most efficient stage combination, namely, two transonic stages plus centrifugal, was used to indicate the engine performance potential by plotting the data on the parametric cycle data curves, Figures 1 through 13. An exception appears in Figure 1, where data for all of the stage combinations were plotted on the graph for fuel consumption. At 75 percent turbine efficiency and low cycle temperature, minimum fuel consumption occurs near a pressure ratio of 12:1; but at 85 percent, which was used subsequently as the attainable turbine efficiency, minimum SFC values are reached near 17:1 pressure ratio for 2100°F (60 percent power) and near 16:1 pressure ratio for 1900°F (30% power). These values may be noted as tentative goals for the part-power operating conditions.

Optimum Performance and Parametric Match Data

An attempt to approach the definition of compressor performance by selecting a 60 percent power design point is illustrated in Figures 21 and 22, the first for an 8:1 pressure ratio and the second for 12:1. Each graph represents an abstract compressor map wherein only cycle parameters appear; no stall line or speed lines are shown. There are, however, three constant turbine inlet temperature lines whose relative locations are based on the assumption of a choked turbine stator. For Figure 21, the design point is assumed to be 2200°F, 8:1 pressure ratio, and 60 percent power.

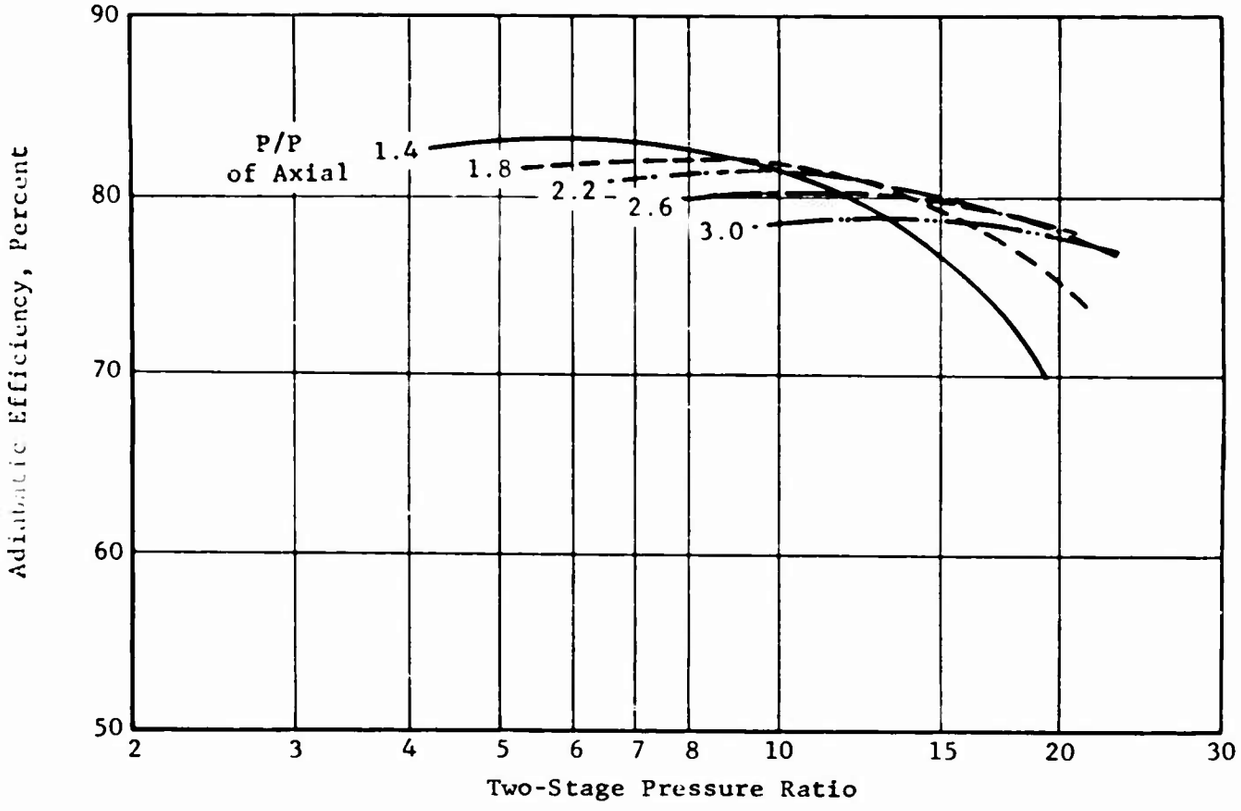

Figure 19. Attainable Efficiency for a Two-Stage Compressor, Incorporating a Supersonic Stage Followed by a Centrifugal Stage.

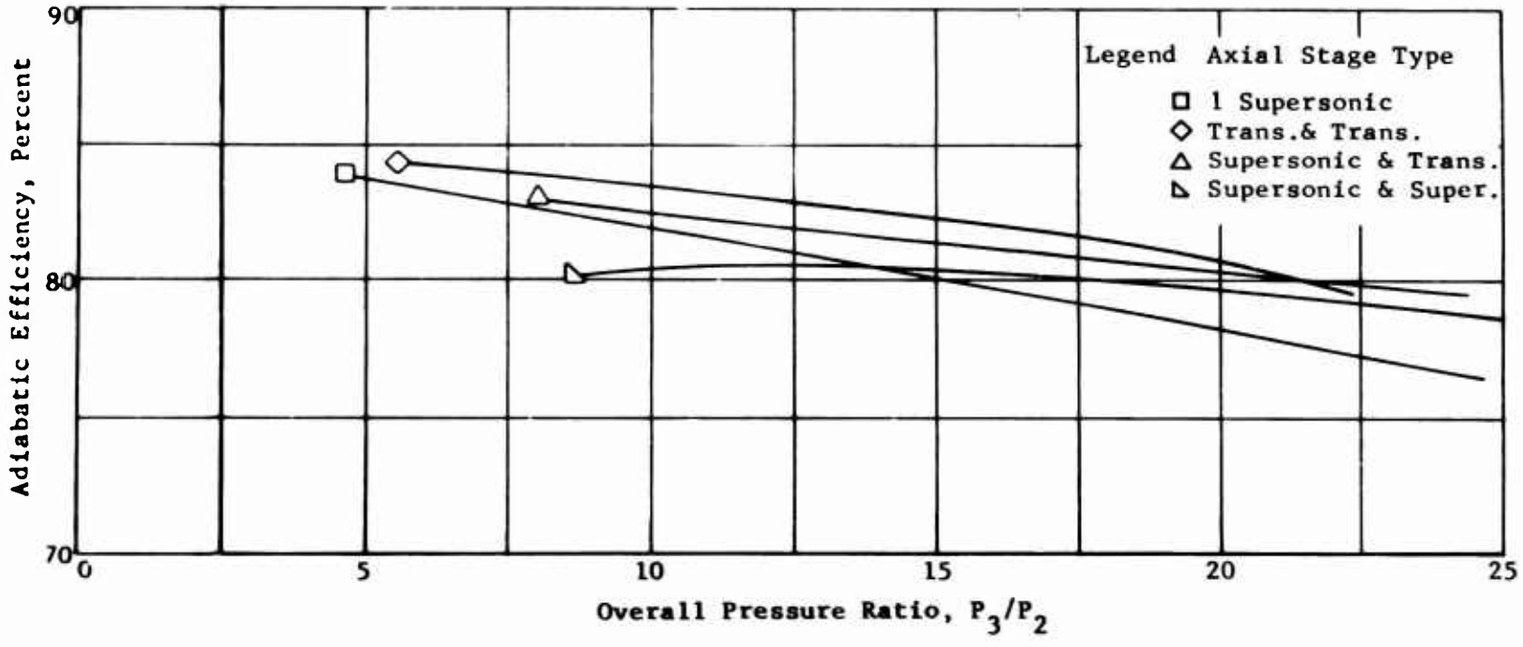

Figure 20. Attainable Efficiency for Two and Three Stage Compressors, Incorporating an Axial Compressor Feeding a Centrifugal Stage.

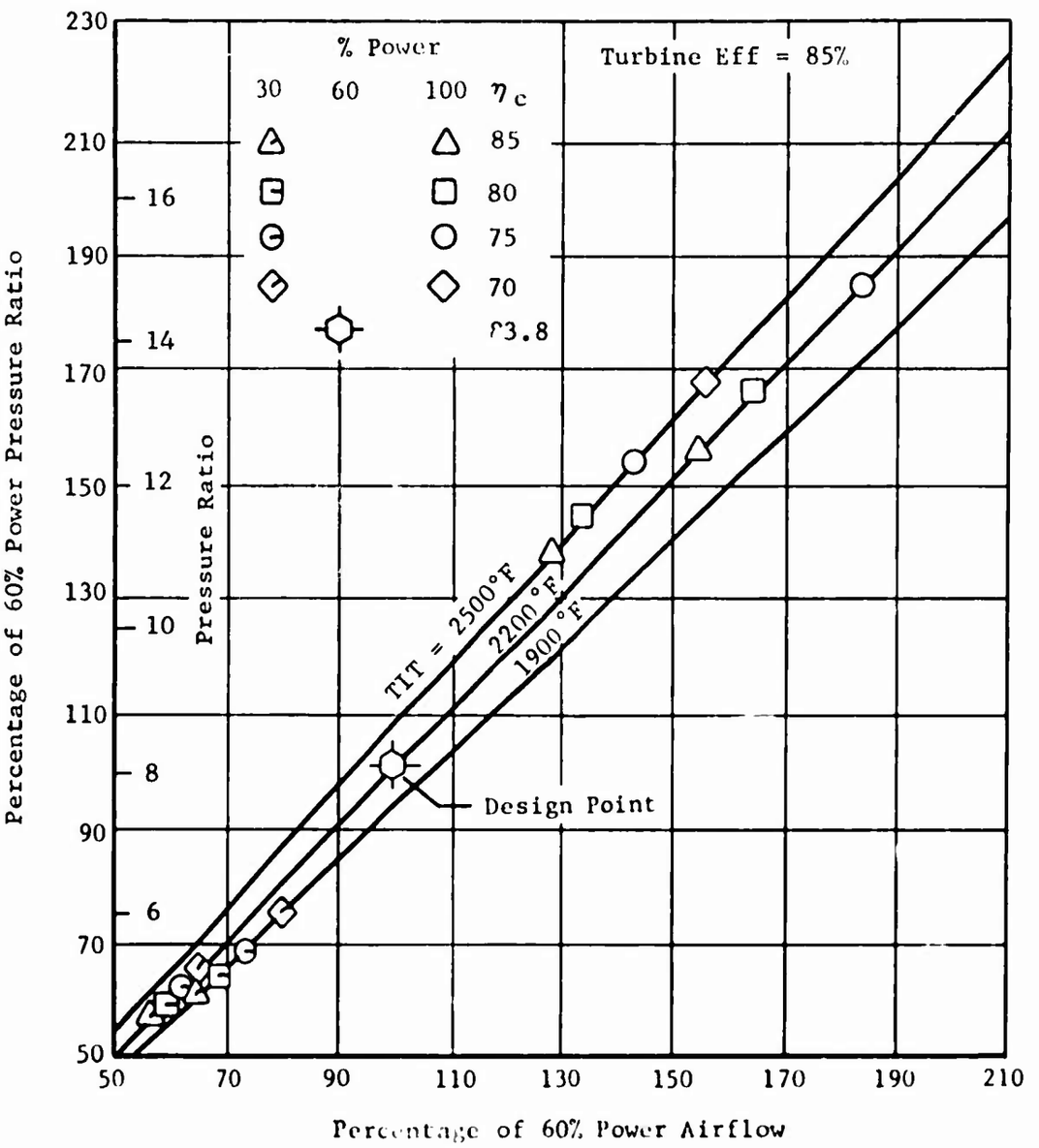

Figure 21. Effect of Compressor Off-Design Efficiency for Compressor Design Point at 60% Power With 8:1 Pressure Ratio.

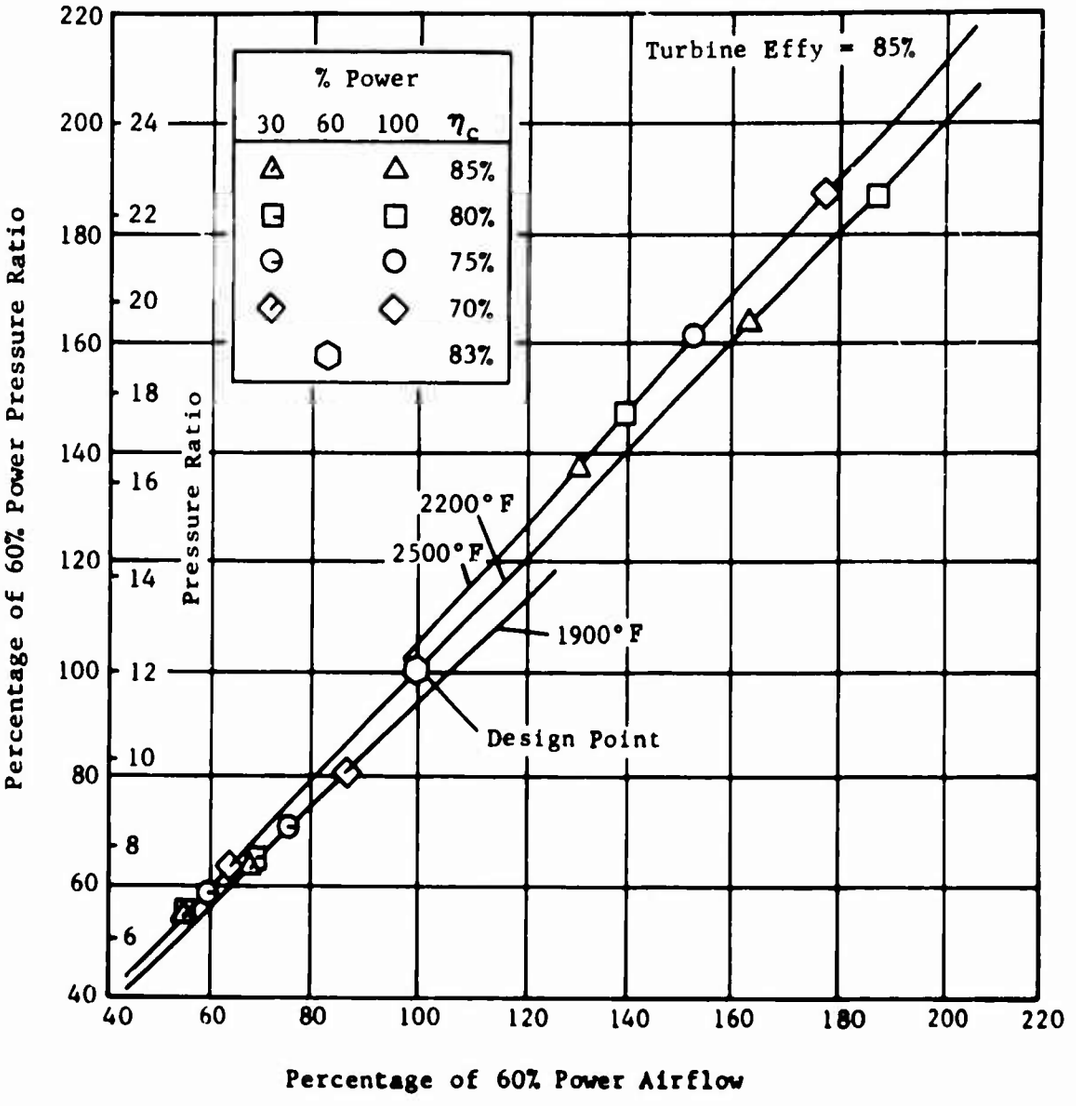

Figure 22. Effect of Compressor Off-Design Efficiency for Compressor Design Point at 60% Power With 12:1 Pressure Ratio.

The compressor efficiency points are located on the temperature lines by use of the cycle parameters, Figures 1 through 14, to define flows which will produce the required 100 percent power or 30 percent power output, as follows. At attainable efficiency, the 60 percent power, 2200°F point defines base point values for pressure ratio and specific power. A given pressure ratio then immediately defines the percentage of pressure ratio. With turbine inlet temperature and pressure ratio known, compressor efficiency determines specific power which, with percentage of power, then defines percentage of flow. From such data, constant compressor efficiency lines are plotted on a graph percentage of pressure ratio versus percentage of flow, and these lines intersect a temperature line like one of those on Figures 21 and 22. These intersections locate the efficiency points on these figures.

The specific fuel consumptions which correspond to compressor efficiency points in Figures 21 and 22 are listed below.

COMPARISON OF BSFC FOR VARIOUS COMPRESSOR EFFICIENCIES AT THREE POWER LEVELS

For 60 Percent Power at 8:1 Pressure Ratio

Compressor Efficiency, percent	70	75	80	83.8	85
100 Percent Power TIT = 2500°F	.46	.44	.42		.415
= 2200°F	.49	.445	.42		.41
60 Percent Power TIT = 2200°F				.47	
30 Perdent Power TIT = 2200°F	.63	.62	.60		.59
= 1900°F	.64	.61	.60		.59

For 60 Percent Power at 12:1 Pressure Ratio

Compressor Efficiency, percent	70	75	80	83	85
100 Percent Power TIT = 2500°F	.43	.40	.39	-	.37
= 2200°F	-	-	.40	-	.39
60 Percent Power TIT = 2200°F	-	-	-	.42	-
30 Percent Power TIT = 2200°F	.55	.53	.52	-	.505
= 1900°F	.56	.53	.50	-	.48

The temperatures and power ratings which should be associated are 2200°F turbine inlet temperature (TIT) for 60 percent of full rated power, 2500°F for 100 percent, and 1900°F for 30 percent. A variation of temperature from 2200°F greatly reduces the excursion of compressor performance from 60 percent values, without penalty in specific fuel consumption.

From Figure 21, it may be noted that 100 percent power pressure ratios as high as about 13 may be required if the design (60 percent power) pressure ratio is 8 and, from Figure 22, as high as 23 if design pressure ratio is 12. The corresponding increased flow values are 155 percent and 180 percent of 60 percent power values. In moving the design P/P from 8 to 12,

much more severe performance demands are placed on the compressor for the 100 percent power point. As shown in the tables above, the reward is an improvement in SFC of about 10 or 12 percent at 30 percent and 60 percent power and about 7 percent at 100 percent power.

It is shown in the above listing that if a 13- or 14-point decrease in compressor efficiency occurs in passing from 60 percent to 100 percent power points, the SFC values will be nearly equal at the two points. At the same time, such an efficiency decrease causes a loss of specific power and a resulting large increase in required flow and pressure ratio at 100 percent power (Figures 21 and 22). It is therefore indicated that attaining full power may be a more sensitive goal than attaining acceptable SFC at 100 percent power.

The preceding study has shown that the pressure ratio and airflow requirements for 100 percent power and the fuel consumption for 30 percent power are critically dependent on changes in off-design efficiency. Heretofore in the study no information has been provided about the probable magnitudes of efficiency changes. This subject was investigated subsequently in the preliminary design phase of the program. Final goals for 30 percent and 60 percent power operating conditions could not be defined with the information available at this stage of the program. General goals could be defined, namely, to maintain high efficiency while seeking for high pressure ratio. The tentative goals noted at the end of the preceding section may still be held for 30 percent and 60 percent power. The corresponding pressure ratios should be 16:1 and 17:1 respectively.

PRELIMINARY DESIGN

Component Configuration

The investigation of compressor configurations encompassed the combination of stages of various types with respect to optimum distribution of pressure ratio between LP and HP compressor, stage matching effects of various compressor combinations, effects of two-spool compressors on front drive, and effects of disc stress and temperature on centrifugal compressor tip speed. Pressure ratio distribution effects are treated above in a section entitled Compressor Performance Curves. Stage-matching of various compressor types is treated below in a section entitled Compressor Characteristics. The two-spool front drive turboshaft compressor is discussed here in relation to the mechanical complexities. The disc-stress analyses were approached in two ways at different points in the program, as described here. A factor in the disc stress approach is the centrifugal compressor flow path configuration, which is discussed here in both mechanical and aerodynamic aspects.

Two-Spool Front Drive Turboshaft Engine

A shafting design arrangement for a two-spool front drive compressor was developed around compressor flow path concepts of this program as shown in Figure 23. The shaft system consists of a central shaft by which a power turbine drives a gearbox, then a coaxial second shaft by which an LP turbine drives the two-stage axial compressor rotor, and finally a third coaxial shaft by which an HP turbine drives the centrifugal rotor. Thus the centrifugal compressor disc must have a central hole large enough to contain at least two shafts and the running clearance spaces. In the design shown, a bore diameter of 2 inches was the largest hole that could be provided concomitant with acceptable disc stresses. This implies limitations on the sizes of the interior shafts and on the critical speeds of shafting. The system of three concentric shafts also presents complexities in the bearing and lubrication systems.

Critical speeds of the shafting shown in Figure 23 were calculated with the following results. The outer shaft critical speed was high, above the engine maximum operating speed of about 50,000 RPM. The intermediate shaft critical speeds were calculated to be in the range between 30,000 and 40,000 RPM, and therefore in the ordinary range of engine operation. The innermost shaft critical speed calculations showed a first critical speed in the range between 8000 and 11,000 RPM and a second critical speed range between 25,000 and 31,000 RPM. Thus, both of the inner shafts will have critical speeds in the engine operating regime.

Critical speeds can be changed by supporting the shaft at appropriate locations in bearings which change the mode of vibration of the shaft.

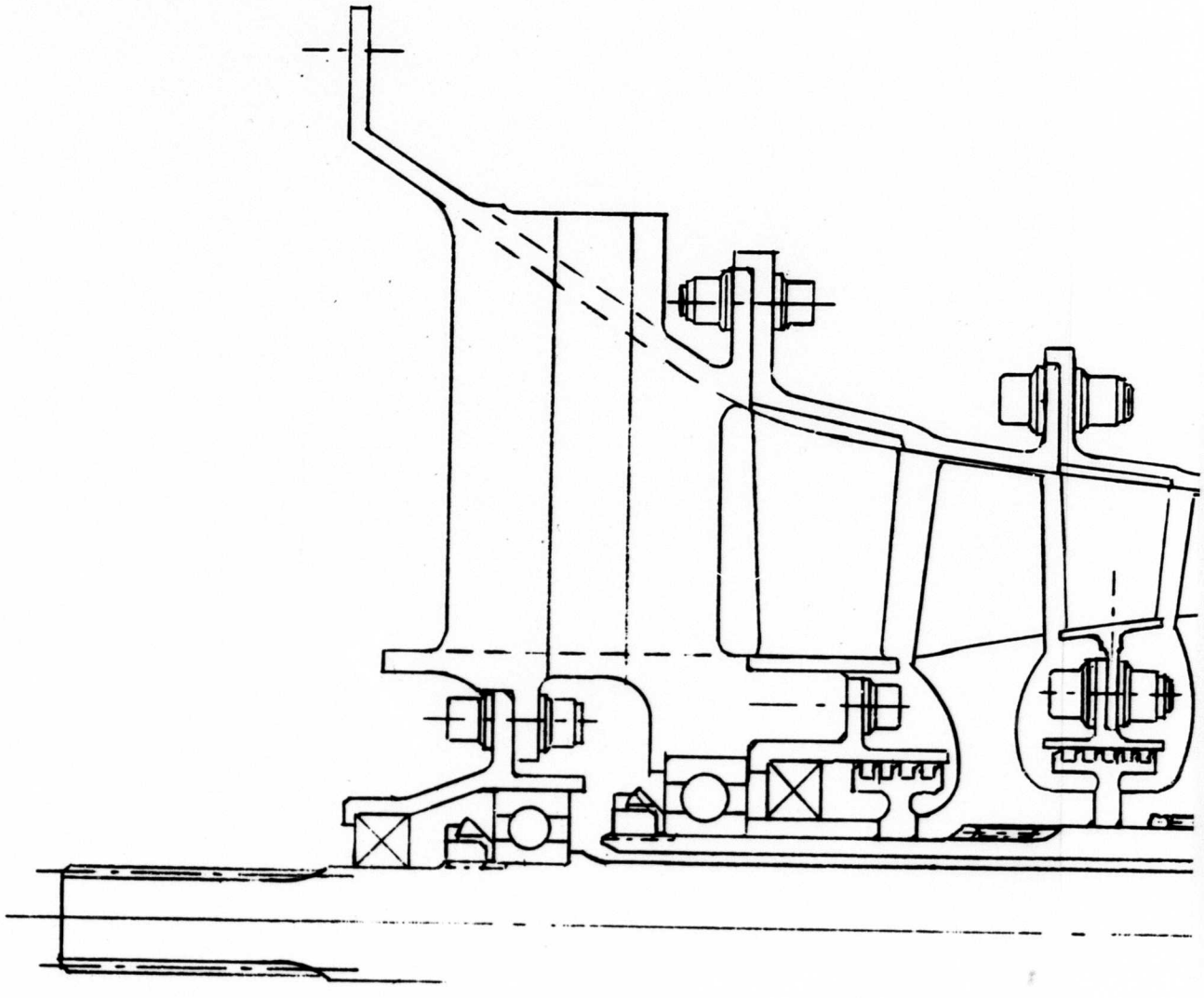

Figure 23. Two Spool Front Shaft Compressor Design.

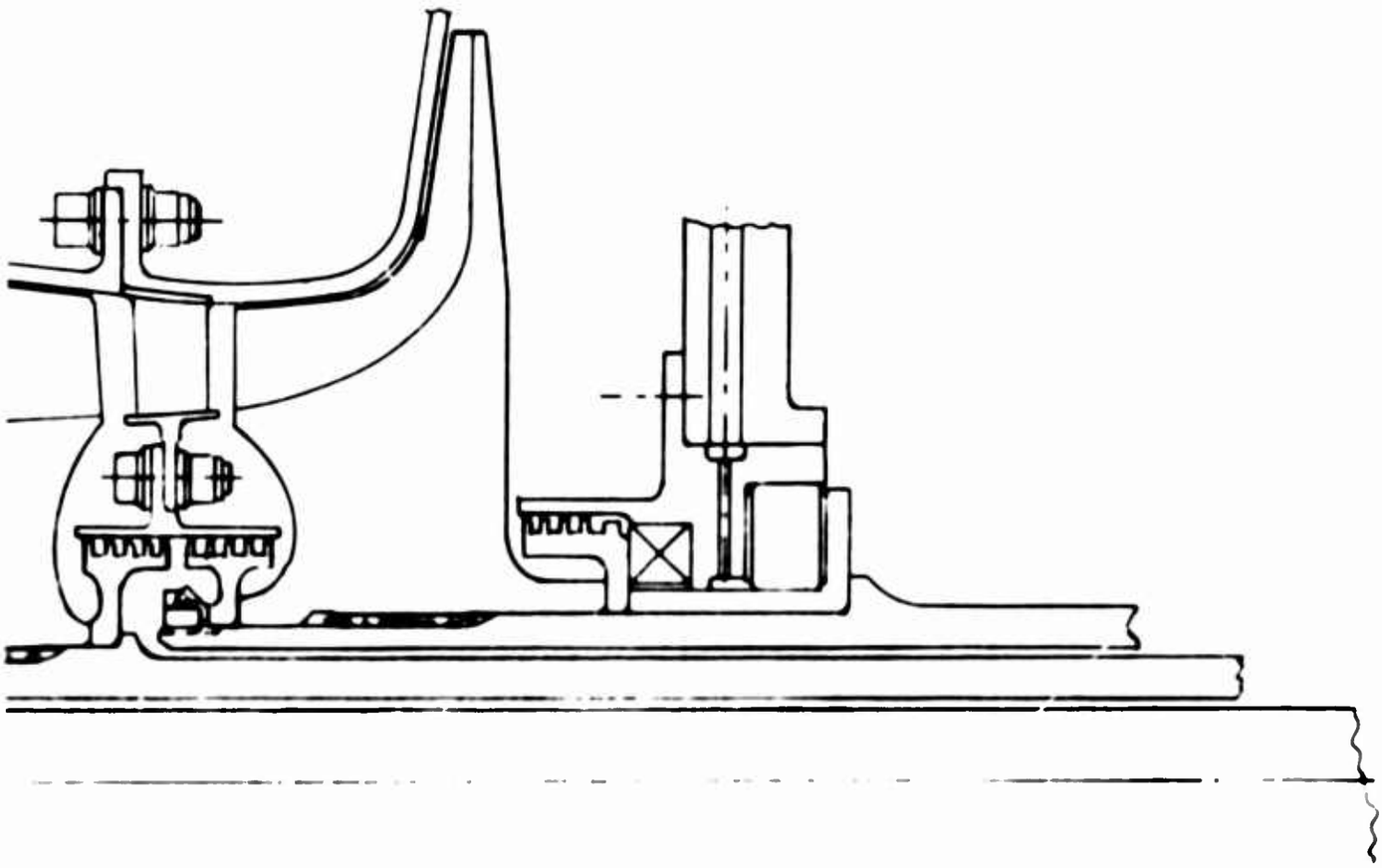

In effect, the shafts support each other between main bearing locations. Because all of the shafts have critical speeds occurring at different RPM and two have criticals in the operating range, a task of great complexity and considerable uncertainty arises in predicting the critical speeds which would result from attempts to control the critical speeds by coupling these elastic systems together through such sleeve bearings.

The lubrication problem is complicated by the need to place snubber bearings between the three shafts. Some sealed path has to be provided for supplying oil to the intershaft snubber bearings, and then a flow path and a motive force have to be provided to carry the heated oil from the bearing to the sump. The motive force can be provided by tapering the bore of a hollow shaft so that an axial component of centrifugal force drives the oil along the shaft. However, the tapering of shafts is restricted because of the small size of the shafting, and the motive force can be nullified if the shaft is bowed under vibration and is unable to run true. Thus, the lack of space for seals and lines and the flexibility of the structure combine to create critical speed problems and to make solutions difficult.

Disc Stress and Tip Speeds for Centrifugal Impellers

The pressure ratio attainable in a centrifugal compressor is directly related to the attainable tip speed. Near the beginning of the study it was noted that supercharging a centrifugal impeller with axial stages would raise inlet temperatures. It was recognized that the increased air temperature would reduce the corrected tip speed of an impeller operated at constant physical speed, and it was suspected that the rise in metal temperature would weaken the metal and reduce the allowable tip speed.

In order to determine maximum allowable impeller speeds for the configurations in this study, an initial investigation was made of the impeller stresses in the Boeing RF2 as reported in reference 10. Maximum stress values with variations in bore diameter, impeller rotating speed, and material were estimated. Figure 24 shows the Boeing impeller form in comparison with the proposed impellers. The initial study was made assuming that impellers in this investigation would be similar in shape to the RF-2 impeller. Therefore, stresses ratioed in the RF-2 impeller would be applicable to the study impeller. Figures 25 and 26 show the results of this study for two materials, Inconel 718 and Titanium Alloy 6Al-4V. The limiting bore stress was set as 1.2 times the 0.2-percent yield strength. The study resulted in limiting the rotor speed to 45,000 RPM for titanium and 42,500 RPM for Inconel 718, both with a bore radius of about 0.6 inch. Based on this study, an 1850-ft/sec limit was placed on centrifugal impeller tip speed.

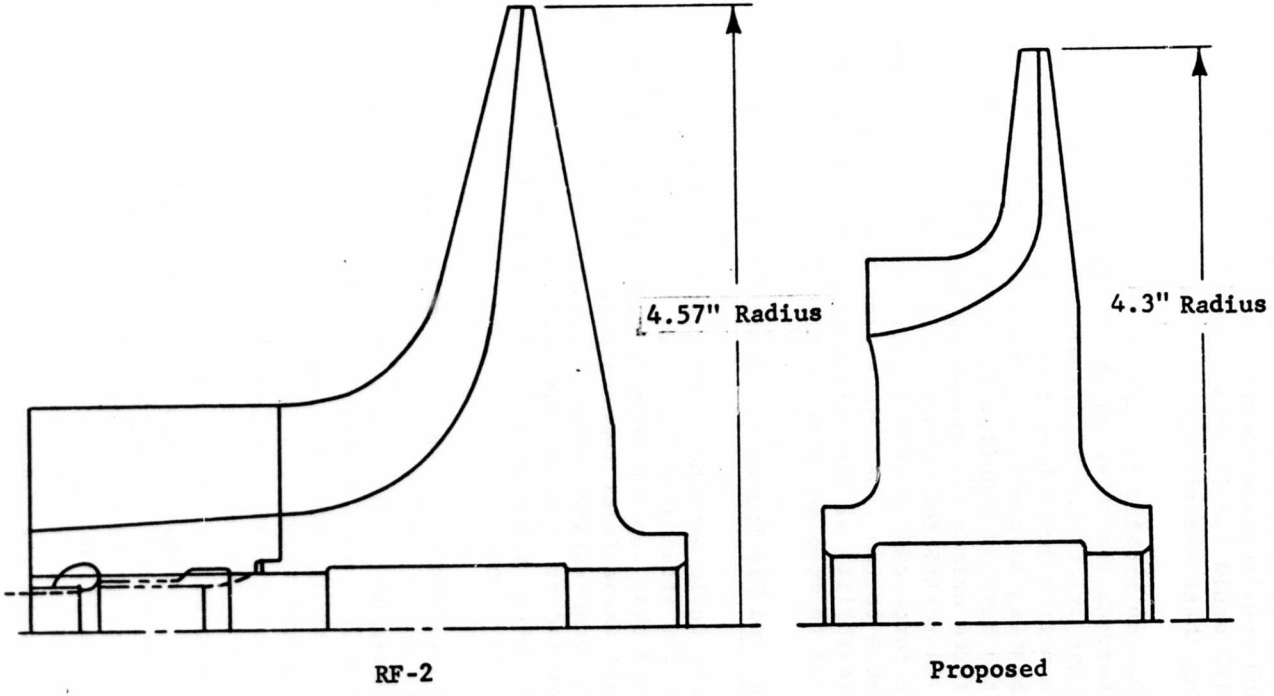

Figure 24. Comparison of Boeing RF-2 and Proposed Centrifugal Impeller Configurations.

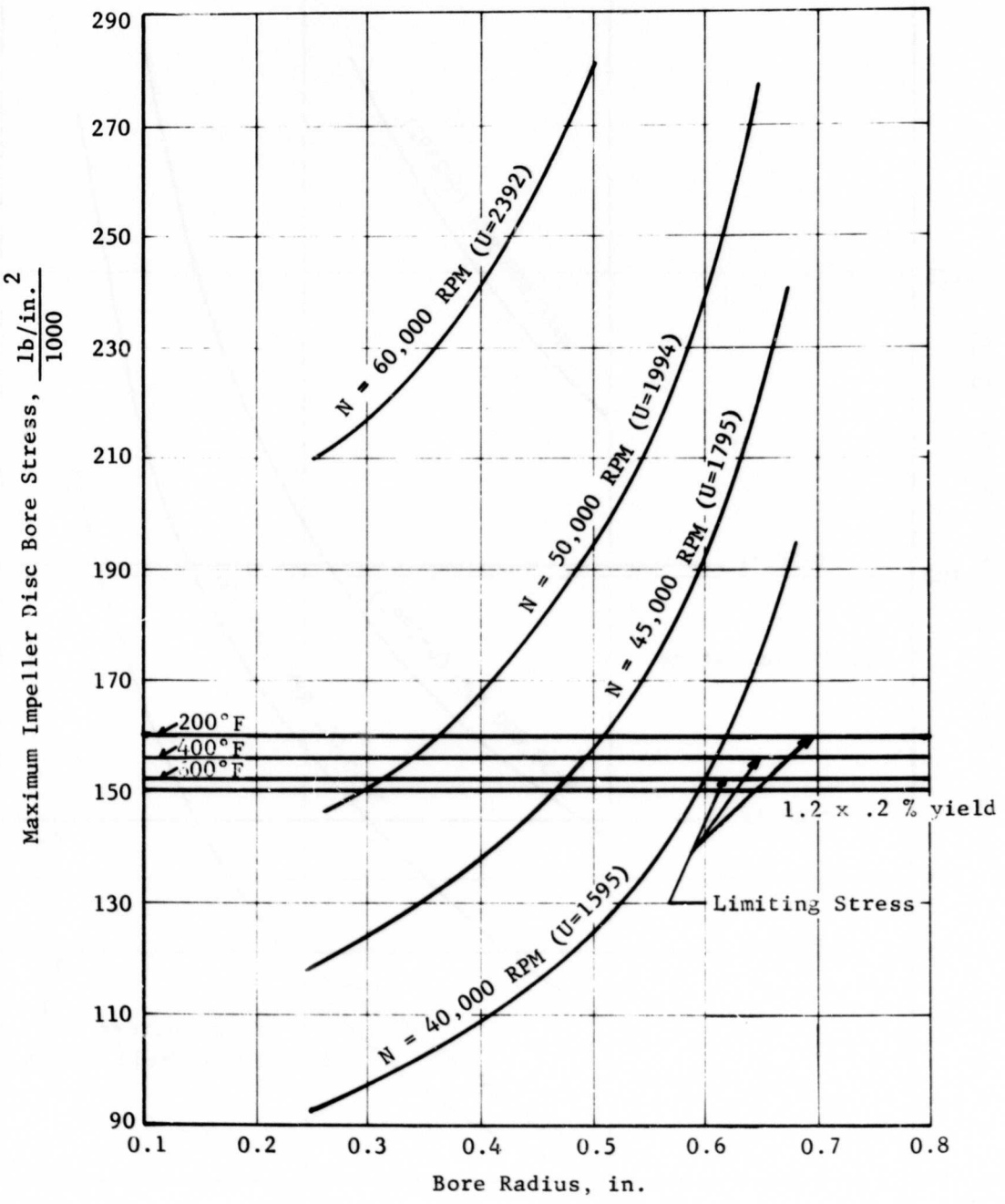

Figure 25. Centrifugal Compressor Disc Stresses Based on Scaling Boeing RF-2 Stresses, for Inconel 718 Material.

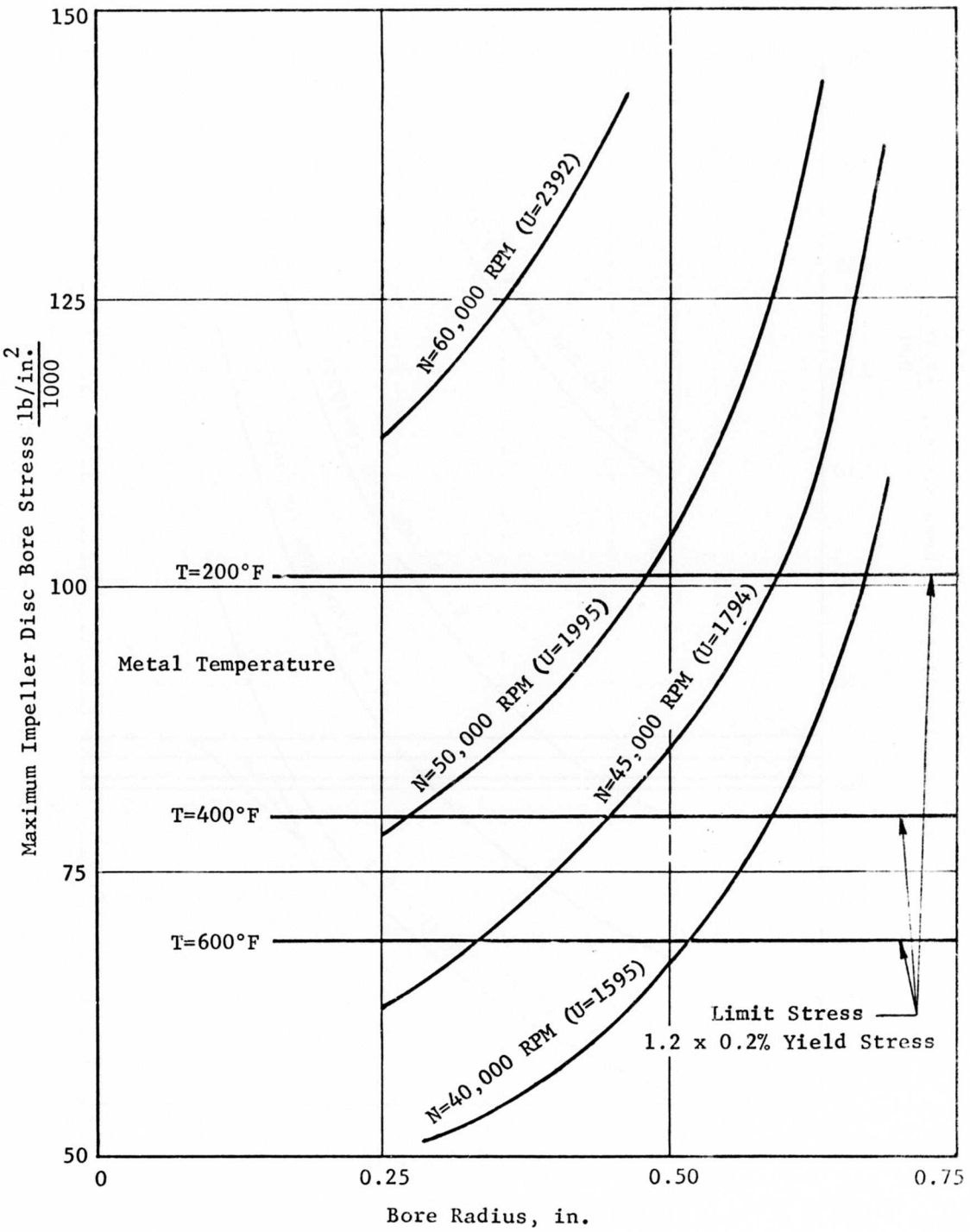

Figure 26. Centrifugal Compressor Disc Stresses Based on Scaling Boeing RF-2 Stresses, for Titanium 6AL-4V Material.

Later in the study, an internal review of the work caused these criteria to be questioned. It was then judged that this approach was conservative, for two reasons. First, the impeller shapes finally proposed for this investigation were markedly different from the Boeing impeller, as shown in Figure 24. The new configuration had more disc material and less dead weight in blade material. Second, bore stress was rejected as a primary criterion for design, because hub flare can usually be changed to reduce bore stress. A different set of criteria was required.

It has been established that the average tangential stress of a rotating disc can be used as a criterion for determining the burst speed, as shown in NACA TN 1667. Since the burst speed can be predicted quite accurately, it is common practice to design the disc or impeller to burst at some speed considerably higher than maximum operating speed. For this study, 130 percent of design speed was used as the burst speed. This results in a value of 1.69 for the ratio of the average tangential stress at burst to the average tangential stress at design. Of course, bore stress must be checked and should not exceed 120 percent of 0.2 percent yield stress.

With the above criteria, a preliminary stress analysis was made of the proposed impeller shown in Figure 24. The average tangential stress for the 4.3 tip radius centrifugal impeller was calculated at various speeds and with bore radii of 0.5, 0.75, and 1.0 inches using Titanium Alloy 7Al-4M and Inconel 718 materials, as shown in Figures 27 and 28.

The impeller tangential stress is somewhat proportional to bore diameter and speed. As the temperature increases, the allowable design stress is lowered. Therefore, all design studies incorporated the smallest bore practical which still allowed space for the required internal shafting. A maximum bore radius of 1 inch was judged to be practical.

As shown in Figure 27, the design speed for a titanium wheel with a 2 inch bore is 62,000 RPM, which results in a limiting design tip speed of 2330 ft/sec. Titanium Alloy 7Al-4M was chosen over Inconel 718 because of its higher strength-to-weight ratio, giving it an average operating tangential stress well below the design stress of 78,000 psi.

The above analysis was made without superimposing the effect of thermal stress. This is justifiable, because the thermal gradients tend to lower the rim stress and increase the bore stress, and it is assumed that the disc could be shaped so as to eliminate any effect of thermal stress on the average tangential stress.

The compressor designs described below in the section entitled Preliminary Design reflect the results of these two studies. The fixed geometry compressor has a centrifugal impeller tip speed of 1840 ft/sec, reflecting results of the first study, and the variable stator compressor has a tip speed of 2050 ft/sec, based on the second stress study.

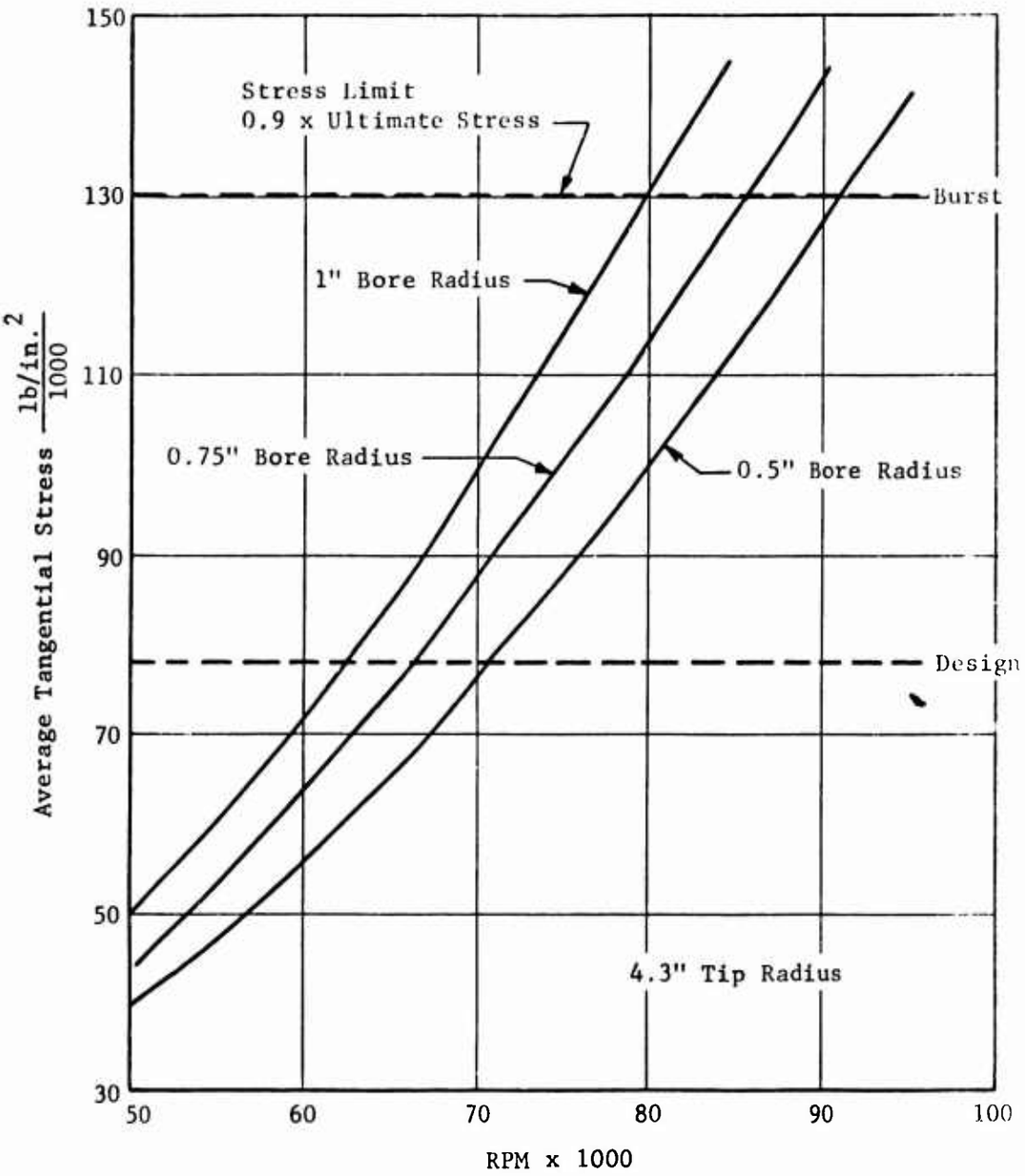

Figure 27. Centrifugal Compressor Disc Average Tangential Stresses in Proposed Disc Configuration for Titanium 7Al-4M Material at 600°F.

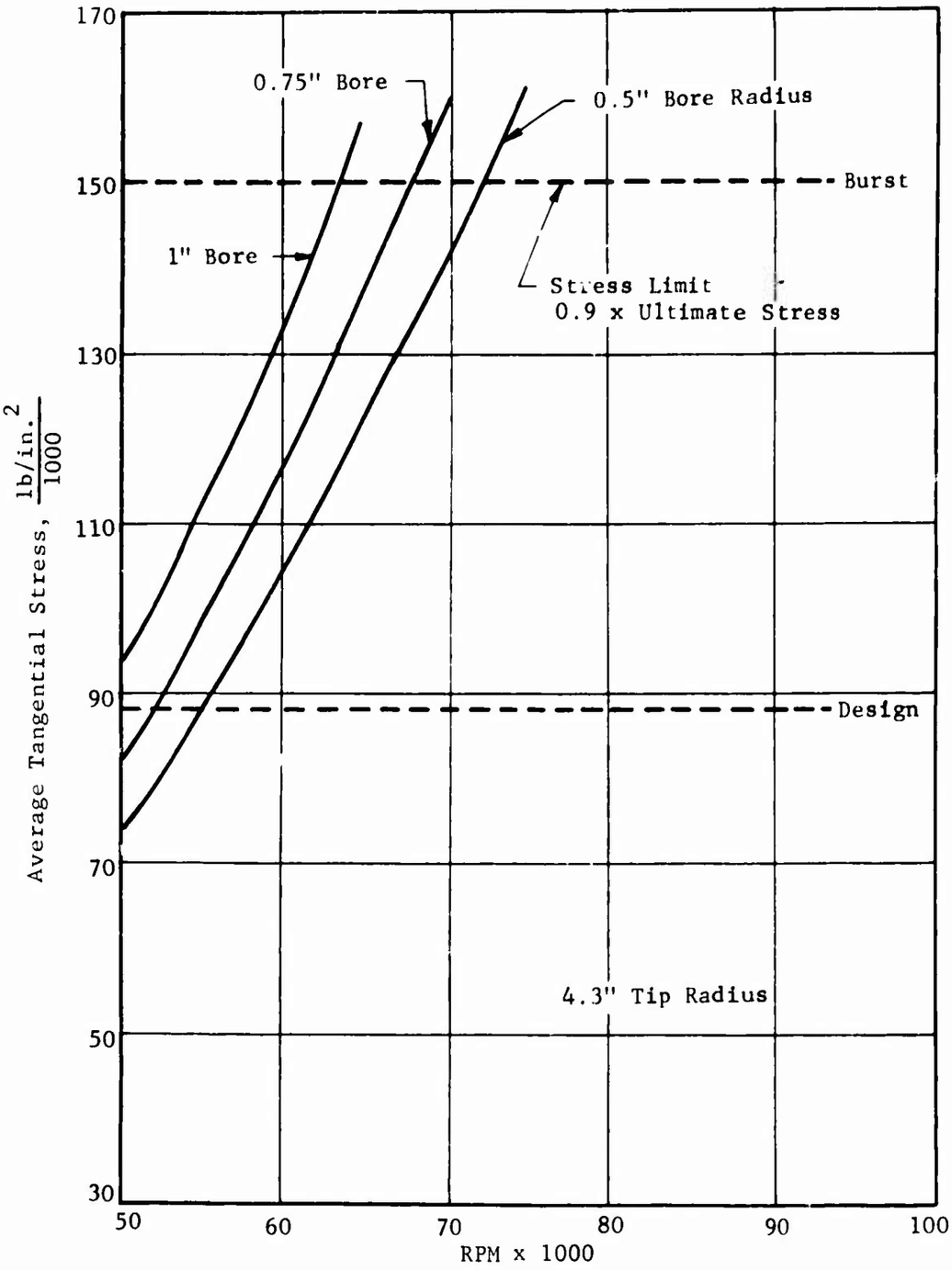

Figure 28. Centrifugal Compressor Disc Average Tangential Stresses in Proposed Disc Configuration for Inconel 718 Material at 600°F.

Centrifugal Compressor Flow Path

The design of a centrifugal compressor may be optimized as a unit alone, and this will lead to the highest possible efficiency for the type. The form that results may be associated with specific speed, as described in Reference 11. The shape of the ideal machine is similar to the Francis impeller, with an inducer hub to tip radius ratio less than 0.5 and an impeller tip to inducer tip radius ratio of about 2. This ideal form of the centrifugal compressor can be scaled for staging with axial boost stages, but there are factors that militate against simple scaling, namely, the connecting duct form and the disc and shafting requirements.

The connecting duct from the axial stage outlet to the centrifugal inlet is required to have a minimum length and a minimum curvature. The axial compressor hub radius quite strongly determines LP compressor work capability because it determines the minimum blade speed in the compressor. It is therefore typical of high stage pressure ratio axial compressors that the inlet hub/tip radius ratio is greater than 0.5 and that the hub radius has a rising slope through the compressor. Inasmuch as LP compressor pressure ratios approaching 3 are being considered, there is a marked reduction in annulus area and in annulus height through the compressor, producing an exit hub/tip radius ratio very likely to be above 0.7. Connecting such an axial stage to a centrifugal of 0.5 hub/tip radius ratio requires carrying the flow through an inward curve to a smaller diameter and through another curve to lead into the flow path of the centrifugal inducer. Increasing duct length reduces duct curvature. Greater duct length raises interpassage pressure losses and increases flow distortions; but increasing duct curvature also leads to flow distortions and increased pressure losses. Only if the radius change is avoided can the curvature be avoided and the length shortened, and this requires having a centrifugal inducer which is designed to receive flow directly from the axial compressor.

The disc of both the centrifugal and the axial compressors must be designed to pass a drive-shaft coaxially forward from the power turbine. The diameter of this shaft is made as great as possible to control shaft critical vibrations, yet small enough to pass through holes in the compressor disc. The permissible centrifugal tip speed decreases as supercharging raises the temperature and reduces metal strength. It also decreases as the central hole is enlarged to accommodate the drive-shaft. In opposition to these effects, raising the inducer rim diameter provides load carrying metal and shortens path length. The compressor shaft is shortened and stiffened, and the drive-shaft is shortened. Thus, the increase of centrifugal inducer radius contributes to raising tip speed and thus work capability, and helps to control shaft critical speeds.

There remain problems of the nonoptimum centrifugal compressor aerodynamic form. The essential change in the compressor problem is that the inducer now has a narrower radial dimension and a higher inlet Mach number, with a smaller radius ratio for radial flow. Though the problems are serious, the designer has recourse to axial compressor research for handling the high Mach numbers. He can raise the number of blades where necessary to keep blade loadings in the same proportion as in the optimum machine, and he will escape some problems of the compressor with long radial passage length, namely, that separation in radial flow passages should be more easily avoided, and that shroud/vane clearances should give less difficulty. It is judged that this type of centrifugal compressor is most appropriate for an axial-centrifugal machine; therefore, it has been selected for the designs of this program.

Compressor Characteristics

The essential program goal is to identify and describe a compressor design that will yield the best engine performance attainable at 60 percent power, within the limits of a three-year development program. Performance at 30 percent power is also important, but 100 percent power performance can be sacrificed for the sake of improving 60 percent power performance. Cycle performance data show that high pressure ratio, high efficiency, and high turbine inlet temperature all favor these goals.

Maximum efficiency for a compressor at the 60 percent power point is theoretically obtainable through design optimization. That is, every blade row is correctly designed for the 60 percent power point. The number of stages is minimum. The inlet Mach number levels, on the average, yield high stage work, yet good lift/drag ratios. Each blade is set at exactly the correct incidence angle for minimum loss, each blade is shaped exactly for the work to be done, and the number of blades in each row is the best for maximum efficiency. In theory, this will give the optimum efficiency for the 60 percent power point; correct stage types, number of stages, and blade speeds will provide the desired pressure ratio at the 60 percent power design point.

As a compressor operating point is moved away from the design point, its efficiency tends to change. As the operating condition moves to lower speeds and lower Mach number, both the loss coefficients and the sensitivity to incidence effects decrease at the same time that incidences (absolute values) increase, and efficiency may hold level or even rise. Going to higher speeds increases all these effects together and efficiency decreases. The effects of losses with the changes of work determine changes of flow and pressure ratio as well as efficiency, and all go together to define the compressor performance map and hence the cycle performance.

A question that must be asked, then, is whether an optimum 60-percent power design point can in fact be used in an engine at 60 percent power.

It is necessary to determine the compressor off-design performance and to investigate cycle performance, so as to identify the speed of the 60 percent power point and to determine whether operations at 30 percent and 100 percent power will allow us to take advantage of an optimum 60 percent power performance.

The compressor performance maps were defined both by a mean-line mapping procedure and by stage matching procedures. The compressor stage matching procedures are described in detail in Appendix I. The maps were then matched to engines in a manner which provided minimum brake specific fuel consumption at 60 percent and 30 percent power. The procedures for preliminary engine matching are described in Appendix II. As a result of the compressor and engine matching work, clear trends were developed about the best compressor matching relations for minimum part-power fuel consumption. To verify these trends and to review the underlying principles, a study was made of the optimum location on the compressor map of the compressor peak efficiency point.

Compressor Mean-Line Mapping Program

An approach to the design of a compressor at the 60 percent power point was made using the Curtiss-Wright mean-line mapping program. Each of three designs incorporated a supersonic axial stage, a transonic axial stage, and a centrifugal stage. This family of compressors shared equal values of the ratio of temperature rise to the square of tip speed and equal values of the ratios of axial velocity to blade speed. The first of the series was designed for perfect matching at a 1700-ft/sec centrifugal tip speed, and it had a pressure ratio above 17 as shown in Figure 29. The second was designed for 1530 ft/sec tip speed, and the third for 1360 ft/sec. Performance maps for these designs are shown in Figures 30 and 31. Each of these designs was to be a compressor capable of operating to a maximum tip speed of 1700 ft/sec. The operating point for 60 percent power was expected to lie at some tip speed between 80 percent and 100 percent of 1700 ft/sec; it was expected that a 60 percent power point speed and a design point speed could coincide, though not necessarily at one of the selected speeds; and it was expected that the three-point curve developed from the study would define the design speed at which 60 percent power would be obtained. None of these expectations was found to be valid.

The performance maps in Figures 29 to 31 show some results of the engine cycle matching procedure. These appear as points indicating engine operation conditions for 100 percent power, 60 percent power, and 30 percent power. The temperature of 2500°F was established as a limiting temperature for 100 percent power. The temperatures of 1900°F for 30 percent power and 2200°F for 60 percent power are estimated values for these power ratings, the actual values being influenced by power turbine area. Subsequently in the program it was proved that the use of these temperatures gave adequate

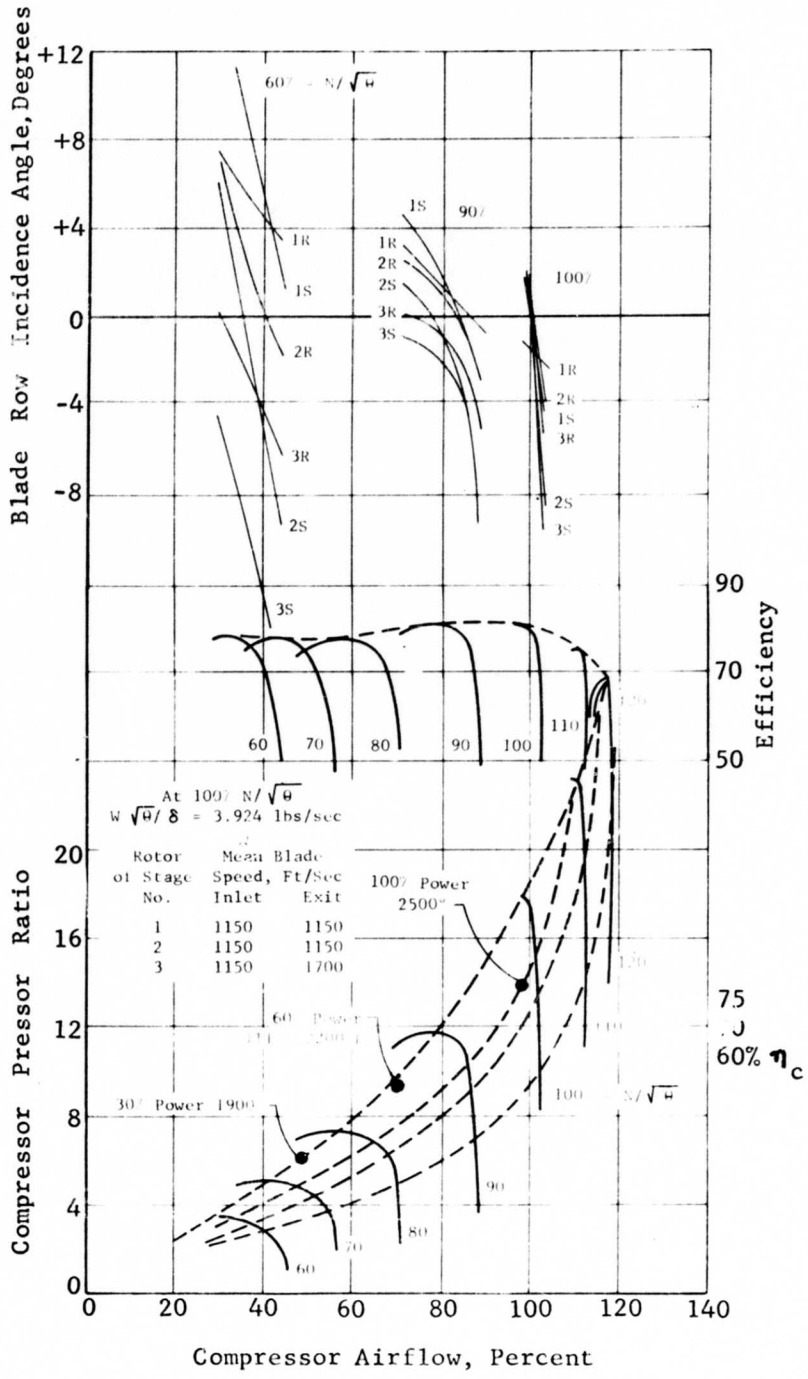

Figure 29. Compressor/Engine Matching Map Mean-Line Mapping Case 1B, U_t = 1700 ft/sec.

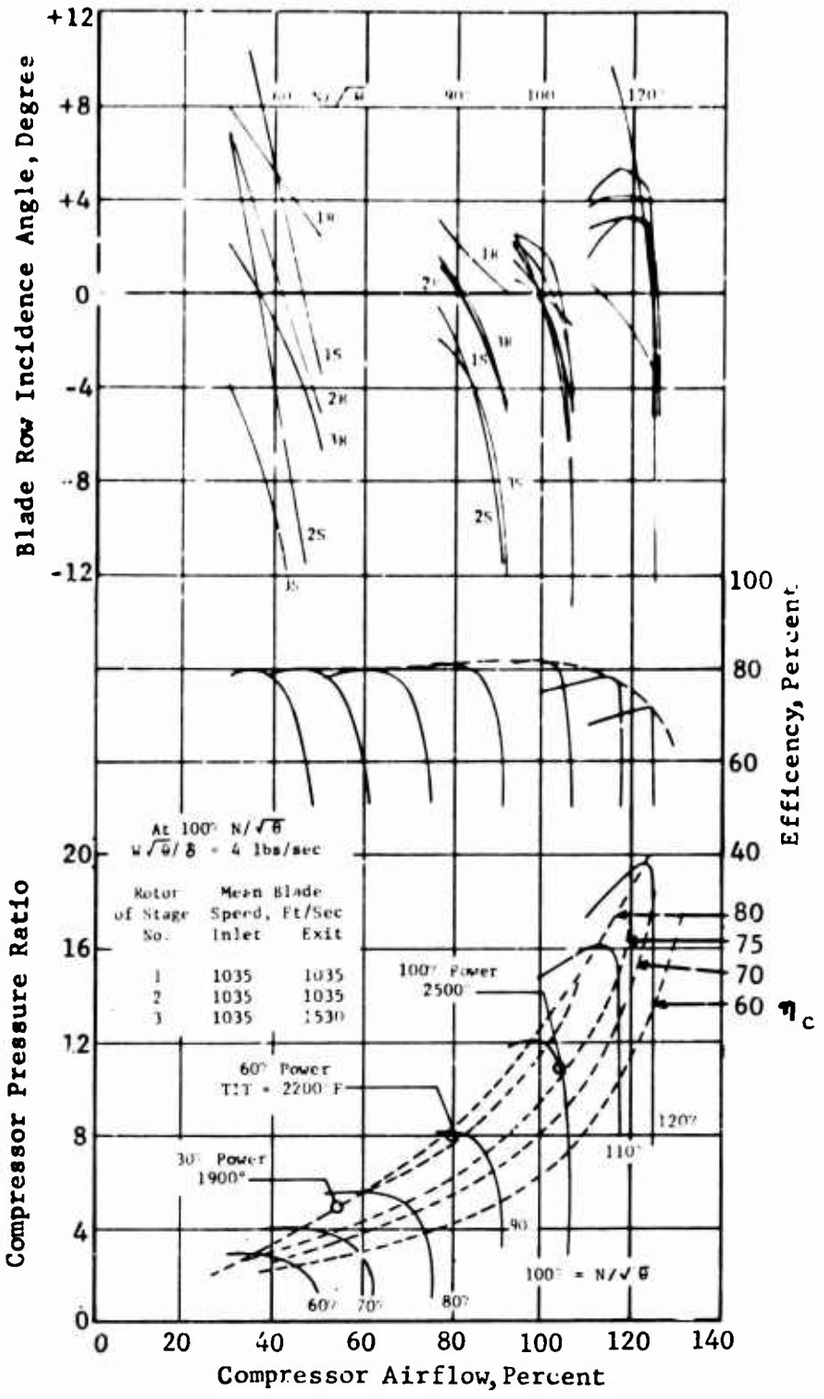

Figure 30. Compressor/Engine Matching Map Mean-Line Mapping Case 2A, U_t = 1530 ft/sec.

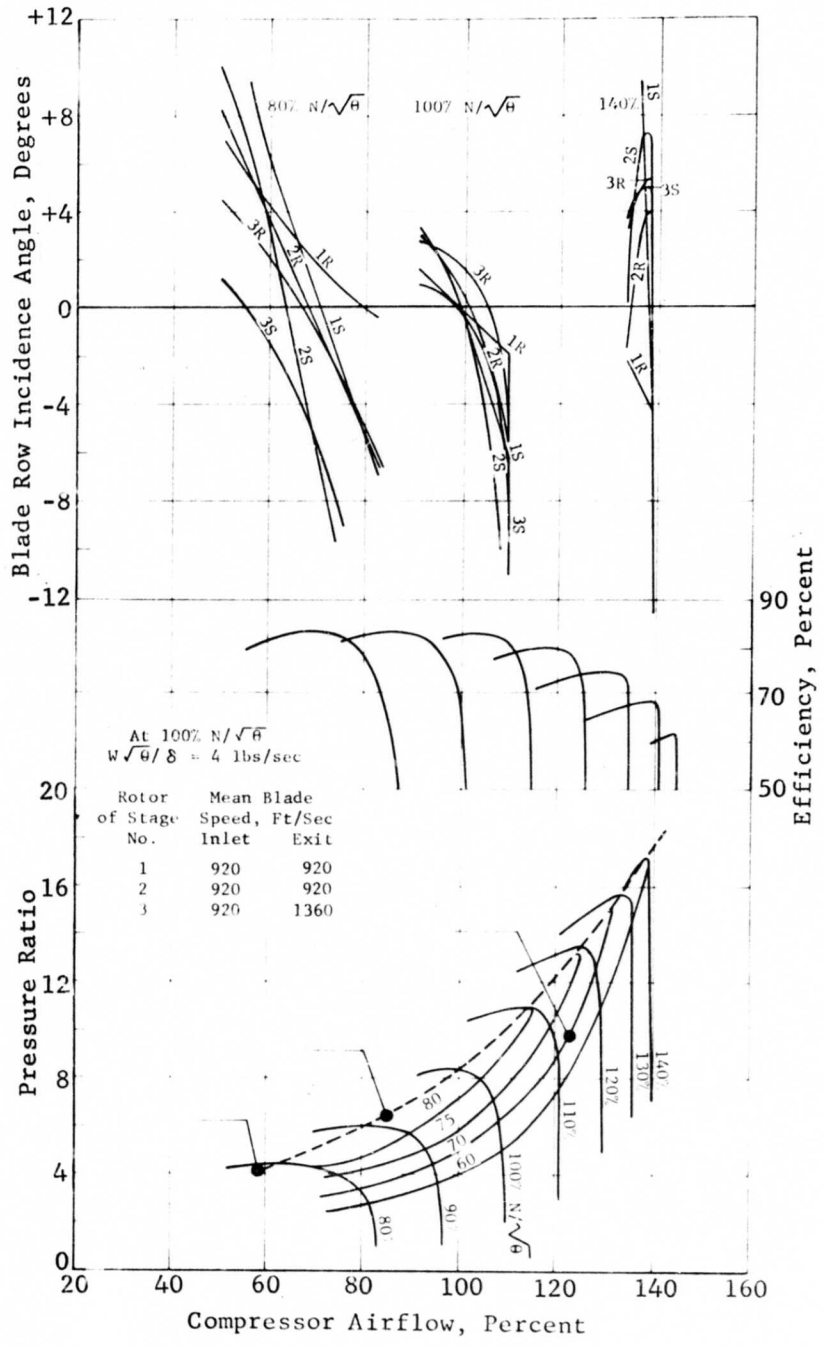

Figure 31. Compressor/Engine Matching Map Mean-Line Mapping Case 3A, U_t = 1360 ft/sec.

TABLE I. SUMMARY OF PRELIMINARY CYCLE PERFORMANCE

		60% Power					30% Power		100% Power								
Case No.	Cycle Match No.	SFC	TIT °F	P/P	Compressor Efficiency	LP % N_D	SFC	LP % N_D	SHP/Wa	SFC	LP % N_D	U_t Centr	Stall-60% Power*	No. of Spools	Match % Speed LP/HP	LP	HP
2,1	1	.505	2200	7.4	79.5	82	.62	73	231	.458	93	1742	Y	1	90/87	S	PW-G
	2	.495	2100	8.1	79	85	.607	73	232	.45	94.5	1771	M	1	90/87	S	PW-G
2,2	1	.48	2100	9	78	88	.61	74	236	.41	96	1799	Y	1	95/90	S	PW-G
	2	.47	2200	8.7	77	87	.61	74	236	.41	96	1799	Y	1	95/90	S	PW-G
2,3	1	.449	2100	11.4	78.5	87	.54	74	237	.405	95	2000	Y	1	95/101	S	PW-G
	2	.455	2200	11.0	78	86	.54	74	237	.405	95	2000	Y	1	95/101	S	PW-G
3	1	.475	2100	10.3	77	84	.54	58	232	.42	100	1890		2	100/95	S	PW-G
	2	.465	2200	9.45	79.5	70	.54	58	232	.42	100	1890		2	100/95	S	PW-G
4,1	1	.46	2100	8.8	81.3	82	.59	70	242	.427	90	1840	N	1	83/88	TT	PW-G
	2	.475	2200	8.65	80.3	82	.59	70	242	.427	90	1840	Y	1	83/88	TT	PW-G
4,1-AAA	1	.475	2100	8.2	82	89	.61	70	235	.435	90	1840	N	1	83/88	TT	PW-G
	2	.485	2200	8	81	88	.61	70	235	.435	90	1840	M	1	83/88	TT	PW-G
4,1-VS	1	.428	2100	12.2	80	90	.52	76	227	.407	100	2030		1	83/88	TT	PW-G
	2	.435	2200	11.5	80	89	.52	76	227	.407	100	2030		1	83/88	TT	PW-G
4,2	1	.455	2100	9.2	81.5	86	.59	78	243	.42	95	1776	Y	1	92/84	TT	PW-G
	2	.465	2200	8.8	81	84.5	.59	78	243	.42	95	1776	Y	1	92/84	TT	PW-G
4,3	1	.455	2100	11.95	77	92.5	.53	80	240	.40	100	1950	N	1	95/92	TT	PW-G
	2	.45	2200	11.8	76.5	91.5	.53	80	240	.40	100	1950	Y	1	95/92	TT	PW-G
4,4-VS	1	.424	2100	14.6	80	89	.49	75	242	.38	95	2050		1	95/105	TT	PW-G
	2	.419	2200	13.5	80	87	.49	75	242	.38	95	2050		1	95/105	TT	
5,1	1	.632	2200	4.5	78	74	.82	62	187	.57	95	1651	N	1	80/85	S	405
5,2	1	.555	2200	5.8	78.5	82	.72	70	210	.51	96	1656	Y	1	90/92	S	405
7,1	1	.58	2100	5.46	80	73	.63	69	203	.54	89	1598	N	1	82/86	ST	405
	2	.578	2200	5.25	80	76	.63	62	203	.54	89	1598	N	1	82/86	ST	405

5,1	1	.632	2200	4.5	78	74	.62	62	187	.57	95	1651	N	1	80/85	S	405
5,2	1	.555	2200	5.8	78.5	82	.72	70	210	.51	96	1656	Y	1	90/92	S	405
7,1	1	.58	2100	5.46	80	73	.63	69	203	.54	89	1598	N	1	82/86	ST	405
	2	.578	2200	5.25	80	76	.63	62	203	.54	89	1598	N	1	82/86	ST	405
7,2	1	.545	2200	6.1	78	81	.67	70	207	.47	95	1725	Y	1	90/92	ST	405
	2	.527	2100	6.87	78.3	82	.66	70	207	.49	95	1725	Y	1	90/92	ST	405
8	1	.5	2200	7.55	79.5	77	.62	65	214	.462	97	1823		2	100/100	ST	405
9,1	1	.542	2200	6.02	80.2	82	.69	70	220	.48	96	1592	Y	1	85/82	TT	405
9,2	1	.505	2100	7.8	80.5	87	.62	76	228	.44	100	1660	Y	1	93/89	TT	405
	2	.51	2200	7.0	80	87	.4	74	228	.45	100	1660	Y	1	93/89	TT	405
10	1	.485	2200	8.4	79	73	.59	64	234	.43	100	1773		2	100/100	TT	405
11,1	1	.425	2100	13.4	81	81	.49	60	238	.395	100	2130		2	100/105	TT	PW-G
	2	.425	2200	12.4	81	76	.48	60	238	.395	100	2130		2	100/105	TT	PW-G
11,2	1	.455	2100	9.3	82	80	.553	63	226	.423	100	1790		2	100/88	TT	PW-G
	2	.458	2200	8.8	82	76	.553	63	226	.423	100	1790		2	100/88	TT	PW-G
11,3	1	.417	2100	11.3	82	76	.514	60	235	.407	100	2000		2	100/99	TT	PW-G
	2	.419	2200	10.6	82	80	.514	60	235	.407	100	2000		2	100/99	TT	PW-G
12	1	.485	2200	8.58	78.2	92	.6	79	235	.43	101	2100	N	1			RF-2
13,1	1	.463	2100	9.9	785	85	.57	74	226	.46	98	1860	Y	1	91/84	ST	PW-G
	2	.48	2200	9	77	83	.56	74	220	.44	96	1822	Y	1	91/84	ST	PW-G
13,2	1	.47	2100	12.1	75	94	.56	81	228	.41	100	1899	Y	1	100/90	ST	PW-G
	2	.468	2200	11.3	77	91	.56	81	228	.41	100	1899	Y	1	100/90	ST	PW-G
13,3	1	.446	2100	12.85	77.5	88	.53	76	231	.402	96	1870	Y	1	95/88	ST	PW-G
	2	.448	2200	12.1	76.5	87	.535	76	231	.402	96	1870	Y	1	95/88	ST	PW-G
14	1	.45	2100	11.85	78	82	.54	66	228	.41	100	1890	N	2	100/90	ST	PW-G
	2	.45	2200	11	79	77	.54	66	228	.41	100	1890	M	2	100/90	ST	PW-G
D1B		.465	2200	9.6	79	86	.56	75	225	.43	98.5	1675		1	100	ST	CENT
D2A		.49	2200	7.7	80.6	80	.61	68	227	.45	92	1565		1	90	ST	CENT
D3A		.515	2200	6.4	83	75	.64	62	220	.47	90	1535		1	80	ST	CENT

* Axial Stage Stall Condition at 60% Power is; Y-yes, in Stall; N-not in Stall; M in Margin of Stall

BLANK PAGE

indications of engine performance. The engine matches represent minimum attainable specific fuel consumption for 60 percent and 30 percent power, as described in Appendix II.

Other results are summarized in Table I. The design speeds and speeds at various power fractions are compared below.

	Case D1B		Case D2A		Case D3A	
	U_t	Percent	U_t	Percent	U_t	Percent
Design	1700	100	1530	100	1360	100
100 Percent Power	1675	98.5	1565	102	1535	113
60 Percent Power	1460	86	1360	89	1270	93.5
30 Percent Power	1275	75	1156	75.5	1045	77

In no case is it optimum to operate the engine at 60 percent power at the intended design point. The design point is most nearly attained for case D3A. But this case also missed most widely the goal of operating the compressor at 1700 ft/sec for 100 percent power. The cycle performance results are summarized below.

	Case D1B	Case D2A	Case D3A
60 Percent Power, 2200°F TIT			
SFC	.465	.49	.515
SHP/Wa	190	187	184
P/P	9.6	7.7	6.4
Compressor efficiency	79	80.6	83
30 Percent Power, 1900°F TIT			
SFC	.56	.61	.64
Design U_t for centrifugal, ft/sec	1700	1530	1360

The best cycle performance for 60 percent power, and for the other powers, occurs for case D1B, because it has the highest pressure ratio. The pressure ratio limitation of the other cases is not structural. It is, simply, that they are matched so that at all the higher tip speeds too much energy is wasted in compressor losses, resulting in reduced efficiency, reduced pressure ratio, and reduced power output for the cycle. Efficiency at the 60 percent power point is indeed better for cases D2A and D3A, but this advantage is overbalanced by the pressure ratio limitation. Evidently it has not been satisfactory to approach the design simply as a design for the 60 percent power point.

Stage Matching

The use of real compressor data allows an examination of matching effects that goes beyond the mean line mapping program investigations.

The mapping program thus far has used a three-stage compressor perfectly matched for a single point. A question can be raised as to the possible benefits of compromising the matching to some extent so that the machine has a larger region where it is relatively well matched, at some sacrifice of performance at the formerly best-matched point.

The map of a developed one-stage or two-stage compressor may be assumed to represent a good state of matching of its components. In general, if matching is a strong factor in compressor performance, the compressor map will show an island of maximum efficiency in the important range of operation. If such an island does not appear in a well developed machine, then effects such as Mach number are overriding. In such cases, lines of maximum efficiency are defined. An island is least likely to appear in low-pressure-ratio machines and in machines with few blade rows. When elements are combined to make a multistage machine with a high-pressure-ratio, matching effects become more important, and these effects have been investigated in this program by combining stage performances to determine overall performance.

The efficiency islands on a stage map may center about a point where the stage is best matched, and from the viewpoint of the matching investigation one may superimpose the maps of two compressors in various ways. Perfect matching at a point results from superimposing the centers of efficiency islands, or the lines of maximum efficiency for two machines. Any other matching implies compromises in maximum efficiency which both broaden the range where efficiency is high and decrease the value of maximum efficiency. The investigations here have focused attention on the intersections of stall lines, and have been restricted by consideration if tip-speed limits. Nevertheless, the matching of efficiency contours, as well as of pressure ratio capabilities, is implicit in every matching case; and the efficiency matches are primary factors in the resulting compressor and engine performance.

The matching procedure used data from five experimental compressors and one hypothetical compressor for which estimated performance is used, as follows:

Type	Model	Max. P/P	Note
Axial	2.8 SS (S)	2.8*	Reference 8
	Transonic (TT)	3.3*	Reference 12
	2.8 SS + Trans (ST)	3.7 & 4.4	Trans. is estimated perf. single stage
Centrifugal	405	3.5**	Curtiss-Wright centrifugal with vaneless space
	PW-G	6.3	Reference 11
	RF-2	12*	Reference 10

The efficiency values for the compressors were incremented by a constant value for each speed line, as follows:

Compressor:	2.8 Supersonic Build 12									
Speed, %	101	100	98	95	90	85	80	70	60	50
Effy. Change	6	6	6	6	5	4	3	3	3	3

Compressor:	2 Stage Transonic (USAAVLABS)							
Speed, %	105	100	95	90	80	70	60	50
Effy. Change	2.5	2.5	2.5	2.5	2.5	2.5	2.5	2.5

Compressor:	Boeing RF-2					
Speed, %	102	100	96.4	86.8	77.2	67.4
Effy. Change	6	6	6	6	6	6

Compressor:	405 Centrifugal						
Speed, %	100	94.6	89.6	84.3	73.8	63.1	52.6
Effy. Change	-3.0	-3.5	-4.0	-4.5	-5.0	-5.5	-6.0

The efficiency change was converted to pressure ratio change by holding actual enthalpy rise constant while changing the ideal (pressure-ratio) enthalpy rise. A change of losses is thus implied. The calculation procedure is given in Appendix III in a FORTRAN procedure called FIXER.

Two other stages were used without correcting efficiencies, the PW-G rotor centrifugal stage and a single transonic stage. The centrifugal stage performance was close to the attainable levels as given. The transonic stage was a theoretical stage with predicted performance at

* Efficiency and pressure ratio raised commensurately, to agree with attainable values.

** Efficiency and pressure ratio lowered commensurately, to account for added diffuser losses.

attainable levels. The 405 centrifugal stage had its efficiency decreased to allow additional losses for a diffuser, for which test data were not available.

The modified compressor performance characteristics are given in Figures 32 through 37.

Matching of the compressors is presented in two formats, one showing the LP/HP compressor matching and the other showing the compressor/engine matching. For selected cases, the LP/HP compressor matching curves are given in Figures 38 through 47. These curves present the interface (LP exit, HP inlet) corrected speed and flow range relations between the two compressors being matched. The compressor/engine matching curves for selected cases are given in Figures 48 through 59. These curves present the compressor performance maps with the engine operating points for 30 percent, 60 percent, and 100 percent power from which part-power minimum specific fuel consumption is obtained.

The staging or matching of two existing compressors generally involves scaling at least one of the machines. True scaling permits, in general, only one practical match point on the HP map for a selected LP operating point, and this match may be far from a desirable one. In true scaling, dynamic and geometric similarity with the prototype are preserved in the scaled machine. In that case, hub-corrected blade speeds for axials and tip-corrected blade speeds for centrifugals are the same in prototypes and derivatives at equivalent performance conditions. In the present matching studies, "free" scaling has been done, preserving these corrected blade speeds and ignoring other requirements for true scaling. This approach is justified in that work capability was provided, leaving design changes and development refinements to subsequent effort. Scaling factors are treated in more detail in Appendix I.

The type of matching synthesis performed involves combining the performance maps of two machines or stages to define the performance of the combination. For two stages to be matched, mass flow continuity must be satisfied and the shafts must rotate, if it is a one-spool machine, at the same speed. Continuity requires that the exit corrected mass flow of the first compressor shall equal the sum of the second compressor inlet corrected mass flow plus the bleed flow. The constant shaft speed requires that the exit-corrected shaft speed for the first compressor shall equal the inlet-corrected shaft speed of the second compressor. Corrected flow is $W\sqrt{\theta}/\delta$ and corrected speed is $N/\sqrt{\theta}$.

For discussion, consider Figure 38, a fixed-stator, single-spool match of the supersonic stage with the PW-G centrifugal stage, case

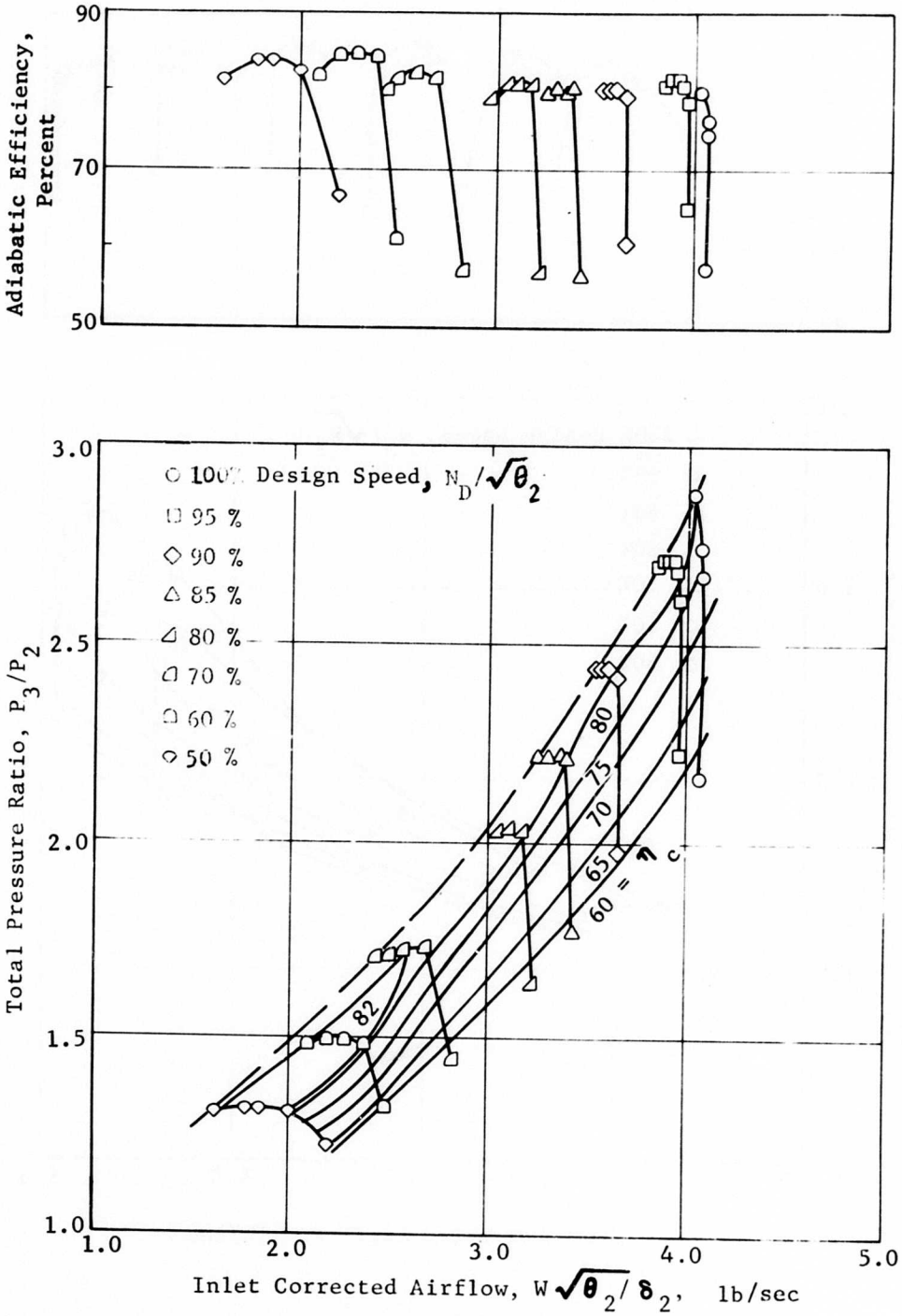

Figure 32. Compressor Test Performance, Modified, 2.8 Supersonic Compressor (F1).

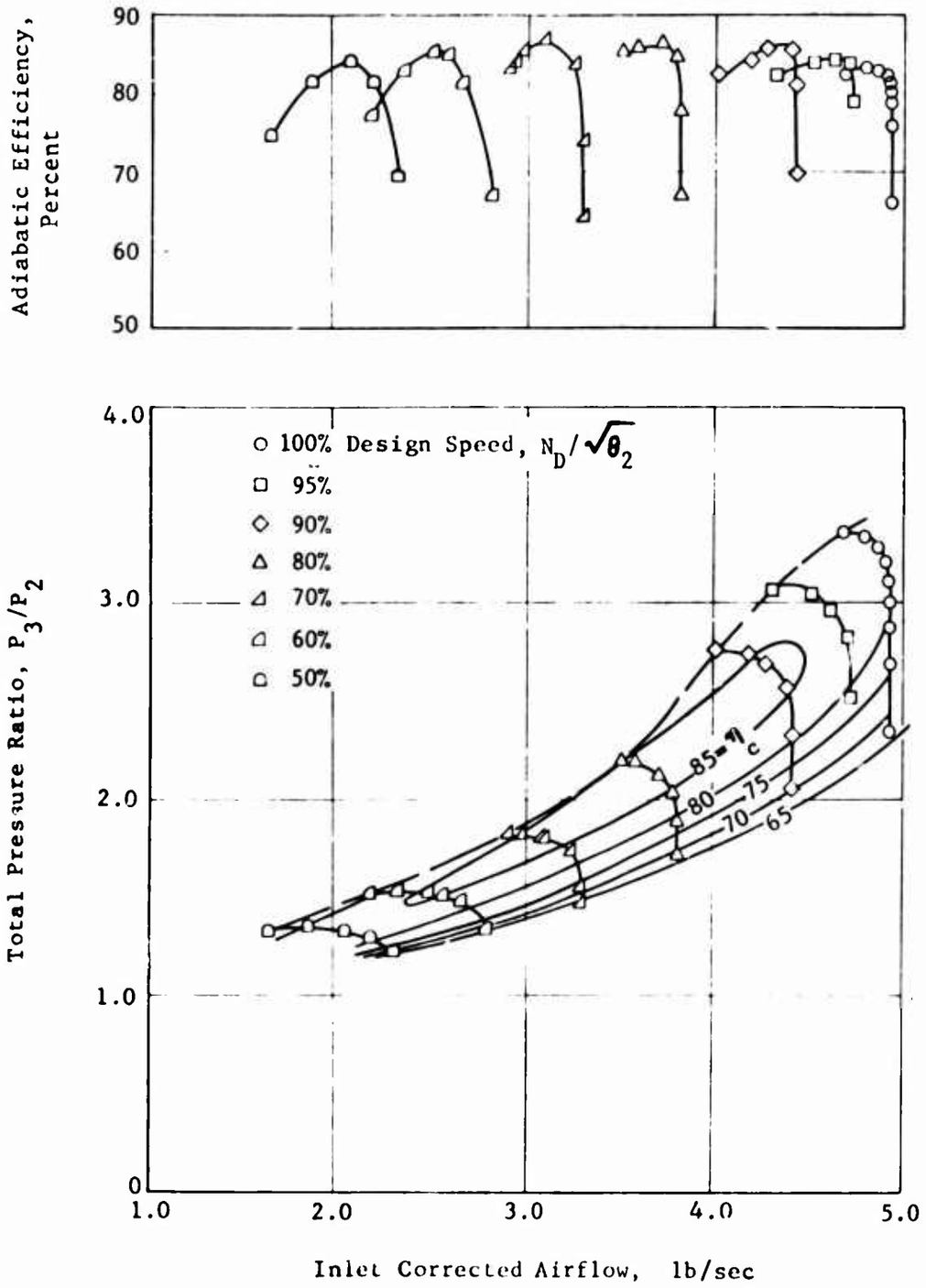

Figure 33. Compressor Test Performance, Modified Two-Stage Transonic Compressor (F1).

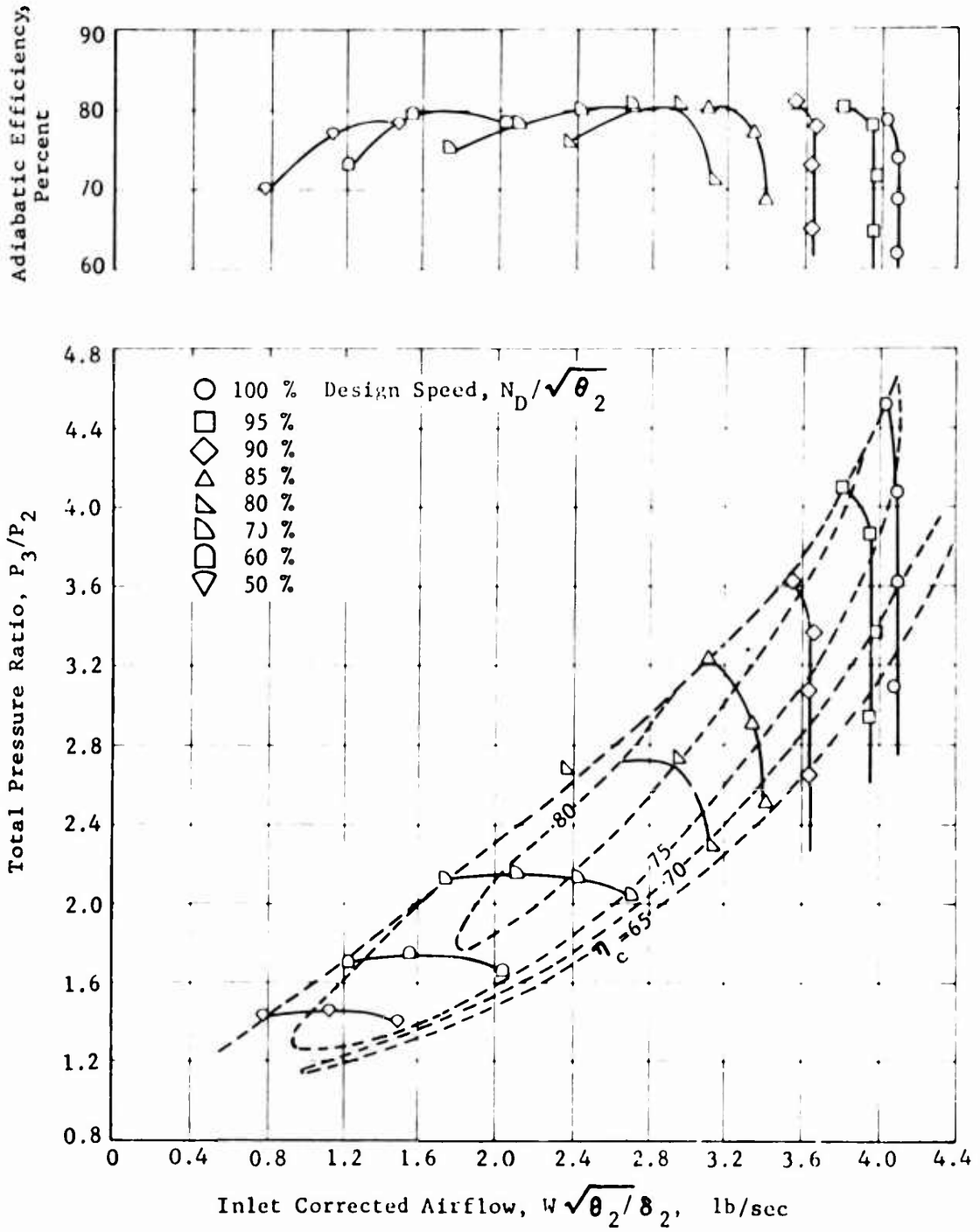

Figure 34. Compressor Base Performance, 2.8 Supersonic (F1) Plus Hypothetical Transonic Stage.

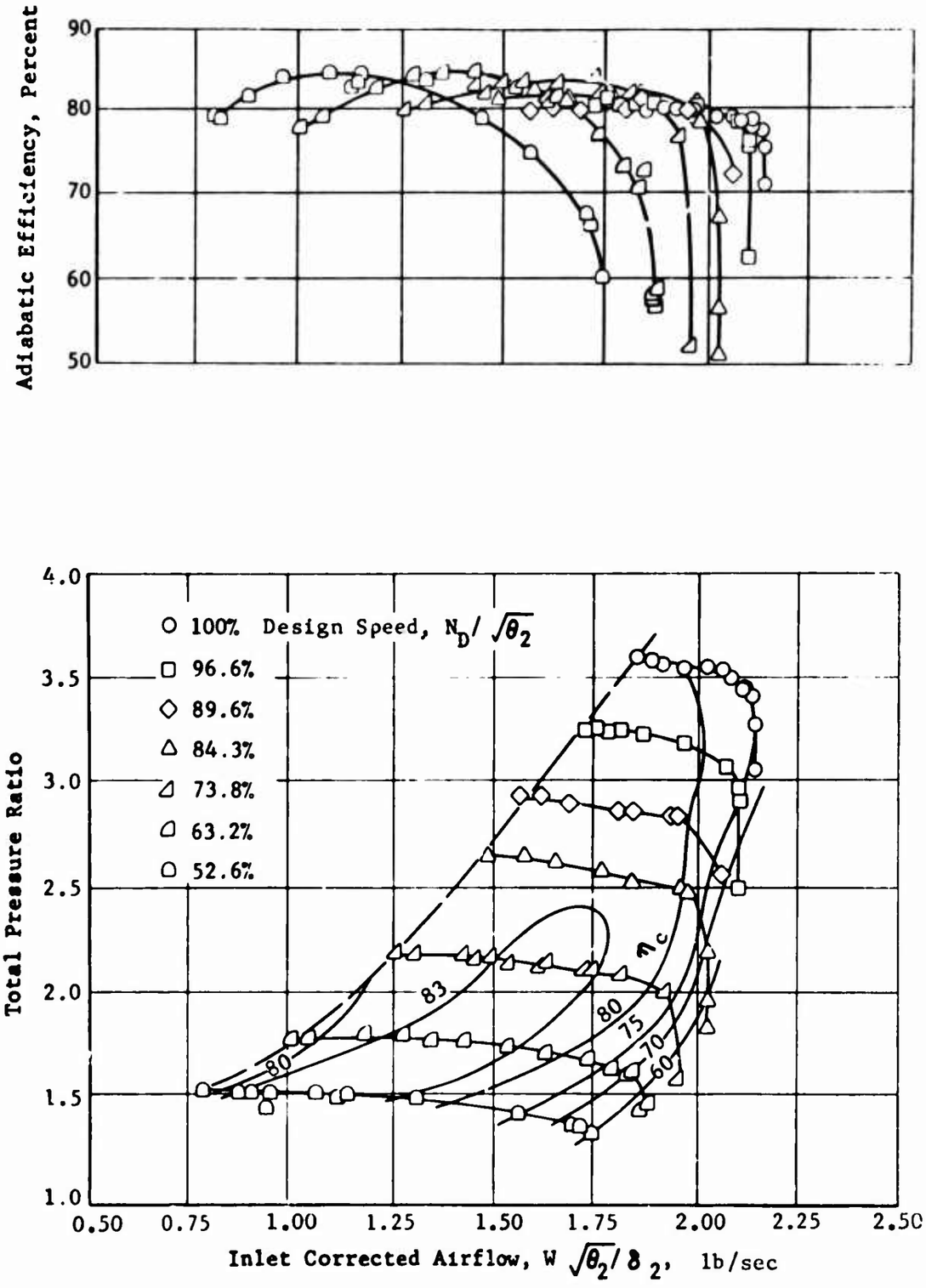

Figure 35. Compressor Test Performance, Modified,405 Centrifugal Compressor (F1).

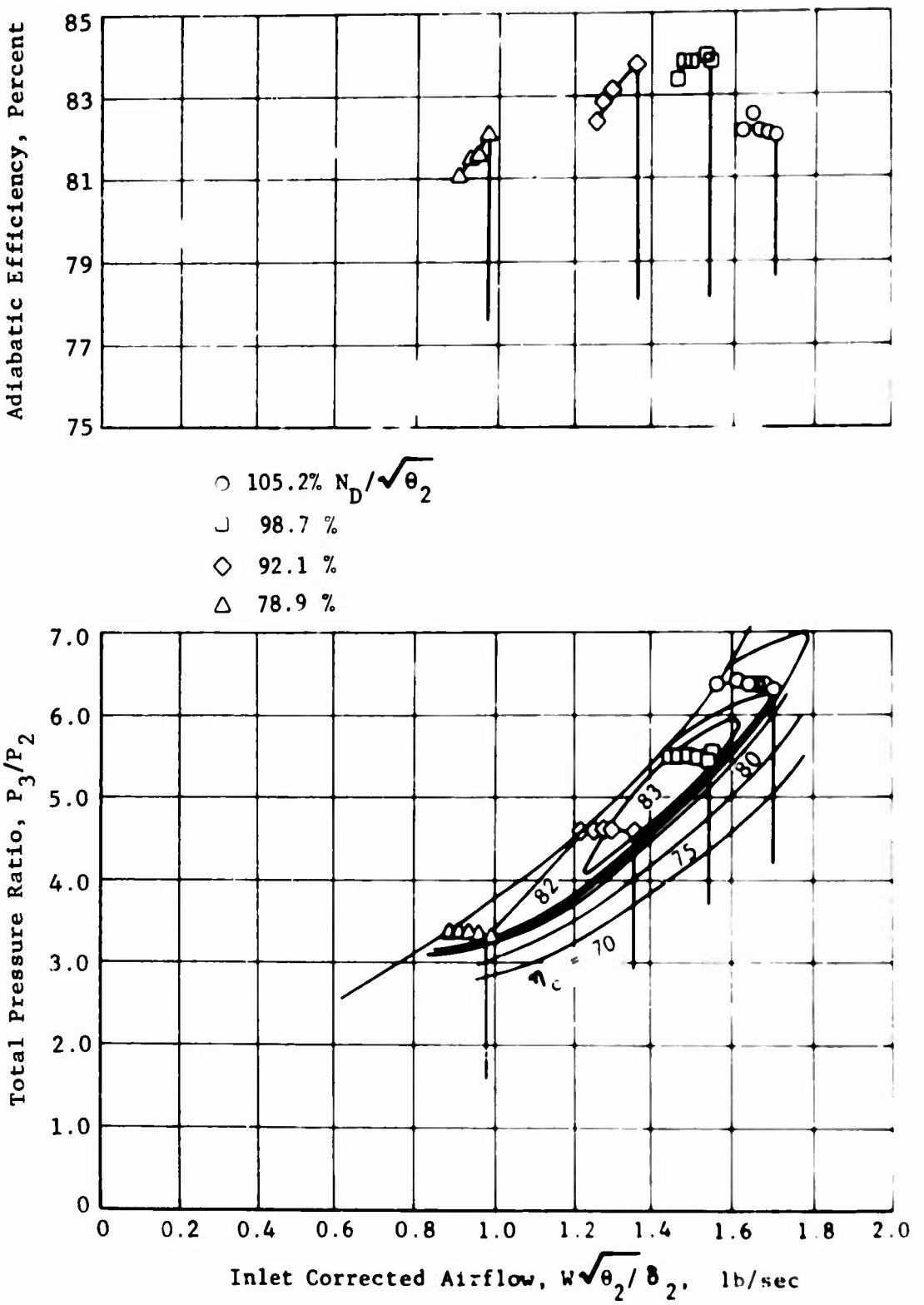

Figure 36. Compressor Test Performance, PW-G Centrifugal Compressor

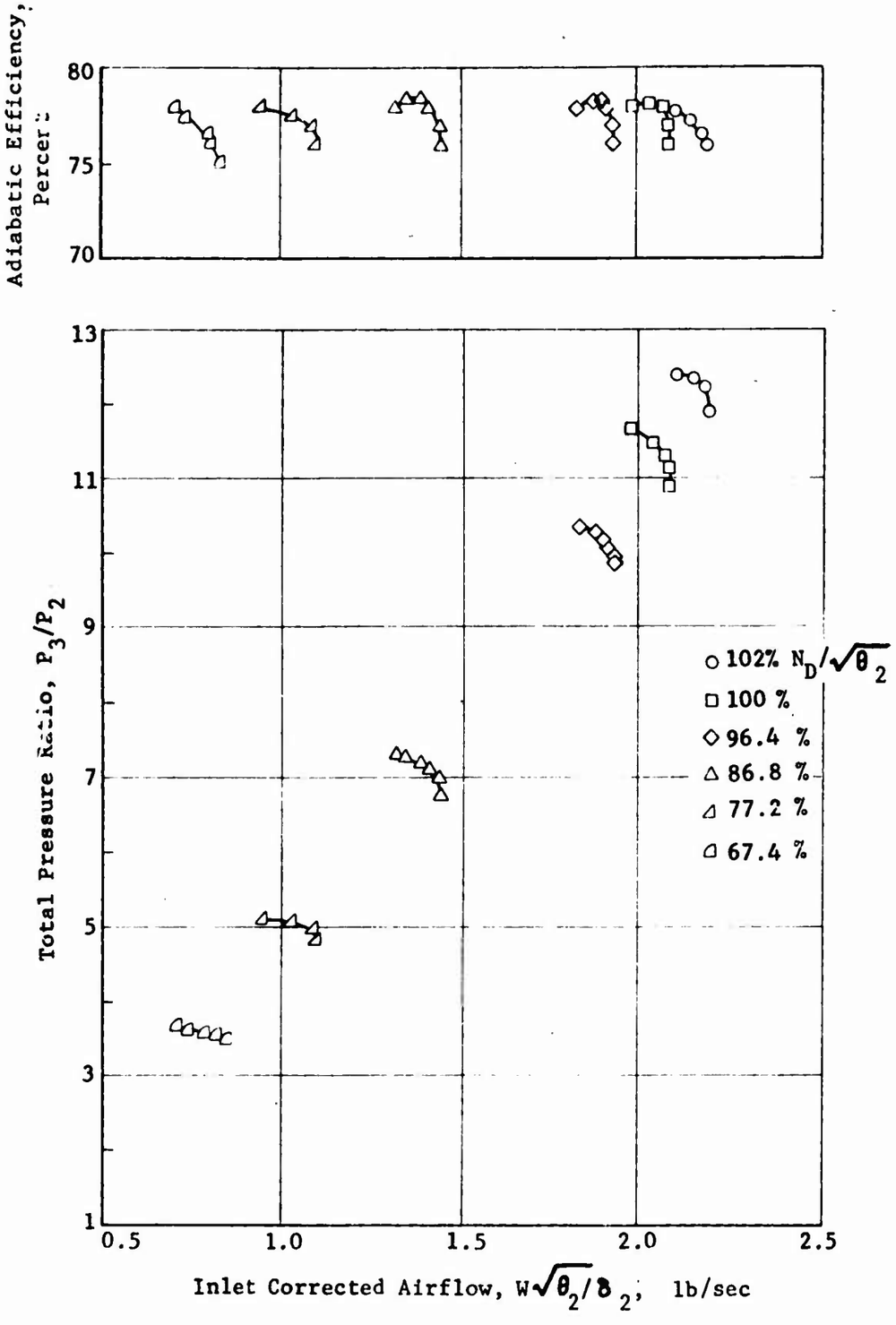

Figure 37. Compressor Test Performance, Modified, Boeing RF-2 Centrifugal Compressor (F1).

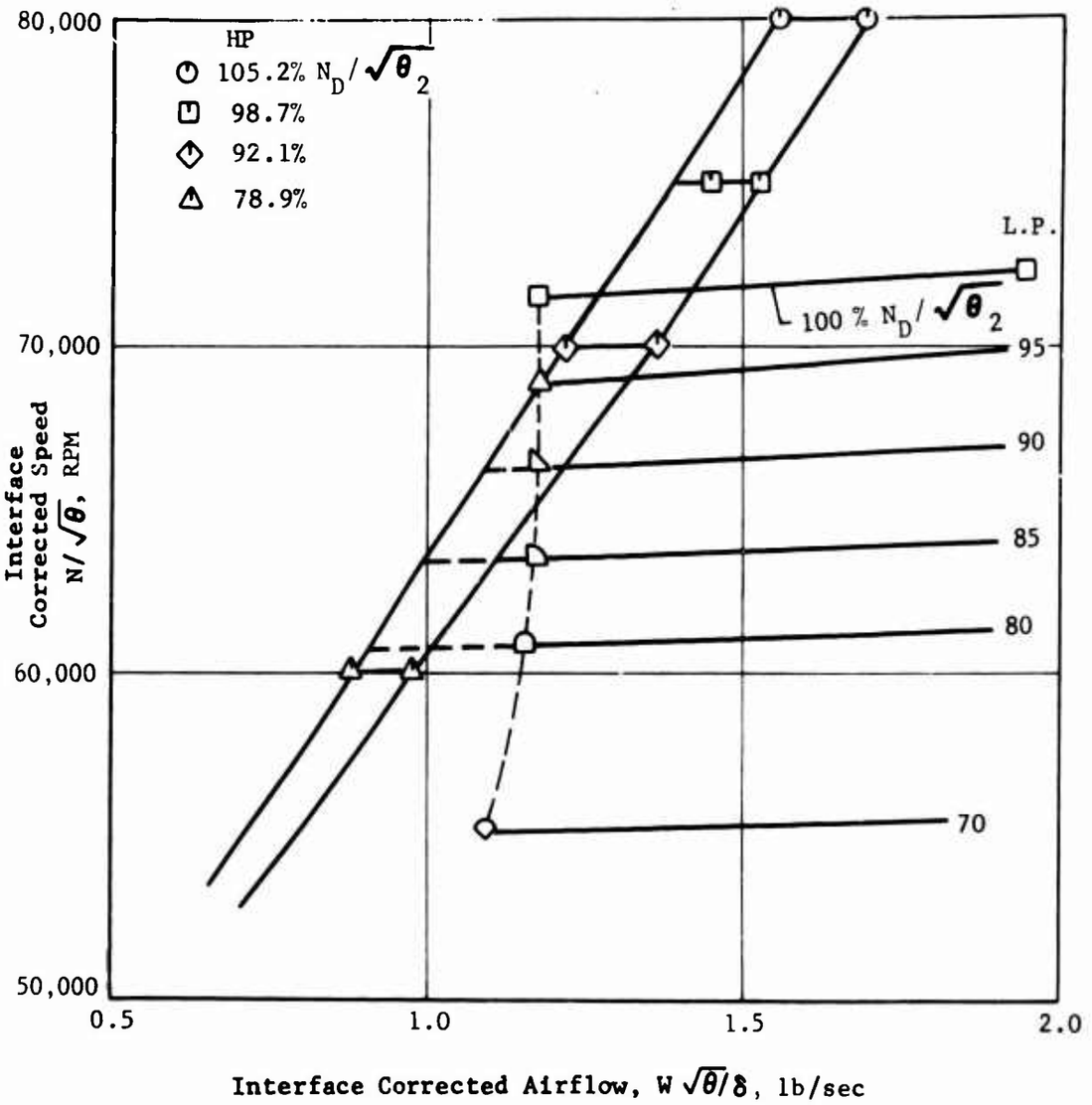

Figure 38. LP/HP Compressor Aerodynamic Match, Supersonic Axial Plus PW-G Centrifugal, Case 2,2.

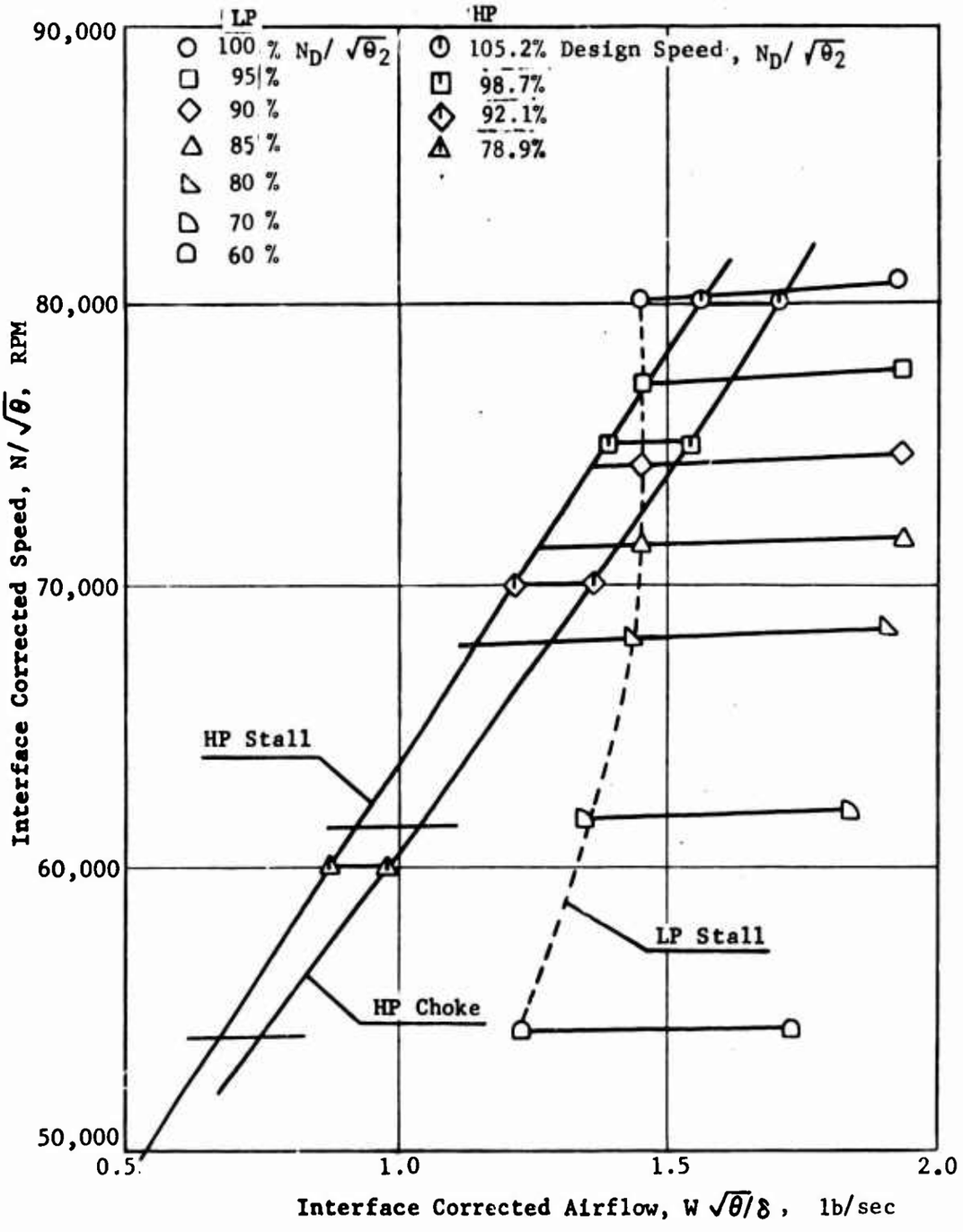

Figure 39. LP/HP Compressor Aerodynamic Match, Supersonic Axial Plus PW-G Centrifugal, Case 2, 3.

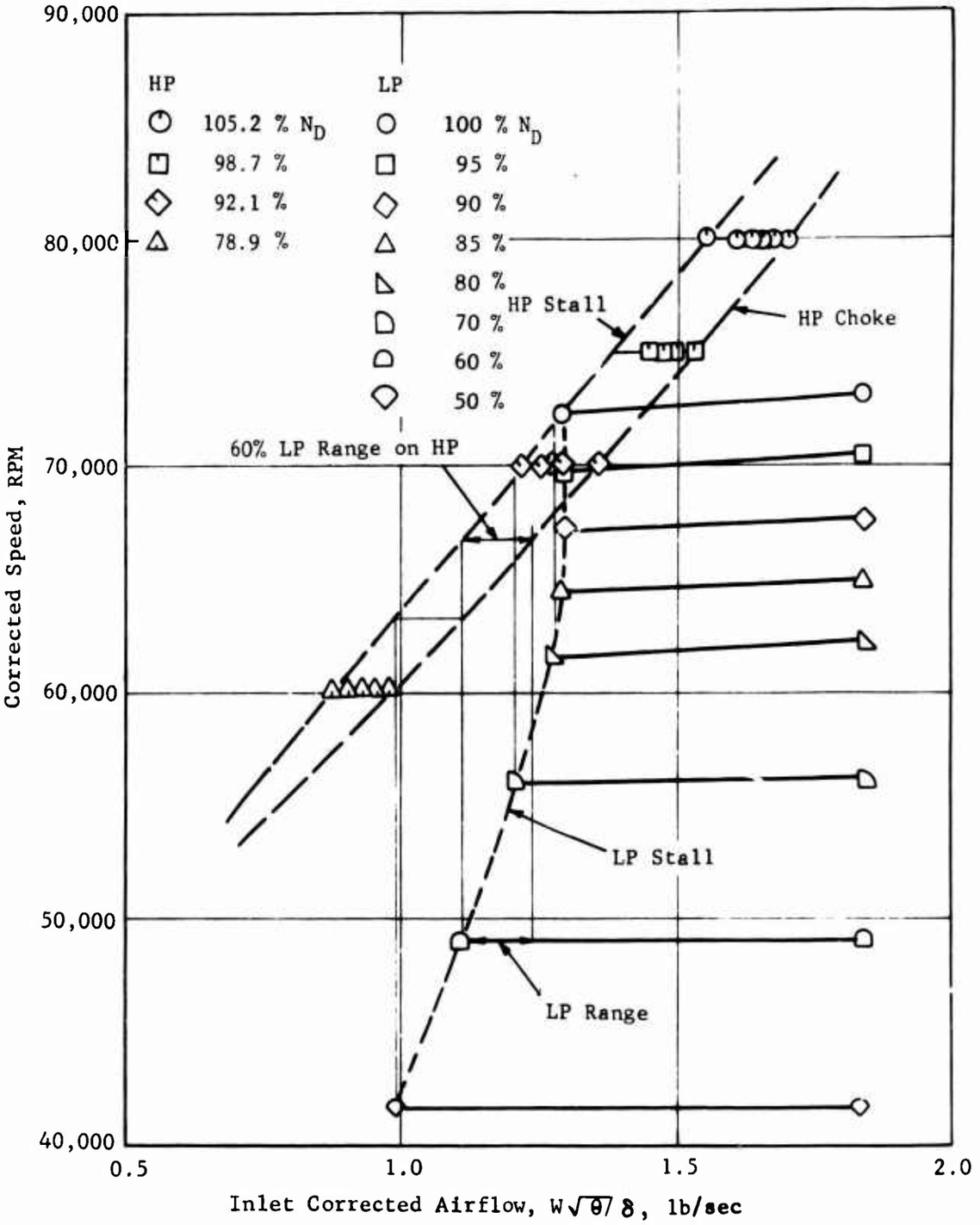

Figure 40. LP/HP Compressor Aerodynamic Match, Supersonic Axial Plus PW-G Centrifugal, Two Spools, Case 3.

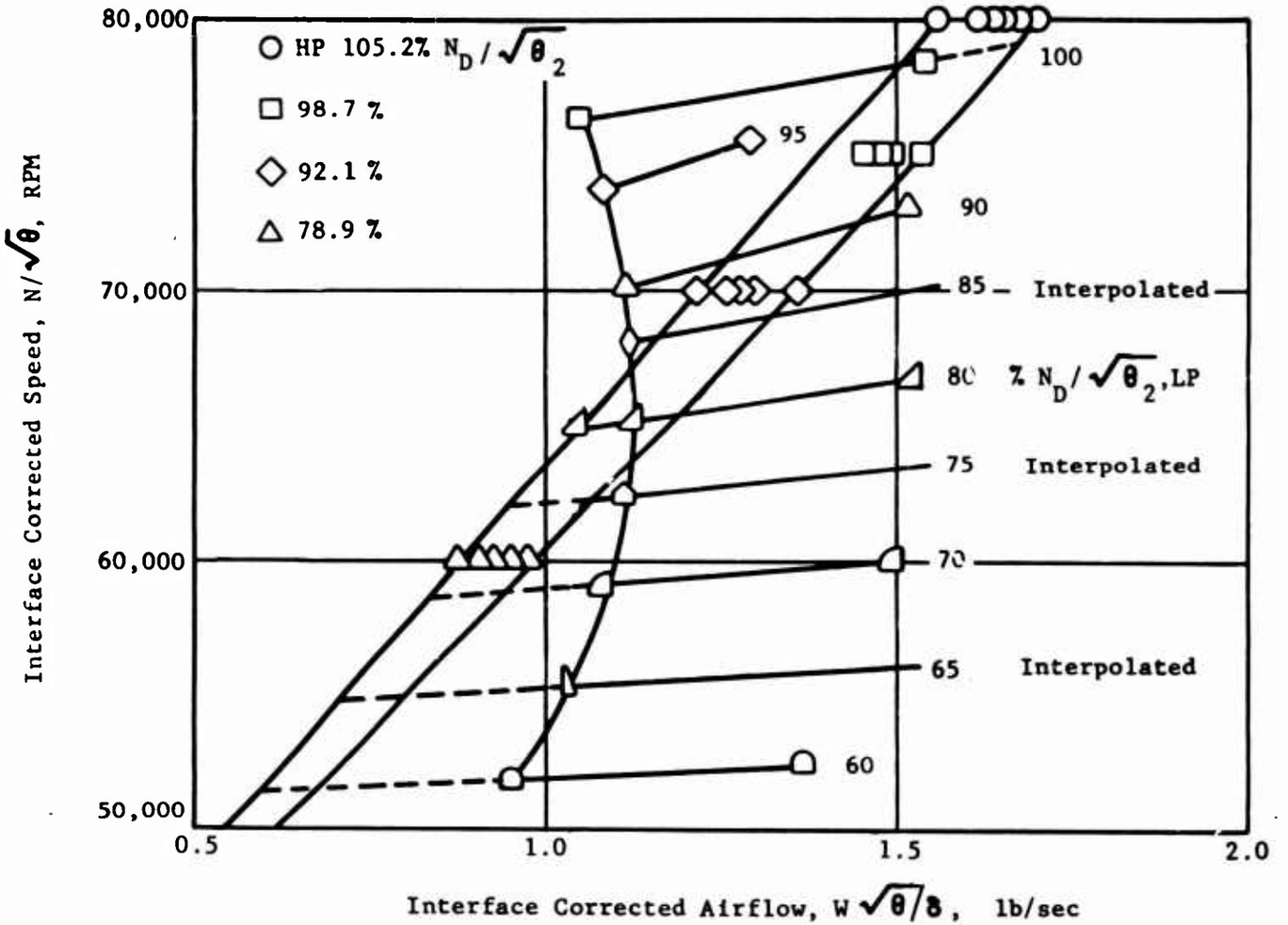

Figure 41. LP/HP Compressor Aerodynamic Match, Two-Stage Transonic Axial Plus PW-G Centrifugal, Case 4,1.

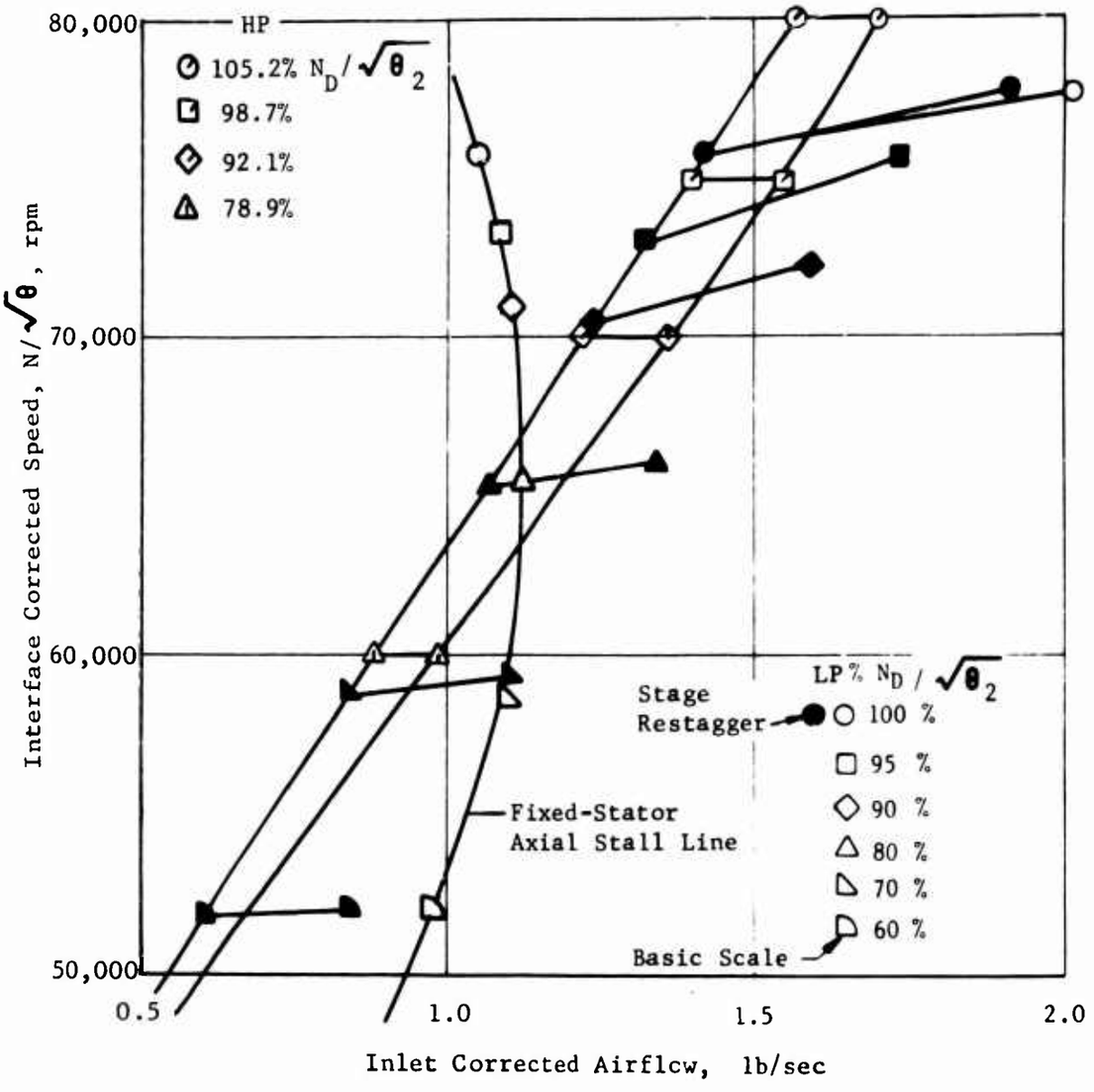

Figure 42. LP/HP Compressor Aerodynamic Match, Two-Stage Transonic Axial Plus PW-G Centrifugal, Variable Stators, Case 4, 1-VS.

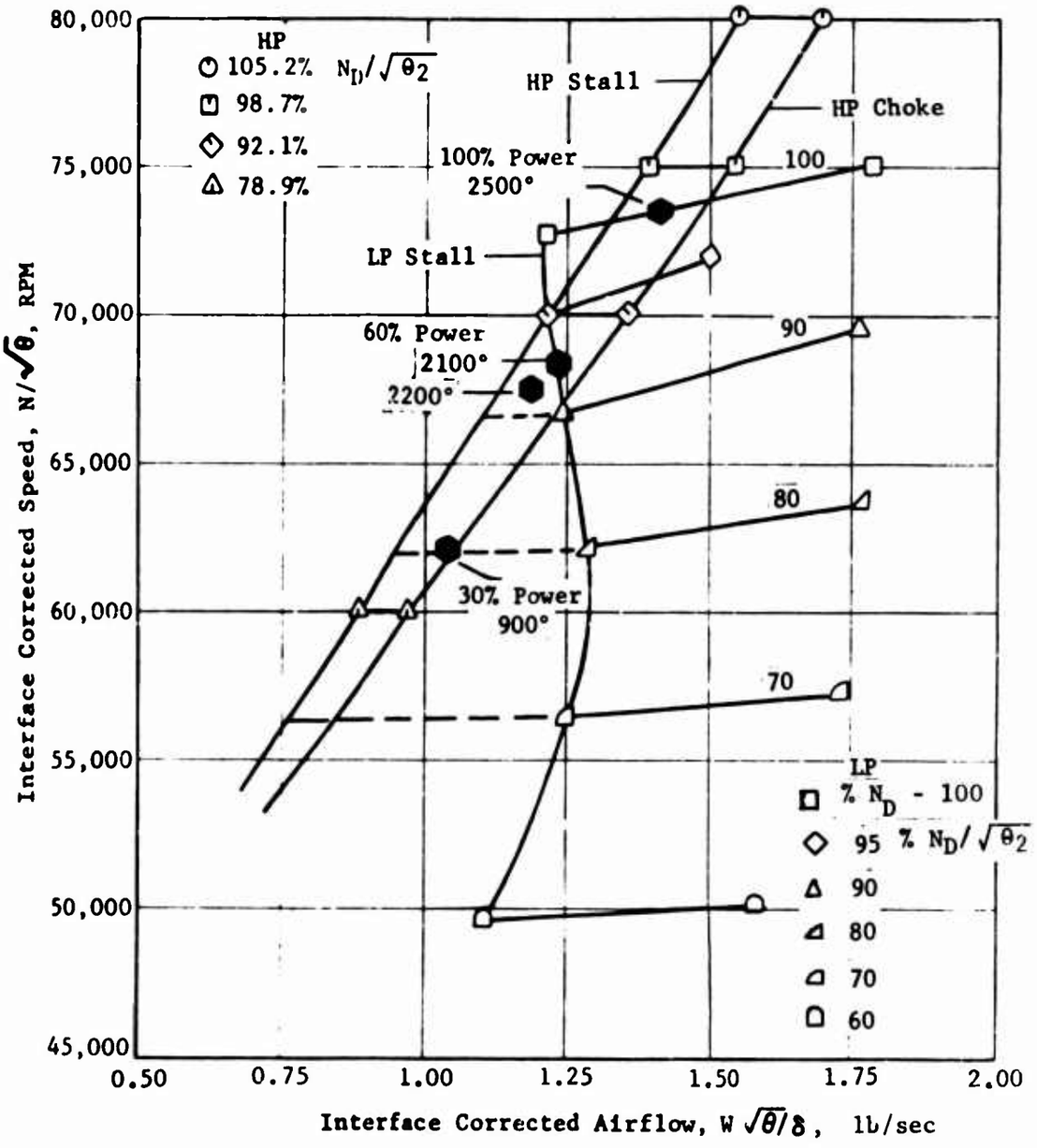

Figure 43. LP/HP Compressor Aerodynamic Match, Two-Stage Transonic Axial Plus PW-G Centrifugal, Case 4,3.

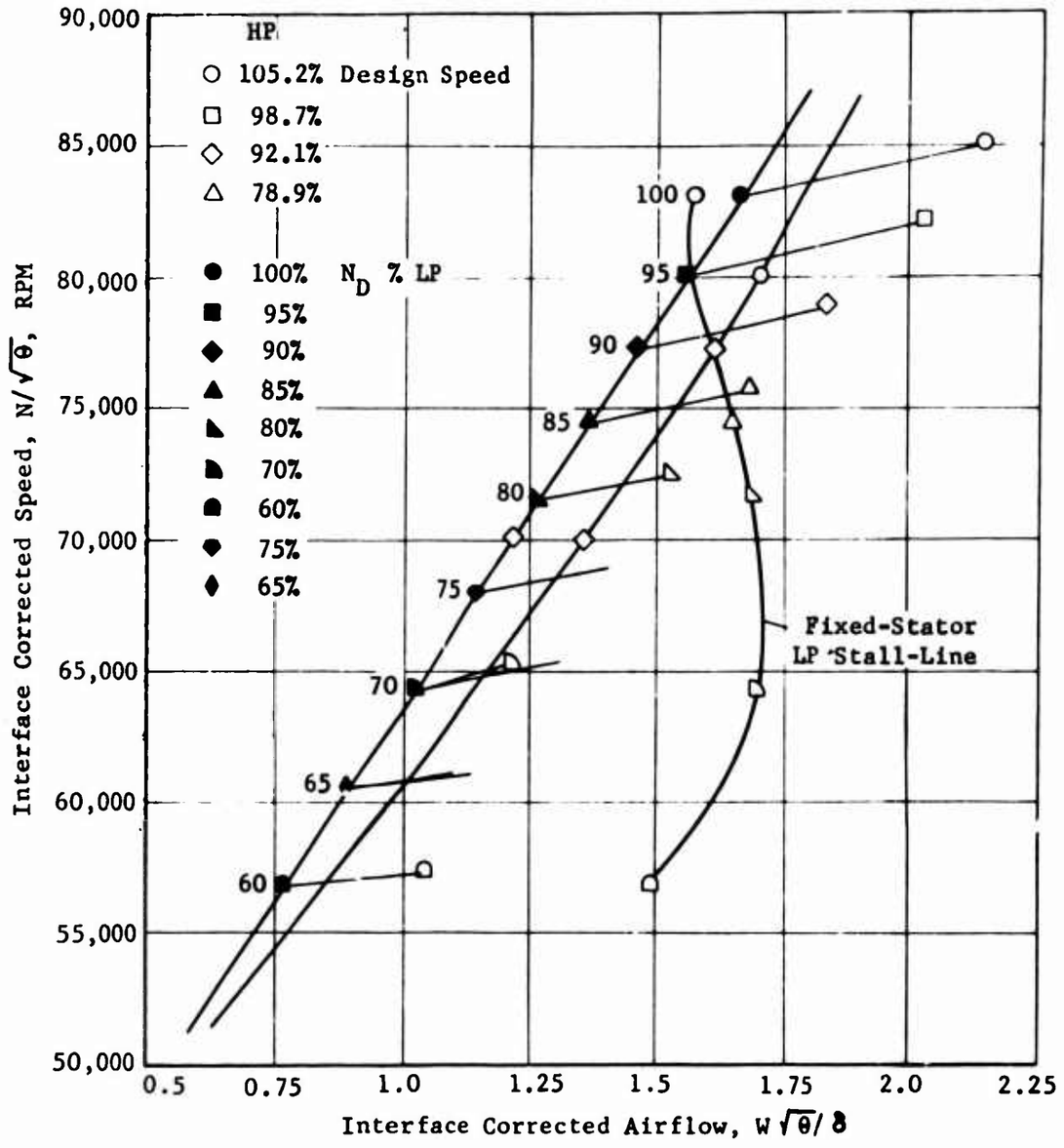

Figure 44. LP/HP Compressor Aerodynamic Match, Two-Stage Transonic Axial Plus PW-G Centrifugal, Variable Stators, Case 4,4-VS.

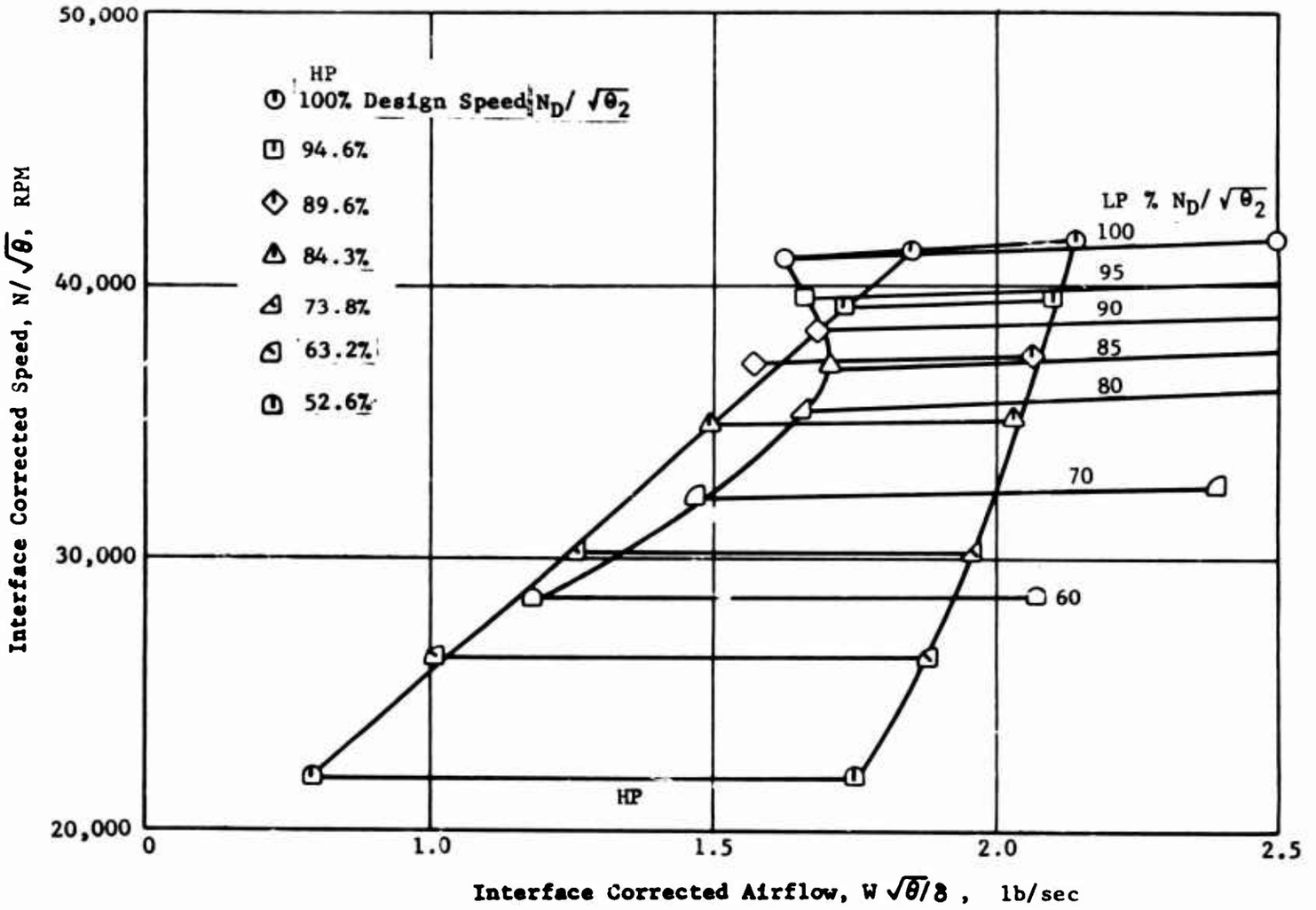

Figure 45. LP/HP Compressor Aerodynamic Match, Supersonic Plus Transonic Axial Plus 405 Centrifugal, Case 7, 2.

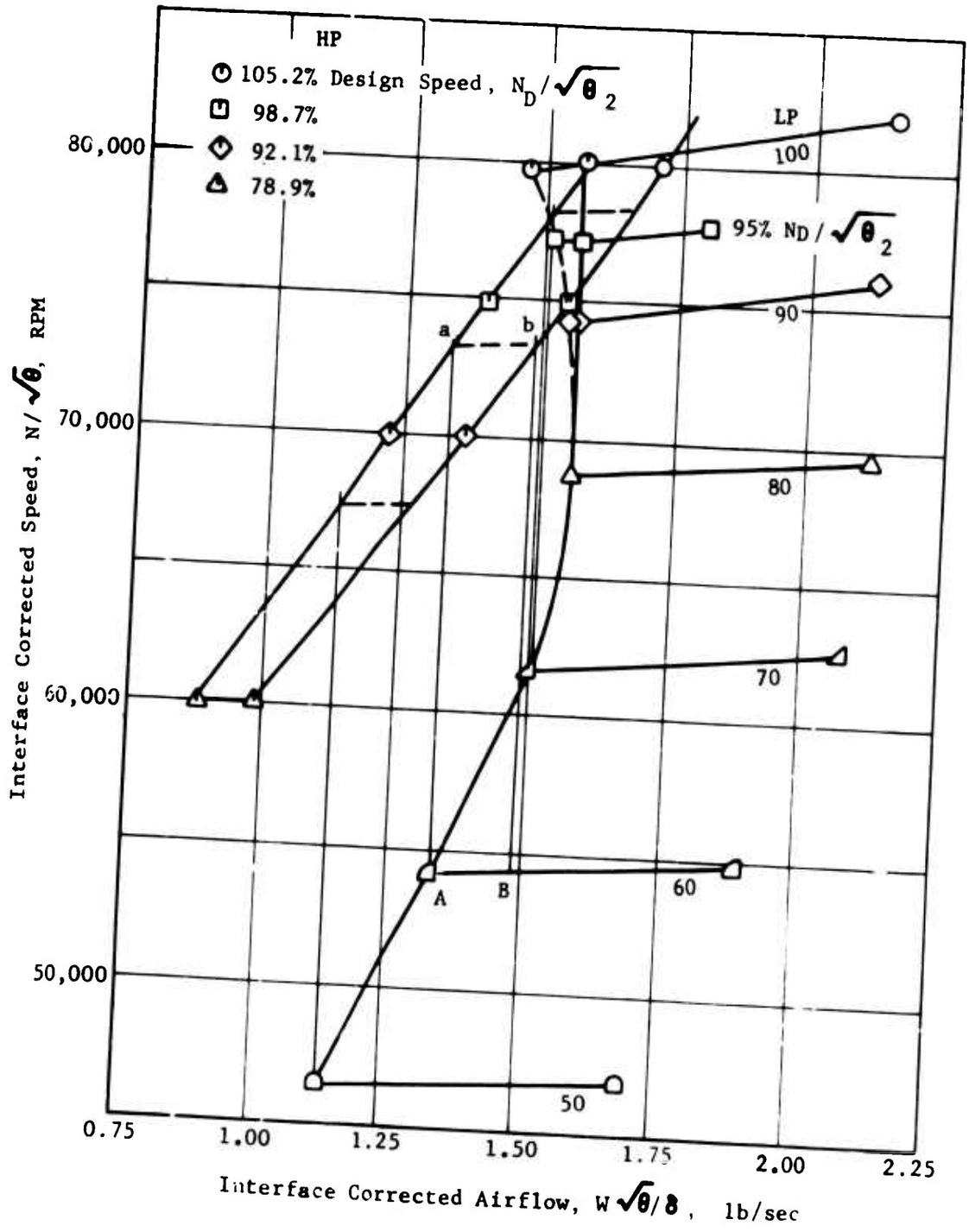

Figure 46. LP/HP Compressor Aerodynamic Match, Two-Stage Transonic Axial Plus PW-G Centrifugal, Two-Spool, Case 11,1.

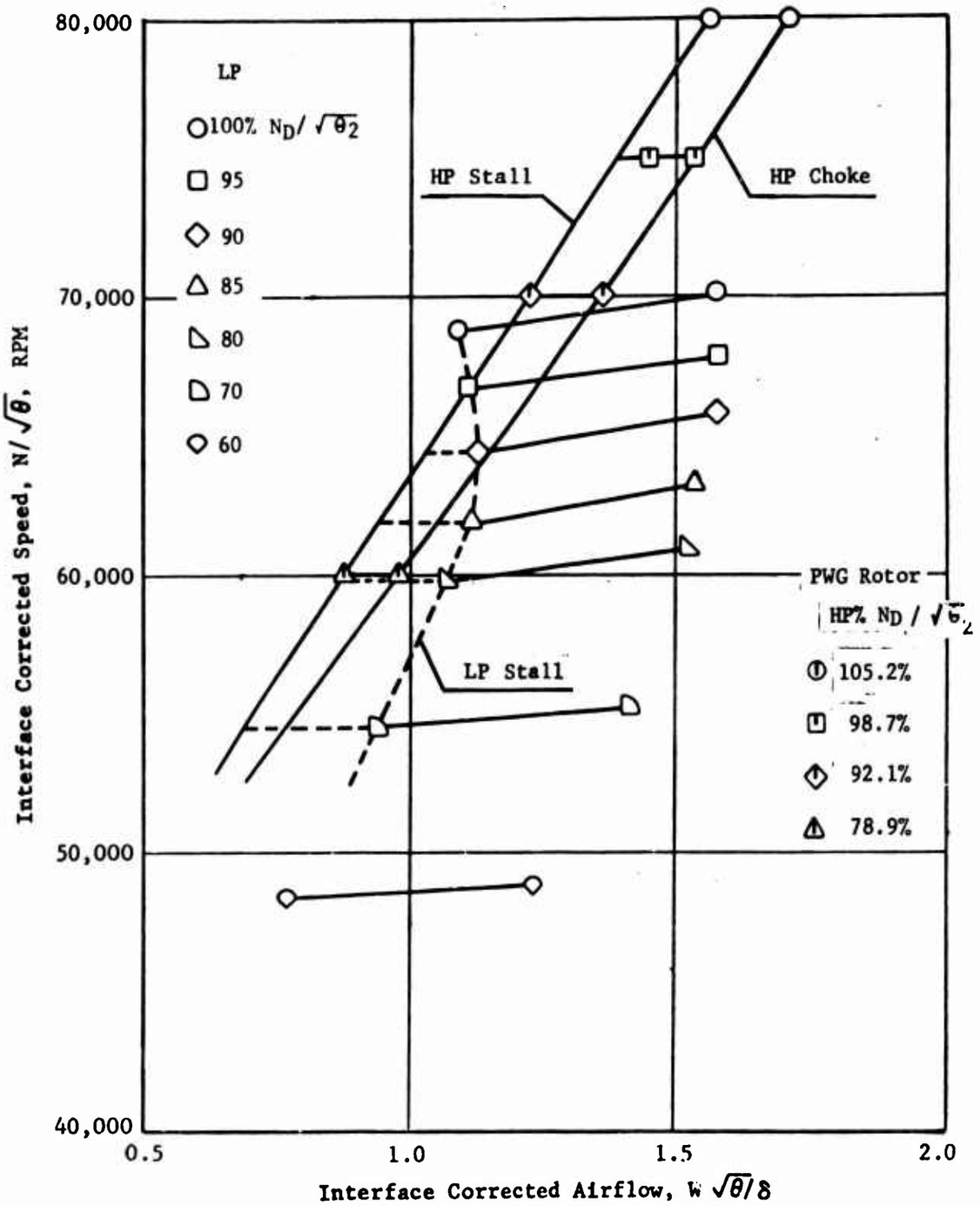

Figure 47. LP/HP Compressor Aerodynamic Match, Supersonic Plus Transonic Axial Plus PW-G Centrifugal, Case 13, 3.

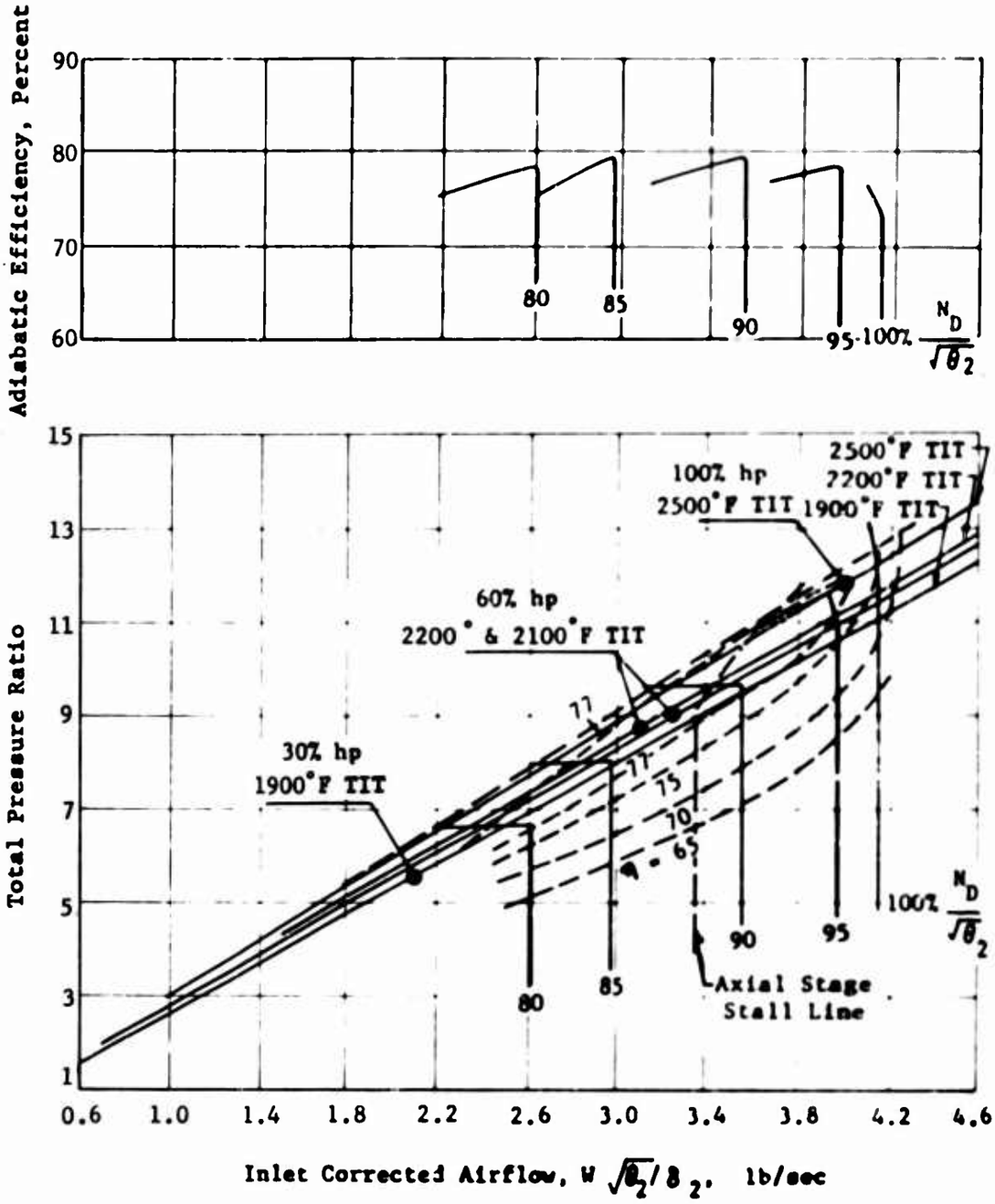

Figure 48. Compressor/Engine Matching Map, Supersonic Axial Plus PW-C Centrifugal, Case 2,2.

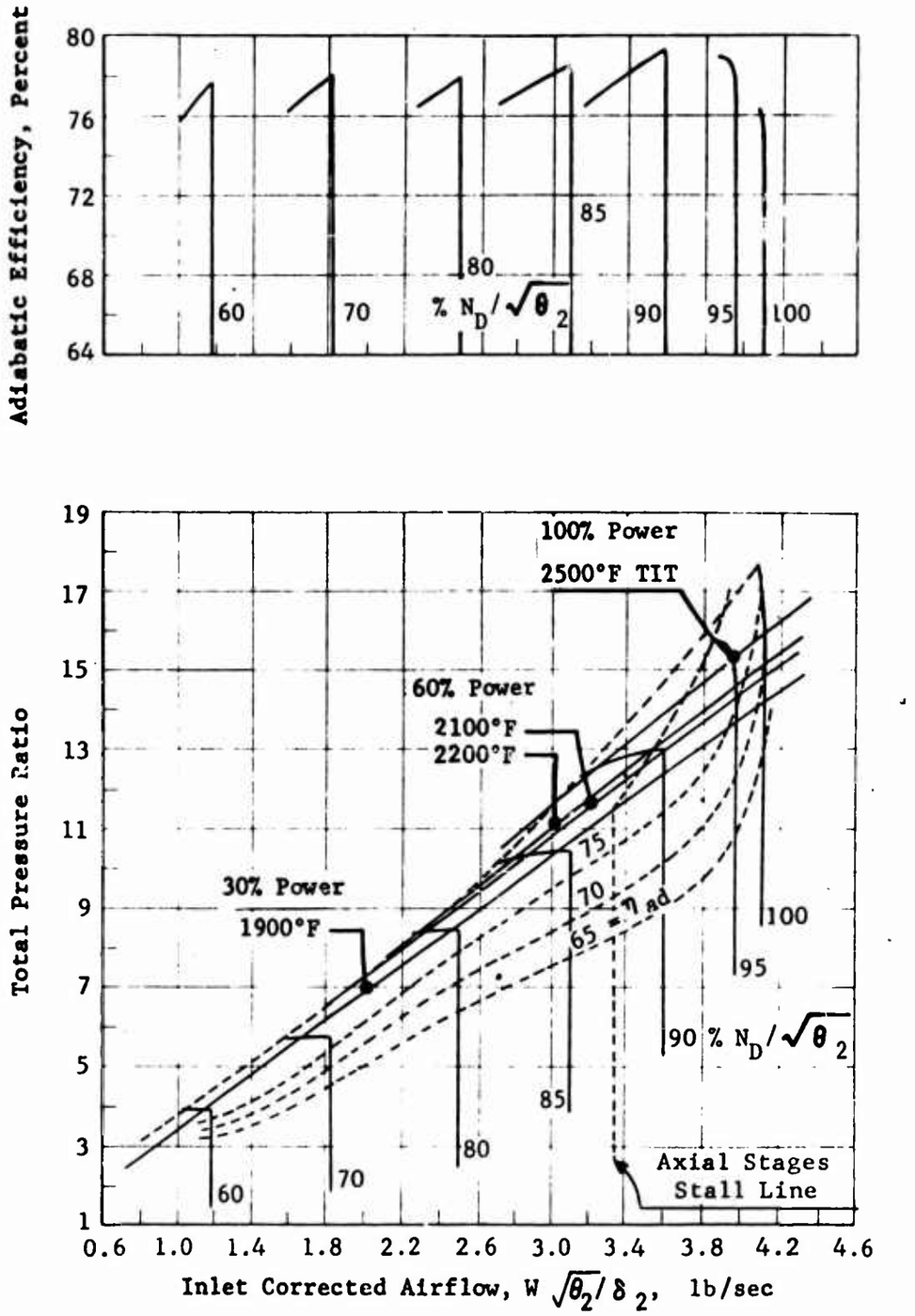

Figure 49. Compressor/Engine Matching Map, Supersonic Axial Plus PW-G Centrifugal, Case 2,3.

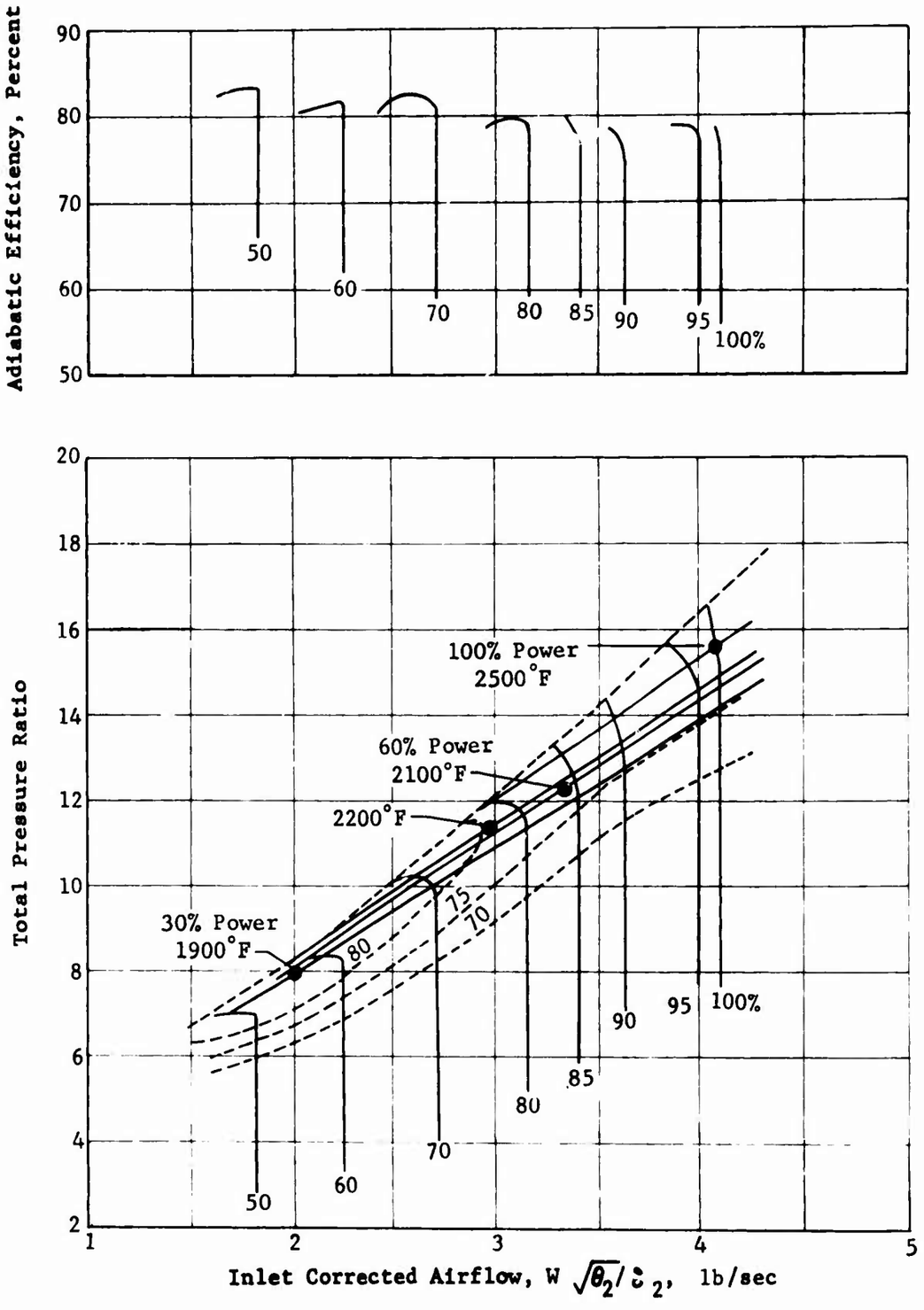

Figure 50. Compressor/Engine Matching Map, Supersonic Axial Plus PW-G Centrifugal, Two-Spool, Case 3.

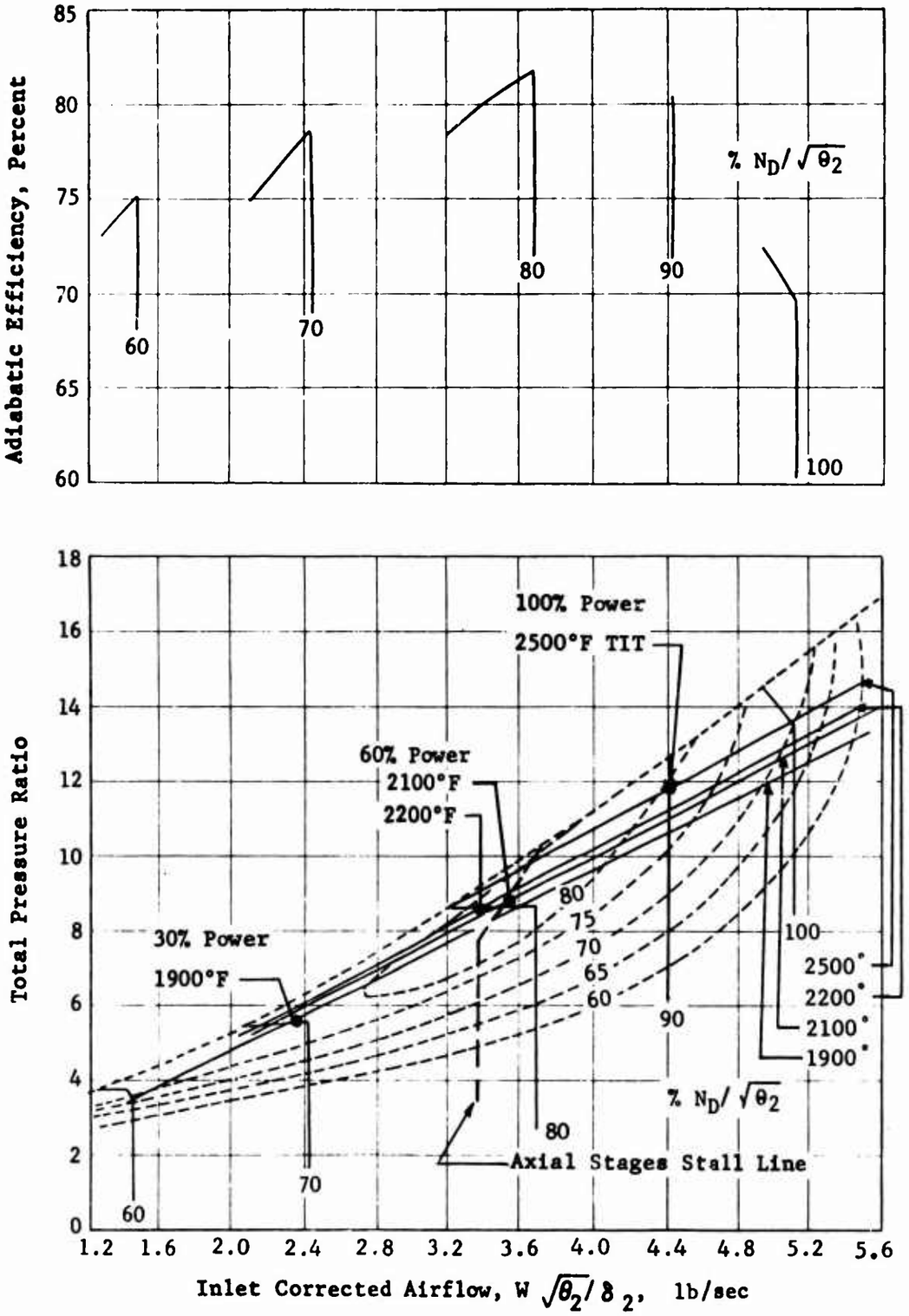

Figure 51. Compressor/Engine Matching Map,Two-Stage Transonic Axial Plus PW-G Centrifugal, Case 4,1.

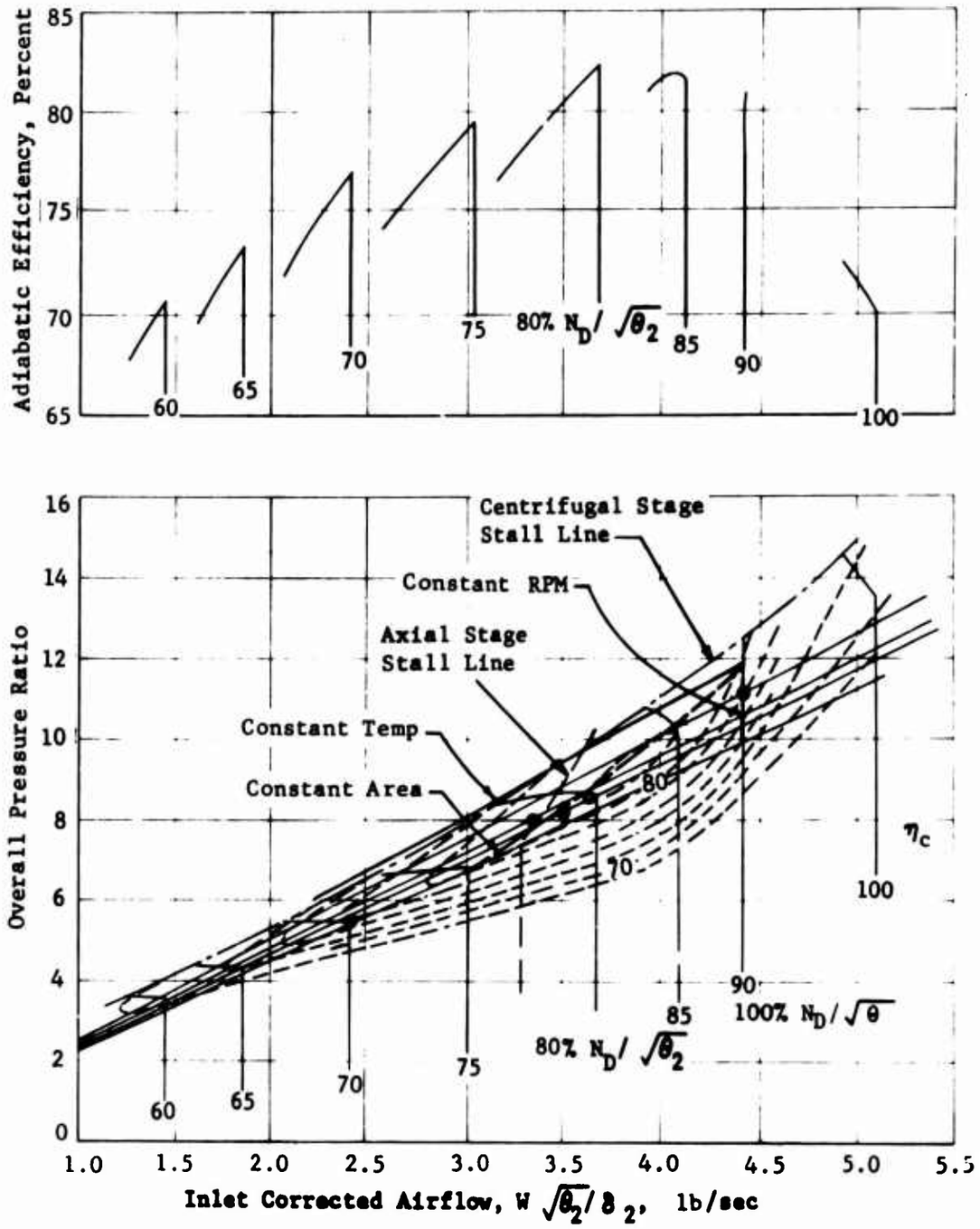

Figure 52. Compressor/Engine Matching Map, Two-Stage Transonic Axial Plus PW-G Centrifugal, Case 4, 1-AAA.

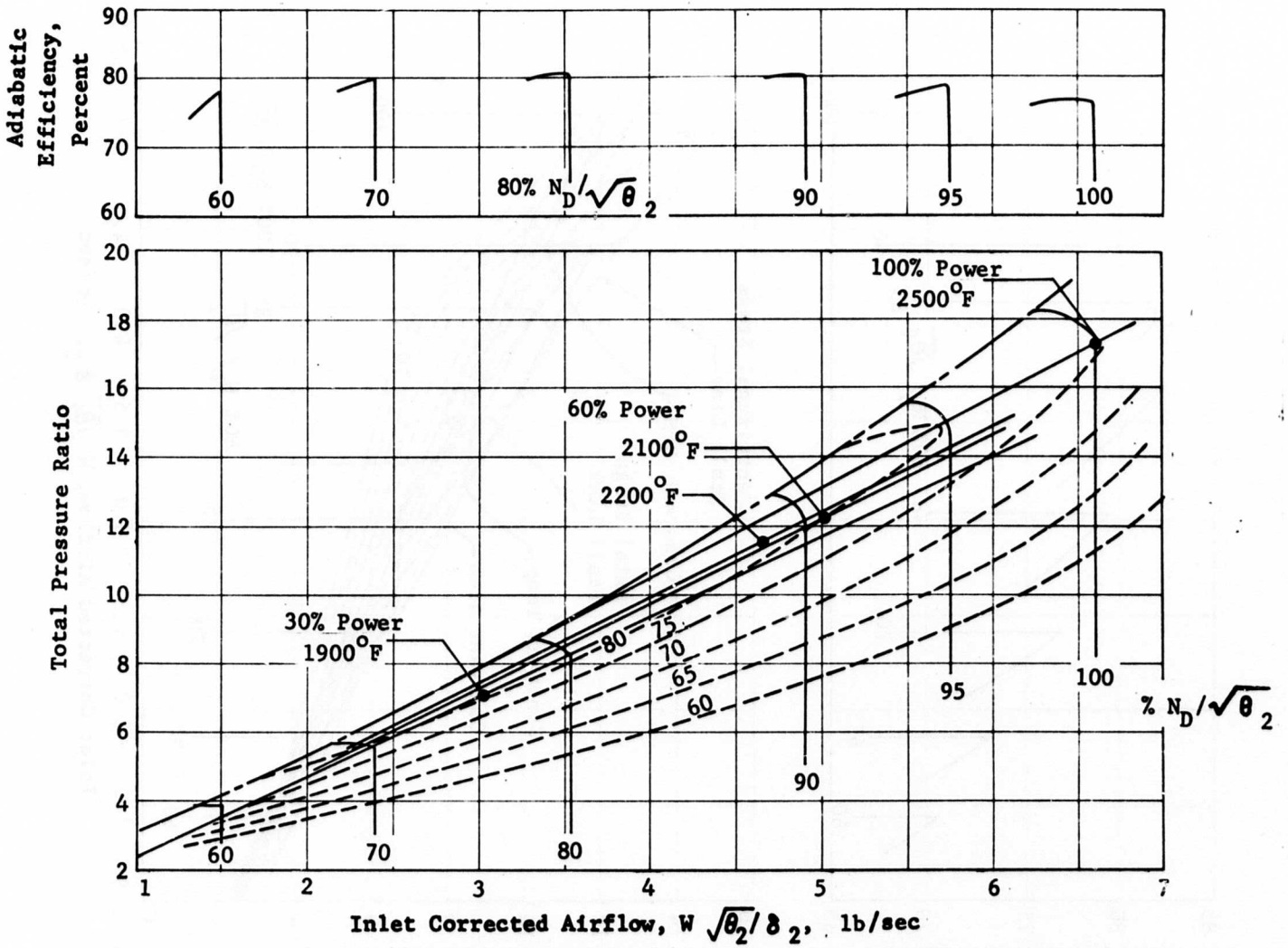

Figure 53. Compressor/Engine Matching Map, Two-Stage Transonic Axial Plus PW-G Centrifugal, Variable Stators, Case 4,1-VS.

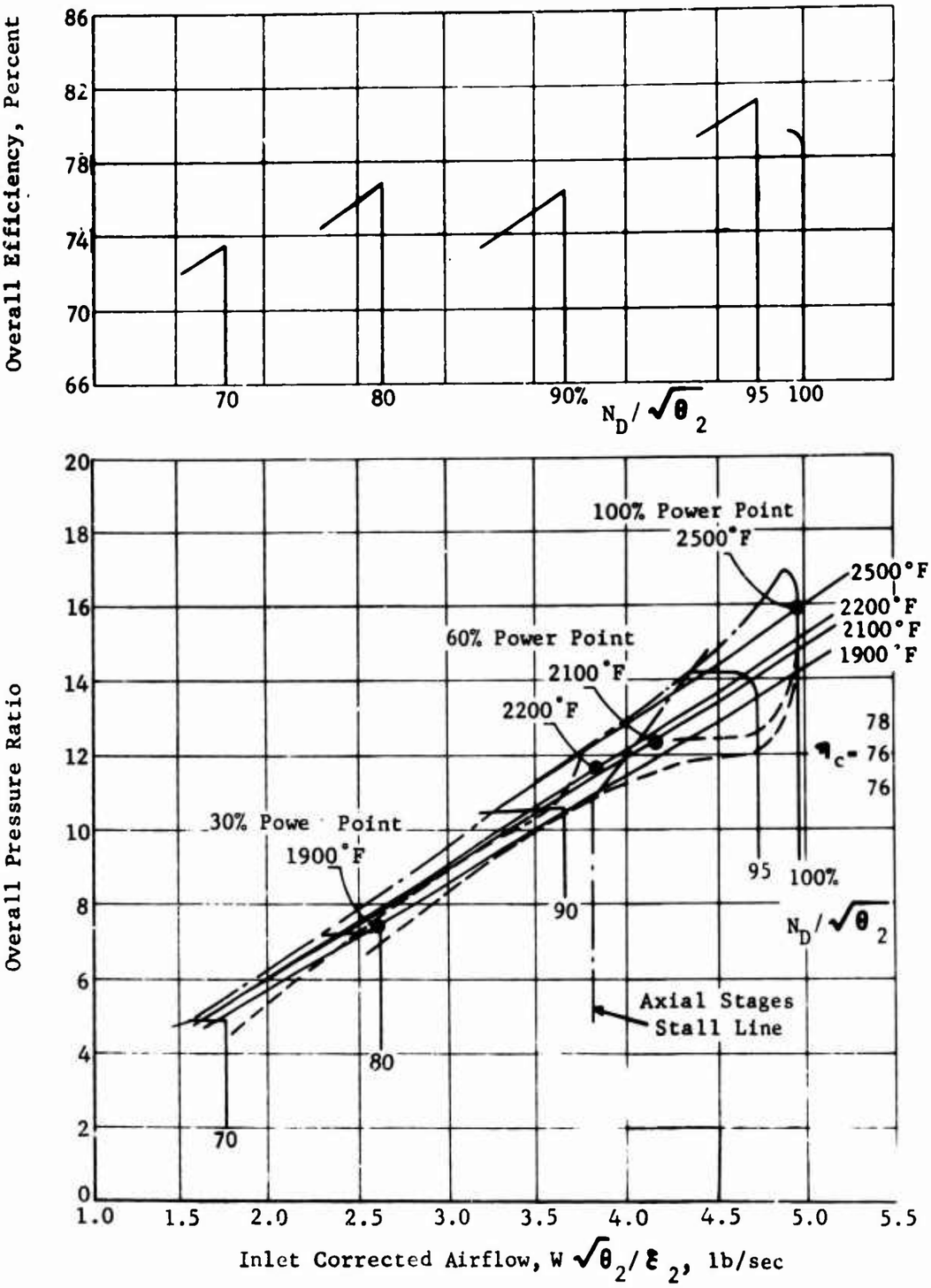

Figure 54. Compressor/Engine Matching Map, Two-Stage Transonic Axial Plus PW-G Centrifugal, Case 4,3.

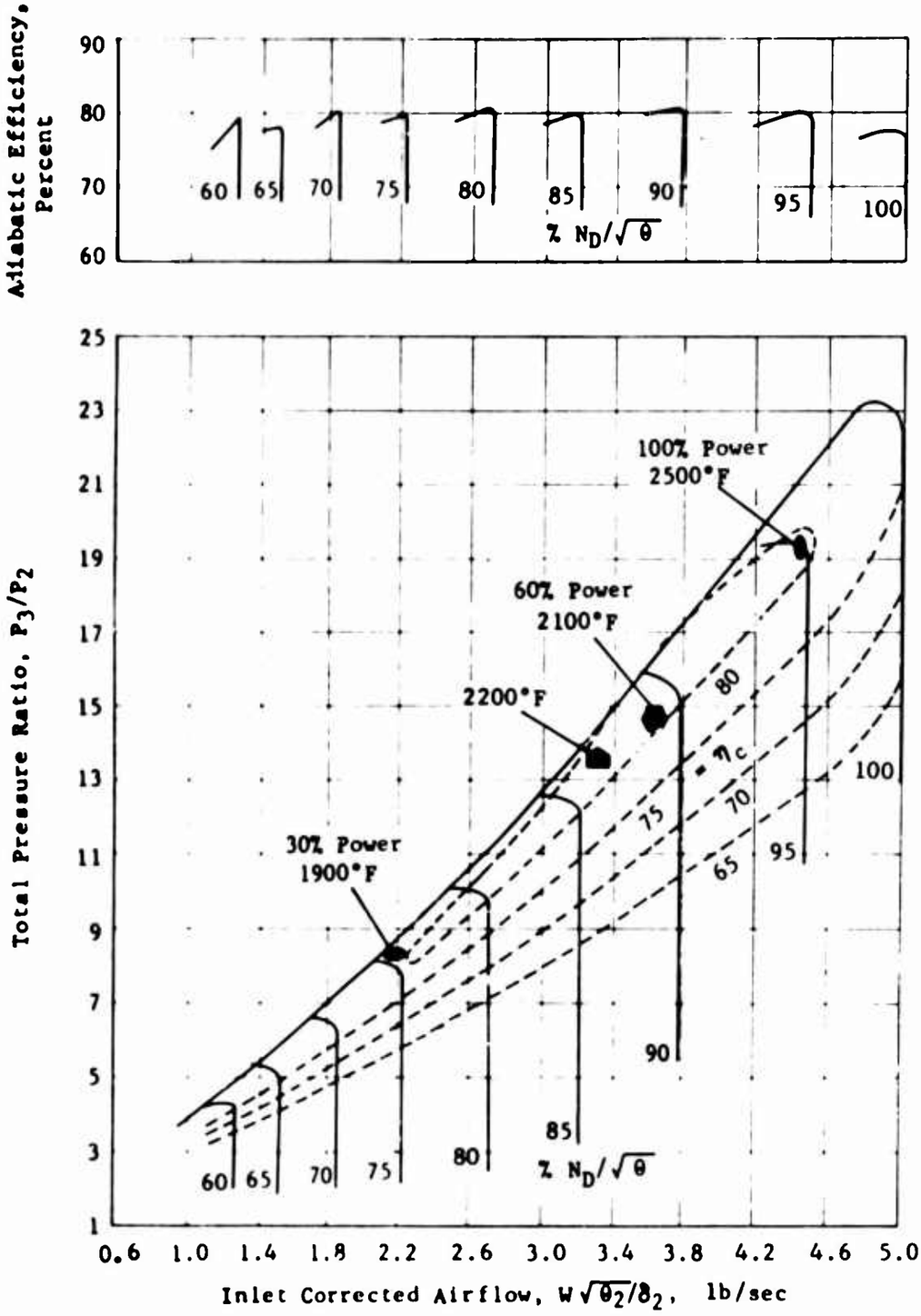

Figure 55. Compressor/Engine Matching Map, Two-Stage Transonic Plus PW-G Centrifugal, Variable Stators, Case 4, 4-VS.

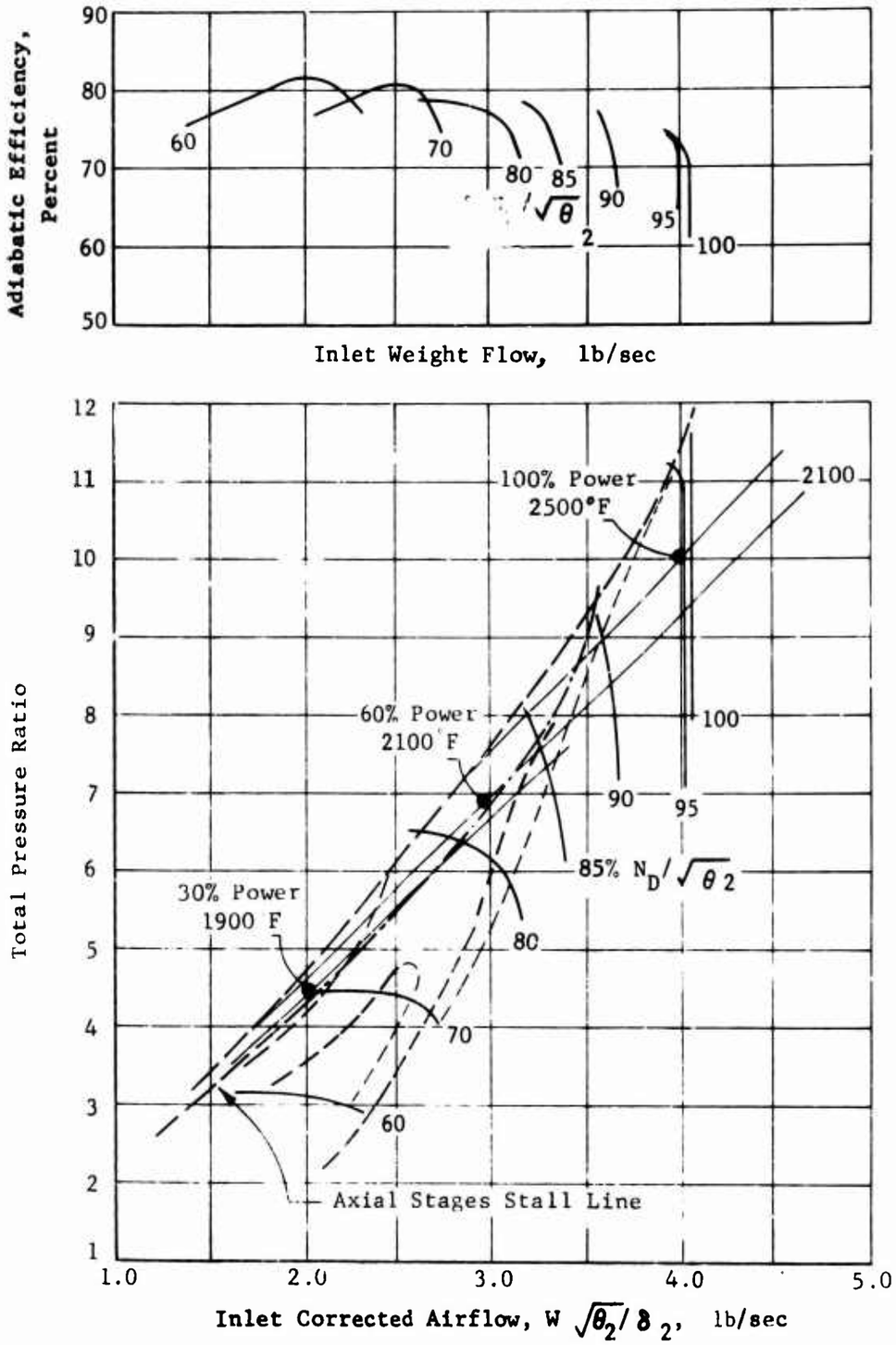

Figure 56. Compressor/Engine Matching Map, Supersonic and Transonic Axial Plus 405 Centrifugal, Case 7,2.

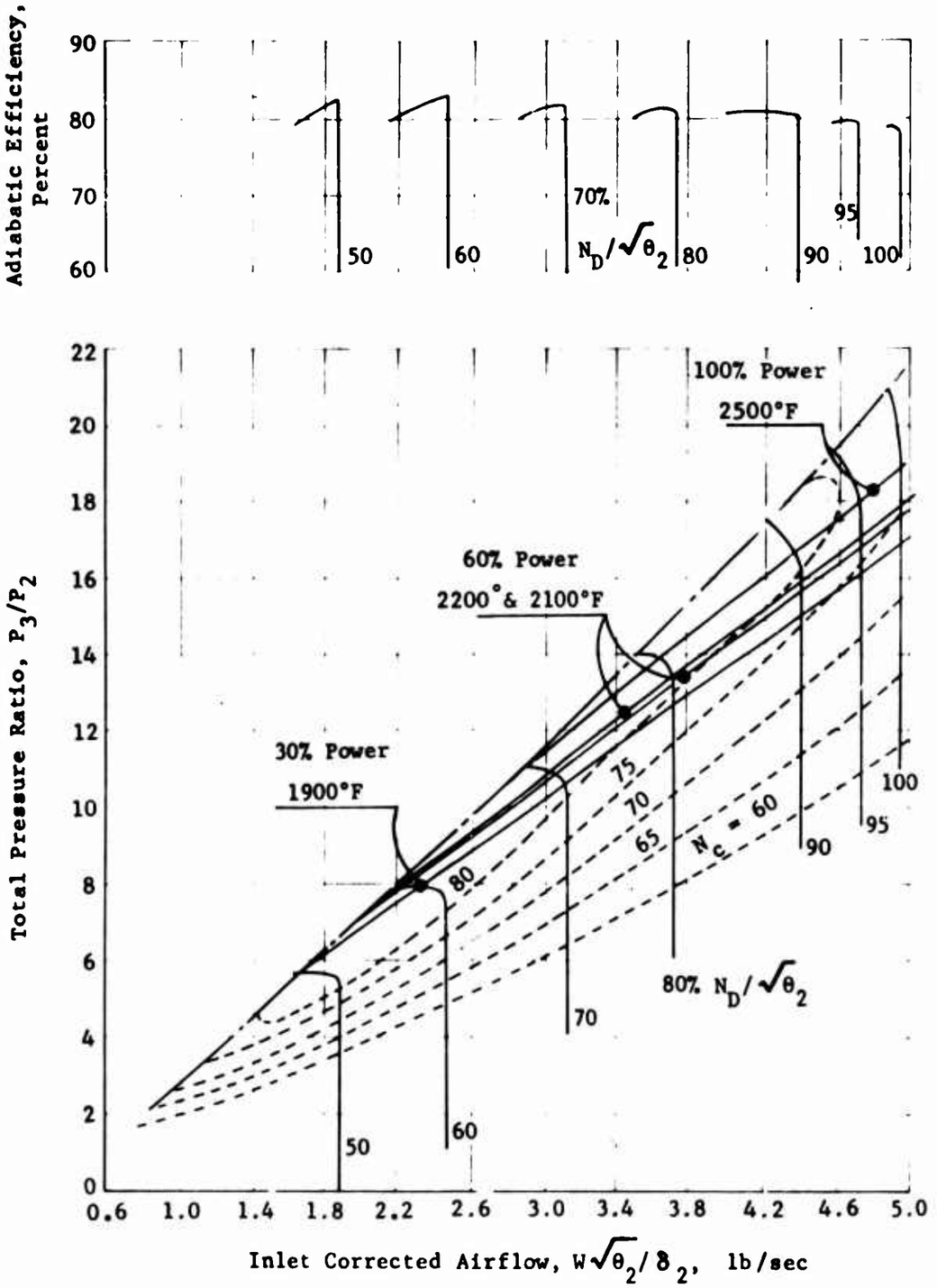

Figure 57. Compressor/Engine Matching Map, Two-Stage Transonic Plus PW-G Centrifugal, Two-Spools, Case 11,1.

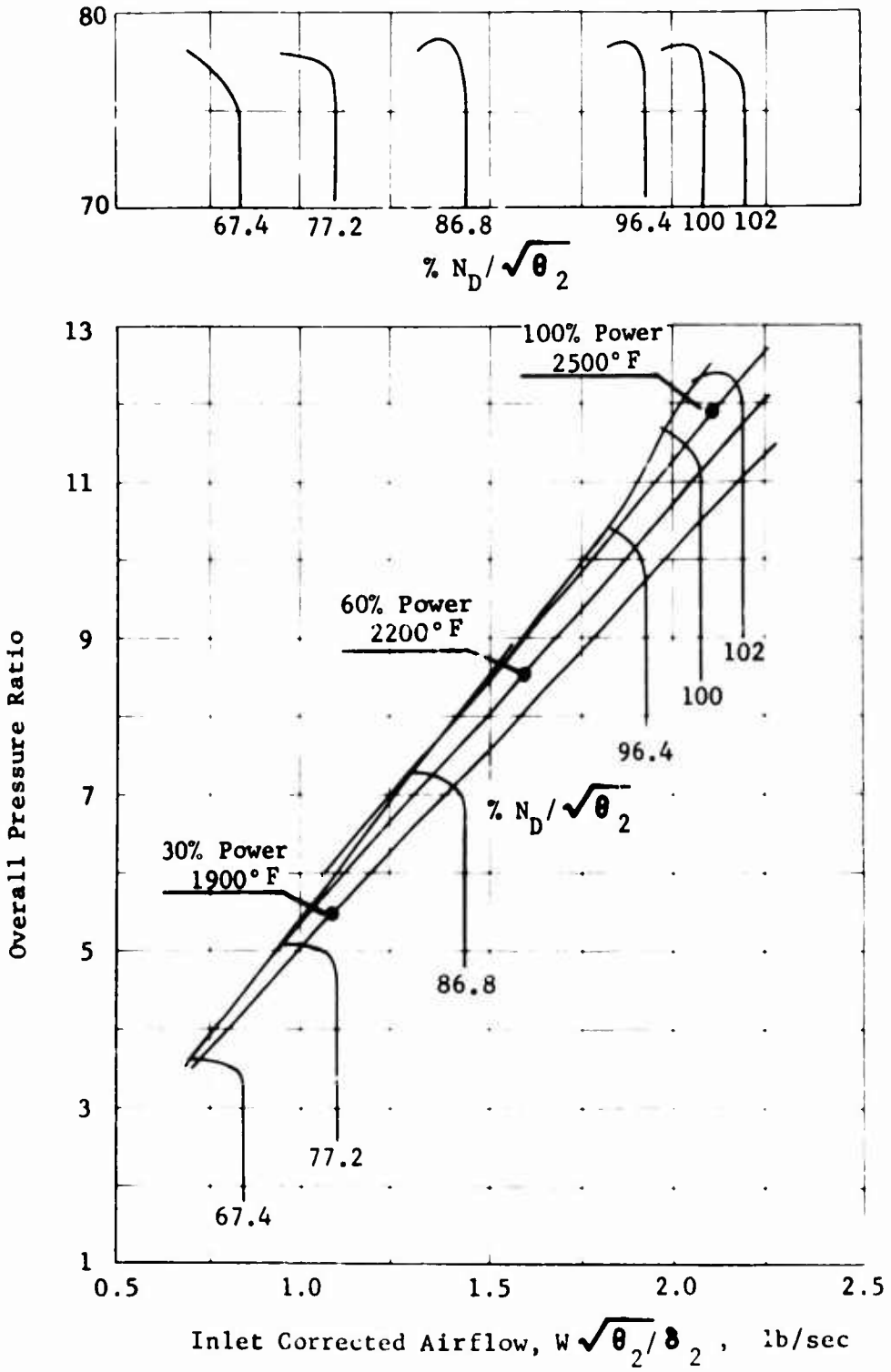

Figure 58. Compressor/Engine Matching Map, RF-2 Centrifugal, Case 12.

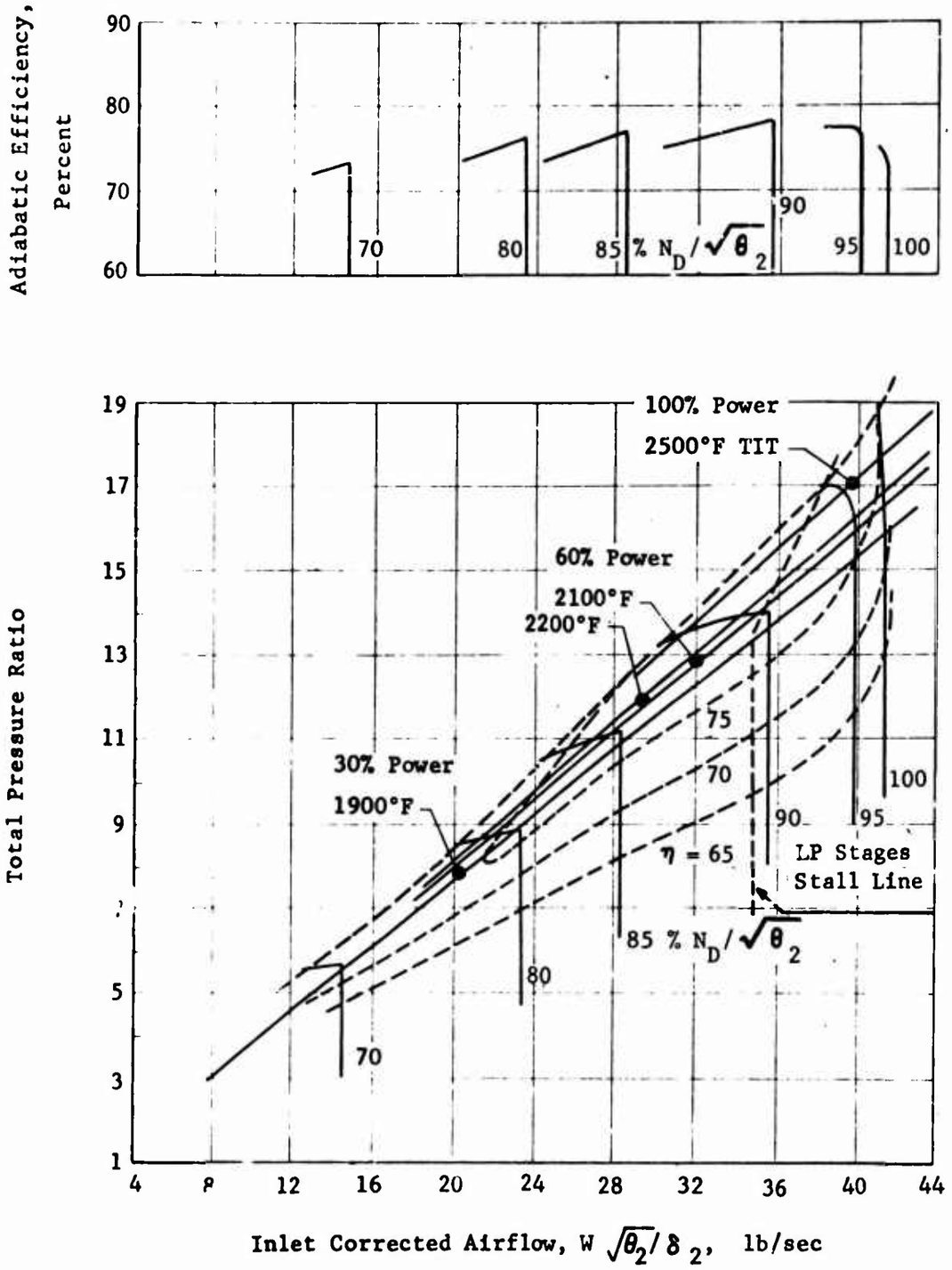

Figure 59. Compressor/Engine Matching Map, Supersonic and Transonic Axial Plus PW-G Centrifugal, Case 13,3.

2,2. The abscissa represents the corrected flow leaving the LP and entering the HP compressor. The values that apply to the interstage situation also apply to the stages when operated separately as in component tests. The ordinate represents the corrected shaft speed at the interstage location, and it also relates to the performance of the stages operated singly. Any point on the graph establishes an operating condition for the individual LP and HP stages and therefore implies the performance for the overall machine. Important features of the graph are the following:

LP speed lines, representing constant values of inlet speed. These lines will represent the inlet corrected speed for the matched combination.

LP stall line, representing the low-flow limit of stable operation for the LP compressor.

HP speed lines, representing values of inlet corrected speed.

HP stall line, representing the low-flow limit of stable operation for the HP compressor.

HP choke line, representing the high-flow limit for the HP compressor.

It is typical of a fixed geometry compressor that the LP and HP stall lines intersect. Above the intersection point, the LP stall line lies to the left of the HP stall line; below the intersection point, the LP stall line lies to the right of the HP stall line, and lower yet, it lies to the right of the HP choke line.

Flow range is limited by choke and stall. HP choke determines the high-flow limit on the match graph; LP exit flow is not limited because the increase in flow volume (corrected flow) depends only on reduction of its outlet pressure. In this study, HP stall has been taken to be the low-flow limit. Therefore the possible compressor operating range lies between choke and stall on the HP and presents the HP with no operating problems. The LP is required to accommodate the HP. At high speed, above the stall-line intersection point, the LP is not subject to stall. The entire compressor surges with stall of the HP before the LP reaches a stalling condition. By the same phenomenon, however, the LP at these speeds is prevented from approaching the pressure ratio and efficiencies that it may have been able to produce near the stall line as a component alone. Below the stall-line intersection, stall comes first to the LP compressor, and the location of the LP stall line has been drawn on fixed-stator compressor maps. At the same time, it has been assumed that the stability of the HP overcomes the instability of the LP. Though information is not presented to support this assumption quantitatively, it is known that LP stages of similar axial-centrifugal compressors do operate in rotating stall at the lower speeds. In the 13-stage axial compressor of the J65 engine, rotating stall in the front stages occurs

from low speeds to as high as 75 percent of design speed. Figure 60 shows a performance map for a five-stage axial compressor. The maximum pressure rise for each stage is located by a line on the map and above the line the stage is operating in stall. Initially in the present study it was assumed that any degree of LP stall could be tolerated outside of the 60 - 100 percent power-operating range. The fixed-stator compressor design was based on this assumption. Later it was assumed that stall should be avoided in the range down to 30 percent power. The variable stator design was based on this assumption.

The LP/HP compressor matching curves imply relationships between all of the compressor operating parameters, including efficiency. The range of the component compressors can be important in defining the range of the overall compressor. As an aid in evaluating the efficiency range of compressors, Figures 61 through 65 show speed lines, stall lines, choke lines, and constant efficiency lines for the experimental (but efficiency-modified) compressors that were matched together. Flows and speeds have been normalized to values near maximum efficiency.

The discussion to this point has dealt with a basic matching problem, the fixed stator compressor. The use of scaling to vary the matching relations of fixed geometry stages is not, however, the end of our matching resources. At a cost in mechanical complexity, bleed and/or variable geometry are available to alleviate matching problems that arise in fixed geometry machines. It is of interest to relate these resources to the compressor match diagram, e.g., Figure 38, discussing bleed, two-spooling, and variable stators in turn.

Bleed is a device for temporarily reducing the size of the LP compressor. In the region below the intersection of stall lines, the LP compressor tends to run in stall because all of its flow cannot be accommodated by the HP. The bleed flow is subtracted at the interface and the LP speed line is moved to the left on Figure 38. This can result in an increase in LP pressure ratio and a decrease in temperature rise with an increase in HP corrected speed and an increase in HP pressure ratio. HP efficiency may then be increased, and the stall line may be moved to higher pressure ratio, permitting an engine to run in a region where it could not run without bleed. A cost is paid in work done on the bled air, and this is likely to result in unacceptably high fuel consumption. Only one bleed case was examined by the methods of this study, and it is not reported; the result was a loss of efficiency with no improvement in stall line. Further work was not carried out because other directions were more attractive.

Two-spooling is a device for removing the speed-matching restrictions on the two compressors. In effect, the LP speed lines in Figure 38 are free to move vertically. Thus the LP 70-percent speed line can be run at 55,000 RPM, while the HP is run at about 90 percent speed or 68,000 RPM, making the two machines comparable in flow and permitting good flow matching to be attained over the whole range of LP speeds. Figure 38 shows that a range of HP speed from about 65,000 to 69,000

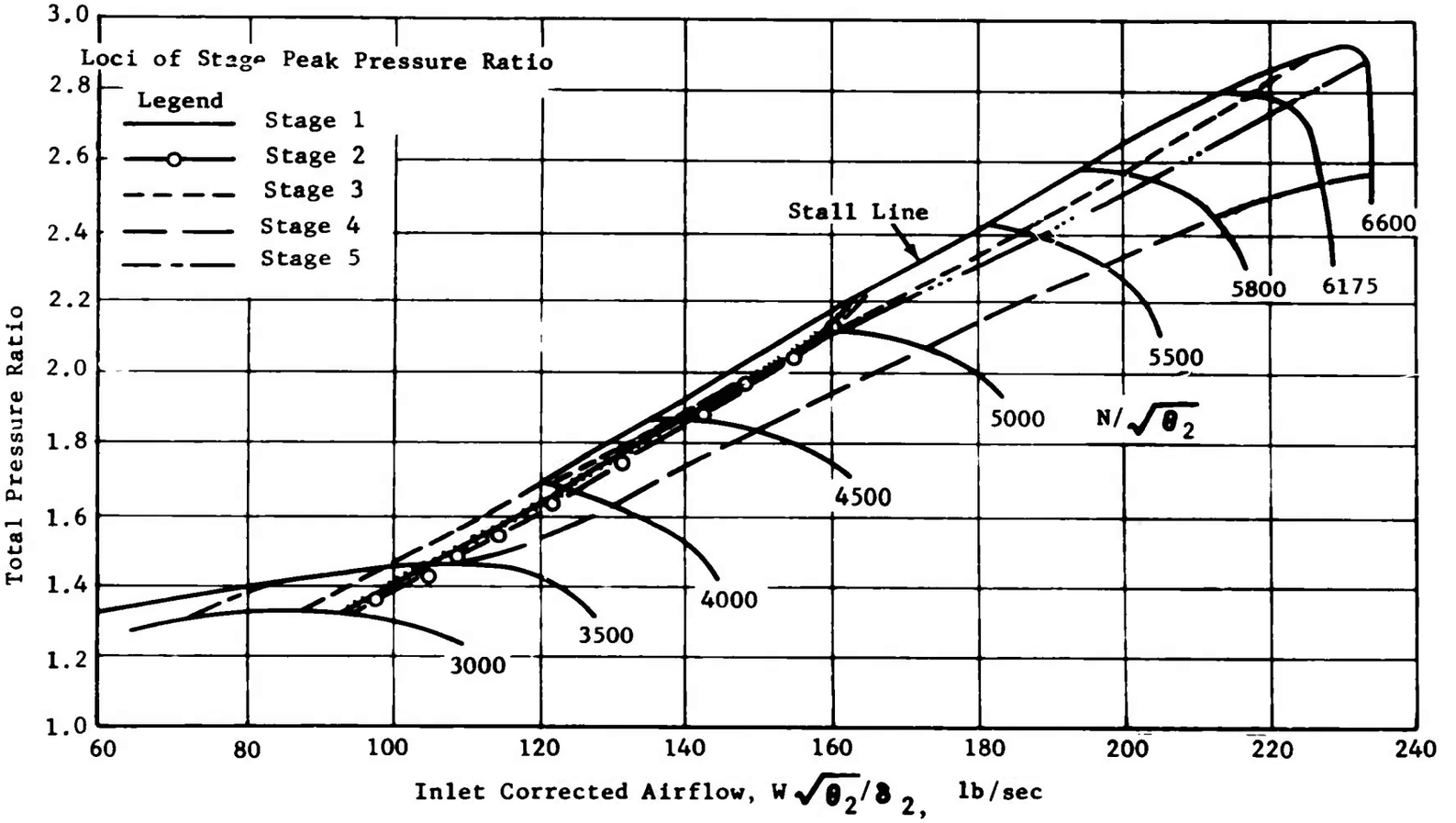

Figure 60. Loci of Stage Pressure Ratio Peak Values on the Performance Map of a 5-Stage Axial Compressor.

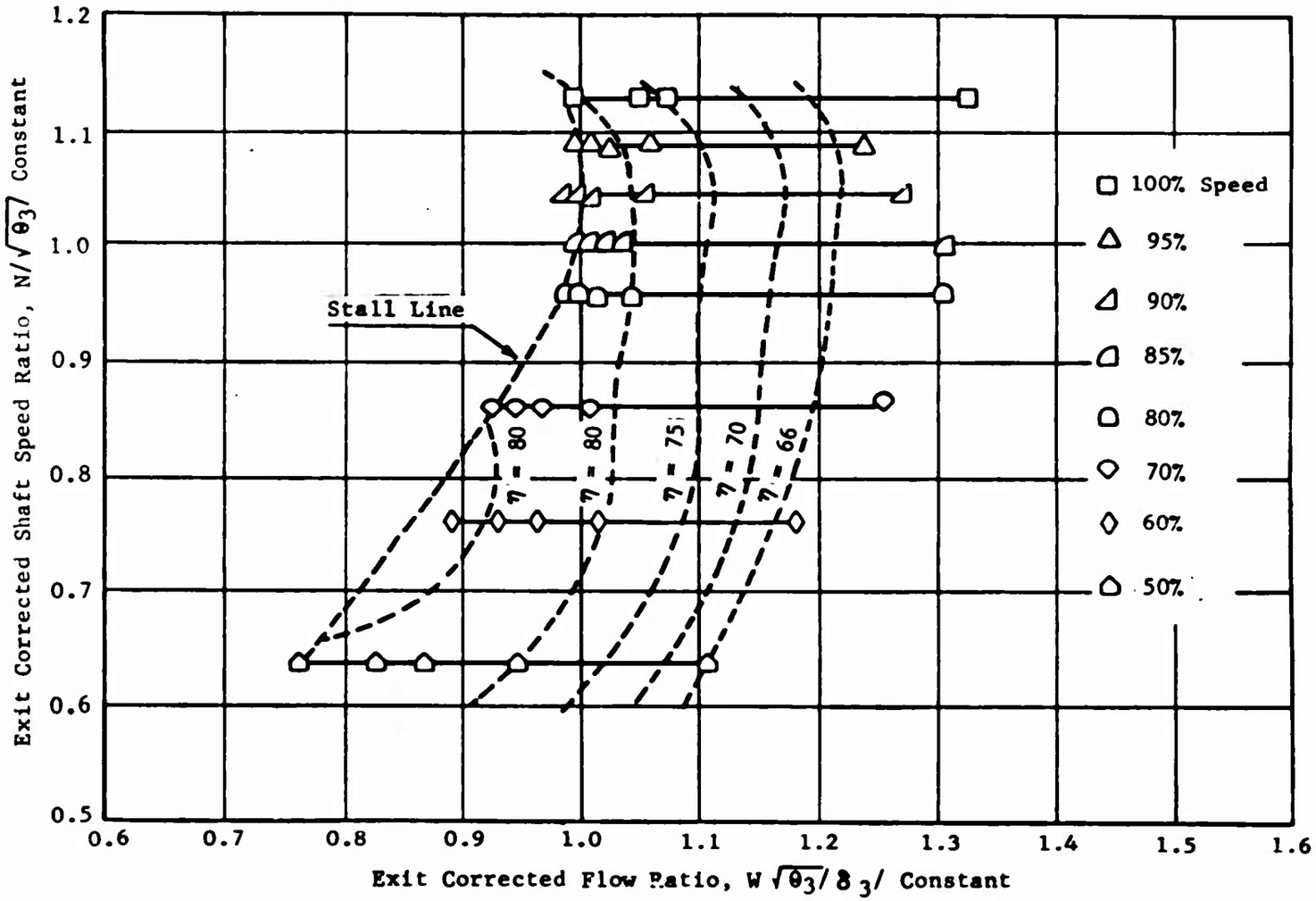

Figure 61. Compressor Stage Speed/Flow-Efficiency Match Relationships, 2.8 Supersonic (F1) Axial LP Compressor.

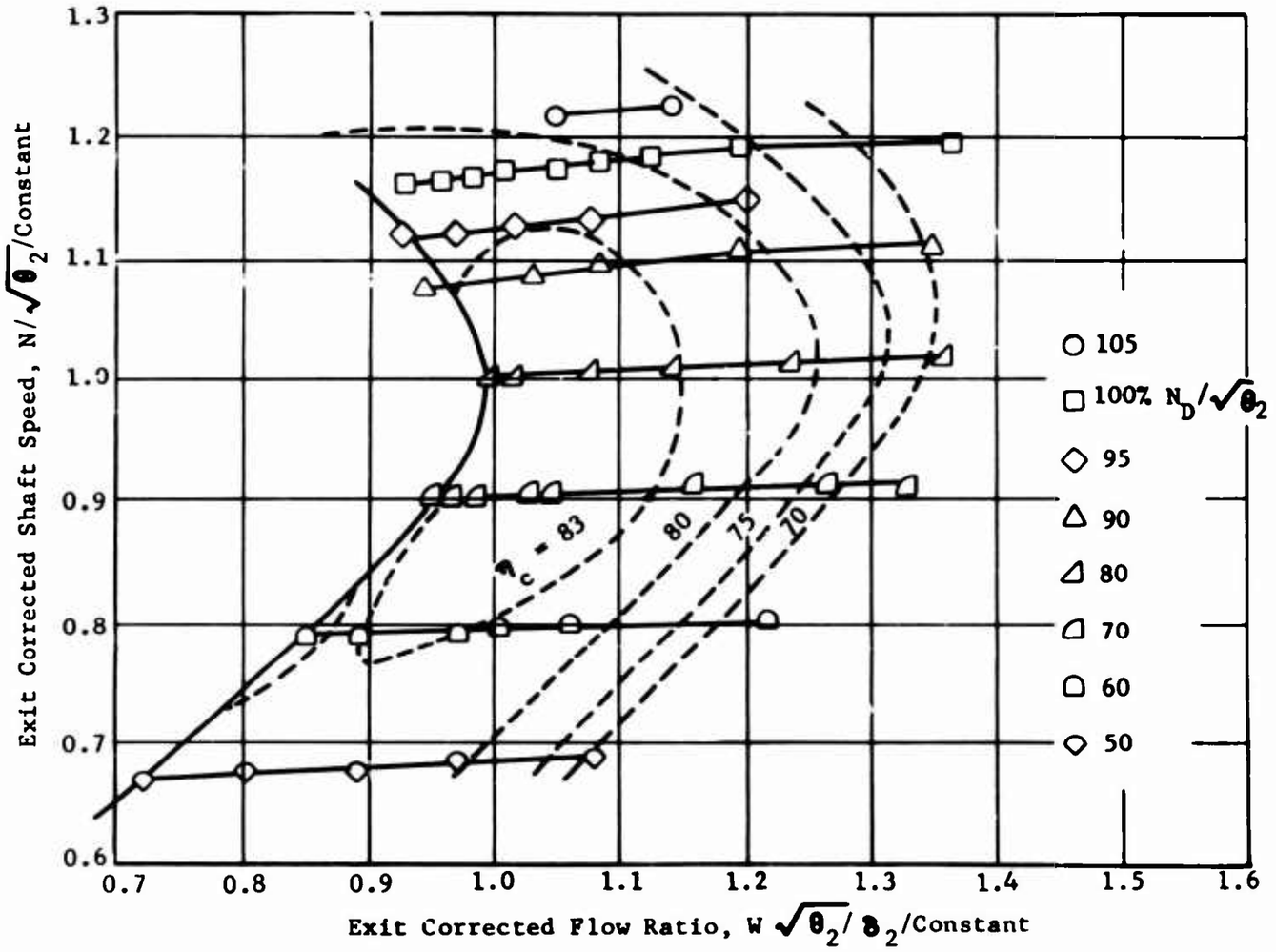

Figure 62. Compressor Stage Speed/Flow-Efficiency Match Relationships, Two-Stage Transonic (F1) Axial LP Compressor.

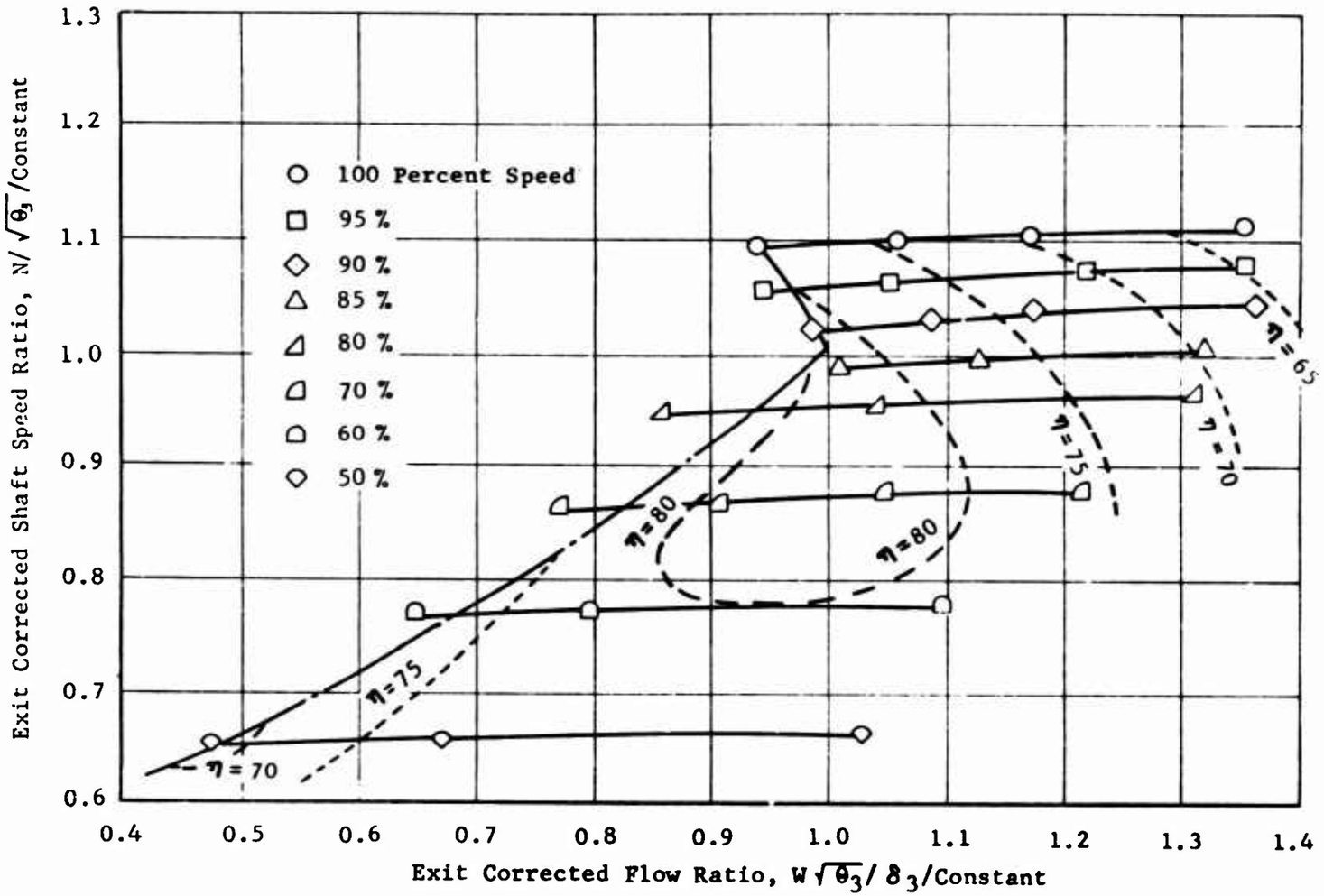

Figure 63. Compressor Stage Speed/Flow-Efficiency Match Relationships, 2.8 Supersonic (F1) Plus Transonic Axial LP Compressor.

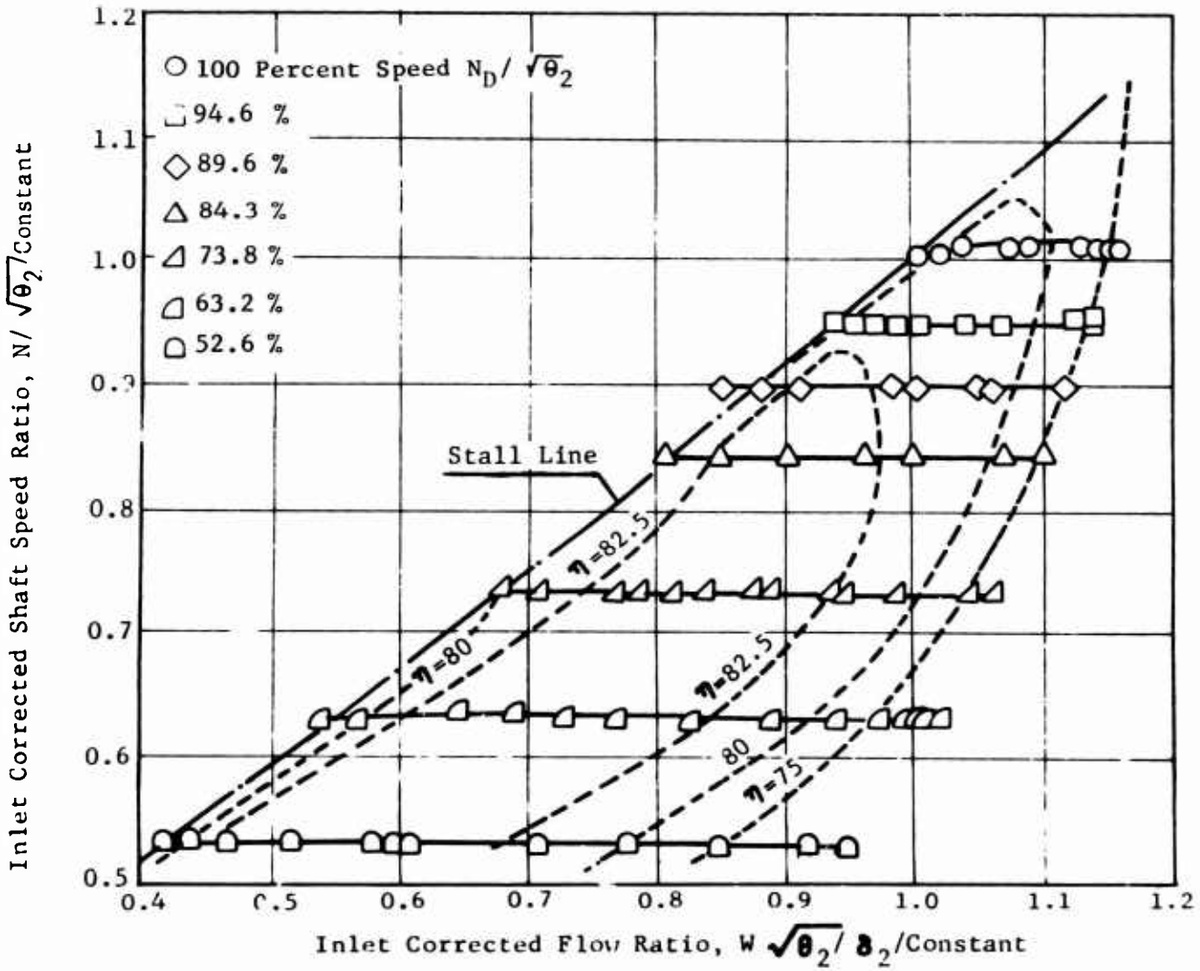

Figure 64. Compressor Stage Speed/Flow-Efficiency Relationships, 405 Centrifugal Stage HP Compressor.

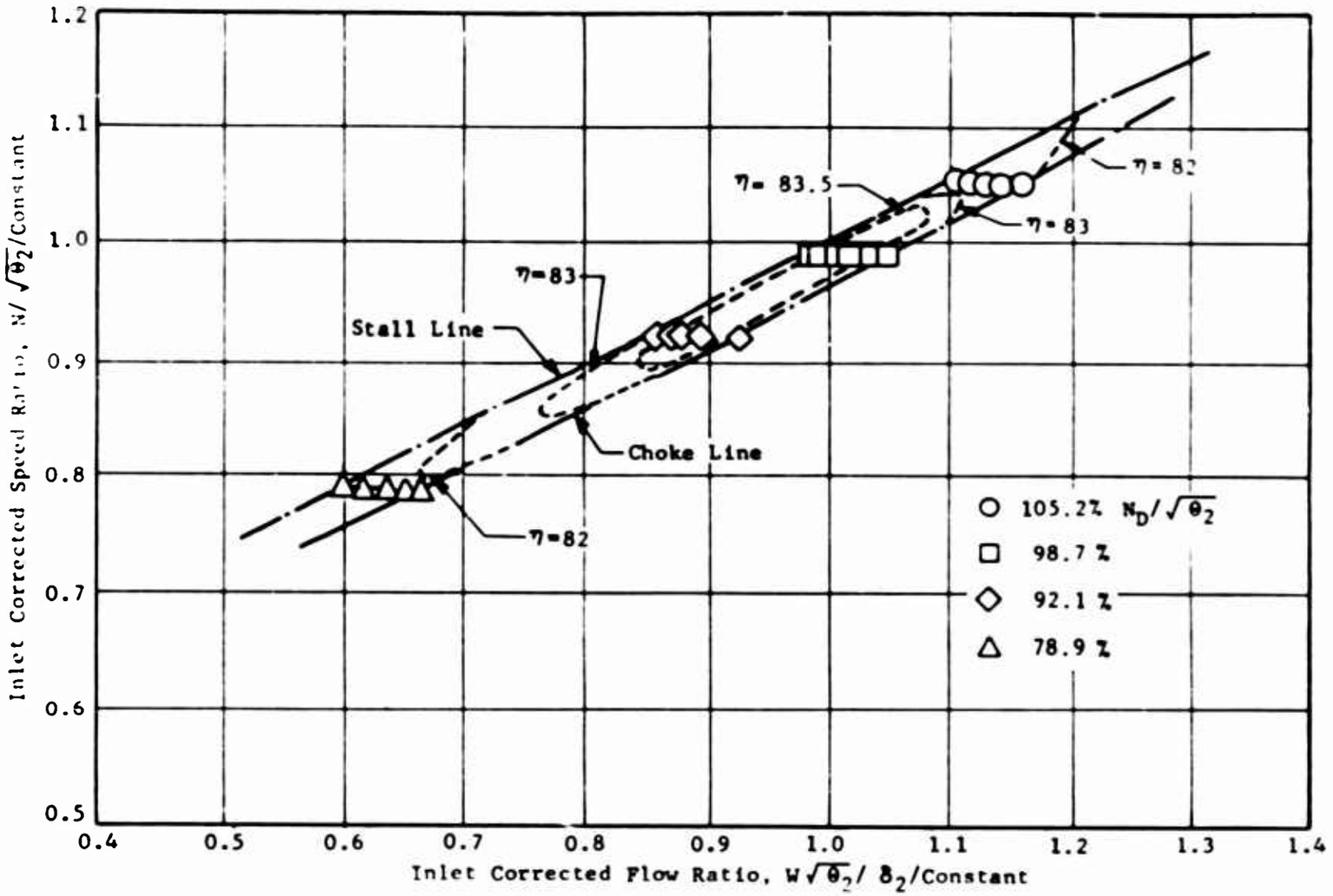

Figure 65. Compressor Stage Speed/Flow-Efficiency Relationships, PW-G Centrifugal HP Compressor.

corrected RPM is required to handle the whole range of LP speeds from 70 percent to 100 percent of design. The HP compressor can be designed to have its maximum efficiency and maximum pressure ratio in this region, thus taking maximum advantage of HP performance potential. The LP compressor performance is then varied to modulate the overall flow and pressure ratio. The actual speed relations in two-spool engines follow this pattern quite closely, but they cannot be determined exactly by study of the compressor alone. The relative speeds are affected particularly by power turbine area, with complex interrelations between turbine and compressor speeds, flows, and powers. Engine performance analyses are required for accurate solutions. The studies performed in the current program simply assumed that LP stall points could be placed on HP stall lines, with exceptions shown on the match diagrams, Figures 40 and 46.

Stator variable setting angles are a device for changing the flow of the compressors, so that the speed lines in Figure 38 are freed to move approximately horizontally. The stators which can be moved include the inlet guide vane and the stator of each axial stage, and the diffuser vanes of the centrifugal compressor. References 8, 10, and 12, respectively, reported that inlet guide vane restaggers alone provided only minor changes in the flow of specific supersonic, centrifugal, and transonic compressors. Rodgers, in Reference 13, reported that a diffuser vane variable setting angle was very effective for changing the flow for radial-flow compressors; this result gives cause to hope for similar effectiveness of exit stator variable setting angles for axial stages. Figures 66 through 68 present the results of a mean-radius mapping study, previously unpublished, on the flow-changing effects of varying the setting angles of inlet guide vanes and both stator rows of a two-stage transonic compressor. The curves are given for 100 percent, 80 percent, and 60 percent of design speed, and show percent variation of flow from design setting angles. Significant variations of flow are indicated. Compressor/engine matching studies in this program have assumed a fixed-geometry, fixed-area gas generator turbine, and fixed-geometry centrifugal compressor. It has become clear that HP compressor flow modulation is not required. In general, all operating points have good efficiency and avoid HP stall regions without HP flow modulation. Therefore, there is no need to vary the centrifugal compressor diffuser vane setting angles. LP compressor stator variable setting angles require a greater variation of HP speed than two spooling, but the variation of LP speed is smaller because the flow is modulated by stator vanes as well as by speed. The use of stator variable setting angles here has been assumed to permit modulating the LP flow so that the LP stall points were placed on HP stall lines, as shown in the match diagrams, Figures 42 and 44.

The basic relations of stage matching have been described to the extent that a reader will be able to follow the stage-matching investigations which are summarized briefly below. Appendix I should be consulted when more detailed information is needed.

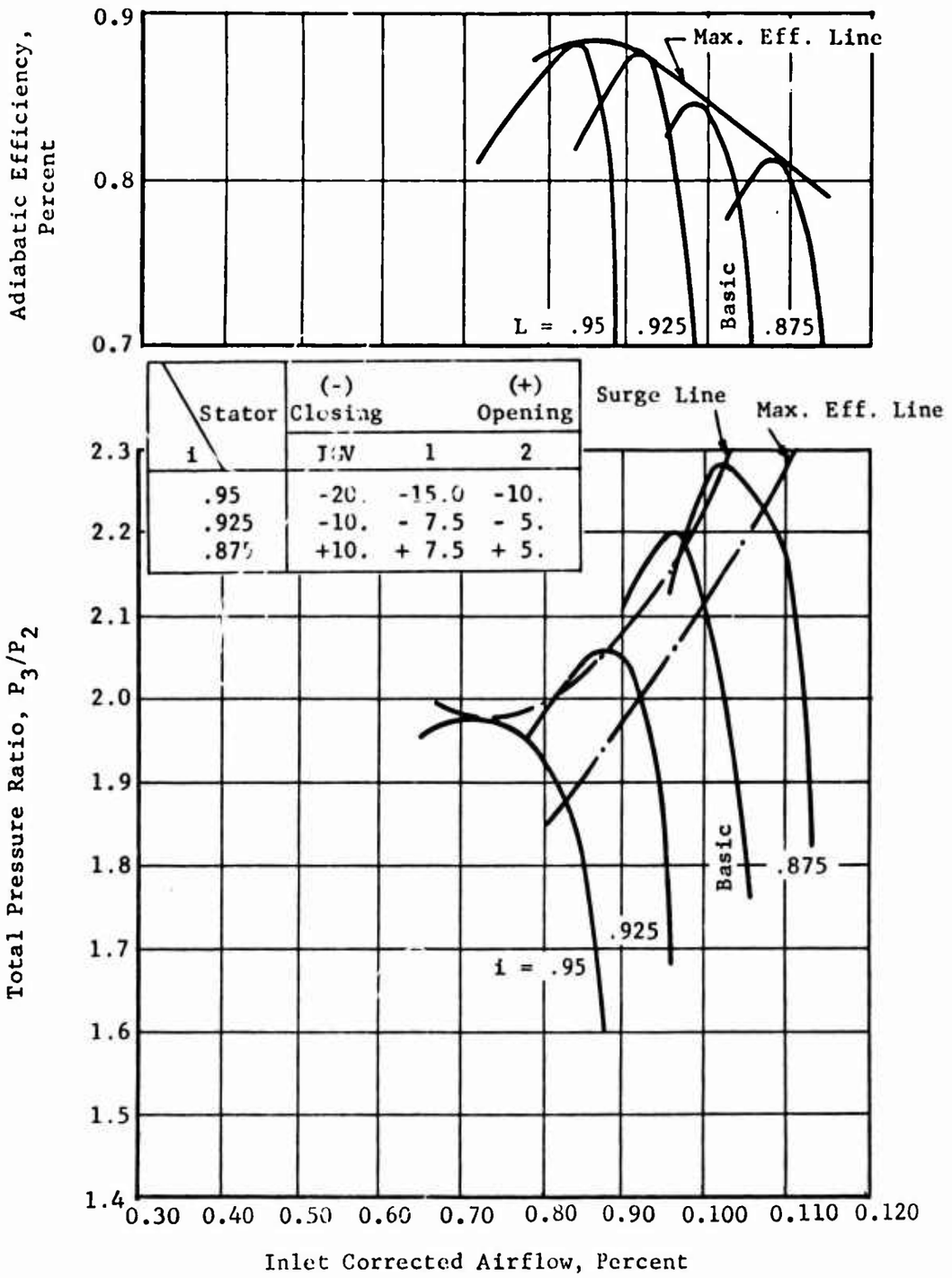

Figure 66. Estimated Performance Variation With Stator Setting Angle Variation at Design Speed.

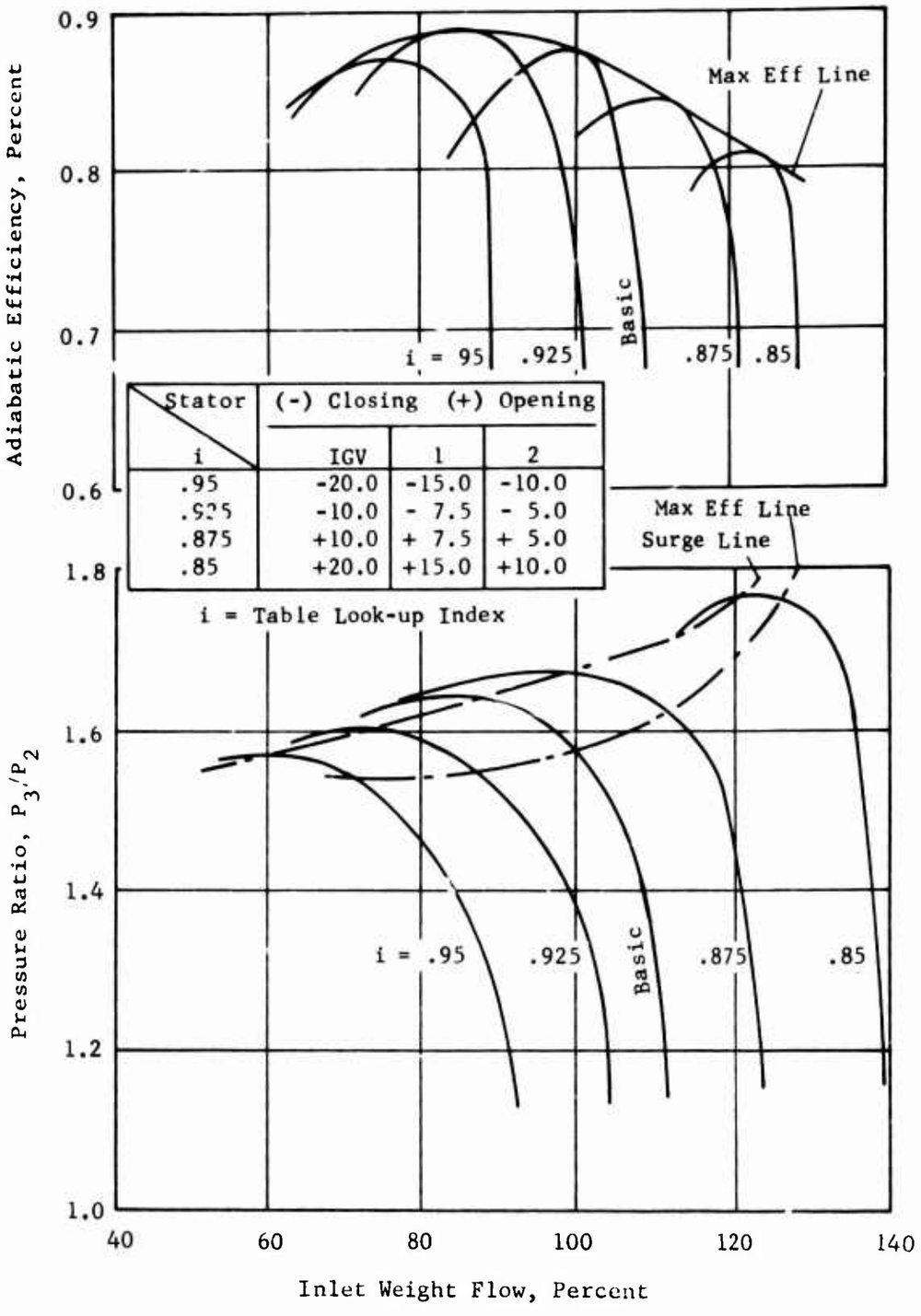

Figure 67. Estimated Performance Variation With Stator Setting Single Variation at 80% of Design Speed.

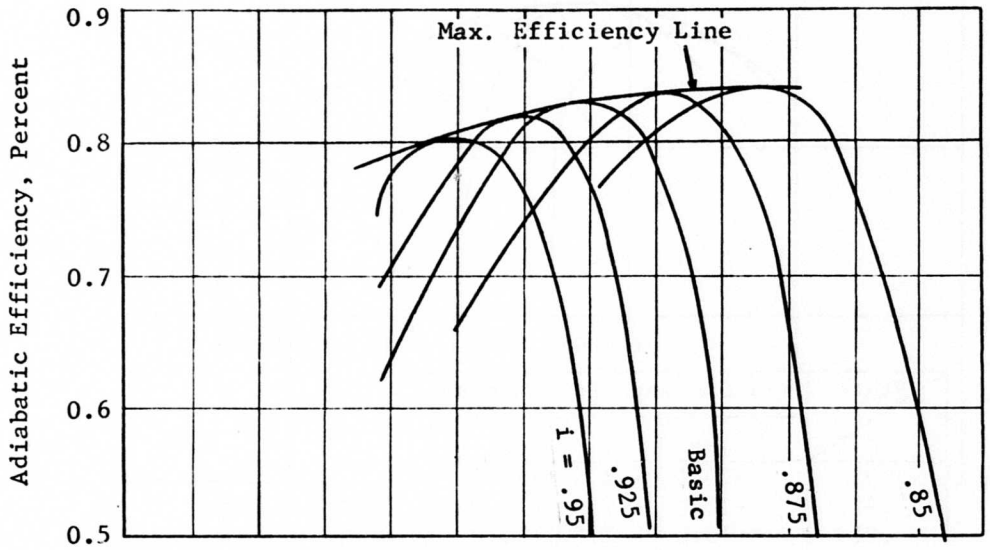

Stator Restagger Table			
Stator	(-) Closing		(+) Opening
i	IGV	1	2
.95	-20.0	-15.0	-10.0
.925	-10.0	-7.5	-5.0
.875	+10.0	+7.5	+5.0
.85	+20.0	+15.0	+10.0

i = Table Look-Up Index

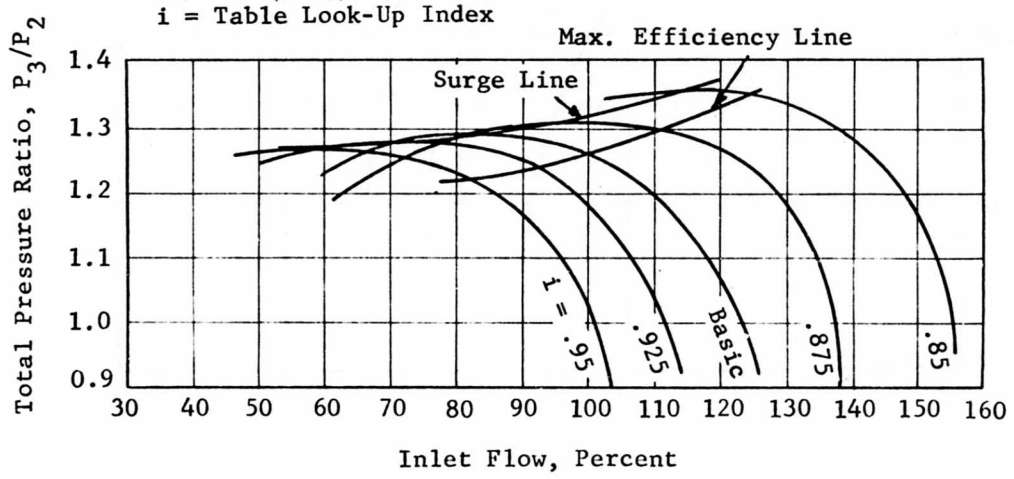

Figure 68. Estimated Performance Variation With Stator Setting Angle Variation at 60% of Design Speed.

1. Fixed Stator Compressors. The study of fixed stator compressors demonstrates many matching characteristics and in particular shows why and how the high-pressure-ratio compressor requires and benefits from variable geometry. The goals and approaches to matching were consistently guided by the need to satisfy the part-load minimum fuel consumption requirements and were influenced by structural considerations. In this discussion it is convenient to exhibit the compressor selections and the matching relations in chart form, as follows:

	S	TT	ST
405			
PW-G	Case 2, 1-90/87	Case 4, -1-83/88 Figs. 41 and 51	
RF-2		Case 1 - 95/94	

This chart shows the cases that were studied in the initial matching phase. Columns indicate which axial compressor was used in each match, and lines indicate which centrifugal, as follows:

S - one axial supersonic stage, see Figures 32 and 61.

TT - two axial transonic stages, see Figures 33 and 62.

ST - one axial supersonic and one transonic, see Figures 34 and 63.

405 - a centrifugal stage with moderate tip speed, see Figures 35 and 64.

PW-G - a centrifugal stage with intermediate tip speed, see Figures 36 and 65.

RF-2 - a centrifugal stage with high tip speed, see Figure 37.

The case numbers are used for reference in Table I, where all data about matching have been summarized. The numbers following the case number indicate the respective LP and HP percents of design speeds at which the stall line intersection occurs for that case. The Figure numbers refer to the LP/HP compressor matching curve and the compressor/engine matching curves, respectively. Graphed data are presented here only for cases of particular interest.

The stage matching work began before the mean-line mapping studies were started and continued after they were completed. Initially, it was supposed that stage combinations would optimize around part speed-points which could serve as 60 percent power points in the engine. Case 2, 1 was relatively high on the LP map according to this theory, but case 4, 1 was consistent with it. Both were relatively low on the HP map. The axial stage (LP) stall line places the 60 percent power operating points for cases 2, 1 and 4, 1 in stall at 2200°F and out of stall at 2100°F turbine inlet temperature. Both cases had maximum pressure ratio limited by maximum power at 100 percent power, a matter which is discussed further in Appendix II. The 60 percent power fuel consumptions of these machines were 0.47 and 0.475 at 2200°F when working at pressure ratios of 8.7 and 8.65 for cases 2, 2 and 4, 1 respectively. For case 1, the 60 percent power fuel consumption was .51 at 7.6 pressure ratio; pressure ratio was power-limited, as were the others, and efficiency was rather low.

A consideration of inlet temperature effects on centrifugal compressors indicated that the full aerodynamic corrected tip speeds developed in cold-air tests would not be available for supercharged stages because of two effects of heating: first, that the heated inlet air will raise the metal temperature, decreasing the permissable stress and permissable actual tip speed; and second, that the heated inlet air will raise the temperature correction and reduce the aerodynamic corrected speed associated with a given actual speed. Based on the design and the material of the RF-2 compressor, a stress scaling study indicated that centrifugal compressor actual tip speed should be limited to values lower than about 1850 ft/sec. By this standard it was found that the RF-2 corrected compressor tip speeds were too high. The design pressure ratio could not be approached, and the available data did not define enough of the low-speed performance. The next set of cases still followed the trend of low match speeds, and the lower speed 405 centrifugal compressor was used extensively.

	S	TT	ST
405	Case 5, 1-80/85	Case 9, 1-85/82	Case 7, 1-82/86
PW-G			Case 13,1-91/84

Data for these cases are given in Table I. The lower pressure ratios resulted in higher 60 percent power SFC values. The best case was 13,1, for which the higher LP match speed gave a higher pressure ratio. In case 5, 1, the LP was free of stall at all speeds because of the low LP match speed and the broad range of the centrifugal. For the other cases, the 60 percent power points were in the stall region of the axial (LP)

stages. Except for case 13,1, the pressure ratios for 60 percent power were power limited, with centrifugal tip speeds below the 1850 ft/sec level. Case 13,1 had 1860 ft/sec tip speed at the power-limit points, and can be regarded as being speed-limited.

The power-limited match cases were unable to develop the potential which was available structurally. That is, the optimum pressure ratio turned out to have a lower value than what could be attained simply by running to acceptably higher speed. At about this point in the program, it was learned from the mean-line mapping program that the design-point had to be moved to speeds near design to minimize part-power fuel consumption. The corresponding lesson from the matching procedures was that the match points had to be moved to higher LP and/or HP speeds. This direction was followed in the next set of stage combinations.

	S	TT	ST
405	Case 5, 2-90/92	Case 9, 2-93/89	Case 7, 2-90/92 Figures 45 and 56
PW-G	Case 2, 2-95/90	Case 4, 2-92/84	Case 13,2-100/90

In each of these cases the pressure-ratio values increased and the fuel consumptions decreased from previous values. The tip speeds in all cases but 13,2 were well below the 1850-ft/sec level and therefore showed potential for further increases. Axial stage stall occurred at 60 percent power for every case. An unusual kind of stall line appears in Case 7, 2 because of the wide operating range of the 405 centrifugal stage. In Figure 56 it may be noted that the 30 percent and 60 percent operating points lie just above the stall line, therefore just inside the stall region. It would be possible, by rematching the engine 100 percent power temperature at a lower pressure ratio, to move both operating points out of stall. At the same time, however, all of the operating points would probably move to lower flow and pressure ratio because of falling efficiency at high speeds. Part-speed specific fuel consumption would suffer seriously.

The broad range of the 405 centrifugal is due to the lack of a vaned diffuser, which can be replaced by a scroll diffuser with a loss in efficiency. It has been concluded from these compressor/engine matching studies that there is no need for this broader range. The stall line forms of the PW-G centrifugal compressors are well adapted to engine operation as developed. It is reasonable to expect that vaned (or channel

type) diffusers can be successfully developed for use with fixed-geometry gas generator turbines as required.

The investigations showed that high pressure ratio and low specific fuel consumption were attainable with fixed geometry at the cost of moving the axial stage stall line above the 60 percent power operating point. This came to be regarded with misgivings. The extrapolation of performance into the stall region was optimistic. There was experience with a two-spool engine in which the LP compressor stalled at exactly the points which were predicted from component tests, despite the stabilizing influence of an HP spool. There was a lack of information about the behavior of compressor components in steady surge or stall at high speeds. There were two ways of avoiding the problem: one, accept a fixed-geometry compressor at lower pressure ratio so that LP stall does not occur at 60 percent power, and rely on bleed to stabilize performance at lower power; two, use variable geometry. Both approaches were pursued. First, fixed geometry.

	S	TT	ST
405			
PW-G		Case 4,1-AAA-83/88 Figures 41 and 52	

This combination of stages was selected because it provided the best 60 percent power specific fuel consumption of the combinations which were free of stall at 60 percent power. It is a modification of case 4, 1, in that a different, more conservative approach was taken to extrapolating into the stall region - see Appendix I - and additional speed lines were interpolated. The 60 percent power point at 2100°F is clear of axial stage stall. Bleed was not incorporated in the calculations of low speed performance, though it was counted as a necessary part of the engine.

The flow path of the compressor was defined and then a review of the program was conducted. It was found that the earlier limit of 1850 ft/sec tip speed was conservative. The use of a different titanium alloy and a change of the centrifugal rotor configuration to a higher hub/tip ratio at inlet, as compared to the RF-2, resulted in raising the permissible speed to a level near 2300 ft/sec. Stages were matched to show the performance potential of the higher tip speed, as follows:

	S	TT	ST
405			
PW-G	Case 2,3-95/101 Figures 39 and 49	Case 4,3-95/92 Figures 43 and 54	Case 13,3-95/88 Figures 47 and 59

The performance for these cases was used in an evaluation of performance as part of a rating system given subsequently. These compressors were fixed-stator machines; cases 2, 3 and 13, 3 were power limited at 2000 and 1870 ft/sec respectively, and case 4, 3 reached 100 percent LP speed at 1950 ft/sec centrifugal tip speed. Axial stage stall was indicated at 60 percent power for cases 2, 3 and 13, 3.

Figure 69 shows the effect of centrifugal compressor tip speed on 60 percent power performance of fixed-geometry compressor engines. Raising tip speed generally raises pressure ratio and reduces brake specific fuel consumption.

2. Two-spool, fixed-stator compressors were matched to determine the potential of this variable-geometry system. The match selections were influenced by the same factors which operated on the fixed-geometry matches described above. Because of the speed flexibility of the two-spool system, the LP match point was always denoted as 100 percent speed, and the HP match point selection tended to be more significant. The PW-G centrifugal was most often used as the HP compressor; as seen in Figure 65, the maximum efficiency region occurred between about 90 and 103 percent of design speed. Higher speeds entailed higher pressure ratio and higher tip speeds, and vice versa. The 405 centrifugal showed maximum efficiency at lower speeds, but was matched at higher speeds for high pressure ratio. An effect of two-spooling is to improve the high-speed matching of the compressor elements to that power-limiting tends to disappear as a factor determining maximum pressure ratio. The following two-spool cases were matched.

	S	TT	ST
405		Case 10-100/100	Case 8-100/100
PW-G	Case 3-100/95 Figures 40 and 50	Case 11,1-100/105 Figures 47 and 57 Case 11,2-100/88 Case 11,3-100/99	Case 14-100/90

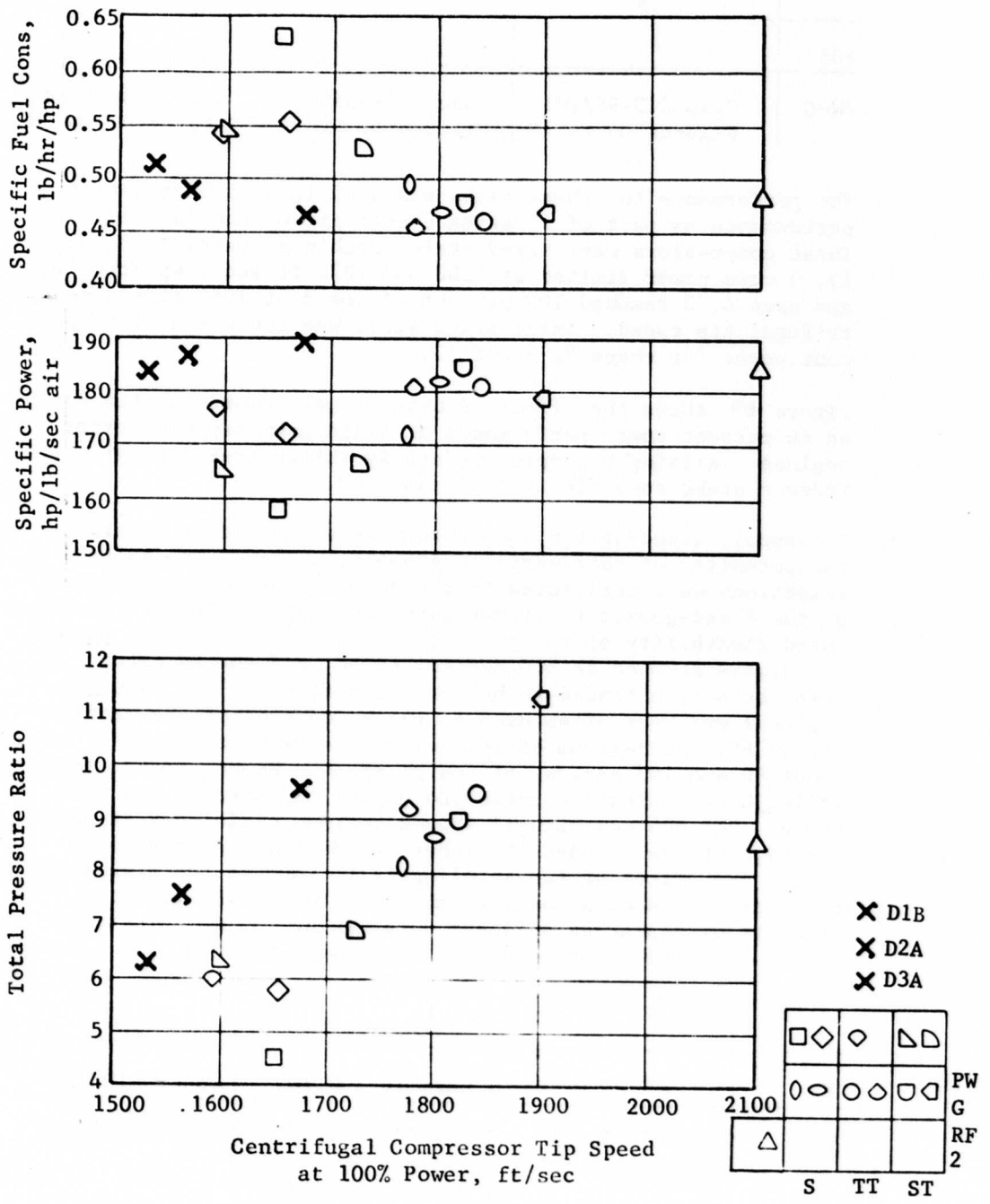

Figure 69. Effects of Centrifugal Compressor Tip Speed on 60% Power Performance of One-Spool Compressor Engines.

The stall line of the matched compressor is the stall line of the HP centrifugal compressor. Axial stage stall coincides with the HP stall. As noted above, the accurate matching of a two-spool engine compressor is not possible without consideration of other engine components in a complete engine system matching analysis; therefore, the present match must be considered to represent a potential of two-spool systems which may not be entirely fulfilled.

The performance of engines incorporating these cases is summarized in Table I. In Figure 70, the 60 percent power engine performance is plotted against centrifugal compressor military power tip speed. It is shown that higher tip speed yields higher pressure ratio and lower fuel consumption, as promised by the parametric cycle data.

3. Variable Stators. The misgivings, noted above, about operating a fixed-geometry compressor at relatively high speeds with LP stages in stall led to the investigation of two stage combinations with variable stators, as follows:

	S	TT	ST
405			
PW-G		Case 4,1-VS 83/88 Figures 42 and 53 Case 4,4-VS 95/105 Figures 44 and 55	

The LP flow in case 4,1-VS was required to be increased for LP speeds above 83 percent to take advantage of the full high-speed LP pressure ratio capability. As a result, the flow at LP design speed increased from 5 to 6.6 lb/sec. The compressor/engine match showed no power limit below design speed and thus presented a theoretic possibility of pushing the military point to 100 percent LP speed, with benefits to 60 percent power specific fuel consumption. At lower speeds, the LP flow was decreased to move the stall line over to the HP stall lines. These moves could be made freely in the matching study without serious questions of actual feasibility.

In choosing the stage combination for the final preliminary design, case 4,4-VS, a more conservative approach was taken. The actual desired match point was 95/105 for the military point and was assumed to be a nominal stator setting angle. The speeds for both LP and HP were at high efficiency (see Figures 62 and 65) but were above the maximum values of efficiency islands to give high pressure ratio from each stage. Operation

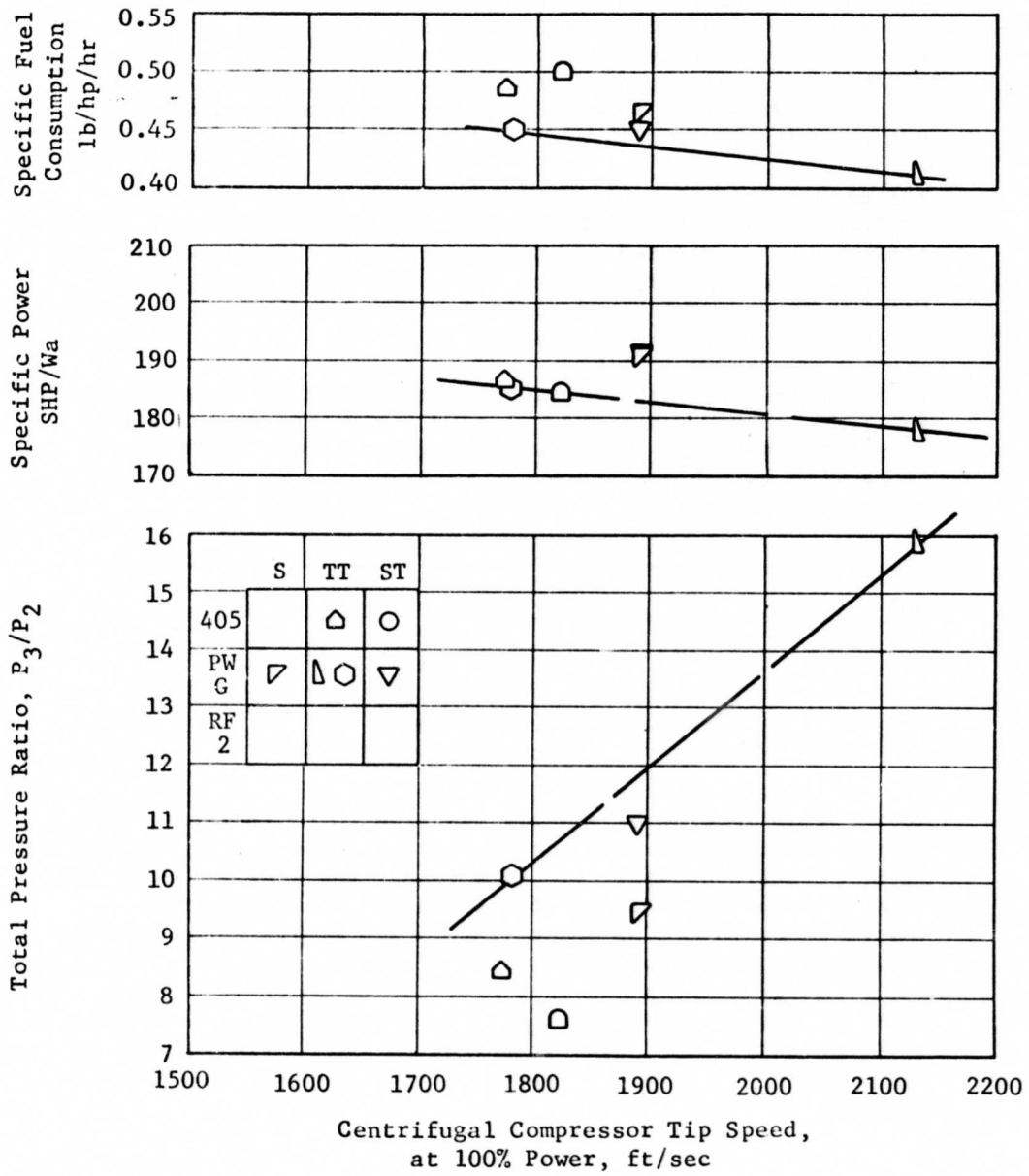

Figure 70. Effects of Centrifugal Compressor Tip Speed on 60% Power Performance of Two-Spool Compressor Engines.

at lower speeds depends on variable stators which decrease LP flow so that the LP stall line falls upon the HP stall line, eliminating LP stall.

The compressor/engine match that resulted was not power limited and permitted operating at the 95 percent speed with military power as desired, with a centrifugal compressor tip speed of 2050 ft/sec.

4. Compressor Peak Efficiency Location. Following the indications about the optimum design point from the mean-line mapping study and about the optimum matchpoint from the stage matching studies, a study was made of the compressor peak efficiency location which would provide minimum 60 percent power fuel consumption. The military power point was assigned a fixed turbine inlet temperature of 2500°F, and the military flow rate was denoted 100 percent flow. The maximum efficiency was determined as previously defined in Figure 20 for an LP compressor with two transonic stages.

   It was noted from experience that compressor efficiency usually comes to a peak at some point in the engine flow range. It was supposed that the peak could be caused to occur at either 50 percent, 75 percent, or 100 percent of military flow, and that efficiency would vary according to a parabolic law at points away from the peak, as shown in Figure 71. With these suppositions, some possible 60 percent power performance points were computed as shown in Figure 72 for military pressure ratios of 10, 15, and 20. It is shown that minimum SFC for 60 percent always occurs for case C, wherein the efficiency peak is located at military power flow. It is also noted that 60 percent power SFC decreases by 8 percent as military pressure ratio is raised from 10 to 15, and by 2 percent as pressure ratio is raised from 15 to 20.

   Further examination shows that the efficiency at 60 percent power minimum SFC is within 2 percent of peak efficiency in every case, a relatively insignificant variation. The decisive effect of peak efficiency location is that the movement of peak efficiency to lower flows also moves the optimum 60 percent power point to lower flow and particularly to lower pressure ratio.

   An insight growing out of this study relates to engine size. Given a military pressure ratio and a peak efficiency value, and other things equal, the best military specific power occurs if peak efficiency is located at military. This gives the smallest possible engine for a given power level. Any other location of peak efficiency gives a larger engine, as reflected in absolute airflow required at military power. For the 15:1

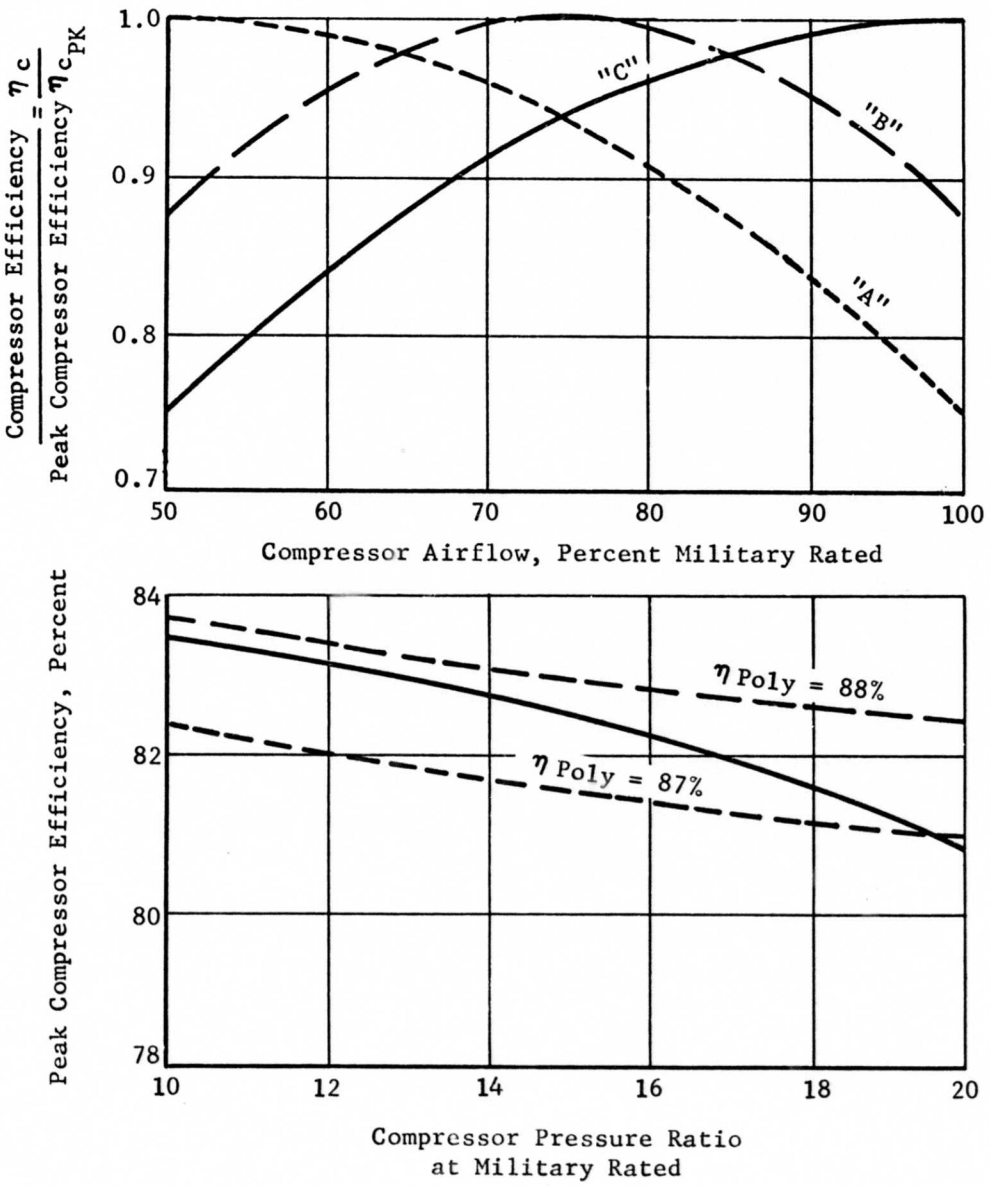

Figure 71. Effects of Compressor Peak Efficiency Location, Efficiency Variation Assumptions.

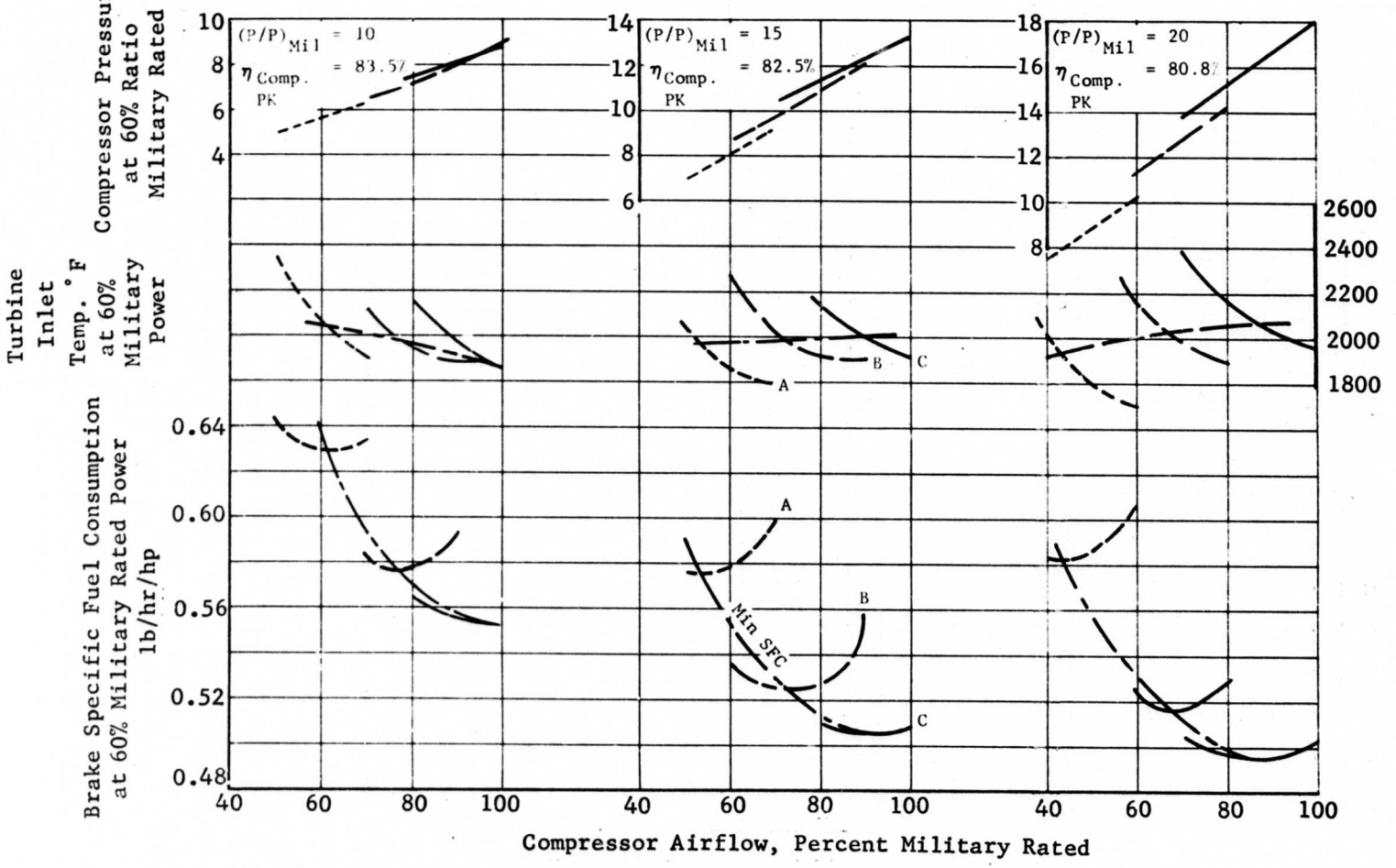

Figure 72. Effects of Compressor Peak Efficiency Location 60 Percent Power Performance vs. Percent Military Airflow for Military Pressure Ratios of 10, 15, and 20 at Turbine Inlet Temperature 2500°F.

military pressure ratio, Figure 73 shows the variation of performance with location of the efficiency peak as a function of absolute airflow. The engine is required to be larger as peak efficiency is moved away from military and as military efficiency decreases. As the engine becomes larger, the 60 percent power minimum SFC gets larger. Therefore, the smallest engine is also the engine which gives the best SFC at part load. The determining factor in size is military efficiency, and the peak can be moved somewhat without causing much change of efficiency or size. Movement to this extent will probably not impair 60 percent power SFC. Movement of the peak toward lower flow will favor part-load performance; but movement toward higher flow should impair part-load performance, because of the decrease of compressor efficiency.

These results agree with the trends of the cycle analysis given in Figures 1 to 13, that BSFC decreases as efficiency is increased and as pressure ratio is increased. They also agree with results of the mean-line mapping and stage matching studies. The mean-line mapping study showed that the design should be optimized for a higher speed, which results in a higher pressure ratio for all operating points and a maximum efficiency near military power. The stage matching study showed that good matching at high speeds is optimum because it too results in a higher pressure for all operating conditions and high efficiency near military power.

Power Turbine Flow Area

The power turbine flow area can be made variable at a cost in mechanical complexity and in somewhat reduced turbine efficiency. The variation of the turbine flow area can be used to change the gas generator operating conditions at various part-load operating conditions. At a given power, reducing the power turbine area will cause an increase in turbine inlet temperature and a reduction in airflow and pressure ratio. Since these changes cause a movement from one point to another on the compressor performance map, a change of compressor efficiency will also be expected to occur. Furthermore, engine specific fuel consumption may be expected to change.

The effect of compressor characteristics on part-load performance of a 2500°F single spool free turbine engine was investigated using a predicted performance map, Figure 52, for the fixed-geometry preliminary design. Engine performance was evaluated using three possible engine operating lines, two being achieved using power turbine variable geometry: (a) using performance map efficiencies and (b) assuming constant efficiency over the entire map to isolate cycle performance effects. The three operating lines, shown in Figure 52, were: (a) fixed power turbine geometry, (b) reducing power turbine area to hold turbine inlet temperature constant at part load, and (c) increasing power turbine area to hold RPM constant at part load.

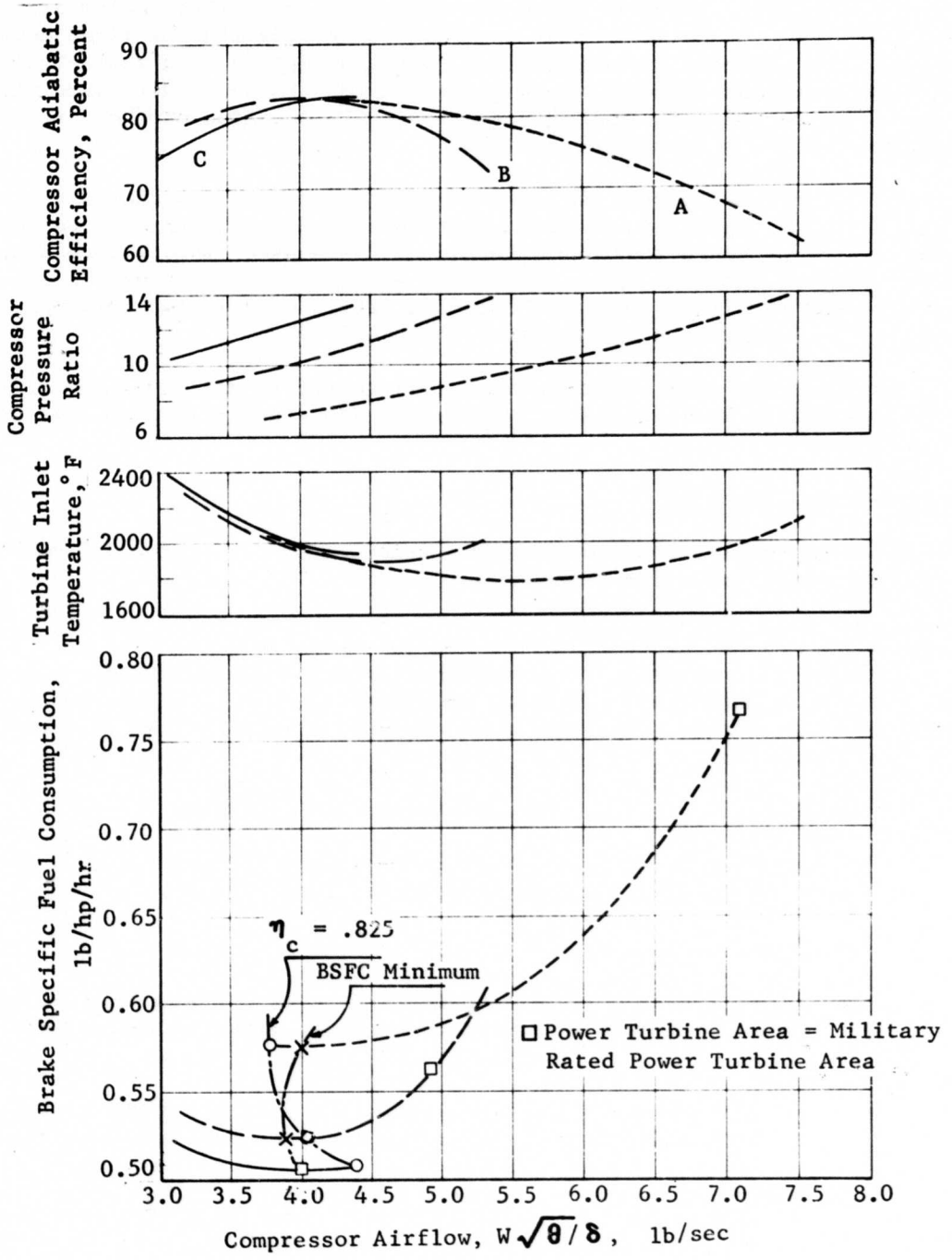

Figure 73. Effects of Compressor Peak Efficiency Location, 60% Power Performance vs. Airflow for Military Pressure Ratio of 12:1 and Turbine Inlet Temperature of 2500°F.

The results of the analysis using the compressor map efficiencies are shown in Figure 74. It is shown that an engine operating line at fixed power turbine area produced lower part-load fuel consumption than that obtained at either constant temperature or constant RPM. These results were attributed partly to the fact that the compressor was operated on the performance map close to the peak efficiency line.

The results of an analysis wherein efficiency was held constant are given in Figure 75. Again it was found that the operating line at fixed power turbine area produced lower part-load fuel consumption than at constant temperature or constant RPM. Therefore, it was shown that there were advantages for the fixed-area case stemming from a complicated interplay between cycle temperature and pressure ratio effects.

This study showed that, in this case, performance is optimized and mechanical complexities are avoided by selecting a fixed power turbine area for the engine.

Selected Configuration

The final compressor configuration was selected by use of the following information and selection procedures.

Two-Spool Versus One-Spool

A rating of compressor types was developed to rationalize the selection between one-spool and two-spool compressors and between several available axial stages. The two-spool compressor received the following considerations.

Two-Spool Compressor With Front Drive Free Turbine

A two-spool compressor provides high pressure ratio with a wide range of flows and pressure ratios at good efficiencies.

Two-spooling is judged to offer benefits as follows:

1. Two-spooling serves the same purpose as variable stators and therefore makes their use unnecessary with the following benefits:

   - Blade ends inside and outside the casing are not cluttered with modifications and parts required for varying blade settings.

   - Leakage at blade ends is better controlled with better performance over a wide range of speeds.

   - Stage type selection, design, and development are freed of consideration of variability requirements and effects.

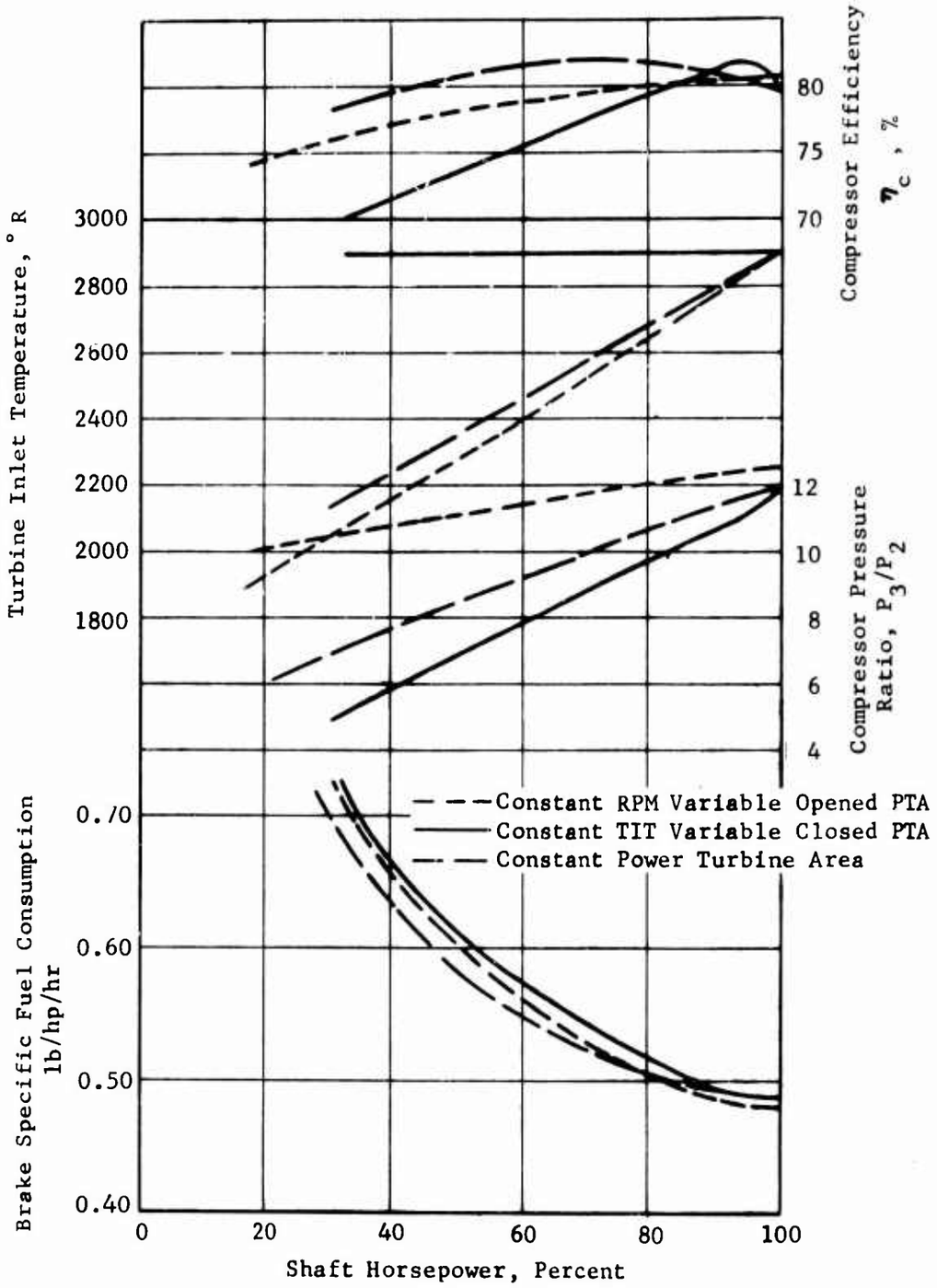

Figure 74. Effect of Variable Power Turbine Area on Part-Load Fuel Consumption, Efficiency Based on Compressor Performance Map, Case 4,1-AAA.

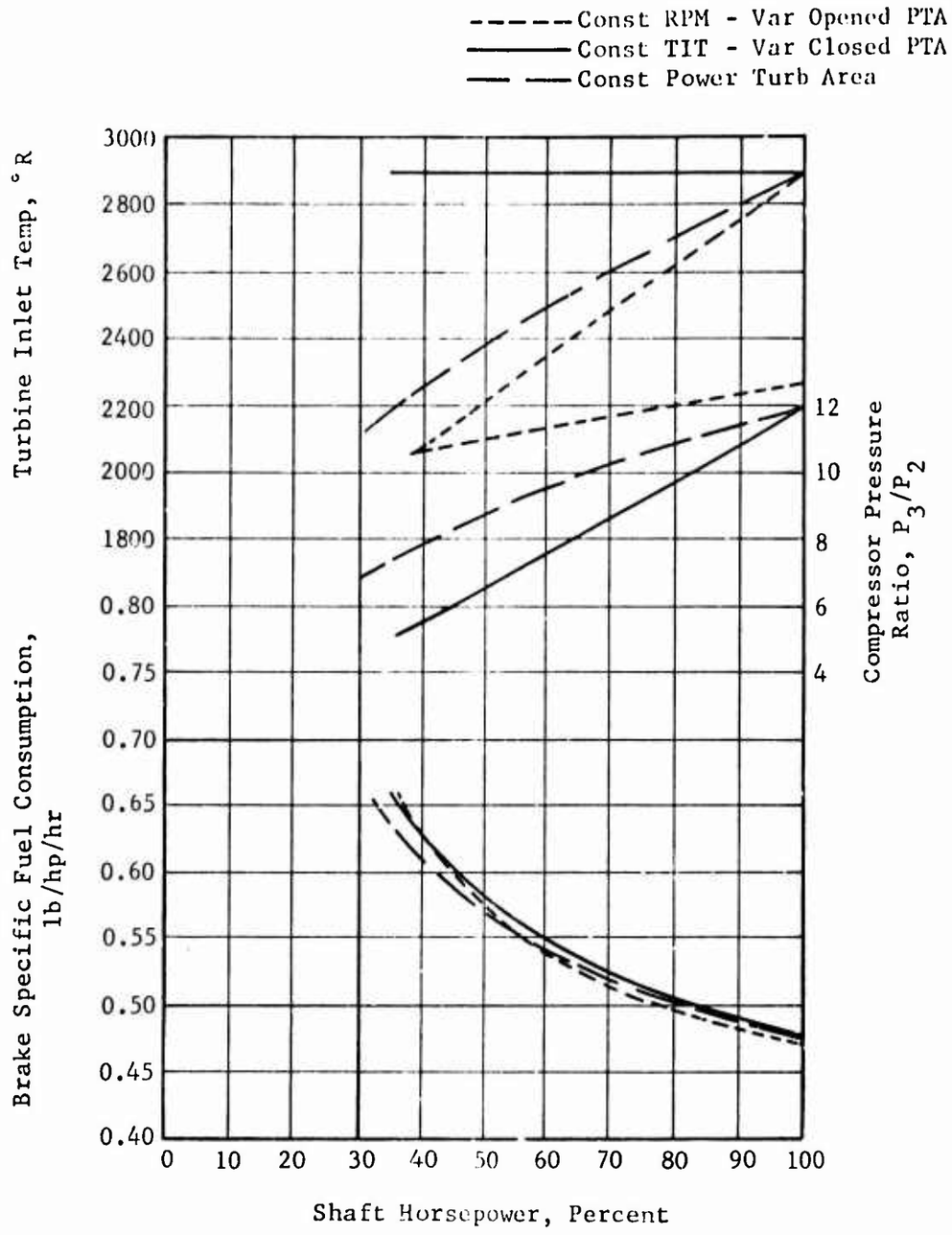

Figure 75. Effect of Variable Power Turbine Area on Part-Load Fuel Consumption With Compressor Efficiency Constant.

2. The axial and centrifugal spools can be designed for different shaft speeds as required for optimization of each.

3. Lubricated, enclosed bearings should give better durability than stator actuation linkage joints and stator trunnions.

4. The cost of corresponding replacement parts, i.e., bearings and seals, should be less than a set of stator trunnion and linkage bushings.

5. Because of detailed flow path smoothness and greater matching flexibility, better overall efficiency will yield better SFC.

Two-spooling with coaxial front shaft is judged to have added weight and to present excessive complications for a three-year development program for the following reasons:

1. A requirement of the system is to minimize the hole diameter in the centrifugal compressor disc, so that useful pressure ratios and tip speeds can be produced. For a 4.4 lb/sec machine, a hole maximum diameter of 2 inches is regarded as reasonable. As a result, the drive shaft is slender and long with critical speeds at about 8000 RPM and 25,000 RPM. Control of vibrations presents excessive development risk.

2. Bearings must operate at or beyond limits of state-of-the-art DN values for rolling element bearings.

3. Oil scavenging with restricted shaft size and limited line access spaces promises serious design compromise and high development risk.

Two-Spool Compressor With Coupled Power Turbine

The advantages of two-spooling prompted the investigation of means other than a coaxial shaft for providing a front-drive engine.

1. LP coupled power turbine. The drive shaft would be fastened to the LP shaft, thus avoiding the need for a third coaxial shaft. This is a feasible cycle which has been investigated at Curtiss-Wright in the past. It is judged to be unacceptable for the following reasons:

   - Helicopter shaft speed is nearly constant from 30 percent to 100 percent power. Holding the LP compressor shaft speed constant prevents flow variation as a means of power modulation. Compressor matching at off-design speeds is inconsistent with cycle requirements.

2. HP coupled power turbine. The drive shaft is coupled through gears to the HP spool, providing a power shaft parallel to, but offset from, the two-spool turbomachinery shafting. The gearing would interrupt the flow path of an axial-flow compressor engine, but the centrifugal compressor discharge can be collected in one or more pipes to bypass the gearing.

   Advantages are:

   . A constant-speed HP spool is better suited to compressor matching than constant-speed LP.

   . Some speed reduction could be taken.

   . Accessory drives could be incorporated in the same gearbox.

   Disadvantages relative to other systems were judged to be overriding, as follows:

   . Engine size and weight would be excessive.

   . Added complexity of gear drive is excessive, for development and maintainability.

The ratings of various stage types were based on the data given in Table II, derived from preliminary matching studies based on fixed-stator configurations, but recognizing a need for variable stators in the projected compressor.

Tables III and IV were developed as an aid in selecting the axial-stage type for a single-spool, variable-stator machine of 60 percent power pressure ratio at 12 or above.

The merit scale is as follows:

Merit Rating	Value Definition
5	Most desirable
4	
3	
2	
1	Least desirable

Weighting factors are given to line items, as noted in the weighting column. Group or category weight factors are calculated on the basis that a maximum value in every line would score the percentage allocated for the category.

TABLE II. ONE-SPOOL COMPRESSOR AXIAL STAGE TYPE RATING DATA

No. of Axial Stages	0	1	2	2
Type Axial Stages	0	S	TT	ST
Matching Case	12	2,3	4,3	13,3
SFC 60 Percent Power	.485	.455	.455	.446
30 Percent Power	.6	.54	.53	.535
100 Percent Power	.43	.405	.40	.402
BHP/Wa 100 Percent Power	235	237	240	235
At 60 Percent Power				
P/P	8.9	11.6	12	12.8
η_c	78.2	78	77	77
Axial Stall	0	Yes	No	Yes
Δ_η (development)	+6	+5	+2.5	+5
At 100 Percent Power				
P/P	11.9	15.3	16.0	17.1
η_c	77	78	79	77
U_t Centrifugal	2100	2000	1950	1870

Note: All axial stators are to be movable to guarantee 30 percent power stall-free operation and adequate starting. No. of movable stators = 1 + No. of axial stages.

TABLE III. ONE-SPOOL COMPRESSOR AXIAL STAGE TYPE MERIT RATINGS

Axial Stage Type	Merit Rating				Weight Factor	Score			
	0	S	TT	ST		0	S	TT	ST
Fuel Consumption									
60 Percent Power	1	4	4	5	5	5	20	20	25
30 Percent Power	1	3	5	4	2	2	6	10	8
100 Percent Power	1	3	5	4	1	1	3	5	4
Sum					8	8	29	35	37
Category Weight 40/40					40	8	29	35	37
Size, Minimum									
SHP/Wa 100 Percent Power	3	4	5	3	1	3	4	5	3
No. of Axial Stages	5	4	3	3	1	5	4	3	3
Sum					2	8	8	8	6
Category Weight 15/10					10	12	12	12	9
Mechanical Complexity, Lack of									
No. of Axial Stages	5	4	3	3	1	5	4	3	3
No. of Variable Stators	5	4	3	3	1	5	4	3	3
Sum					2	10	8	6	6
Category Weight 10/10					10	10	8	6	6
Cost, Minimum									
No. of Axial Stages	5	3	1	1	1	5	3	1	1
No. of Variable Stators	5	3	1	1	1	5	3	1	1
Sum					2	10	6	2	2
Category Weight 10/10					10	10	6	2	2
Development Status									
Compressor Efficiency	2	3	5	4	1	2	3	5	4
LP Stall Alleviation	5	2	4	3	2	10	4	8	6
Shaft Critical Speeds	5	4	3	2	1	5	4	3	2
Sum					4	17	11	16	12
Category Weight 15/20					20	12.75	8.25	12	9.00
Durability									
Variable Stators	5	4	4	4	1	5	4	4	4
Sum					1	5	4	4	4
Category Weight 5/5					5	5	4	4	4
Maintainability									
Variable Stators	5	3	1	1	1	5	3	1	1
Sum					1	5	3	1	1
Category Weight 5/5					5	5	3	1	1

TABLE IV. ONE-SPOOL COMPRESSOR AXIAL STAGE TYPE MERIT RATING SUMMARY

Category	Weight Factor	Axial Stage Type 0	S	TT	ST
Fuel Consumption	40	8.0	29.0	35.0	37.0
Size, Minimum	15	12.0	12.0	12.0	9.0
Mechanical Complexity Lack of	10	10.0	8.0	6.0	6.0
Cost, Minimum	10	10.0	6.0	2 0	2.0
Development Status	15	12.75	8.25	12.0	9.0
Durability	5	5.0	4.0	4.0	4.0
Maintainability	5	5.0	3.0	1.0	1.0
Sum	100	62.75	70.25	72.0	68.0

The following cases are considered in the rating systems.

Rating Case	Definition
0	There is no axial stage. The centrifugal stage is the Boeing RF-2 with improved efficiency.
S	The 2.8 supersonic stage with improved efficiency is the axial stage.
TT	The two-stage transonic compressor with improved efficiency in the axial stages.
S.	The axial stage consists of the 2.8 supersonic plus a transonic stage.

In types S. TT, and ST the centrifugal stage is based on the PW-G stage.

The highest ranked and selected axial compressor is type TT, the two-stage transonic compressor.

Rating comments are as follows: Type 0, with no axial stage, suffered because of low ranking for fuel consumption. In development status, a large efficiency increment requirement was balanced by the desirable lack of

stator variability and a short-length front shaft. Type S, with 1 supersonic stage, suffered in fuel consumption rank and in development status, where need is seen to demonstrate flow-variation capability. There is also a substantial efficiency increment. Type ST shared the limitations of the supersonic stage but showed better fuel consumption because of higher pressure ratio capability. Type TT showed less development risk with good fuel consumption, and this overbalanced the disadvantages of the added stage.

Comments about development status are relevant to future and current research work. The anticipated efficiency gain requirement risks for the supersonic and transonic stages presently favor the transonic axial compressor, a picture which can be altered by the current supersonic compressor stator research program. It is clear from these matching studies that single-spool compressors require axial stage flow variation as a means to give useful high-pressure-ratio performance, either by two-spooling or by variable stators. The capability of the supersonic and transonic stage for variable stator flow movement is an important factor in selecting and applying a type of stage, and it cannot be really known without experimental evaluation of theory. Therefore, the investigation of the flow-variation potential of both of these stages is of great interest. Ability to decrease flow at lower speeds is the required direction of flow variation.

Preliminary Design of Selected Configurations

Two preliminary compressor designs were produced: a fixed-geometry compressor and a variable-stator compressor. The discussion here takes up first the aerodynamic aspects of both compressors and then the structural or design aspects of both machines. The variable-stator compressor is the selected compressor and received more comprehensive definition than the other.

Fixed-Geometry Compressor Aerodynamics

The compressor consists of two transonic axial stages and a centrifugal stage. Based on the previous findings of the study, the military-rated operating point was selected as the design point. Table V gives the design point operating conditions, the stage design point performance values, and the flow path dimensions. The overall pressure ratio is 11.8.

The selection of the design point is based on LP/HP and compressor/engine matching analyses discussed previously under Compressor Characteristics. To summarize those considerations briefly, a match was selected to give a 60 percent power point free of LP stall, at high efficiency, and high pressure ratio. It is expected that bleed will be required to provide satisfactory low-speed performance, but provisions for bleed have not been detailed. The matching data are presented in Figures 41 and 52 and Table I for Case 4,1-AAA.

The selection of pressure ratio value is based on three factors; namely, efficiency, stall margin, and work capability. The centrifugal stage with radial blades was chosen to give the highest pressure ratio commensurate with a temporarily adopted tip speed limit of 1840 ft/sec. The two-stage transonic LP compressor of high pressure ratio was selected for its wide operating range and high efficiency, and was matched at less than maximum pressure ratio to favor part-power stall conditions. The result was a compressor which would deliver a maximum pressure ratio from the available resources, as defined in a performance map. The compressor/engine match was speed-limited, not power-limited, permitting the compressor structural resources to be fully exploited.

It may be noted that this design does not place the peak efficiency at the military power point and, therefore, is contrary to the study results, under Compressor Characteristics above, about the optimum location for compressor peak efficiency. There are two ways of meeting that requirement, but both can be shown to give results contrary to program objectives. First and simplest, one could match the engine so as to place the military rated point at the compressor peak efficiency point, where pressure ratio is lower. This would contravene program objectives because part-power operating points would have lower pressure ratio and efficiency and therefore higher specific fuel consumption. Second, one could retain the pressure ratio and raise the

TABLE V. FIXED-GEOMETRY COMPRESSOR FLOW PATH AND MILITARY RATED DESIGN POINT PERFORMANCE

$P/P = 11.8$, $W\sqrt{\theta_2}/\delta_2 = 4.42$ lbs/sec, $\eta_c = 80.0\%$,

$N/\sqrt{\theta_2} = 49{,}400$ RPM

	Transonic Axial					Centrifugal Stage		
	Stage 1			Stage 2				
Blade Row Exit	IGV	Rotor	Stator	Rotor	Stator	Inducer	Impeller	Diffuser
Flow Path								
Axial Location, in.	0	0.75	1.50	2.25	2.85	3.5	4.25	4.25
Tip Radius, in.	3.07	2.89	2.88	2.74	2.73	2.66	4.27	6.25
Mean Radius, in.	2.44	2.44	2.47	2.44	2.45	2.44	4.27	6.25
Hub Radius, in.	1.81	1.98	2.07	2.13	2.17	2.22	4.27	6.25
Annulus Height, in.	-	0.91	0.81	0.61	0.56	0.44	0.16	0.30
Stage Performance								
Total Pressure Ratio	-	-	1.56	-	1.55	-	-	4.9
Exit Pressure, psia	-	-	22.9	-	35.5	-	-	174.
Exit Temperature, °R	518.7	-	604.7	-	698.5	-	-	1178.
Stage Efficiency, %	-	-	82.	-	86	-	-	83.

efficiency by adding a stage, reducing stage loading, and matching stages so that efficiency would decrease toward lower flows. This would contravene program objectives by failing to fully utilize the stage work resources. In both instances, LP stall would exist at 60 percent power, increasing the uncertainties about performance at all part-load operating conditions.

The design approach is to define an attainable overall performance through stage matching of realistic components, to establish a military rated power design point, and then to determine the compressor configuration required for attaining the design point. Later phases of the design would investigate the requirements for meeting stall line and part-power operating requirements.

The definition of the flow path was the initial step in determining the compressor geometry. A mean-line compressor design program L2050 was used in this work.

A systematic variation of meridional velocity, blade speed, stage pressure ratios, and stator leaving angles was carried out in about 20 runs of the program. Satisfactory values of diffusion factor and DeHaller number served as tests for changing variables in the various runs. The velocity diagram parameters are listed in Table VI, and velocity diagrams are depicted in Figure 76. The flow path is depicted in Figure 77. The flow path selected for this axial compressor shows a smooth curve for the hub wall, with a broken line for the tip wall. The centrifugal compressor annulus is directly aligned and closely connected to the axial annulus. The reasons for selecting this configuration are given in the section above on Component Configuration. The inducer is slightly supersonic and is given a large axial length so that the swirl and the radial pressure gradient can be raised prior to the turn to radial, and so that the required large inducer diffusion can be performed gradually. At impeller exit, the passage height was 0.16 inch, a larger value than the 0.12 inch estimated to have been used in the PW-G impeller. The diffuser represented is a channel type of the pattern developed in Reference 10.

Variable-Stator Compressor Aerodynamics

The compressor consists of two transonic axial stages and a centrifugal stage. The military-rated operating point was selected as the design-point. In addition, operating conditions at the estimated 60 percent and 30 percent power points were investigated to determine the stator restaggers associated with these conditions. Table VII gives the design point operating conditions, the stage design-point performance values, and the flow path dimensions. The flow path is depicted in Figure 78.

The axial compressor type for this design was selected according to the section above denoted Selected Configuration. The centrifugal compressor was configured with an inducer annulus aligned to and close-coupled to

TABLE VI. FIXED-GEOMETRY COMPRESSOR PRELIMINARY DESIGN VELOCITY DIAGRAM DATA

	Transonic Axial					
	Stage 1		Stage 2		Centrifugal Stage	
Blade Row	IGV	Rotor	Stator	Rotor	Stator	Inducer	Diffuser
U_1, ft/sec	-	1050	1050	1065	1050	1056	1840
V_{m1}, ft/sec	-	500	560	570	610	620	620
M_1	-	1.06	0.65	1.02	0.66	0.96	1.14
α_1, deg	0	64.5	42.5	61.8	42.7	59.6	69.0
α_2, deg	0	43.8	0	38.6	0	19.9	-
DeHaller Number	-	0.67	0.75	0.64	0.75	0.63	-
D-Factor	-	0.47	0.49	0.50	0.49	-	-
Pressure Recovery	-	0.94	0.98	0.96	0.98	0.84	0.93

Subscripts:
1 - inlet of blade row
2 - exit of blade row
m - component in meridional plane (axial or radial)

Symbols:
U - rotor blade section speed
V - air velocity
M - Mach number
α - air angle measured from meridional plane

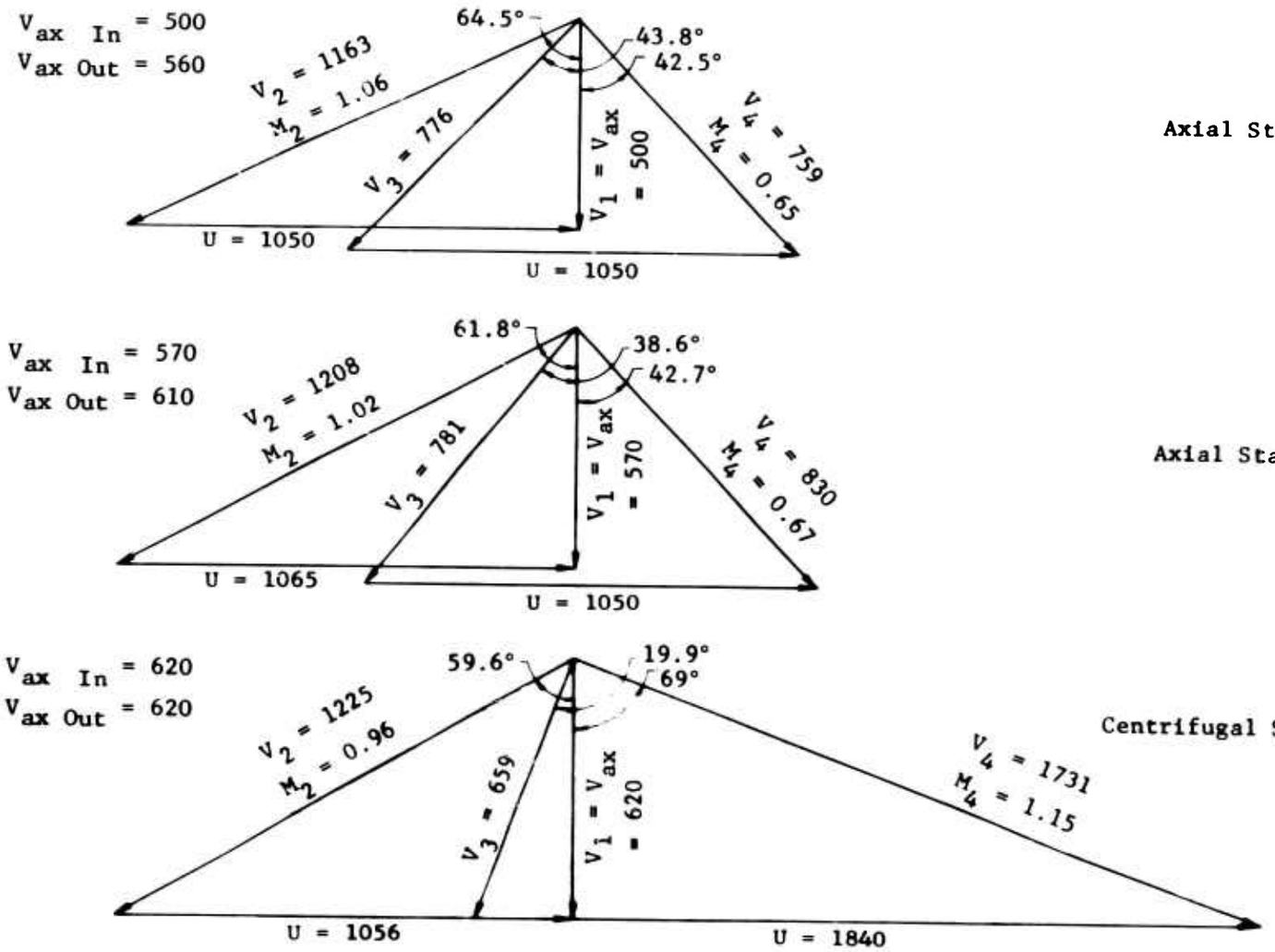

Figure 76. Fixed-Geometry Compressor Velocity Diagrams at 100 Percent Military Rated Power Design Point.

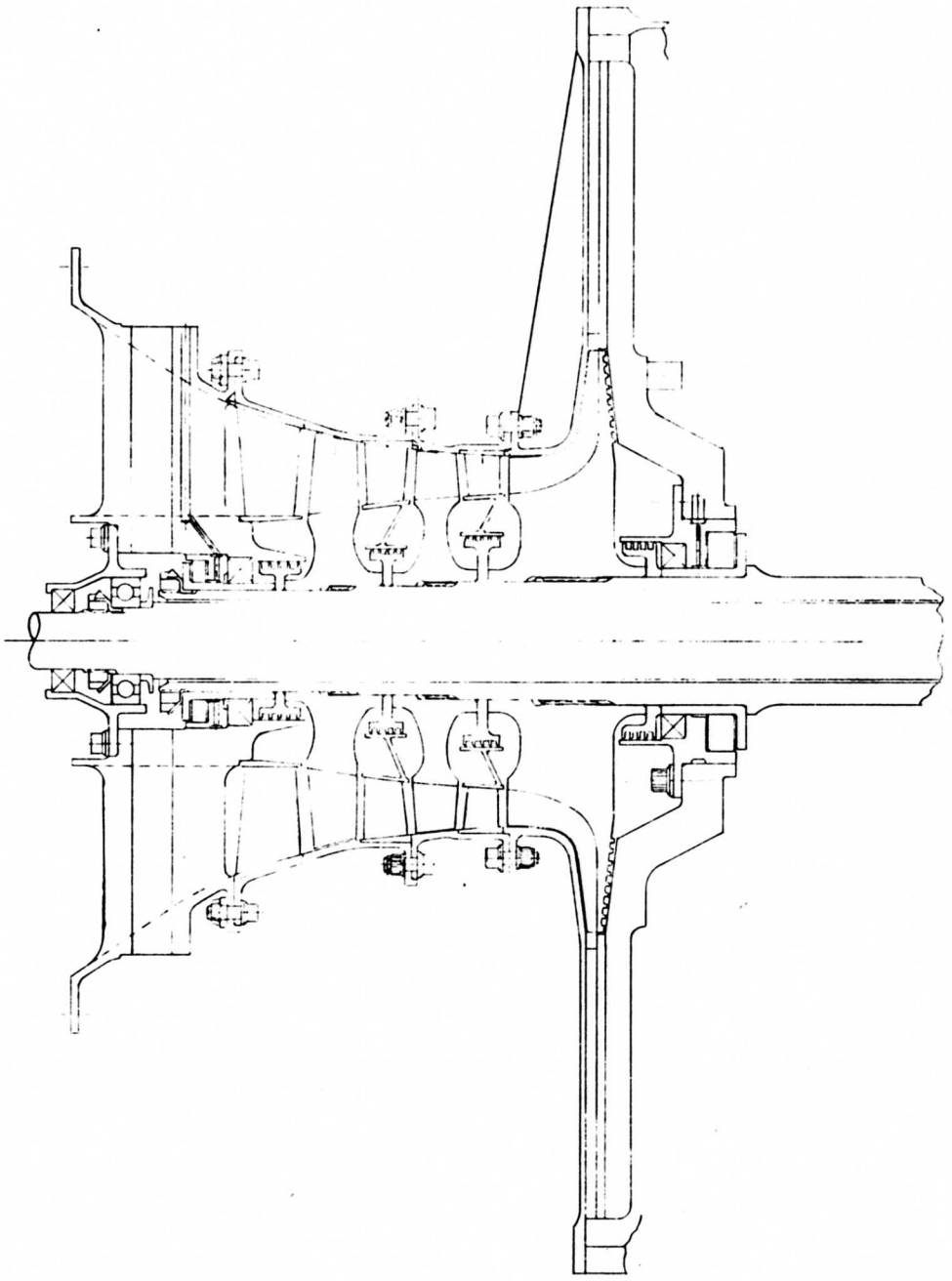

Figure 77. Fixed-Geometry Compressor Design.

TABLE VII. VARIABLE-STATOR COMPRESSOR FLOW PATH AND MILITARY RATED DESIGN POINT PERFORMANCE

$P/P = 19.09$, $W\sqrt{\theta_2}/\delta_2 = 4.48$ lbs/sec, $\eta_c = 80\%$

$N/\sqrt{\theta_2} = 56{,}600$ RPM

	Transonic Axial					Centrifugal Stage		
	Stage 1			Stage 2				
Blade Row Exit	IGV	Rotor	Stator	Rotor	Stator	Inducer	Impeller	Diffuser
Flow Path								
Axial Location, in.	0	0.85	1.50	2.15	2.65	3.5	4.4	4.4
Tip Radius, in.	2.83	2.68	2.63	2.56	2.53	2.55	4.15	7.00
Mean Radius, in.	2.12	2.23	2.23	2.28	2.28	2.33	4.15	7.00
Hub Radius, in.	1.42	1.78	1.82	2.00	2.02	2.11	4.15	7.00
Passage Height, in.	1.41	0.90	0.81	0.56	0.51	0.44	0.12	0.40
Stage Performance								
Total Pressure Ratio	-	-	1.72	-	1.66	-	-	6.67
Exit Pressure, psia	-	-	25.2	-	41.9	-	-	280.
Exit Temperature, °R	518.7	-	624.3	-	738.0	-	-	1375.5
Stage Efficiency, %	-	-	82.4	-	85.6	-	-	83.4

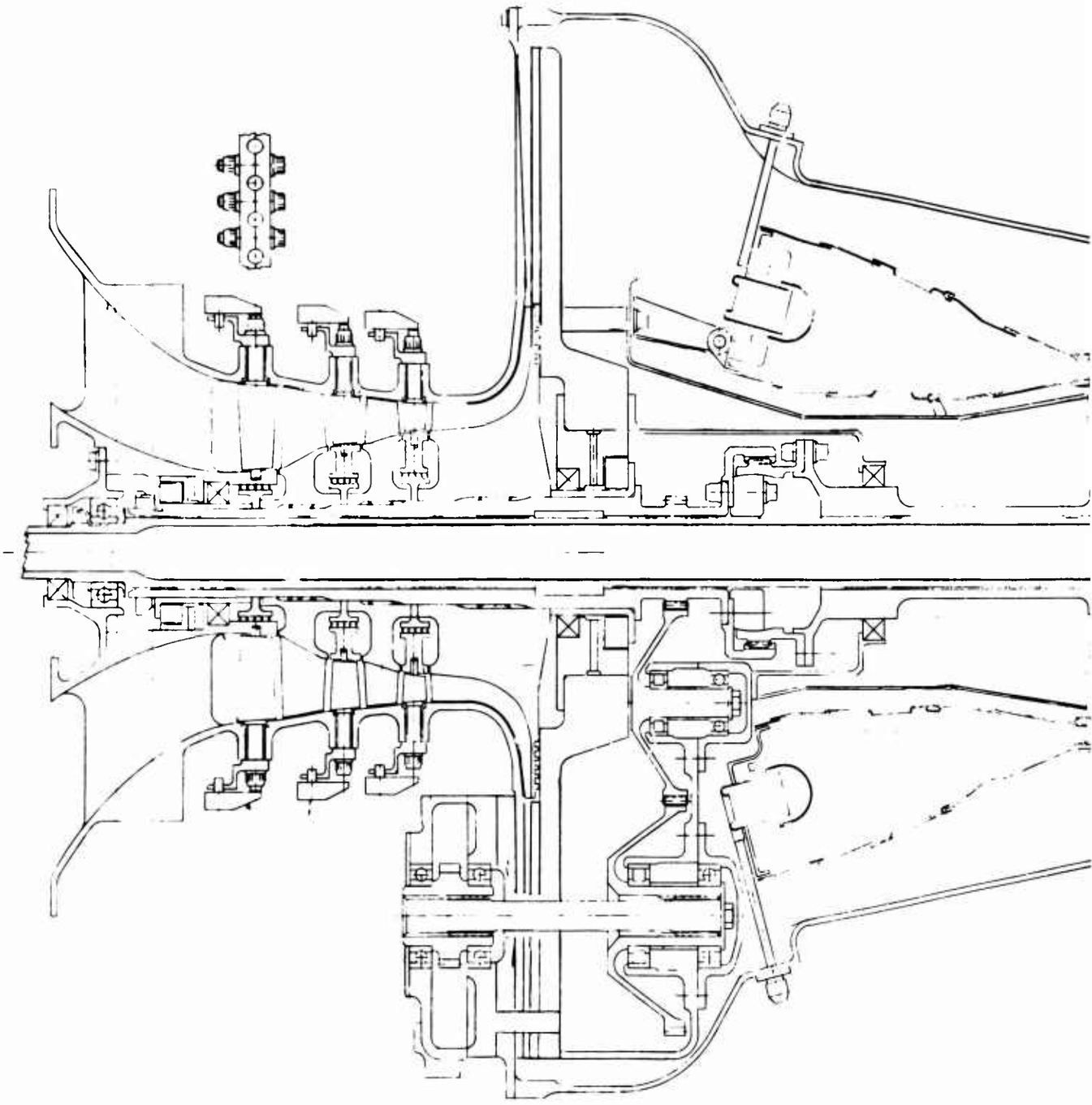

Figure 78. Variable-Stator Compressor and Engine Design.

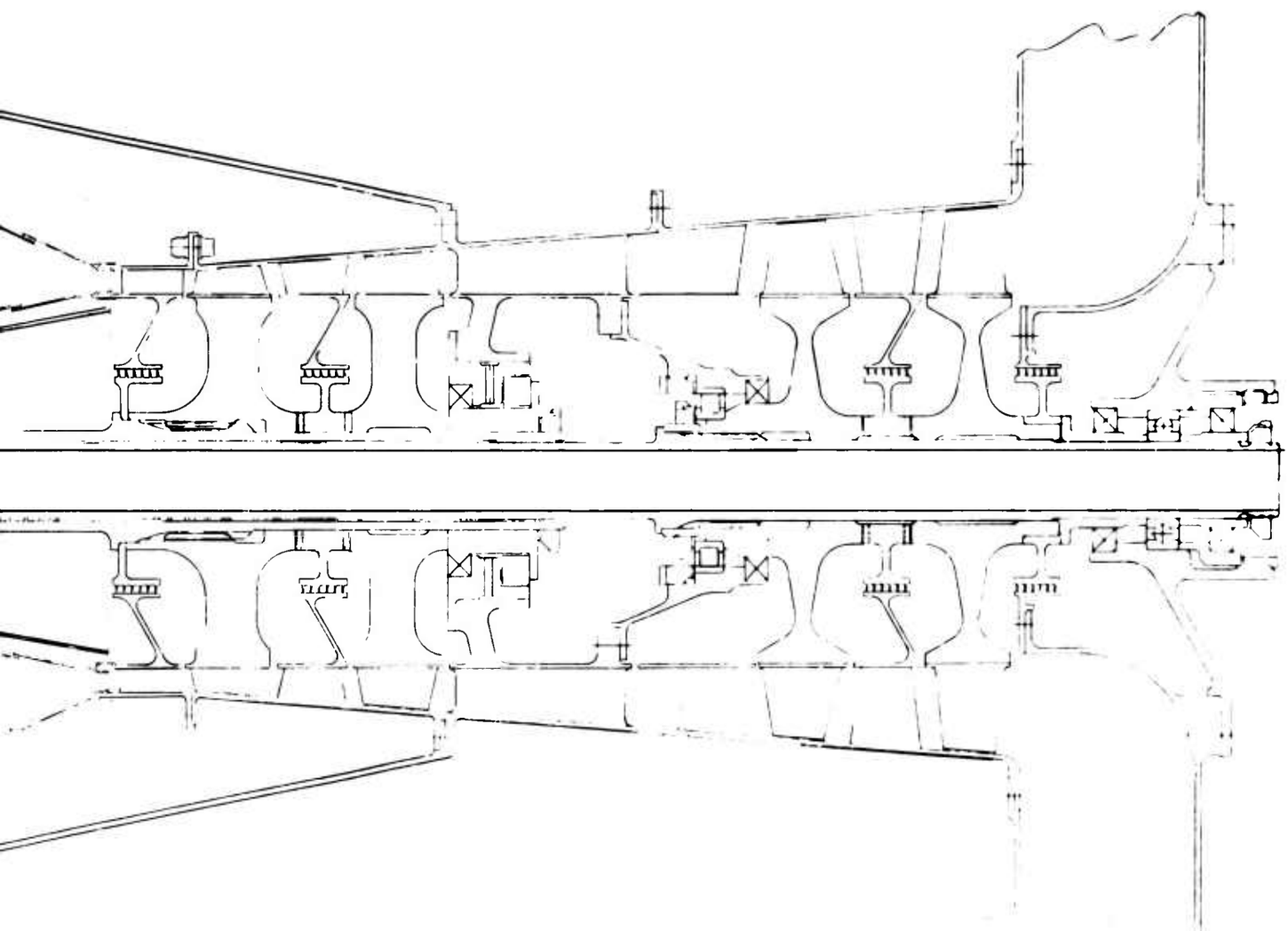

BLANK PAGE

the axial stages. The basic stage matching was based on the military rated point, with the part power performance improved by varying stator setting angles. The LP compressor speed of 95 percent was just above the maximum efficiency island, as shown in Figure 62. A conservative approach was taken in that the LP stage work level was reduced by 4 percent to bring stage work back to the levels of the experimental machine with efficiencies still being kept high as in the modified case. The HP compressor speed of 105 percent was also just above the maximum efficiency island as shown in Figure 65. This was the highest speed and gave the highest pressure ratio that could be derived directly from the tests of the PW-G centrifugal stages, and it resulted in a centrifugal compressor tip speed of 2050 ft/sec and an overall military rated pressure ratio of 19.23. No established limit prevented pushing to higher pressure ratios; it was judged that the selected design point represented a reasonable extension of current state of the art for a three-year development program. The LP/HP matching relations are shown in Figure 44, and the compressor/engine match is shown in Figure 55. The compressor/engine match was not power-limited, and the military rated point was located at 95 percent of the design speed of the transonic axial compressor. An 80 percent efficiency island covers most of the operating range of the map, due to the matching improvements to be effected through the variable-stator setting angles.

The flow path dimensions were established by using the design program L2050 in the manner described above for the fixed-geometry compressor. Blade speeds, axial velocities, and stage pressure ratios were varied systematically in over 24 runs of the program to establish acceptable design values for the velocity diagram parameters given in Table VIII. Velocity diagrams are shown in Figure 79.

The annulus form for the axial compressor began with a hub/tip radius ratio of 0.5, a lower value than the 0.6 value used for the fixed-geometry design. The mean radius tip speed was increased at each rotor exit to give a broken-line wall at both hub and tip of the annulus. The function of this wall form is to provide local streamline curvature effects which have in the past produced efficient stages. As compared to the fixed-geometry compressor, a higher shaft speed resulted from the decreased inlet hub/tip ratio and led to smaller diameters and larger passage heights through the axial compressor. The centrifugal compressor flow path was made long in the inducer section, before the turn, in accord with the philosophy of Reference 10.

The blade sections selected for the variable-stator compressor are listed in Table IX, showing camber and stagger angles for each of the axial compressor blade rows. Stagger angles for the inlet guide vanes and first and second stators are given for the 60 percent and 30 percent power conditions based on calculations described in the section on Compressor Performance Prediction.

TABLE VIII. VARIABLE-STATOR COMPRESSOR PRELIMINARY DESIGN MEAN RADIUS VELOCITY DIAGRAM DATA AT THREE POWER LEVELS

	Transonic Axial					Centrifugal Stage	
	Stage 1			Stage 2			
Blade Row	IGV	Rotor	Stator	Rotor	Stator	Inducer	Diffuser
U_1, ft/sec							
100% power	-	1050	1100	1100	1125	1125	2050
60% power	-	966	1012	1012	1035	1035	1886
30% power	-	840	880	880	900	900	1640
V_{m1}, ft/sec							
100% power	-	500	580	590	650	660	660
60% power	-	372	452	453	528	533	604
30% power	-	233	302	303	376	379	502
M_1							
100% power	-	1.06	0.70	1.04	0.70	1.00	1.25
60% power	-	0.88	0.65	0.88	0.64	0.88	1.20
30% power	-	0.67	0.58	0.69	0.57	0.71	1.08
α_1, deg							
100% power	0	64.5	44.9	61.8	43.1	59.6	70.6
60% power	0	67.5	53.1	64.5	48.8	61.6	70.6
30% power	0	71.7	63.1	68.1	57.2	64.6	71.4
α_2, deg							
100% power	0	41.9	0	38.4	0	14.9	-
60% power	10	42.1	7.5	39.2	5	15.5	-
30% power	30	43.1	22.5	40.0	15	16.2	-
DeHaller Number							
100% power	-	0.67	0.72	0.66	0.74	-	-
Diffusion Factor							
100% power	-	0.49	0.53	0.49	0.50	-	-

Subscripts 1 - inlet of blade row
2 - exit of blade row
m - component in meridional plane (axial or radial)

Symbols U - rotor blade section speed
V - air velocity
M - Mach number
α - air angle measured from meridional plane

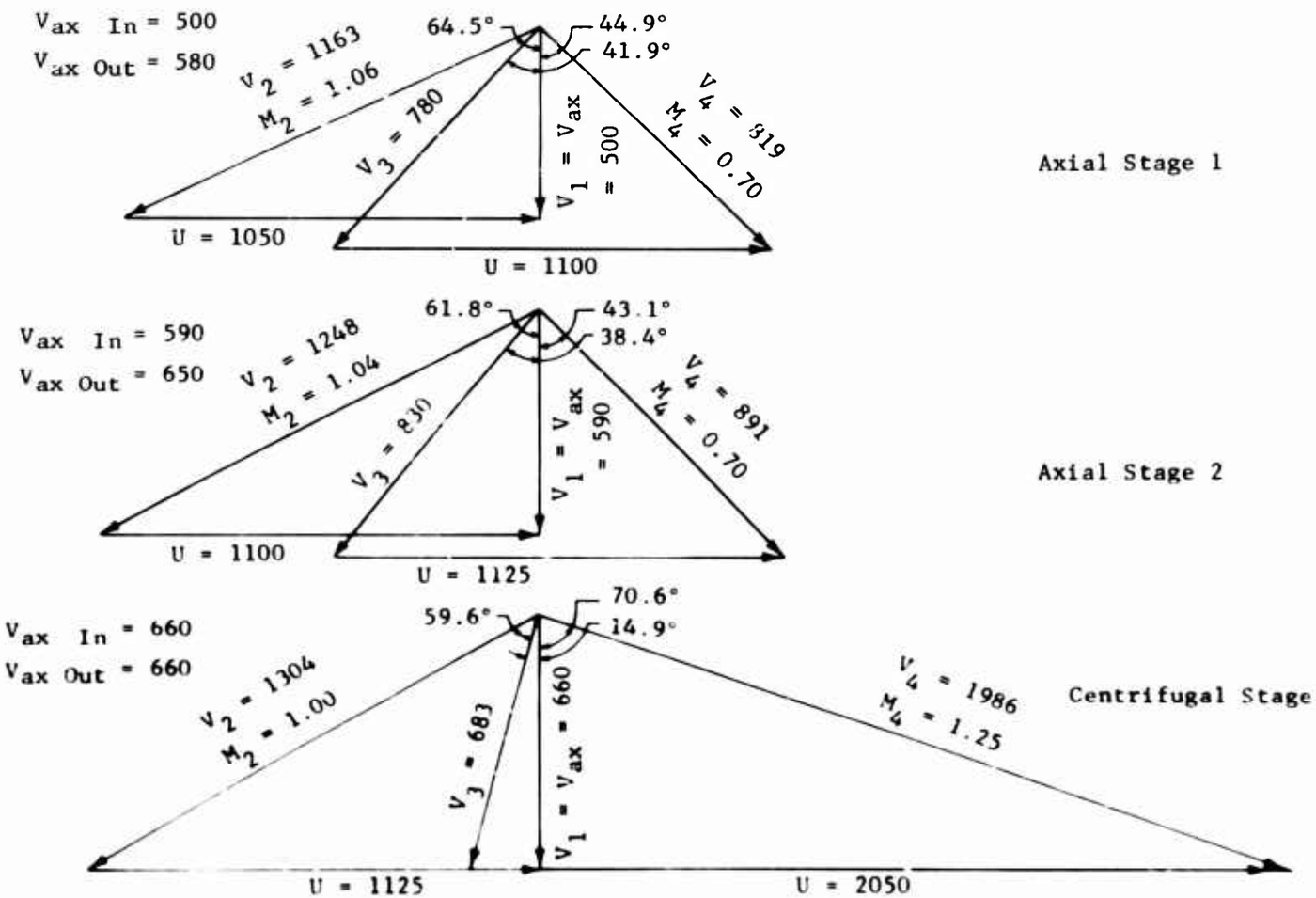

Figure 79. Variable-Stator Compressor Velocity Diagrams at 100 Percent Military Rated Power Design Points.

TABLE IX. VARIABLE-STATOR COMPRESSOR BLADE GEOMETRY AT MEAN RADIUS SECTIONS

	Transonic Axial					Centrifugal Stage		
	Stage 1			Stage 2				
Blade Row	IGV	Rotor	Stator	Rotor	Stator	Inducer	Impeller	Diffuser
Inlet Radius, in.	2.10	2.12	2.23	2.23	2.28	2.28	2.33	4.40
Blade Type	NACA63	MCA	CA/65	MCA	CA/65	MCA	Channel	Channel
Camber, C_{lo}	7.0	-	-	-	-	-	-	-
, deg	-	30.3	56.1	31.1	53.8	-	-	-
Blade Angle, Inlet, deg	-	64.5	41.6	59.8	39.8	57.6	-	68.6
Exit, deg	-	34.2	-10.7	31.5	-10.2	-	0	-
Chord, in.	0.60	1.15	0.52	0.80	0.47	-	-	-
Max. Thickness/Chord	0.10	0.06	0.09	0.06	0.09	-	-	-
Stagger Angle, deg								
100% power	-10	49.3	16.8	46.3	16.2	-	-	-
60% power	0	49.3	24.1	46.3	21.2	-	-	-
30% power	+20	49.3	36.5	46.3	30	-	-	-
No. of Blades	32	19	39	29	43	15	30	26

The blade types are selected according to the blade operating conditions. The inlet guide vane is given a camber which enables it to function well at off-design conditions, even though at design conditions it is required to do no turning at all. The NACA 63 section has a mean line with a maximum camber located well forward. It is well suited to serve as an accelerating, or swirl imparting, cascade airfoil section. The rotor blade sections are identified as MCA, signifying multiple circular arc sections with maximum camber located toward the rear of the section. With high inlet Mach numbers, these blades have thin profiles. The detail design of these blades is performed with quasi-channel design methods which account for intra-blade work distribution and blade blockage effects. Reference 3 describes such a method. The stator blade sections have relatively low inlet Mach numbers and therefore have circular arc mean lines and thicker subsonic airfoil sections, capable of accommodating large variations of incidence angle which are imposed as the setting angles are varied to keep the LP stages out of stall over a wide range of operating conditions.

The inducer can be designed by methods similar to those used for designing transonic axials, or alternatively by the blade-to-blade velocity computation procedures, derived by Stanitz, Dallenbach, Welliver, and others and used for designing the centrifugal compressor impellers in recent years. One such program is described in detail by Welliver and Acurio in Reference 15. The detail design of the impeller is conceived to follow the successful paths reported in References 10 and 11; namely, to particularly avoid separation of flow in the impeller, by adding splitter blades to reduce loading and by avoiding a reduction of meridional velocity in the radial flow region where the radial static pressure gradient is high due to the rotation of flow.

It is conceived that the inducer is divided in the rotation plane into two parts with the same number of blades in each section. The forward section is rotated by a third of a blade pitch in a backward direction so as to discharge its unseparated but thickened wakes between the blades of the downstream inducer section, thus causing the start of new, thin boundary layers at the leading edges of the downstream blades. Success with this approach was reported by Ball, Bell, and Mann in Reference 14, though it was abandoned by them for reasons of cost and structural difficulty. The present application has more to gain from it because of higher aerodynamic loading requirement and may present less structural difficulty because of the relatively smaller blade span. Two other concepts discussed in Reference 14 are judged to be applicable to this detail design; namely, the introduction of splitter vanes in the impeller with their leading edges placed so as to divide the channel flow evenly despite the nonuniform blade-to-blade meridional velocity, and a diffuser with marked divergence in the meridional plane. The passage height at centrifugal impeller exit is 0.12. It is judged that the vaneless space should be treated as a mixing region with a constant area on the circumferential surface at all radii. The radius ratio from impeller exit to diffuser channel inlet is in the

order of 1.06, as described in reference 10. The proportions of the diffuser pickup channel throat would then, for 26 channels, be in the order of 0.11 by 0.35 inch. A divergence from the narrow dimension is of great advantage in providing the shortest path for accomplishing a given degree of diffusion or in a given space for giving the highest degree of attainable diffusion. The diffuser channel exit section is either square or circular, circular sections being preferred if feasible to minimize wetted areas. Diffuser channels downstream of pickup sections are straight, and pickup leading edges are designed as sharp wedges to facilitate attachment of entering supersonic flows.

Fixed-Geometry Compressor Design

The fixed-geometry compressor structural design is essentially the same as the variable-stator compressor design described below except for the stator support system and the compressor housing. Figure 77 depicts the arrangement of the fixed-geometry compressor.

Like the variable-stator compressor housing, the fixed-geometry housing consists of shroud rings stacked axially and secured at each stage by a circumferential ring of bolts. The stator blades and rings are integrally cast of corrosion-resistant steel in complete assemblies. The inside shroud forms the stationary part of the interstage labyrinth seal for the 2nd and 3rd stages.

The "Z" cross section of the inner shroud provides axial stiffness by which the diaphragm can better resist the pressure difference across the stator. The outer shroud is bolted axially at the flanged joint of the compressor housing. Torque is transferred from the stator rings to the housing by lugs on the rings that fit into slots in the housing. Assembly of the compressor is accomplished in essentially the same manner as for the variable-stator configuration, by stacking forward from the centrifugal impeller, alternately installing rotor discs and stator rings.

This method of constructing and assembling the stators is simple, thereby lowering the fabrication cost.

Variable-Stator Compressor Design

The variable-stator compressor design consists of two axial stages and a centrifugal stage mounted on a single shaft, with a coaxial inner shaft through which an aft power turbine drives a front gearbox. Variable blade setting angles are provided for the IGV and the first- and second-stage stators. The design of the compressor and the general engine configuration are shown on Figure 78.

The compressor structure consists of housings with stator blades, flow passages, and bearing supports; of shafting with bearings and seals; and of rotors with blades and airseals. The axial compressor housings

are machined from aluminum alloy castings. The stator blades are precision cast of steel. The centrifugal compressor shroud is machined from a steel casting; steel is required to retain adequate strength at the elevated temperatures of the compressor exit air. Slipper bearings carry the compressor shaft, and the coaxial inner drive shaft is carried by rolling element bearings at the ends, with an intermediate intershaft sleeve bearing to control power shaft vibration amplitudes. Axial stage rotor discs and blades are integrally machined from titanium or steel; a detail design study would evaluate the lower cost of steel against the lighter weight of titanium. The centrifugal impeller is machined from titanium.

The compressor is assembled by mounting the shaft in the rear main bearing support and then alternately stacking rotors on the shaft and stators on the shroud until the front main bearing support is installed to complete the assembly. The casing circumferential flanges are bolted together; there is no meridional split line or flange. Compared to split casings, the proposed construction facilitates stator blade installation, controls rotor blade tip clearances more effectively, and provides a continuous airseal structure.

The main features of the design are discussed below in detail, covering in particular the variable stators, the rotors, the bearings, and the shafting.

The cast steel stator blades have trunnions on each end. The outer trunnion extends through a replaceable bushing which is carried in the housing flange. The compressor housing is split circumferentially at the stator trunnion centerline of each stage, allowing for axial stacking of shroud sections during assembly. The flanges are bolted together between stator trunnions. The stators are actuated by circumferential unison rings with small trunnions which fit into small flexible bell cranks extending from each stator trunnion. The bell cranks provide enough flexibility to deflect out-of-plane during actuation, due to the unison ring travelling in a cylindrical plane and the bell crank turning in a flat plane. The stator inner trunnion passes through a hole in a ring which forms the annulus hub wall and extends to lower radius to form the airseal shroud ring.

The rotors are splined to the shaft for transmission of torque, and the splines are located in the part of the disc which is most deformed under centrifugal loading at high speed. Concentricity is maintained at all speeds by locating disc bore pilot diameters at the ends of the bore, away from the radial growth region. The airseal rotors are clamped between the bladed rotors and need not be keyed to the shaft. Each labyrinth seal rotor has four lands.

The shafting layout of the complete engine is shown in Figure 78. The major rotating components are (a) the compressor driven by (b) the gas generator turbine, and (c) the free power turbine driving a gearbox

through the coaxial inner shaft. Straddle bearings are provided for the compressor and the power turbine, with high critical speeds and good control of blade tip clearances. The gas generator turbine is supported at the rear by a bearing and at the front by the compressor shaft through a spherical-seated coupling, which avoids the redundancy of a three-bearing system; a similar coupling is used successfully in the J65 engine for the same purpose.

The size and speed of the gas generator shaft require the use of special bearings. At 60,000 RPM, a DN value of 2.9 million would result, a value considered excessive for rolling-element bearings. Therefore, a floating sleeve or slipper type of bearing was selected for the outer shaft. This bearing type has two advantages: first, it can operate at high surface speeds (500 ft/sec); and second, it has sufficient running clearances to allow a well balanced wheel to spin about its mass center of gravity, thus lowering the vibratory forces transmitted to the support.

The power turbine is straddle supported on rolling-element bearings with the rear bearing taking the thrust. The thrust bearing DN value is 1.2 million, a value well within the state of the art. The front of the shaft is supported by a ball bearing via struts through the air passage. A floating sleeve bearing is installed between the two concentric shafts, to force a node on the inner shaft and, thereby, increase the critical speed. The compressor and power turbines can probably be designed to operate well below the first critical speed, principally due to the closely supported straddle mounting of these two components. There are other contributing factors; for example, the critical speed with compressor rotors made of steel was calculated as 101,000 RPM, but for rotors made of lighter titanium it was 138,000 RPM.

However, the compressor turbine and the long power turbine shaft first mode critical speeds will be below the maximum operating speed. It is possible and desirable to design the shafting in these cases with the first critical in the lower half of the speed range and the second critical above the maximum operating speed. This allows rapid acceleration through the first critical speed and thus prevents a buildup of excessive vibratory amplitude. The floating intershaft sleeve bearing near the middle of the long power turbine shaft would tend to force a partial node at this location and prevent excessive amplitude buildup. Lubrication to this bearing can be provided through the inner shaft and out through holes to the inside diameter of the sleeve. Scavenge is to the same cavity as the rear compressor bearing.

COMPRESSOR PERFORMANCE PREDICTION

Performance predictions for both the fixed-geometry compressor and the variable-stator compressor were produced on an overall basis by stage matching procedures. The considerations and methods involved in these matches are discussed at length previously in the section entitled Preliminary Design under topics entitled Compressor Characteristics and Preliminary Design. Further analysis of the off-design performance for the variable-stator compressor was performed using the mean-line mapping program and is detailed here.

Fixed-Geometry Compressor Performance

The predicted overall performance for the fixed-geometry compressor is plotted in Figure 52. This map shows the total pressure ratio and adiabatic efficiency values for inlet-corrected constant speed lines plotted against inlet-corrected airflow. Operating points are shown for the preliminary compressor/engine matching at 100 percent, 60 percent, and 30 percent power. This performance map was used for predicting engine performance in the study described above in the section entitled Power Turbine Flow Area, which showed that fixed turbine area gave better performance than variable area. The map was also used in predicting engine performance reported below in the section entitled Engine Performance Prediction, with the operating line shown in Figure 80.

Variable-Stator Compressor Performance

The predicted overall performance for the variable stator compressor is plotted in Figure 55. The performance map shows the total pressure ratio and adiabatic efficiency values for inlet-corrected constant speed lines plotted against inlet-corrected airflow. Engine operating points for 100 percent, 60 percent, and 30 percent power are shown based on the preliminary matching. The map was used in predicting engine performance presented below in the section entitled Engine Performance Prediction, and the resulting engine operating line is shown in Figure 81.

Performance for the variable-stator compressor was predicted at approximate 60 percent and 30 percent power points by the use of the mean-line mapping program in order to determine the kind of off-design stator angle restaggers that would be expected to be required. This work was carried on concurrently with the engine performance prediction, and the results of that work were not available to define the 60 percent and 30 percent power operating conditions. Therefore, the operating conditions were taken to be the values shown on Figure 55, based on the initial compressor/engine matching studies. The predicted speed lines and the operating points are shown in comparison with the basic map in Figure 82.

The procedure for defining the speed lines used the design parameters established at the military rated design point, with variation of speed and setting angles in the axial stages. A pattern of setting angles was

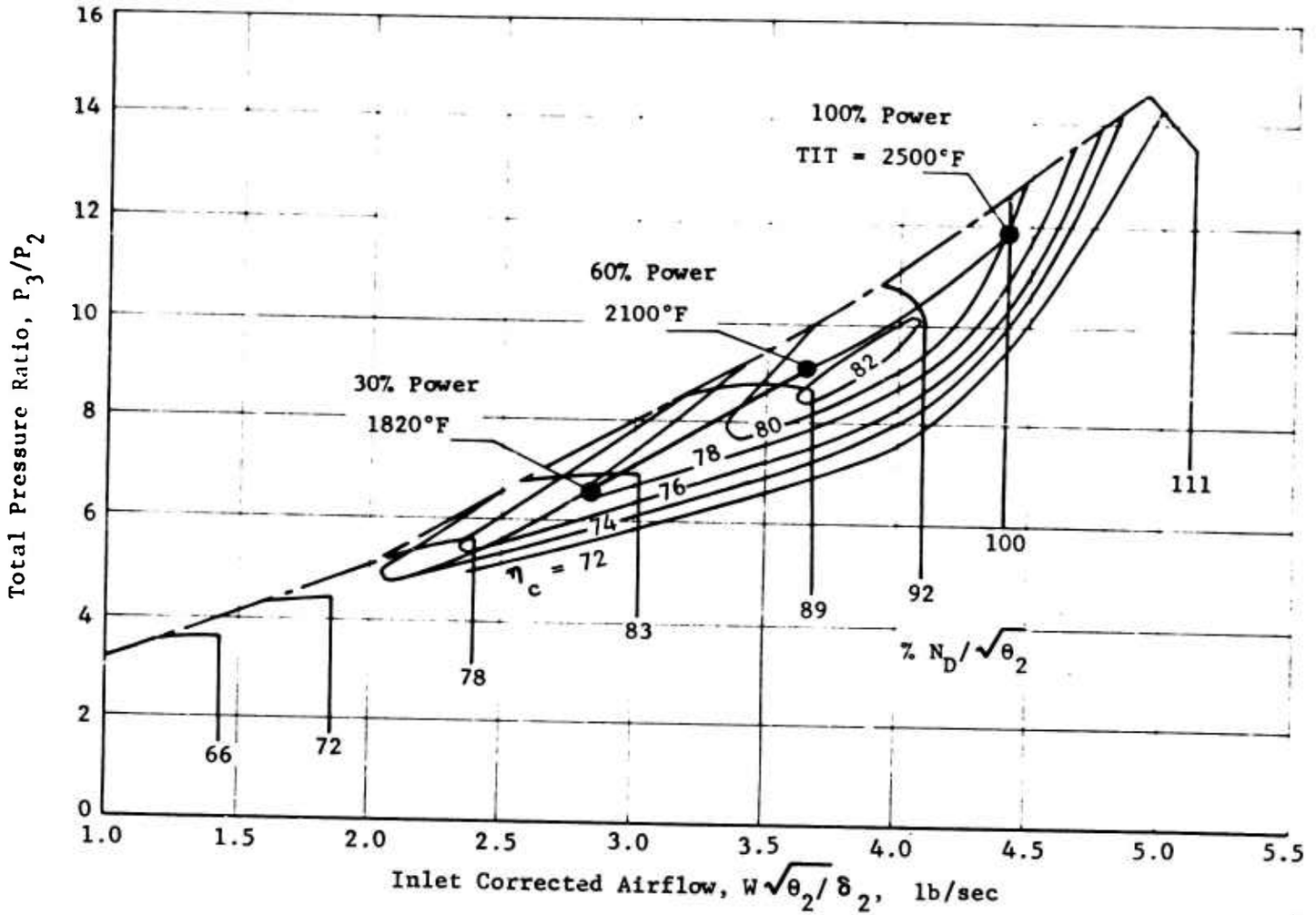

Figure 80. Fixed-Geometry Compressor Performance Map With Engine Operating Line Superimposed.

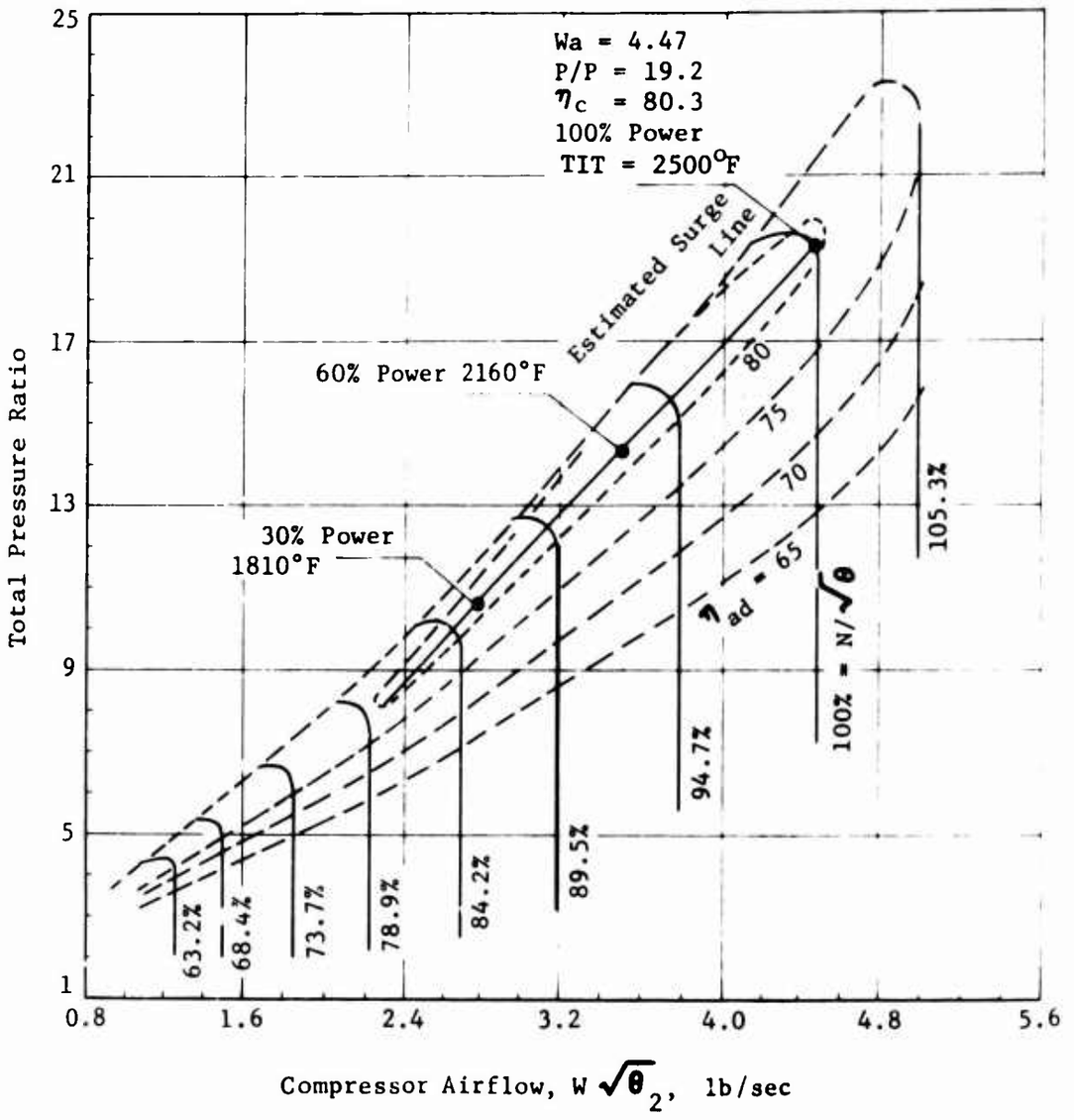

Figure 81. Variable-Stator Compressor Performance Map With Engine Operating Line Superimposed.

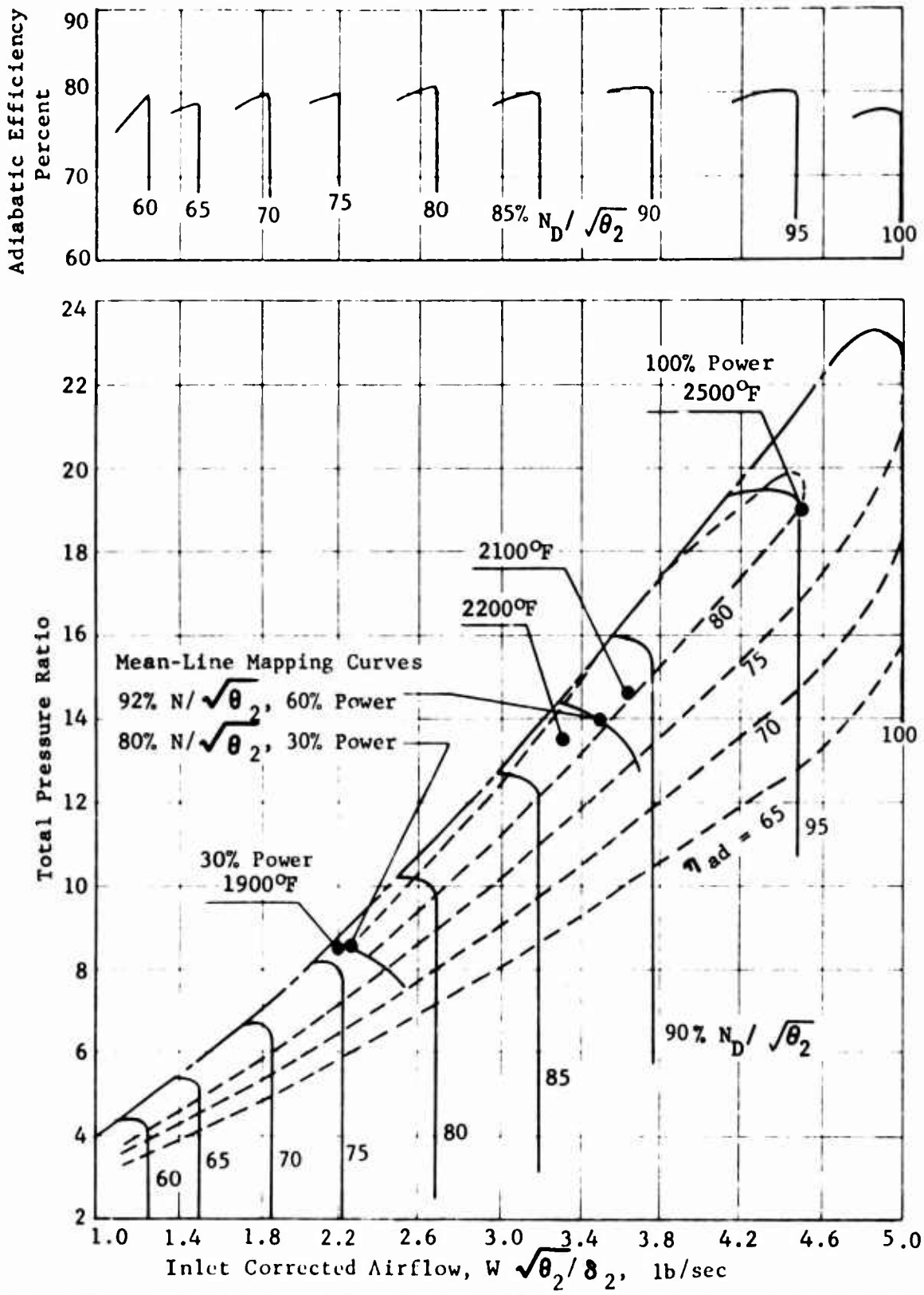

Figure 82. Variable-Stator Compressor Off-Design Performance Prediction Based on Mean-Line Mapping Program Compared With Overall Performance.

developed in an earlier study, where it was found to be the best of a number of various patterns tried, and was used exclusively here. The first stator restagger was 75 percent of the IGV restagger and the second stator restagger was half of the IGV restagger.

For the 30 percent power point, a speed was selected and several speed lines were run in the mean-line mapping program at various restagger levels until a restagger level was found which passed a line close to the desired operating point. Data from the line point nearest to the desired one were examined to determine whether the incidence angles were low at the axial stages and the inducer. Then another speed was chosen, and a new set of stagger values was found, as described above, resulting in a new data point close to the desired point. The pattern of incidence angles was again examined and compared with those of the previous speed, and in this manner a speed and stagger angle combination was found which minimized the incidence angles. This was selected as the preliminary operating point for the 30 percent power point.

The same process was carried out with different speeds and staggers to establish the preliminary operating point for the 60 percent power operating point.

The results of the off-design performance calculations appear as velocity diagrams for 60 percent and 30 percent power in Figures 83 and 84; as lists of incidence angle, inlet Mach number, blade row pressure recovery, stage pressure ratio, and stage efficiency in Table X, comparing values at the three power levels; as lists of velocity diagram parameter blade speed, meridional velocity, and inlet and outlet angles in Table VIII, comparing values at three power levels; and as lists of stator blade stagger angles for the three power levels in Table IX.

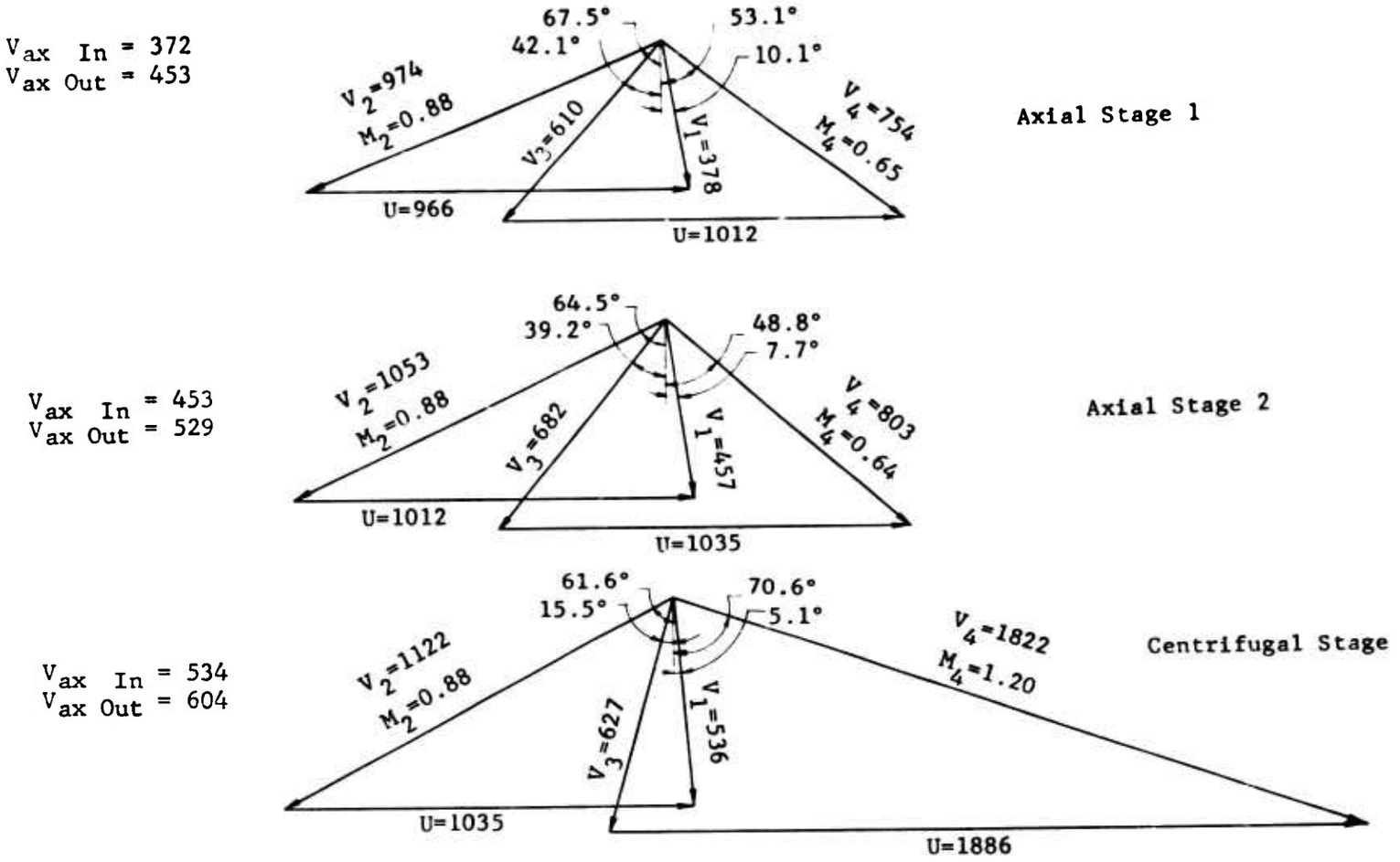

Figure 83. Variable-Geometry Compressor Velocity Diagrams at 60% of Military Power Operating Point.

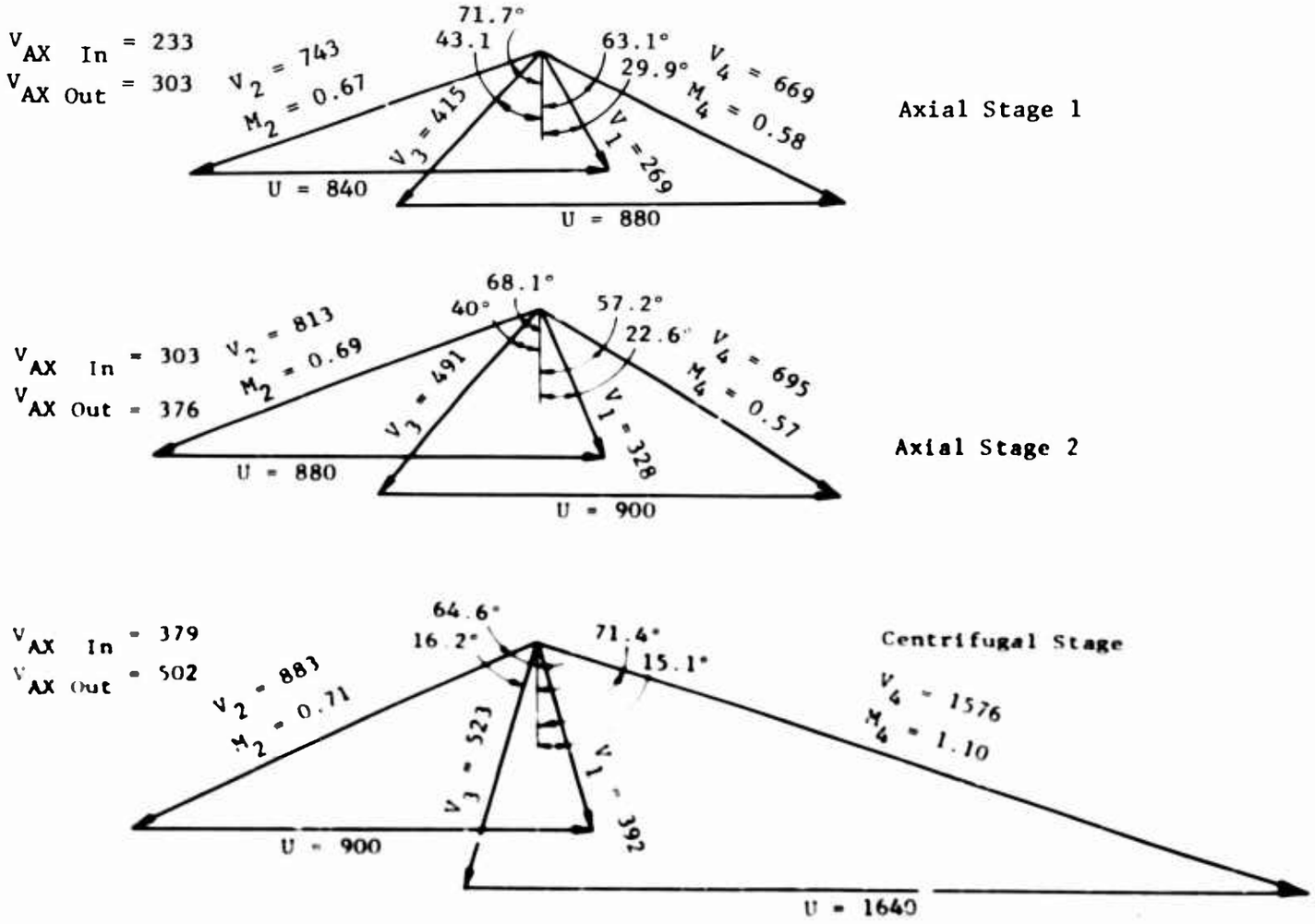

Figure 84. Variable-Geometry Compressor Velocity Diagrams at 30% of Military Power Operating Point.

TABLE X. VARIABLE-STATOR COMPRESSOR BLADE INCIDENCE ANGLES, INLET MACH NUMBER, AND PRESSURE RECOVERIES AT THREE POWER LEVELS

	Transonic Axial				Centrifugal Stage	
	Stage 1		Stage 2			
Blade Row	IGV	Rotor	Stator	Rotor	Stator	Inducer	Diffuser
Incidence Angle, deg							
100% power	-9	0	0	0	0	0	-.1
60% power	+1	0.5	0.4	2.2	0.4	1.5	-.1
30% power	+21	3.8	-5.0	4.8	-1.6	3.7	0.7
Inlet Mach Number							
100% power	-	1.06	0.70	1.04	0.70	1.00	1.25
60% power	-	0.88	0.65	0.88	0.64	0.88	1.20
30% power	-	0.67	0.58	0.69	0.57	0.71	1.08
Pressure Recovery							
100% power	-	0.931	0.978	0.945	0.978	0.824	0.917
60% power	-	0.955	0.981	0.958	0.981	0.840	0.923
30% power	-	0.971	0.983	0.973	0.984	0.864	0.930
Pressure Ratio							
100% power			1.72		1.66		6.68
60% power			1.63		1.55		5.54
30% power			1.46		1.41		4.14
Efficiency, %							
100% power			82		86		83.5
60% power			86		87		83.8
30% power			88		88		84

ENGINE PERFORMANCE PREDICTION

In order to establish a higher confidence level in the preliminary designs presented for (a) a moderate-pressure-ratio (12:1) fixed-geometry compressor and (b) a high-pressure-ratio (19:1) variable-stator compressor, off-design (matched) engine performance was predicted from 100 percent to 20 percent military power. These performance predictions were obtained with a rather sophisticated computer program, in which the performance characteristics of all engine components are introduced in tabular form, and a series of iterative calculations is performed to satisfy the fundamental relationships of flow continuity and total energy conservation of the working medium with varying gas properties as it passes through the engine. In this manner, any off-design operational problem areas are uncovered at this early stage of design.

Performance Results

The significant matched engine performance for the two engine cycles, incorporating the fixed-geometry and variable stator compressor configurations described earlier, is tabulated below:

TABLE XI. SINGLE-SPOOL TURBOSHAFT PERFORMANCE COMPARISON - SEA LEVEL STATIC, STANDARD DAY

(Turbine Inlet Temperature at Military = 2500°F)
(100% Power Turbine Speed - Except as Noted)

	Fixed-Geometry Compressor			Variable-Stator Compressor		
	100% Mil.	60% Mil.	30% Mil.	100%	60%	30%
Brake Specific Fuel Cons. lb/SHP/hr	.454	.504	.632*	.408	.451	.540*
Compressor Pressure Ratio P_3/P_2	11.8	9.1	6.6	19.2	14.6	10.6
Turbine Inlet Temperature T_4 °F	2500	2100	1820	2500	2160	1810
Compressor Adiabatic Efficiency η_c %	79.5	81.3	78.3	80.3	80.6	80.2
Gas Generator Speed N_{GG} %	100	89.6	82.2	100	93.3	85.9
Compressor Airflow $W_a\sqrt{\theta_2}/\delta_2$ lb/sec	4.42	3.65	2.83	4.47	3.59	2.81
Shaft Horsepower SHP hp	976	586	293	1000	600	300

*Power Turbine Speed = 80%

1. A single-spool nonregenerative turboshaft engine with (a) BSFC = .451 lb/SHP/hr at 60 percent of military power, (b) 1000 SHP at 2500°F military rated turbine inlet temperature, 4.47 lb/sec airflow, and (c) BSFC = .54 lb/SHP/hr at 30 percent power, is feasible, using a two-transonic stage and one-centrifugal-stage compressor with variable axial stators capable of 19.2 P/P and 80.3 percent adiabatic efficiency at military.

2. This engine will have a 10 percent lower BSFC at 60 percent power and a 15 percent lower BSFC at 30 percent power than a similar engine using a two-transonic stage and one-centrifugal stage compressor with fixed axial stators capable of 11.8 P/P and 79.5 percent adiabatic efficiency at military.

3. There appear to be no foreseeable operational problems associated with either engine cycle with regard to:

   a. High-speed compressor surge

   b. Low-speed compressor surge

   c. The need for variable turbine geometry

The part-load specific fuel consumption versus percentage of power for both engines is presented in Figures 85 and 86; power turbine operation at and near 100 percent speed produces minimum BSFC from military to 60 percent power. At 30 percent power, minimum BSFC occurs between 70 percent and 80 percent power turbine speed. This condition is discussed later.

Component Characteristics at Part-Load

The major components for which part-load performance characteristics were assumed are:

1. Overall Compressor

2. Combustor

3. Compressor Turbine (with air cooling)

4. Power Turbine (uncooled)

In addition, the following component assumptions were made:

5. Inlet Diffuser - 100 percent total pressure recovery

6. Lower Heating Value of Fuel - 18,400 Btu/lb

7. Gasifier Shaft Mechanical Efficiency - 99 percent

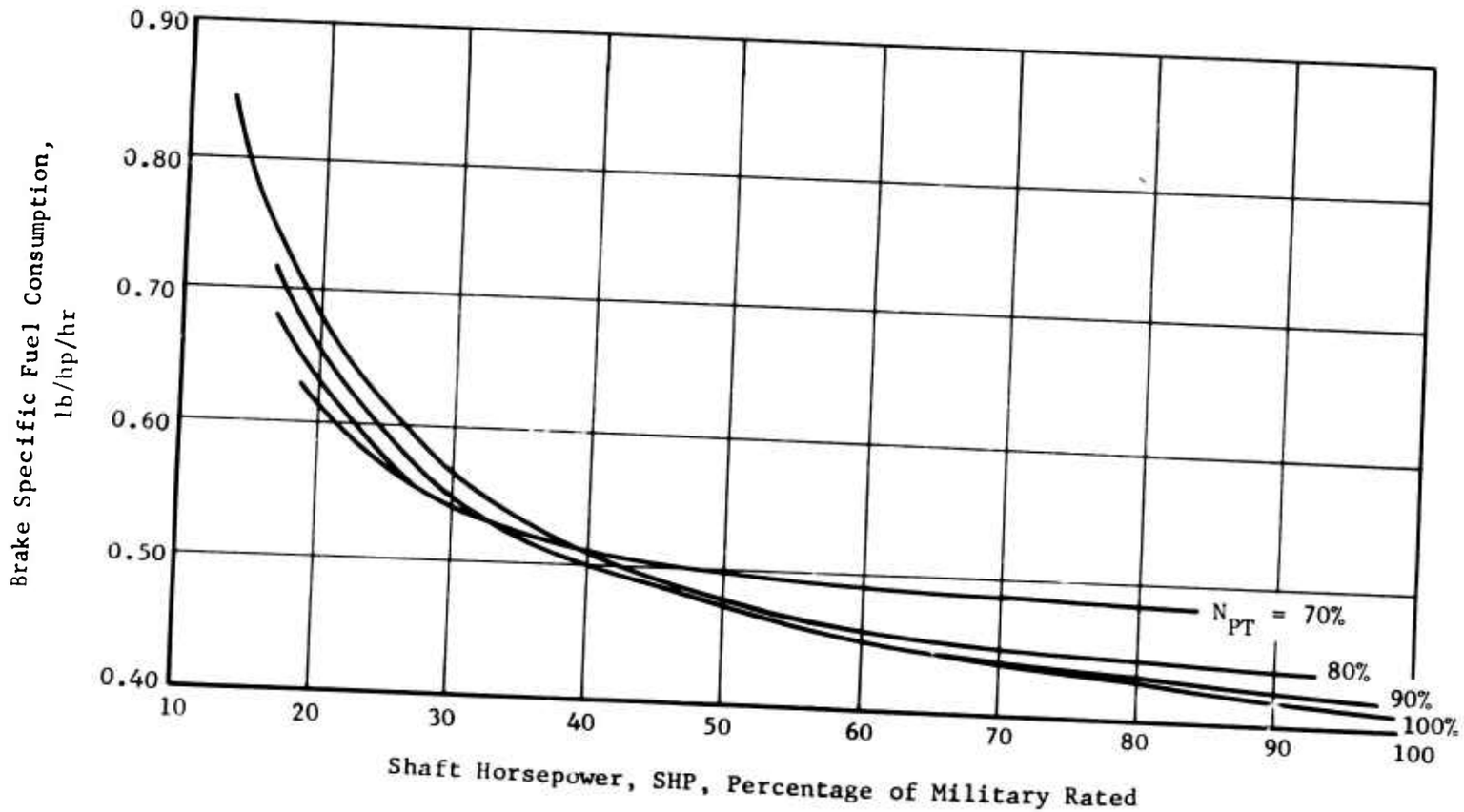

Figure 85. Variable-Stator Compressor Turboshaft Engine Part-Load Brake Specific Fuel Consumption at Sea Level Standard Day With Military Rated Power Point at P/P = 19.3/1, TIT = 2500°F, Wa = 4.47 lb/sec.

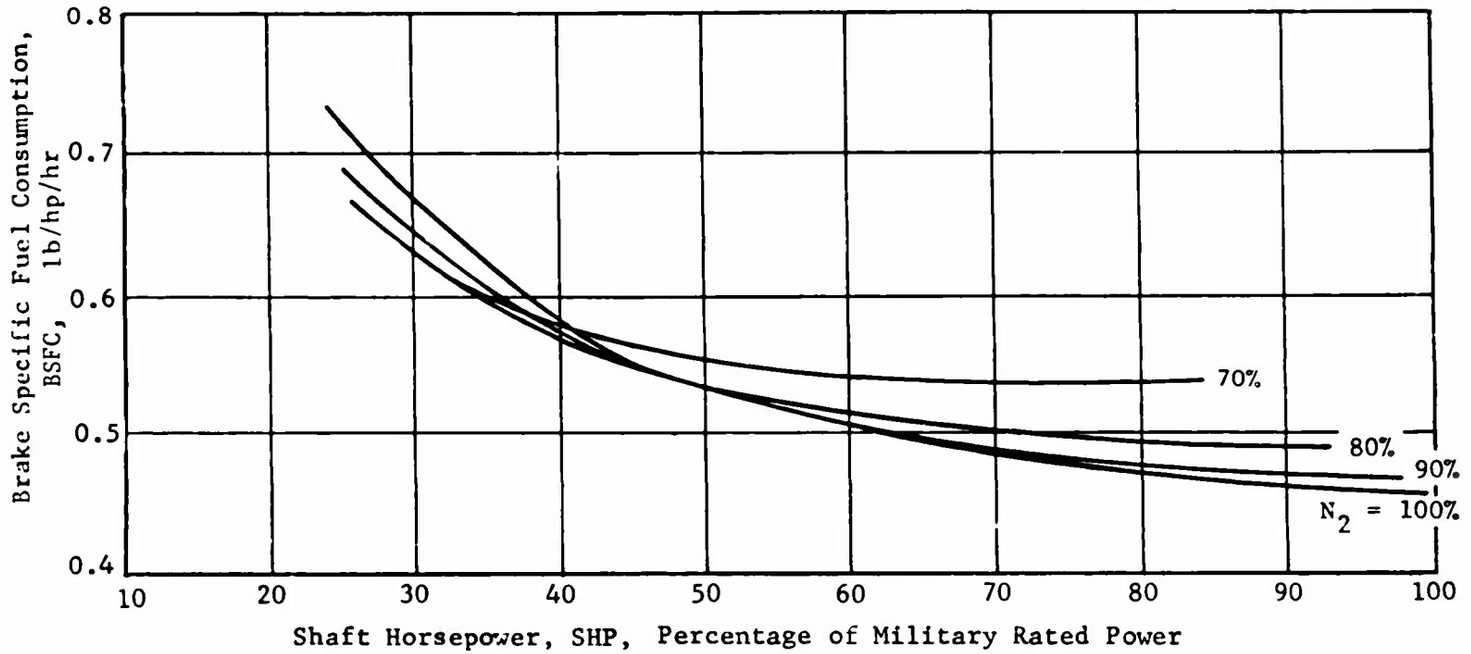

Figure 86. Fixed-Geometry Turboshaft Engine Part-Load Brake Specific Fuel Consumption at Sea Level Standard Day With Military Rated Power Point at P/P = 11.8/1, TIT = 2500°F, Wa = 4.416 lb /sec.

8. Power Turbine and Output Shaft Mechanical Efficiency - 99 percent

9. Seal Leakage and Overboard Bleed - 0 percent

10. Inter-Turbine (Compressor Turbine to Power Turbine) Pressure Loss - 0 percent

11. Power Turbine Exit Total Pressure to Ambient - 1.030 @ military, 1.007 @ 20 percent military

12. Compressor Turbine 1st Stator Cooling Air - 4 percent of compressor airflow discharged and mixed upstream of 1st turbine rotor to do work in turbine.

13. Compressor Turbine Rotor Cooling Air - 3 percent of compressor airflow discharged and mixed downstream of last turbine blade row to do no work in turbine.

Overall Compressor

The predicted overall compressor characteristics with engine operating line superimposed are presented in Figure 81 for the variable-stator compressor. It can be seen that the engine operating line for part load passes directly through the large 80 percent adiabatic efficiency island. Adequate surge margin at both the high- and the low-speed regions is readily apparent. The 60 percent power operating point is located at 14.6 P/P, 80.6 percent adiabatic efficiency, 3.59 lb/sec (80.3 percent of military) airflow, and 93.3 percent speed. The required turbine inlet temperature is 2160°F, within the range of 2100°F to 2200°F used in the cycle analysis and preliminary matching studies. The acceleration characteristics of the engine with this compressor are judged to be excellent due to the high cruise speed levels and large surge margin.

The same type of presentation is made in Figure 80 for the fixed-geometry compressor with engine operating line superimposed. In this case, the part-load engine operation from 100 percent to 30 percent power is also within the 80 percent adiabatic efficiency island with 60 percent power occurring near the peak efficiency of 82.6 percent. Adequate high- and low-speed surge margin is also evident. The 60 percent power operating point is located at 9.1 P/P, 81.3 percent efficiency, 3.65 lb/sec (82.6 percent of military) airflow, and 89.6 percent speed. All these characteristics with the exception of efficiency and airflow are lower than described above for the variable-stator compressor, and contribute to the 10 percent higher engine specific fuel consumption. The acceleration potential of an engine with these compressor characteristics is judged to be good.

A comparison of the compressor airflow and speed variation with output shaft horsepower for the fixed-geometry and variable-stator compressors is presented in Figure 87. The application of variable stators

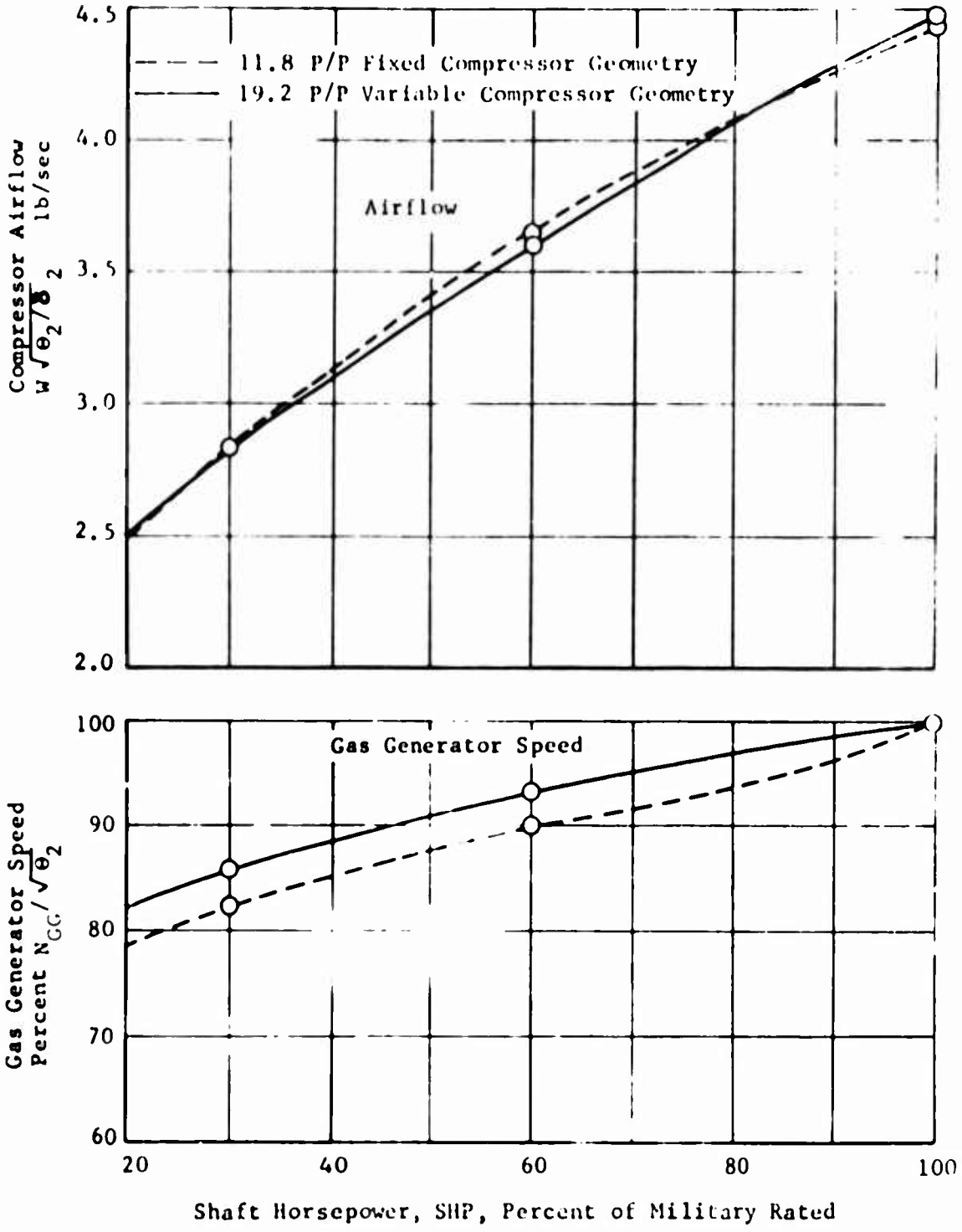

Figure 87. Comparison of Fixed-Geometry Compressor with Variable-Stator Compressor for Gas Generator Airflow and Speed Characteristics at Power Turbine 100% Speed and Sea Level Static Conditions.

is seen to (1) reduce airflow and (2) increase speed at the 60 percent power level. The airflow reduction is basically due to engine matching of the almost constant efficiency compressor. The speed increase, on the other hand, is accomplished by the variable-stator airflow modulating characteristics.

Combustor

Realistic performance characteristics terms of combustion efficiency and burner pressure drop, for typical annular combustor were incorporated in the off-design (matched) engine performance prediction program. However, the combustion efficiency remained essentially constant at 99 percent, and the total pressure recovery varied only slightly from 96 percent at military power to 95 percent at 20 percent power due to the small variation in inlet velocity and burner temperature rise.

Compressor Turbine

The off-design performance characteristics of this component were scaled from a typical fixed-geometry two-stage compressor turbine. The variation of adiabatic efficiency from the assumed design value of 85 percent is shown to be less than 1.0 percent from military to 20 percent power in Figures 88 and 89 for the two different compressor-configured engine cycles. The flow characteristics were for choked flow over the engine operating range investigated. The turbine cooling air treatment described previously is representative of this contractor's experience with transpiration cooled blades and is consistent with the turbine efficiency definition used in the compressor to turbine power balance.

Power Turbine

The off-design power turbine flow and work characteristics were also scaled from a typical fixed geometry uncooled two-stage power turbine map. These characteristics are presented in Figure 90, with engine operating lines of 70 percent, 80 percent, 90 percent, and 100 percent actual power turbine speeds superimposed. It can be seen from the map and from the curves at the bottom of Figures 88 and 89 that the power turbine efficiency with 100 percent speed remains near the peak value of 85 percent as power is reduced from 100 percent to 60 percent military rated. Below this power level, the output shaft speed (free power turbine RPM) should be reduced slightly to 80 percent at 30 percent power to maintain peak efficiency and minimum engine specific fuel consumption.

Advancement Potential

In the initial Engine Cycle Analysis section above, it is noted that tentative optimum pressure ratio values for 30 percent and 60 percent power were 16:1 and 17:1 respectively. The variable stator compressor

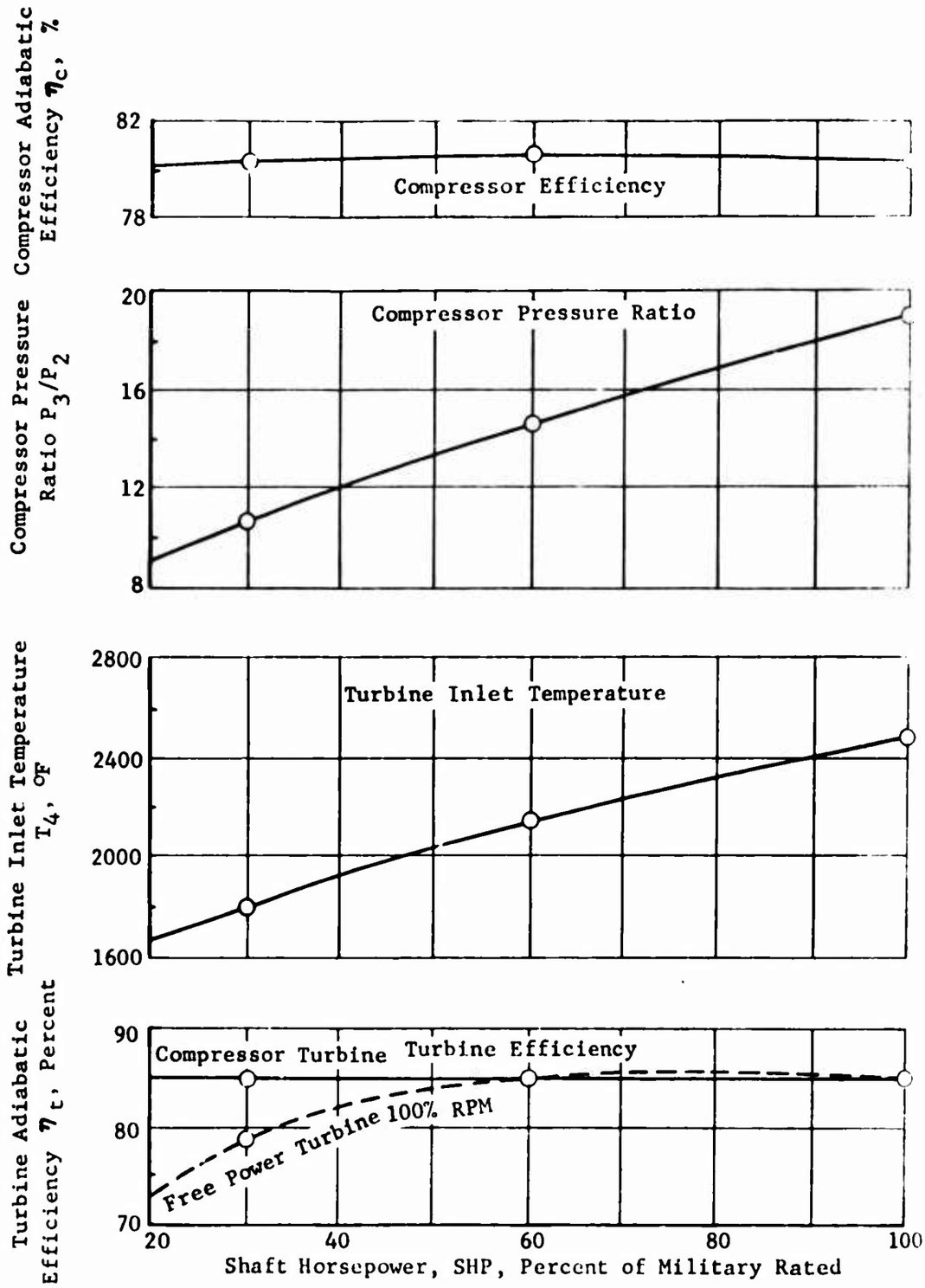

Figure 88. Variable-Stator Compressor Turboshaft Engine Part-Load Performance Characteristics at 100% Power Turbine Speed at Sea Level Standard Day.

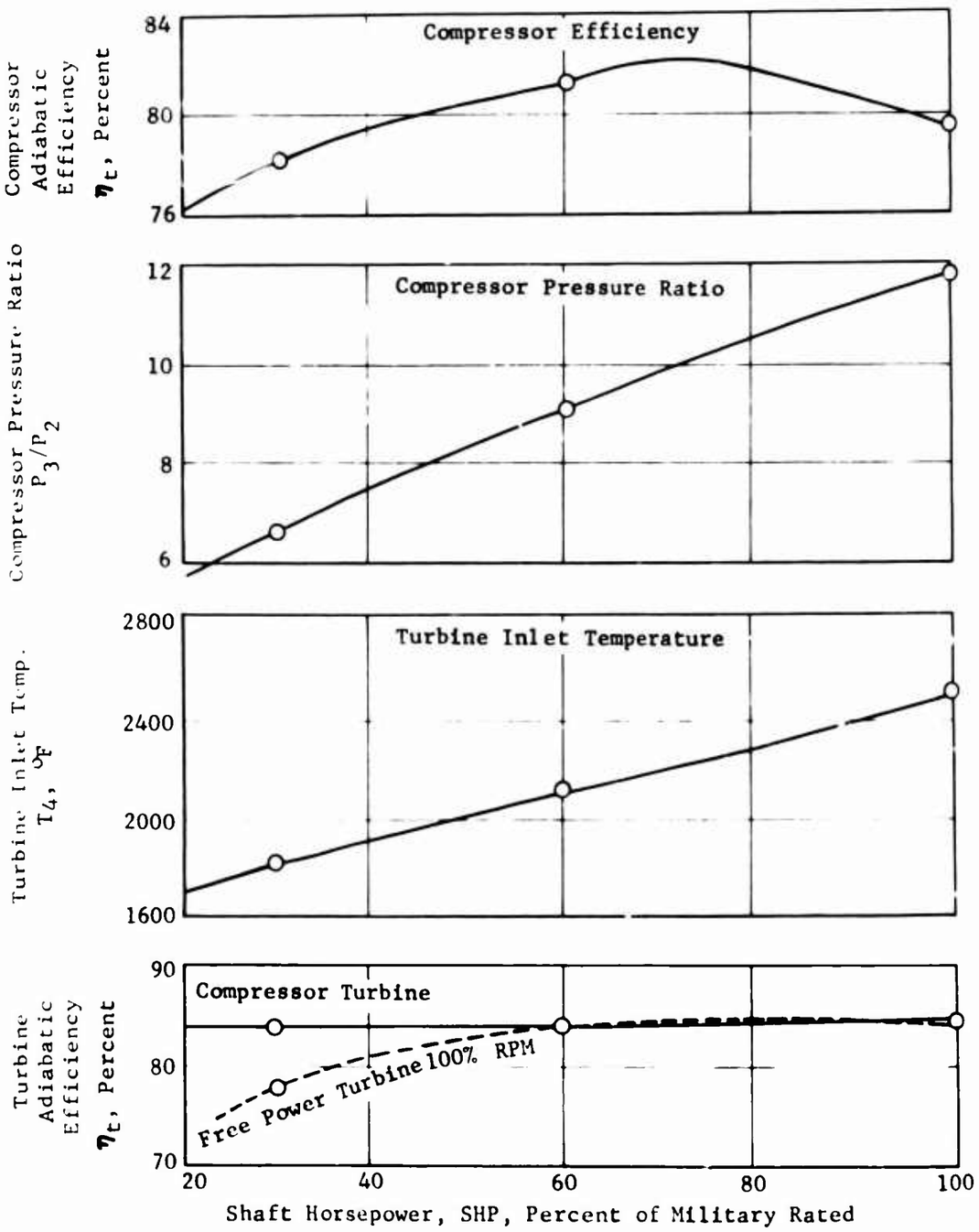

Figure 89. Fixed-Geometry Compressor Turboshaft Engine Part-Load Performance Characteristics at 100% Power Turbine Speed at Sea Level Standard Day.

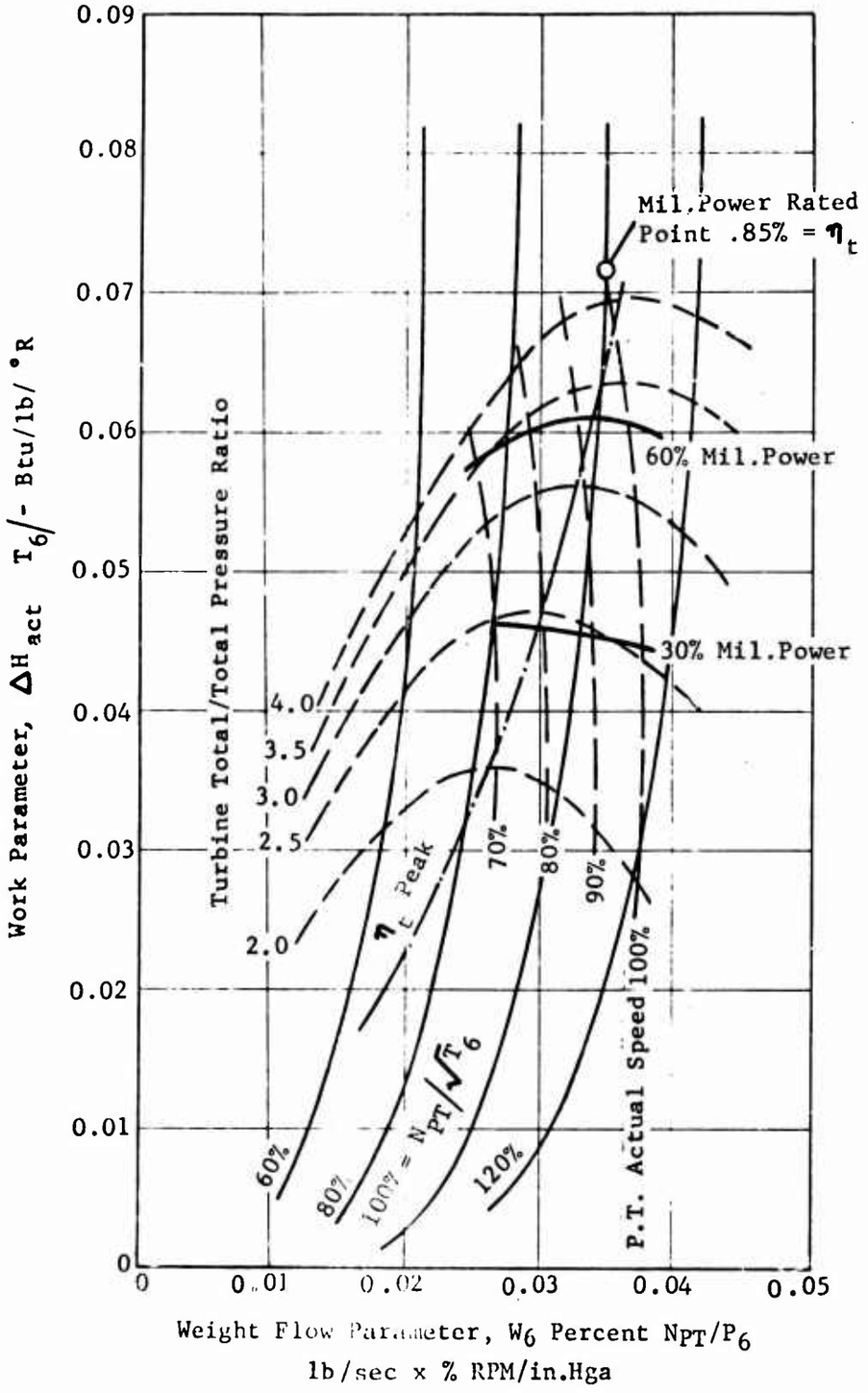

Figure 90. Power Turbine Performance Characteristics With Superimposed Engine Operating Lines for Variable-Stator Compressor Turboshaft Engine.

engine operates at corresponding pressure ratio values of 10.6:1 and 14.6:1 as shown in Table XI. It is of interest to explore the implications of these differences in respect to fuel consumption and military rated pressure ratio. For 30 percent power, using Figure 3, cycle performance at 1900°F and 85 percent turbine efficiency, the corresponding fuel consumptions are .435 and .452, for a decrease of 4 percent between the selected cycle and the tentative optimum. For 60 percent power, using Figure 5, cycle performance at 2100°F and 85 percent turbine efficiency, the corresponding fuel consumptions are .405 and .400 for a potential decrease of about 1 percent. The potential values can be calculated as fractions of values given in Table XI, thus at 30 percent power the potential specific fuel consumption would be .52, and at 60 percent power it would be .445.

Assuming that military power pressure ratio and part-load pressure ratios would be in the same proportions, the optimum compressor for 30 percent load would have a 30:1 pressure ratio at military power, and the optimum compressor for 60 percent load would have a 22.5:1 pressure ratio, compared to the 19.2:1 value of the selected compressor.

The desirability of these performance gains must be weighed against the increased risk and increased complexity associated with the increased pressure ratios.

CONCLUSIONS

The following conclusions were reached in the study of a front-drive free power turbine engine with fixed gas generator turbine geometry and 2500°F turbine inlet temperature at military rated power.

1. The compressor, to be developed with high confidence in three years, incorporates two transonic axial stages with variable setting angles in IGV and stators and a centrifugal stage in a single spool. At 60 percent power, the engine fitted with this compressor operates at a pressure ratio of 14.6:1, a turbine inlet temperature of 2160°F, and a specific fuel consumption of 0.45. The pressure ratio at military rated power is 19.2:1.

2. Minimum 60 percent and 30 percent power fuel consumption would be obtained at pressure ratios of about 17:1 and 16:1 respectively. The specific fuel consumption for these cycles is lower by about 1 percent and 4 percent respectively than that associated with the selected compressor, but military pressure ratios are increased to 23:1 and 30:1 respectively. The higher pressure ratios require additional compressor stages and/or a decrease in development confidence.

3. No advantage in part-load fuel consumption is attainable by accepting significant increases of military rated power fuel consumption. Conversely, for a given cycle pressure ratio, a high efficiency at military rated power favors low specific fuel consumption at part-load operating conditions.

4. The avoidance of part-power compressor stall and surge in high-pressure-ratio (near 20:1) compressors requires variable compressor geometry. Either two-spool or variable-stator compressors provide satisfactory modes of geometry variation.

5. A front-drive engine with two-spool compressor presents developmental obstacles associated with shaft vibration critical speeds. The related difficulties favored the selection of a single-spool variable-stator compressor for a development program.

6. Variable axial compressor stators are necessary and probably sufficient for obtaining the necessary compressor matching effects. Variable inlet guide vanes alone are not sufficient, and variable centrifugal diffuser vanes are not necessary.

7. A two-stage transonic axial compressor offers advantages in efficiency and performance range over a supersonic stage. These advantages depend in part on a superior capability of the transonic stage to accommodate variations of flow by means of variable-stator setting angles.

RECOMMENDATIONS

A three-year experimental program should be undertaken to develop the variable-stator axial-centrifugal compressor described herein, including the following phases:

1. Final aerodyanmic and structural design, including detailed investigation of operating conditions at 60 percent, 30 percent, and 100 percent power operating points defined herein.

2. Experimental development of the variable-stator axial compressor to produce high efficiency at the required flow and pressure ratio, to develop the required part-speed flow range by means of variable IGV and stator setting angles, and, finally, to define the performance in terms of both inlet-corrected and outlet-corrected flow and speed parameters.

3. Experimental development of the centrifugal compressor with a high inlet hub/tip radius ratio to produce high efficiency at required flow and pressure ratio and to define performance in terms of inlet-corrected flow and speed parameters.

4. Analytic investigation of component matching concurrently with component development to verify that components are compatible and to predict design and off-design performance of the combination.

5. Experimental investigation of the complete axial-centrifugal compressor with evaluation of the matching characteristics.

LITERATURE CITED

1. Jones, B.A., and Oscarson, R.P , SINGLE STAGE EXPERIMENTAL EVALUATION OF VARIABLE GEOMETRY GUIDE VANES AND STATOR BLADING, Volume III and Volume IV, Pratt & Whitney Aircraft, PWA FR-2638 and 2639, NASA CR 54557 and 54557, National Aeronautics and Space Agency, NASA Lewis Research Center, Cleveland, Ohio, 31 December 1968.

2. Kovach, K., and Sandercock, D.M., EXPERIMENTAL INVESTIGATION OF A FIVE-STAGE AXIAL-FLOW RESEARCH COMPRESSOR WITH TRANSONIC ROTORS IN ALL STAGES. II COMPRESSOR OVERALL PERFORMANCE, National Advisory Committee for Aeronautics, NACA RM E54G01, NASA Lewis Research Center, Cleveland, Ohio, 1954.

3. Wright, L.C., and Novak, R.A., AERODYNAMIC DESIGN AND DEVELOPMENT OF THE GENERAL ELECTRIC CJ805-23 AFT FAN COMPONENT, The General Electric Company, ASME paper 60-WA-270, 1960.

4. Groh, F.W., and Robb, W.L., HIGH EFFICIENCY CAN BE ACHIEVED IN SMALL SIZE TRANSONIC COMPRESSOR ROTORS, The Boeing Company, SAE 820C, Society of Automotive Engineers, Inc., 485 Lexington Ave., N.Y. 17, N.Y., 1964.

5. Lieblein, S., and Johnsen, I.A., RÉSUMÉ OF TRANSONIC-COMPRESSOR RESEARCH AT NACA LEWIS LABORATORY, NACA Lewis Laboratory, Journal of Engineering for Power, Vol. 83, Series A, No. 3, July 1961.

6. Knowles, D.W., DEVELOPMENT OF A 3500-HP MARINE GAS TURBINE, Curtiss-Wright, ASME paper 59-A-199, American Society of Mechanical Engineers, 345 East 47th Street, N.Y., N.Y. 10017, 1959.

7. Mills, R.G., and Pitt, P.A., 1100-HP GAS TURBINE FOR MARINE APPLICATIONS, BuShips, U.S. Navy, and Solar Aircraft Co., ASME paper 60-GTP-11, 1960.

8. Muller, C.H., and Cox, L.R., SINGLE-STAGE AXIAL COMPRESSOR COMPONENT DEVELOPMENT FOR SMALL GAS TURBINES, Vol III Curtiss-Wright, USAAVLABS Technical Report 68-90C, U.S. Army Aviation Materiel Laboratories, Fort Eustis, Virginia, June 1969, AD857498.

9. Schwartz, F., GAS TURBINE ENGINEERING HANDBOOK, Gas Turbine Publications, Inc., 80 Lincoln Ave., Stamford, Conn., 1966.

10. Welliver, A.D., and Acurio, J., DESIGN AND DEVELOPMENT OF SMALL, SINGLE-STAGE CENTRIFUGAL COMPRESSOR, The Boeing Company; USAAVLABS Technical Report 67-47, U.S. Army Aviation Materiel Laboratories, Fort Eustis, Virginia, September 1967, AD385595.

LITERATURE CITED - Continued

11. Morris, R.E., and Kenny, D.P., HIGH PRESSURE RATIO CENTRIFUGAL COMPRESSORS FOR SMALL GAS TURBINE ENGINES, United Aircraft of Canada, Limited, P.O. Box 10, Longueuil, Quebec, Canada, June 1968.

12. Davis, James V., and Dellert, Edmund J., ADVANCEMENT OF SMALL GAS TURBINE COMPONENT TECHNOLOGY, ADVANCED SMALL AXIAL COMPRESSOR, VOL II, REDESIGN, Continental Aviation and Engineering Corp.; USAAVLABS Technical Report 69-10B, U.S. Army Aviation Materiel Laboratories, Fort Eustis, Virginia.

13. Rodgers, C., VARIABLE GEOMETRY GAS TURBINE RADIAL COMPRESSORS, Solar Div., Int. Harvester Co., ASME paper 68-GT-63, 1968.

14. Ball, G.A., Bell, A.H., and Mann, L.B., THE DEVELOPMENT OF THE CHRYSLER AUTOMOTIVE CENTRIFUGAL COMPRESSOR. CENTRIFUGAL COMPRESSORS. TECHNICAL PROGRESS SERIES, VOL 3, Society of Automotive Engineers, Inc., 485 Lexington Ave., New York 17, N.Y., December 1961.

15. Welliver, A.D., and Acurio, J., ELEMENT DESIGN AND DEVELOPMENT OF SMALL CENTRIFUGAL COMPRESSOR, VOL II, The Boeing Company, USAAVLABS Technical Report 67-30, U.S. Army Aviation Materiel Laboratories, Fort Eustis, Viriginia, August 1967, AD384924.

GLOSSARY

camber	a blading parameter, either 10 times the nominal lift coefficient of the prototype wing section or the angular difference between tangents to section mean lines at leading and trailing edges.
DeHaller number	an aerodynamic loading parameter, the ratio of blade row outlet to inlet relative velocity.
diffusion factor	an aerodynamic loading parameter, the value of the equation: $1 - V_2/V_1 + (V_{1tan} - V_{2tan})/2\,V_1$ solidity
DN	a bearing limit parameter, the product of shaft speed in RPM and the bearing inside diameter in millimeters.
HP	high-pressure compressor, always a single-stage centrifugal compressor.
LP	low-pressure compressor, an axial compressor of one or two stages.
plus	in the description of a multistage compressor, e.g., supersonic plus centrifugal, plus indicates that the first-named stage is the inlet stage and that it discharges flow to the next named stage.
power-limited	indicates that engine power at 2500°F burner temperature is the decisive factor in establishing optimum performance, rather than some other limit such as maximum cycle pressure or compressor tip speed. Appendix II treats this topic in more detail.
PW-G	a centrifugal compressor stage with high efficiency and pressure ratio about 6:1, from data in Reference 11. Performance is given in Figure 36.
RF-2	a centrifugal compressor stage with pressure ratio near 10:1 and efficiency raised from test values given in Reference 10. Performance given in Figure 37.
solidity	a blading parameter, the ratio of blade section chord length to spacing between blades.

GLOSSARY - Continued

stagger	a blading parameter, the angle between the section chord line and the compressor shaft centerline.
S	a supersonic axial compressor stage with pressure ratio near 3 and efficiency raised from test values given in Reference 8. Performance given in Figure 32.
ST	a two-stage axial compressor based on stage S above and a hypothetical transonic stage. Performance given in Figure 34.
TT	a two-stage transonic axial compressor with pressure ratio near 3 and efficiency raised from test values given in Reference 12. Performance given in Figure 33.
405	a centrifugal stage with scroll collector from Curtiss-Wright unpublished data on test of impeller plus vaneless space and efficiency reduced. Performance given in Figure 35.

APPENDIX I
LP/HP COMPRESSOR MATCHING PROCEDURES

The compressor matching procedure combines the performance characteristics of a low-pressure compressor (called LP) and a high-pressure compressor (called HP) to define the overall performance of the assembled configuration. The performance data is processed into a form suitable for matching studies, following which one of the compressors is scaled to produce a desirable match. The overall performance is then computed.

The LP compressor takes air at ambient conditions, compresses it, and delivers it to the HP compressor, which then further compresses the air and delivers it to a receiver. In a gas turbine engine, the receiver is a combustor or a regenerator heat exchanger. In a test rig, the receiver is a throttlable collecting chamber.

PROCESSING PERFORMANCE DATA FOR MATCHING

The point of LP discharge and HP intake is the interface point. It is assumed in the present case that there is no cooling or pressure drop between stages; any deviations from this assumption are accounted for in the LP performance data. Bleed at the interface point is a recognized possibility. The law of continuity requires that flow leaving the LP must be admitted by the HP or bled off at the interface point. There are no changes of pressure or temperatures, therefore,

$$(W\sqrt{\theta}/\delta)_{\text{LP exit}} = (W\sqrt{\theta}/\delta)_{\text{HP inlet}} + \text{BLOOD}$$

where BLOOD is the bleed flow. For single-shaft compressors, the shaft speeds of both compressors are identical and there are no changes of temperature, therefore,

$$(N/\sqrt{\theta})_{\text{LP exit}} = (N/\sqrt{\theta})_{\text{HP inlet}}$$

The two equations written above dictate terms according to which the test data must be used for the stage matching procedure. The match is defined in terms of interface corrected airflow and speed in Figure 91 for a typical LP compressor and in Figure 92 for a typical HP compressor. In Figure 91 exit corrected speeds are plotted against exit corrected flows. The constant speed lines represent constant inlet corrected speeds, and the stall line passes through the lowest corrected airflow points of each line. In Figure 92, inlet corrected speeds are plotted against inlet corrected flows. The speed lines represent constant inlet corrected speed, and the stall line passes through the lowest corrected airflow points of each. The choke line passes through the highest corrected airflow points of the HP map.

The definition of compressor element performance utilizes corrected enthalpy values, as follows:

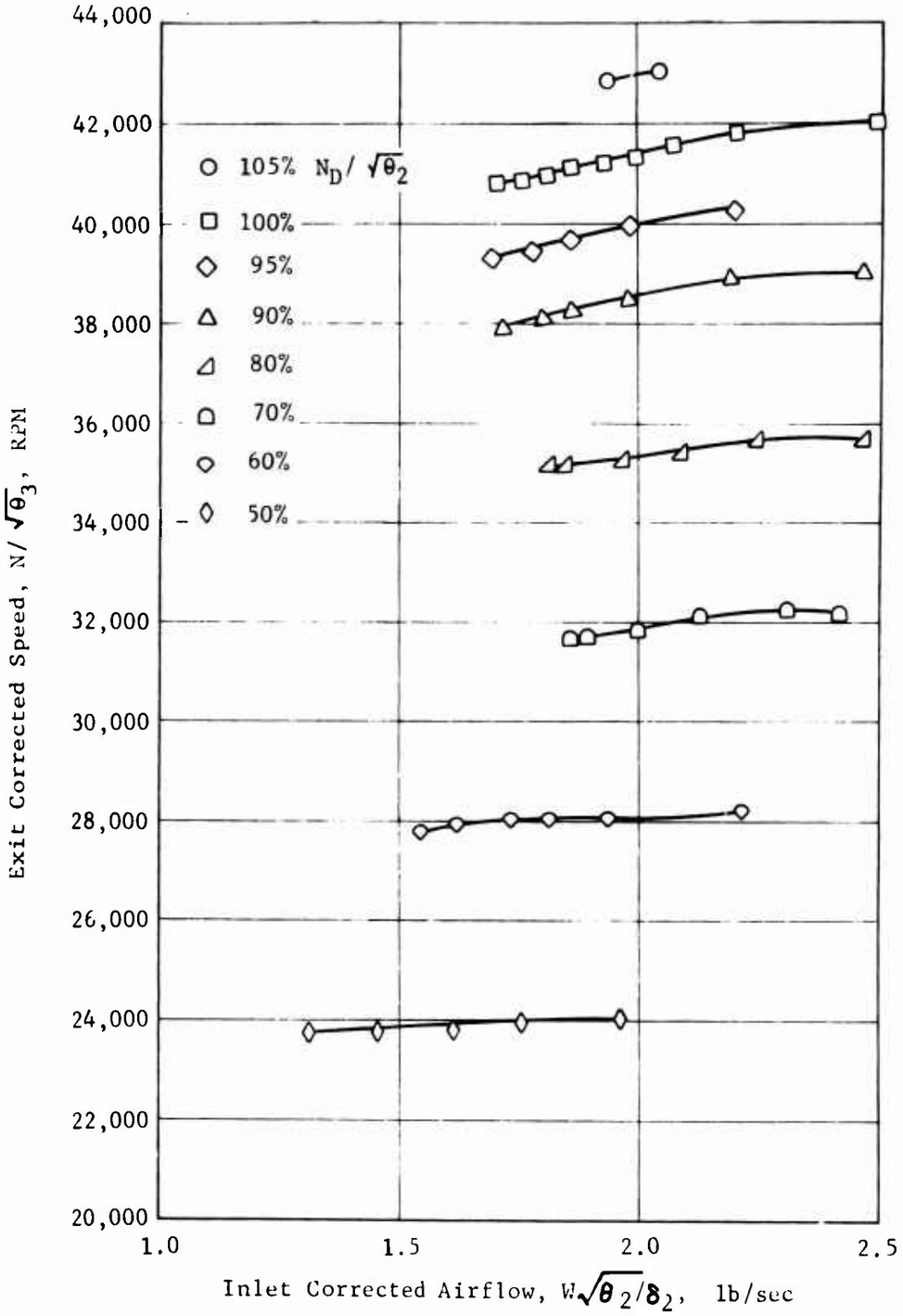

Figure 91. Typical LP Compressor Matching Base Data, Two-Stage Transonic Compressor (F1), Corrected Speed.

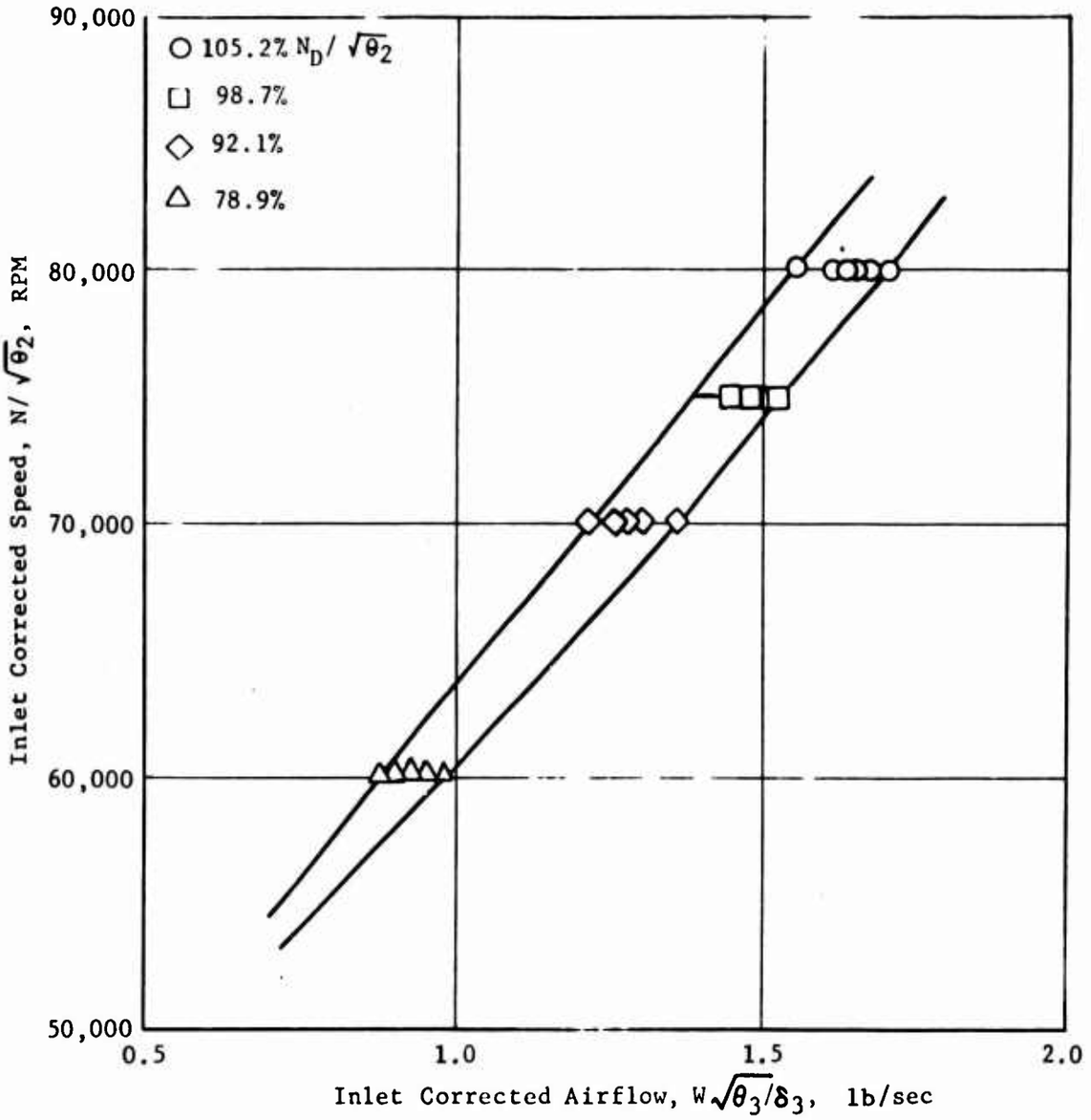

Figure 92. Typical HP Compressor Matching Base Data, PW-G Centrifugal Stage, Corrected Speed.

HCOI = isentropic enthalpy rise divided by the square of the speed ratio

HCO = HCOI divided by stage efficiency

The value of HCOI is determined from test data corrected to standard inlet conditions and therefore implies a correction for inlet temperature ratio. The inlet corrected speed ratio is referred to design speed. Division of enthalpy rise by the speed squared collapses the range of values which must be plotted; also, it brings to attention any systematic variations of speed line form that may be characteristic of the machine, and it facilitates interpolation between speed lines when this is required. In typical fashion, Figures 93 and 94 show values of HCO and HCOI, respectively, plotted against outlet corrected airflow for lines of constant inlet-corrected speed for the LP compressor. Similarly, Figures 95 and 96 show values of HCO and HCOI, respectively, plotted against inlet corrected airflow for lines of constant inlet-corrected speed for the HP compressor.

The computation of the corrected performance parameters in proper form for matching was done with the aid of a small FORTRAN IV program called BLAH, which is presented in Appendix III.

Superimposing the data of Figure 91 directly upon the data of Figure 92 represents direct staging of the compressors. There would be a serious mismatch in speed, with the LP design speed near 41,000 and the HP design speed at 75,000 RPM; some degree of scaling is necessary.

SCALING

There is only one valid method of scaling, which is to change all dimensions in the same proportion, to associate a certain pressure ratio with the identical set of temperature-corrected tip speeds and gas velocities, and to expect corrected flow to vary in proportion to the square of the radius ratio. This method is here called true scaling. True scaling was tried in the original stages of the program. For a given point on an LP map a line can be superimposed on the HP map in order to show all the possible points where the selected LP point can be located using true scaling. It is easy to choose the one point on the line where the LP should be located, but it is more difficult to accept any combination of performance reached in that manner. This problem led to a requirement for more freedome, and to a simplified approach to scaling called free scaling.

With true scaling, in order to perform the required work, it is necessary to secure the same axial compressor corrected hub speeds and the same centrifugal compressor corrected tip speeds in the original and the derivative components. It was assumed that this would be done in free scaling also, but that the other requirements of true scaling would not be met. However, other details of design would be handled as well in the final design of the free-scaled derivative as in the original compressor, though not by scaling. It was not necessary in the matching work to do anything to ensure

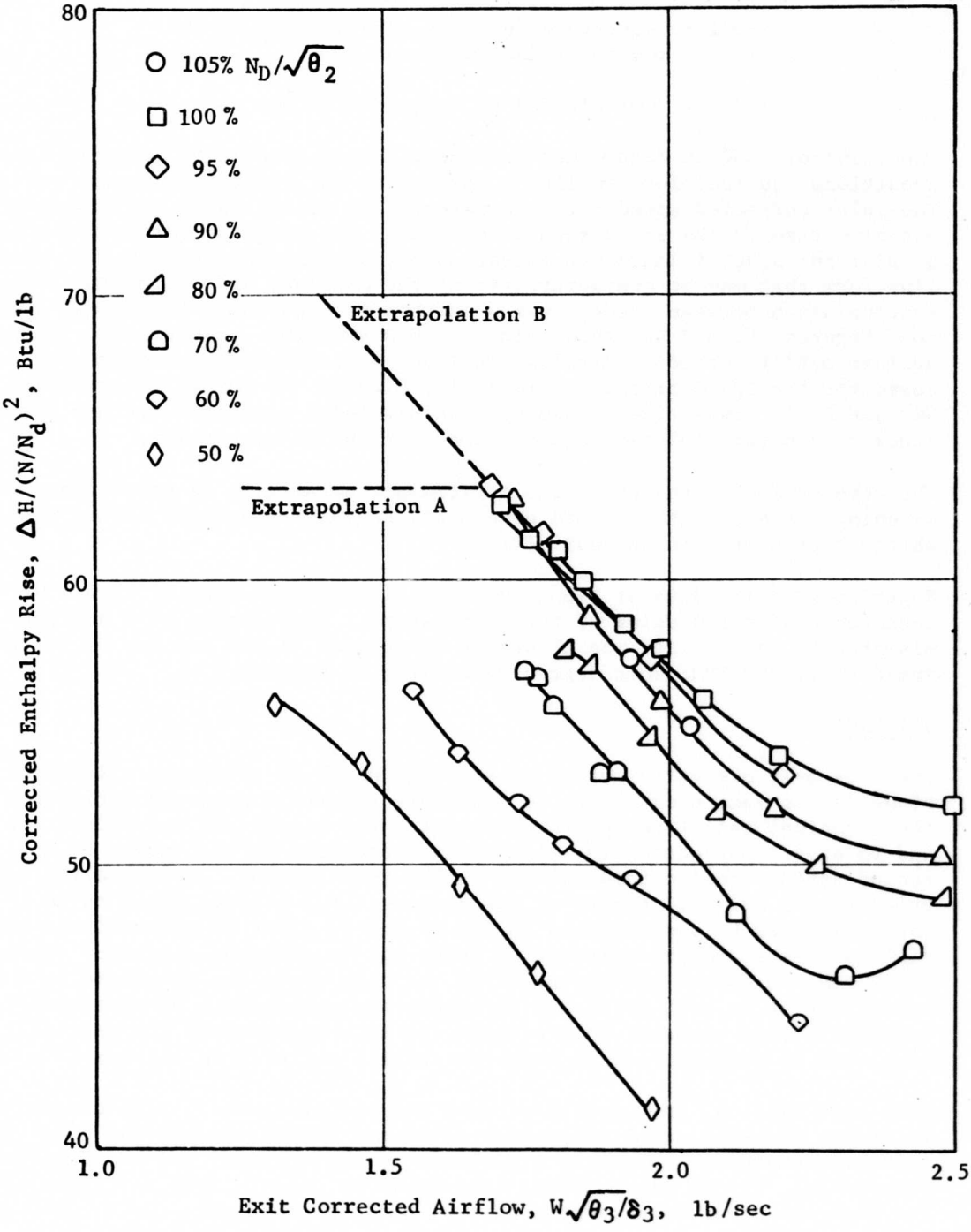

Figure 93. Typical LP Compressor Matching Base Data, Two-Stage Transonic Compressor (F1), Corrected Enthalpy Rise.

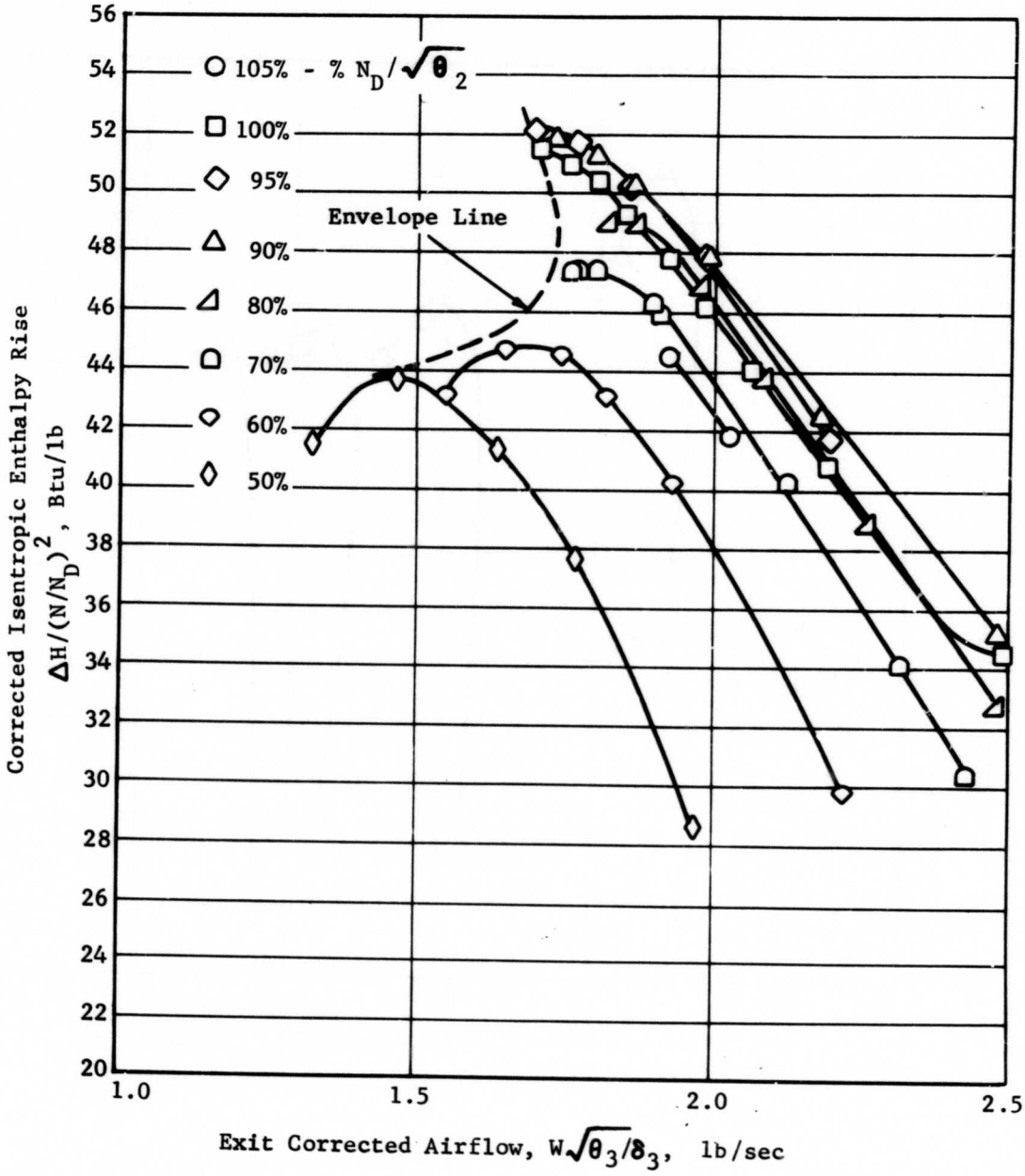

Figure 94. Typical LP Compressor Matching Base Data, Two-Stage Transonic Compressor (F1), Corrected Isentropic Enthalpy Rise.

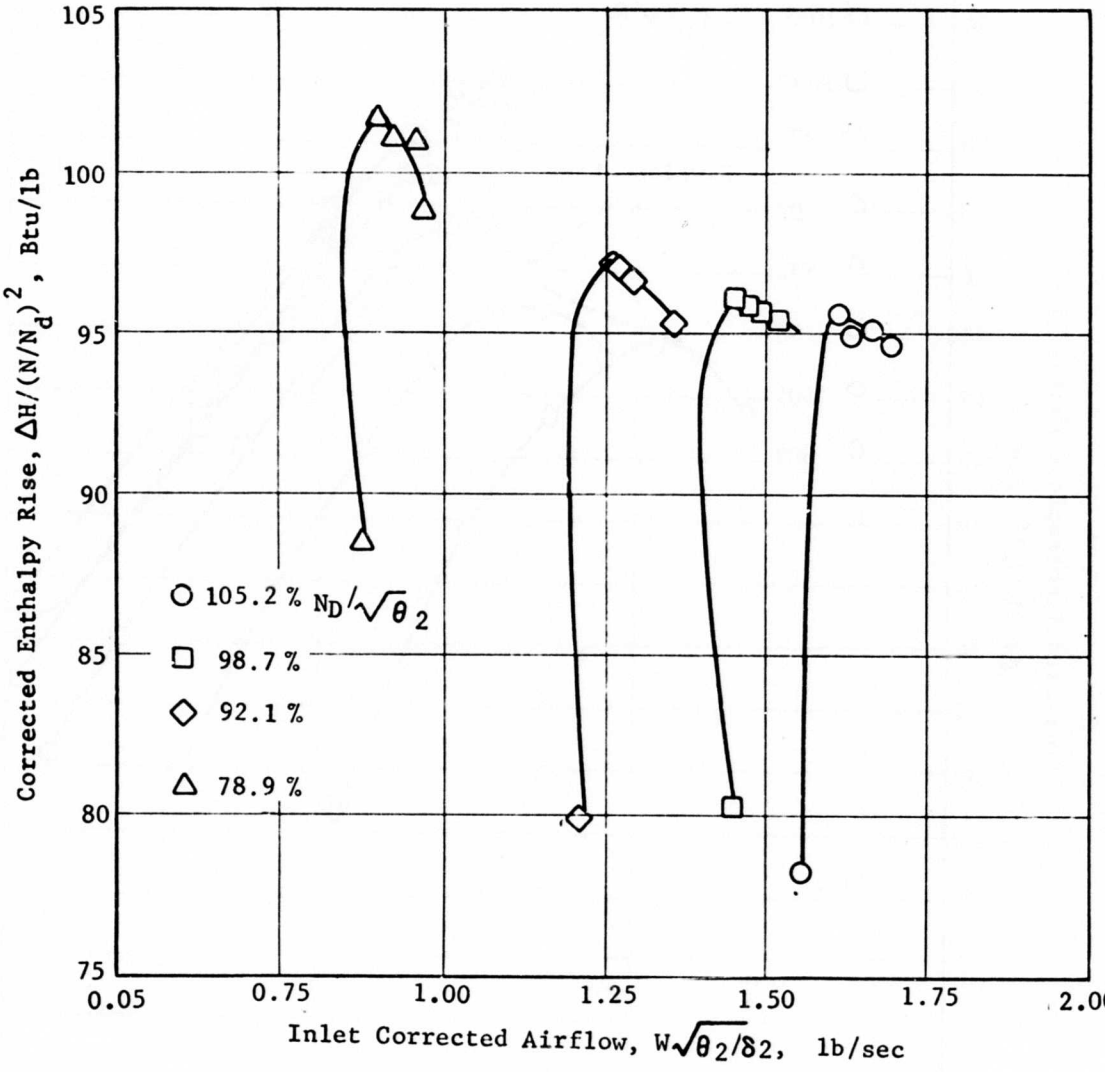

Figure 95. Typical HP Compressor Matching Base Data, PW-G Centrifugal Stage, Corrected Enthalpy Rise.

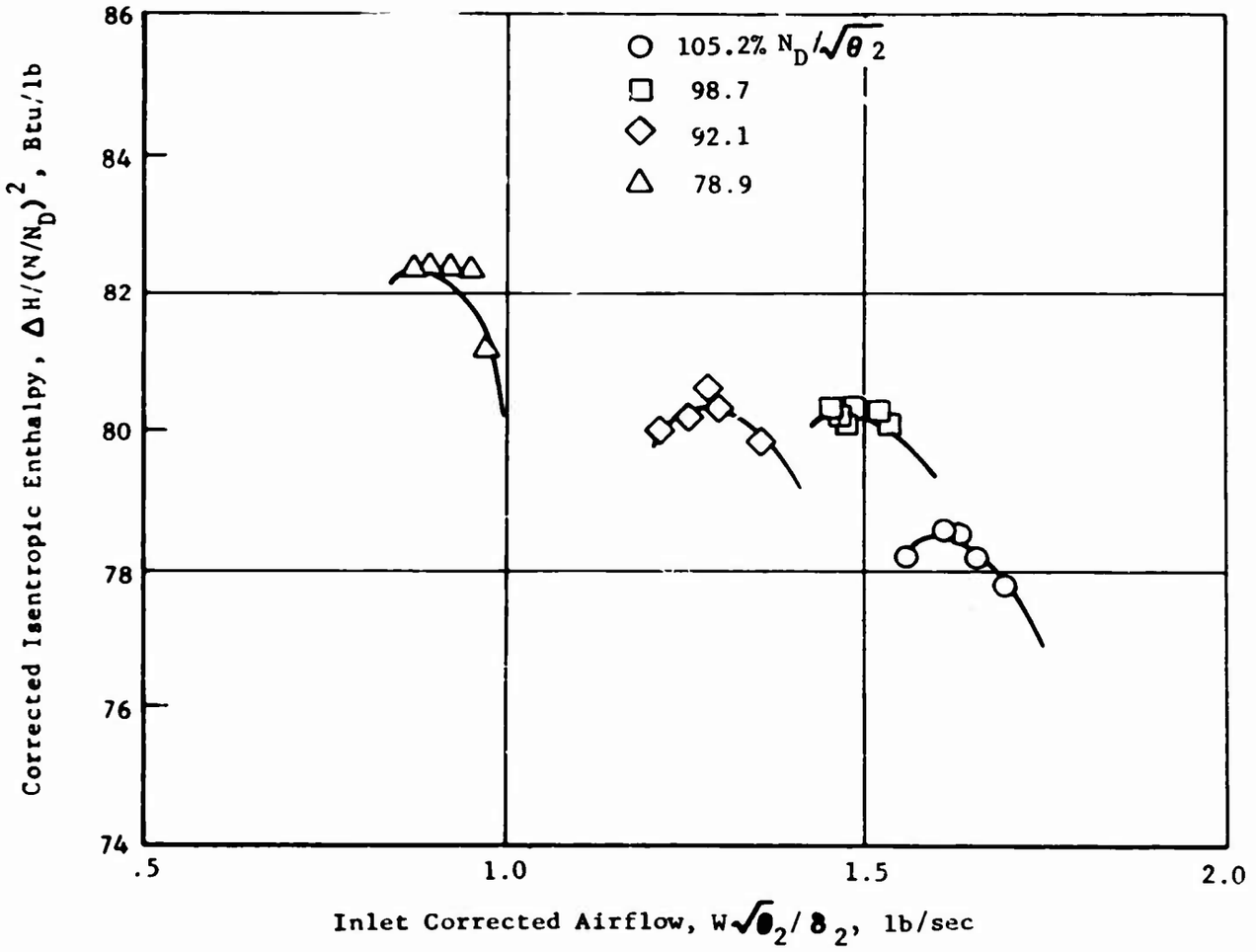

Figure 96. Typical HP Compressor Matching Base Data, PW-G Centrifugal Stage, Corrected Isentropic Enthalpy Rise.

this adherence to good design practices. The assumption merely gives explicit recognition to the fact that in free scaling an element of new design was introduced.

Important scaling relations are detailed below in the description of data input preparation.

COMPUTING INPUT DATA PREPARATION

Some relations which must be used in computing matched compressor performance are outlined below:

1. For true scaling it may be shown that

$$(W\sqrt{\theta}/\delta) \times (N/\sqrt{\theta})^2 = K1$$

It has become the practice to superimpose an LP match map on an HP match map, e.g., Figure 38. A true scale line can be put on such a map according to the following formula:

$$W\sqrt{\theta}/\delta = K1/(N/\sqrt{\theta})^2$$

where K1 is computed from values taken at a selected point on the LP map. A true-scale line is approximately perpendicular to an HP stall line, resulting in free choice of stall relations but little variation of flow and speed. Free scale departure from true scale has usually been toward lower centrifugal compressor specific speeds.

2. The scale factors for flow and speed are used whether scaling is true or free. There is a scale factor for speed:

$$C_N = N_{HP}/N_{LP}$$

and a scale factor for flow:

$$C_W = W_{HP}/W_{LP}$$

In the case of true scaling it may be shown that:

$$C_W = 1/C_N^2.$$

In any case the scale factors may be calculated after LP flow W_{LP} and speed N_{LP} and HP flow W_{HP} and speed N_{HP} have been selected. All scaling is done at the interface using the LP/HP matching maps.

3. Design speeds must be supplied as inputs for the matching computation. In the present study the LP compressors were not scaled; hence the design inlet corrected speeds were used:

XND1 = LP design inlet-corrected shaft speed, RPM.

For the HP compressor the following formula was used:

XND2 = (HP design inlet-corrected speed)/C_N, RPM,

where C_N is the speed scale factor defined in the preceding section.

4. The physical, i.e., uncorrected, tip speed of the centrifugal compressor was used as a limit and as information. The following equation was used in calculating the value of tip speed U for single-spool machines:

$U = C_N \times XND1 \times (\text{HP design tip speed})/(\text{HP design shaft speed})$.

This is the tip speed at LP design speed, and if the compressor for some reason does not attain LP design speed the tip speed is correspondingly lower.

For a two-spool compressor, the following formula was used:

$U = \sqrt{T_3/518.7} \times (\text{HP design tip speed}) \times ENPC2/100.$

Here T3 is the LP compressor exit temperature and the radical term is the interface value for $\sqrt{\theta}$. The value of the radical can alternatively be computed as the applicable ratio of LP inlet/exit corrected speeds. ENPC2 is an input percent speed value for the HP compressor, determined in a manner described subsequently.

5. Superimposing the LP map on the HP match map is accomplished with the use of the above-defined scale factors C_N and C_W. On the LP map, for each LP speed line values of speed and flow are read at two points or more, and the corresponding HP map values are calculated using the scale factors. The resulting values are then plotted on the HP match map to show the LP speed lines and stall lines in relation to the HP as showr in Figure 38.

For two-spool compressors the map is constructed just as above, and the effect of two-spooling is handled by the manner in which data is taken from the match map.

For variable-stator compressors an initial map was drawn just as above, and then the LP speed lines were moved horizontally until the LP stall line fell on the HP stall line, thus defining the flow

variation required of the LP. The input quantity, FLORAT was defined for each speed line as follows:

$$FLORAT = (W_{HP} - W_{LP}) \times 100/W_{LP}$$

where W_{LP} and W_{HP} are LP stall point flows before and after the flow shift accomplished by varying stator angles.

For air bleed, the input quantity BLOOD is defined as follows:

$$BLOOD = (W_{LP} - W_{HP})/C_W$$

where $W_{LP} - W_{HP}$ is the quantity of bleed flow on the match map and the scale factor C_W converts it to unscaled LP size.

6. The input values ENPC1 and ENPC2 are percent speed values for the LP and HP compressors. The ENPC1 values identify the LP constant inlet corrected speed lines used in presenting LP performance on the match map and elsewhere. Points on the ENPC1 lines determine the operating conditions for both LP and HP compressors. Since the match map is drawn on the HP map, HP speeds are read on the ordinate scale and percent speed ENPC2 is referred to HP design speed.

   For two-spool compressors the speeds are not bound together. ENPC1 speed lines again define the LP compressor, but the flow range can be associated with HP flows at other speeds. One approach taken was to associate the LP speed with the HP speed at which stall lines coincide. A later approach was to choose the LP stall point which had maximum flow and choose the corresponding HP speed ENPC2. to be used for that LP speed and all higher LP speeds. This resulted in some under-loading of the LP at high speeds but was regarded as more reasonable.

7. Access to the data in performance curves, Figures 93, 94, 95, and 96, is by way of percent speed and corrected airflow. The corrected flow values W_{HP} for reading HP performance curves were read directly from the match map between the limits of HP stall and HP choke. If the LP stall line crossed the speed line in this range, the flow at that point was taken as one of the points.

   A flow value W2 is required as program input and is defined as follows:

$$W2 = W_{HP}/C_W$$

   Both W_{HP} and C_W are defined above.

   For reading LP data in most cases, including two-spool cases, a value W_{LP} was defined as follows:

$$W_{LP} = W_{HP}/C_W.$$

For bleed cases,

$$W_{LP} = W_{HP}/C_W + \text{BLOOD}.$$

For variable stator cases

$$W_{LP} = W_{HP}/1 + \text{FLORAT}/100.)$$

In single-spool fixed-stator cases at low speeds, the possible HP flow range often fell to the left of the LP flow range, indicating that the LP was operating in stall, where performance was not defined. In such cases, the LP speed line was usually extended horizontally to the left from the stall point. In other cases, particularly for case 4,1-AAA, the speed lines were simply extended along the speed line itself.

8. The values of HCO and HCOI were read from typical Figures 93 and 94 at values of W_L for the LP, and from typical Figures 95 and 96 at values W_H for the HP. The extrapolation into the LP stall region is the only questionable aspect of the matching procedure. As shown in Figure 93, two extrapolations for temperature rise (HCO) were used. For most cases a horizontal extrapolation from the maximum value on the speed line was used. For case 4,1-AAA, Figure 52, an extrapolation along the line of the speed line was used. As shown in Figure 94, for the pressure ratio (HCOI), only one type of extrapolation was used, following the envelope of values for all speed lines. With respect to the HCO extrapolations, it can be argued that a fair comparison resulted from treating most cases in the same way. In retrospect, the second method is preferred; it was applied to the fixed-geometry design case where it tended to give lower part-speed efficiencies.

The computation procedures for stage matching were performed by a computer according to two FORTRAN programs, which are described in Appendix III. All of the inputs for these programs have been defined above.

APPENDIX II
COMPRESSOR/ENGINE MATCHING PROCEDURES

The compressor/engine matching procedure defines an optimum set of operating conditions for 60 percent, 30 percent, and 100 percent power by a process which is very simple and yet was reached only after a number of ineffective or inefficient approaches had been tried and finally rejected. One of the most troublesome concepts to establish has been that an optimum condition for minimum 60 percent and 30 percent power fuel consumption does actually exist. Some of the difficulty arises in the need to take, as a beginning, a compressor map of some kind.

Figure 97 shows the type of compressor map that is required. This map has a stall line and enough lines of constant efficiency to determine the efficiency at any point of interest. There are no speed lines, since none are required until consideration of compressor speed limitations begins. Initially, there is no definition of engine cycle pressure ratio for any operating condition. Optimization of engine performance at some power level and pressure ratio establishes the operating region on the compressor map. This map can be one based on test data, on an LP/HP matching procedure, or on a mean-line mapping program. The pressure ratio and flow parameters may have any desired values, and the efficiency islands any plausible shapes. The basic requirement is for a definition of representative compressor operating characteristics, in order that optimum engine performance can be related to a particular compressor map. This map also has lines of constant burner temperature, positioned using the assumption of a choked turbine nozzle, governed by the following equation:

$$k = W\sqrt{T}/(P/P)$$

The value of k is established by placing one point for one burner temperature on the graph. Thereafter, any temperature line can be located from the following equation:

$$P/P = \sqrt{T}/k \times W$$

The location of the family of temperature lines is restricted only in that it is desirable to place the operating points in regions of maximum efficiency and reasonable stall margin.

The next step is to read from the curve, along one burner temperature line, values of pressure ratio, airflow, and efficiency. The range of flows covered should extend above and below the pressure ratios at which a given power point is expected to fall. In the present study, a 2500°F burner temperature was chosen for military power. For 60 percent power, temperatures of 2100° and 2200°F were investigated, and for 30 percent power a 1900°F temperature was used. These values were based on experience and were not verified until the last phase of the study involving calculation of detailed engine performance.

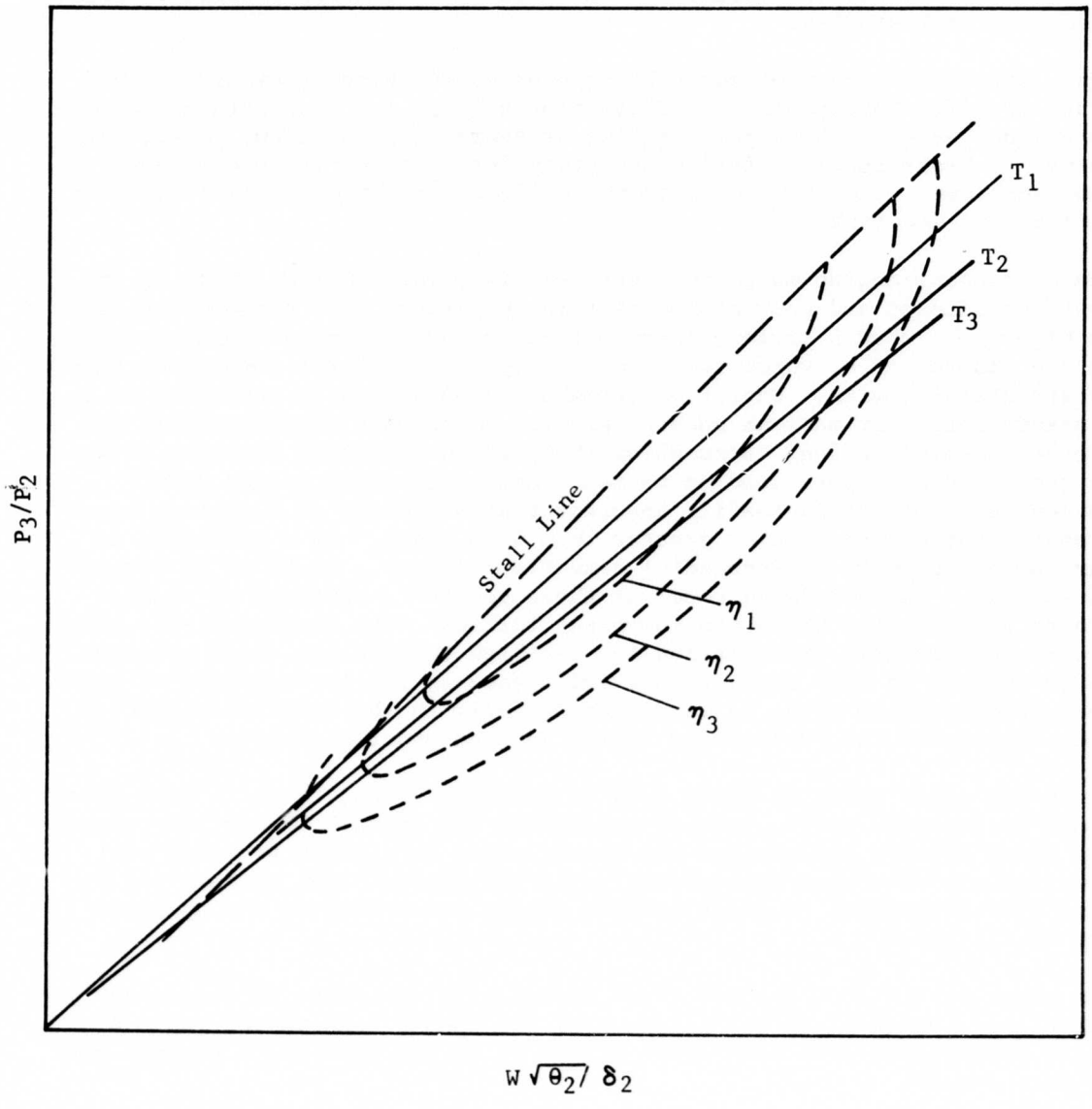

Figure 97. Sketch of Compressor Performance Map for Compressor/Engine Matching.

Next, from Figures 3, 5, 8 and 12 at the new-found values of pressure ratio and compressor efficiency, read values of Brake Specific Fuel Consumption and Brake Specific Horsepower. It may be noted that in the present study, an 85-percent efficiency was used for the turbine based on experience in past studies.

Next, determine values of shaft horsepower as the product of airflow and brake specific horsepower. Finally, plot a graph for each burner temperature line, as shaft horsepower versus pressure ratio or flow. Also, plot curves of brake specific fuel consumption for each temperature against the same abscissa. Such a graph appears in Figure 98 where pressure ratio is used as the abscissa.

The compressor/engine match in Figure 98 is power limited, which is the most significant and pervasive factor in the study. The performance data in Figure 98 show a maximum power output at 2500°F burner temperature at 15.3 pressure ratio, which is below the capability of the compressor based on structural limits. Engine performance is optimized by selecting 15.3 pressure ratio for maximum power. Figure 98 shows a characteristic increase in specific fuel consumption (SFC) which occurs as pressure ratio is reduced during part-load operation. Again referring to the 2500°F horsepower plot, it is readily apparent that selection of a maximum power pressure ratio less than or greater than 15.3 results in a reduction in maximum power, with corresponding reductions in power at 60 or 30 percent of maximum. Since reduced power at these points is obtained at reduced pressure ratio, the SFC would increase, following the characteristic noted above. Performance optimization for the high temperature, high pressure ratio engines in this study is not influenced by the introduction of variable power turbine area, as is discussed fully in the Power Turbine Flow Area section of the Preliminary Design section under Discussion.

There are cases where no power peak is defined. Then, there is some other limit to pressure ratio, such as compressor tip speed. The optimum operating point is then the maximum tip-speed, since this point provides part-power points with maximum pressure ratio and minimum fuel consumption. This operating point produces maximum engine power limited not by power, but by tip speed.

The shape of the 2500°F power curve varies with the shape of compressor map efficiency contours and the location of the 2500°F line on the map. A sharp power-limit peak such as in Figure 98 is not typical; a rounded peak is more common.

Power-limited engine configurations usually incorporate fixed-geometry compressors. In the study, either two-spooling or using variable stators has raised high-speed compressor efficiency to the point where maximum speed becomes the limiting factor. The speed limit is taken to be either 100 percent LP speed or a specified centrifugal tip speed. In the absence of other limits, it is certain that power limiting will occur with engines of any kind operated at overspeed conditions, due to decrease of component efficiency.

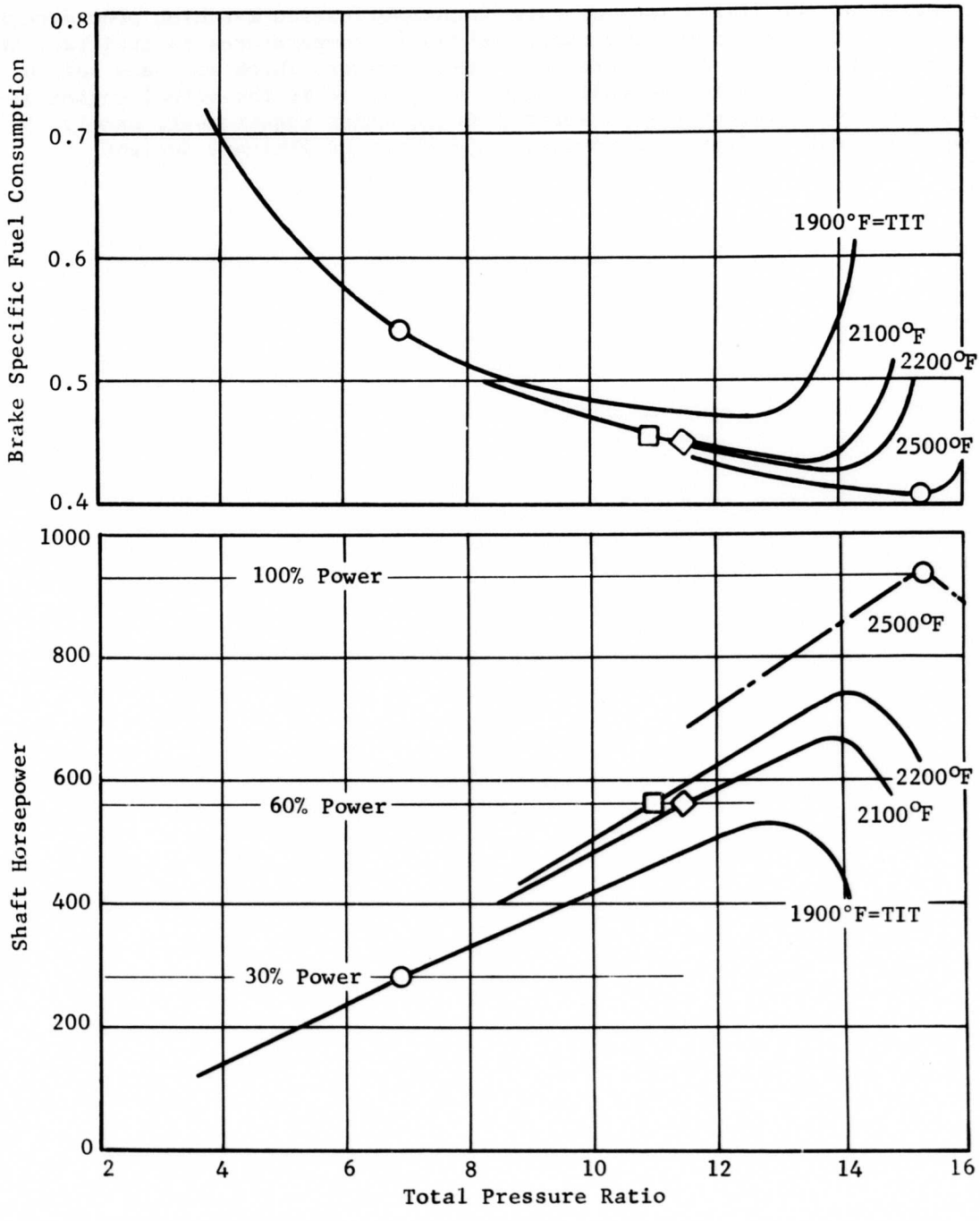

Figure 98. Compressor/Engine Matching Performance, Power and Brake Specific Fuel Consumption as a Function of Pressure Ratio for Temperatures of 1900°, 2100°, 2200° and 2500°F, 2.8 Supersonic Plus PW-G Centrifugal, Case 2,3.

A review of the limitations of this compressor/engine matching procedure is in order at this point. The choice of burner temperatures is arbitrary and results in somewhat inaccurate performance values, which are only set in proper perspective in the full engine analysis or in the actual engine operation. The procedure does satisfy an important requirement, namely, to expeditiously evaluate and compare a number of preliminary designs.

APPENDIX III
COMPUTATION PROCEDURES

Many of the computations in this study were performed using an IBM 360/44 digital computer. Some fairly large proprietary programs were used: a mean-radius compressor design program, L2050, and a compressor mapping program, L2048; a turboshaft design point cycle performance program, L2089, and a single-spool turboshaft off-design engine performance program, L2159. Other small FORTRAN programs were prepared and used for executing the program work. They deal with the matching of the compressor stages as described in APPENDIX I and in the DISCUSSION under Compressor Performance Curves in ENGINE CYCLE ANALYSIS, and under Compressor Characteristics in PRELIMINARY DESIGN.

This appendix gives the input lists, the FORTRAN program listings, and samples of program printed output for the following small FORTRAN programs.

Program Name	Purpose
ADDER	Given pressure ratio and efficiency for two compressors, find overall pressure ratio and efficiency when compressors are staged.
FIXER	Given compressor performance on cards, raise efficiency by a constant amount on each speed line, compute corresponding pressure ratio, and punch out cards giving new performance data.
BLAH	Given compressor performance on cards, calculate corrected enthalpy rise values and exit-corrected speed and flow values.
ONE-SPOOL COMPRESSOR MATCH	Given performance data for an LP and an HP stage, calculate overall performance. Also punch cards giving performance in format used in BLAH and FIXER.
TWO-SPOOL COMPRESSOR MATCH	Given performance data for an LP and an HP stage, calculate overall performance.

The input lists give the card type, card fields, input format, FORTRAN name of variable, and definition of variable. Card type identifies each card for a subsequent list showing the sequence of cards in the input deck. The input format code signifies the following:

A	alphanumeric, a combination of letters and numbers used to write a title, placed anywhere in the field of allotted card columns.
I	integer, a number without a decimal point, placed in the last (right-most) column in the allotted field.
D	decimal, a number which has a decimal point; number may be placed anywhere in the allotted field.

The information about the programs is given in subsequent tables as follows:

	Input List	Sample Output	FORTRAN Listing
ADDER	XII	XIII	XIV
FIXER	XV	-	XVI
BLAH	XV	XVII	XVIII
ONE-SPOOL MATCH	XIX	XX	XXI
TWO-SPOOL MATCH	XXII	XXIII	XXIV

Subroutine SNARF is used in all of these programs. The listing for this subroutine is given with the listings for BLAH, Table XVIII.

TABLE XII. ADDER INPUT LIST

Card Type	Column	Input Format	Name	Definition
A	1-10	I	JO	Number of axial LP compressor cases
	11-20	I	KO	Number of centrifugal HP compressor cases
B	1-10 11-20 to 61-70	D	APOP	Total pressure ratio for the axial compressor; up to 7 values in fields of 10 columns
C	1-10 11-20 to 61-70	D	AETA	Adiabatic efficiencies for the axial compressor, corresponding to total pressure above (one AETA for each APOP on Card B)
D	1-10 to 61-70	D	CPOP	Total pressure ratio for the centrifugal compressor, up to 7 values in fields of 10 columns.
E	1-10 to 61-70	D	CETA	Adiabatic efficiency for the centrigugal compressor (one CETA for each CPOP on Card D)

Each input case requires one data set of cards consisting of the following card types in sequence

A	Beginning of a case
E,B,B,B,	B cards to give data for JO cases at 7 per card
C,C,C,	C cards to give data for JO cases at 7 per card
D,D,D,D	D cards to give data for KO cases at 7 per card
E,E,E,E	E cards to give data for KO cases at 7 per card
A	Beginning of a new case

INPUT FORMAT LEGENDS: A = Alphanumeric
I = Integer
D = Decimal

TABLE XIII. ADDER SAMPLE OUTPUT

AXIAL COMPRESSOR PERFORMANCE IS 1.500 PRESSURE RATIO
0.820 ADIABATIC EFFICIENCY

-- CENTRIFUGAL PERFORMANCE ---				*	OVERALL PERFORMANCE				
PRESSURE RATIO	EFFY. AD.	P3 PSIA	T3 DEG.R	*	PRESSURE RATIO	EFFICIENCY AD	POLY	P4 PSIA	T4 DEG.R
5.00	0.820	22.0	596.3	*	7.50	0.804	0.852	110.2	1013.2
8.00	0.800	22.0	596.3	*	12.00	0.786	0.849	176.4	1184.0

AXIAL COMPRESSOR PERFORMANCE IS 2.000 PRESSURE RATIO
0.800 ADIABATIC EFFICIENCY

-- CENTRIFUGAL PERFORMANCE ---				*	OVERALL PERFORMANCE				
PRESSURE RATIO	EFFY. AD.	P3 PSIA	T3 DEG.R	*	PRESSURE RATIO	EFFICIENCY AD	POLY	P4 PSIA	T4 DEG.R
5.00	0.820	29.4	660.5	*	10.00	0.789	0.847	147.0	1117.8
8.00	0.800	29.4	660.5	*	16.00	0.772	0.846	235.1	1303.5

```
 0A2171
/&
```

TABLE XIV. ADDER FORTRAN LISTING

```
FORTRAN IV    MODEL 44  PS       VERSION 3,  LEVEL 2   DATE  69338

              C     PROGRAM ADDER
              C
              C     THIS PROGRAM DETERMINES OVERALL EFFICIENCY FOR COMBINATION OF AN
              C    *AXIAL AND A CENTRIFUGAL.IT USES AIR PROPERTIES FROM SUBROUTINE
              C     *SNARF
              C
              C APCP IS TOTAL PRESSURE RATIO FOR THE AXIAL COMPRESSOR
              C AETA IS ADIABATIC EFFICIENCIES FOR THE AXIAL COMPRESSOR
              C CPCP IS THE TOTAL PRESSURE RATIO FOR THE CENTRIFUGAL COMPRESSOR
              C CETA IS THE ADIABATIC EFFICIENCY FOR THE CENTRIFUGAL COMPRESSOR
              C   P3 IS INTERSTAGE PRESSURE, LBS/SQUARE IN.
              C   T3 IS INTERSTAGE TEMPERATURE, DEGREES R.
              C OPCP IS OVERALL PRESSURE RATIO
              C OETA IS OVERALL EFFICIENCY
              C OETAP IS POLYTROPIC EFFICIENCY
              C   P4 IS EXIT PRESSURE, LBS/SQUARE IN.
              C   T4 IS EXIT TEMPERATURE, DEGREES R.
              C
0001                DIMENSION APCP(20),AETA(20),CPCP(20),CETA(20),P3(20),T3(20),
                   1     OPCP(20,20), OETA(20,20), OETAP(20,20), P4(20,20), T4(20,20)
              C
              C******THE COMPUTATION LOOPS USING ONE AXIAL FOR ALL CENTRIFUGALS
              C          WRITING IS DONE AFTER ALL COMPUTATIONS ARE FINISHED
              C
0002                T2 = 518.7
0003                P2 = 14.696
0004                T2L = ALOG(T2)
0005                CALL SNARF( 4, T2, YT,  PR2, YP,  H2, YH,   CP,   GAM )
0006           10   READ 902, JD, KD
0007                READ 904, ( APCP(J), J = 1, JD )
0008                READ 904, ( AETA(J), J = 1, JD )
0009                READ 904, ( CPCP(J), J = 1, KD )
0010                READ 904, ( CETA(J), J = 1, KD )
              C****** COMPUTATION BEGINS WITH LOOP ON AXIALS
              C
0011                DO 100 J = 1, JD
0012                  P3(J)  = P2 * APCP(J)
0013                  PR3 = PR2 * APCP(J)
0014                  CALL SNARF(4, H3I, YT, PR3, YP,  H3I,  YH ,   CP,  GAM )
0015                  H3 = H2 + ( H3I - H2 ) / AETA(J)
0016                  CALL SNARF(5, T3(J), YT, PR3,YP,  H3, YH , CP, GAM )
              C*******THE CENTRIFUGAL LOOP BEGINS HERE
              C
0017                  DO 100 K = 1, KD
0018                    P4(J,K) = P3(J) * CPCP(K)
0019                    PR4 = PR3 * CPCP(K)
0020                    CALL SNARF(6, T4I, YT,  PR4, YP, H4I, YH, CP, GAM )
0021                    H4 =  H3  +  ( H4I - H3 ) / CETA(K)
0022                    CALL SNARF(5, T4(J,K), YT, XP, YP, H4, YH, CP, GAM )

0023                    OPCP(J,K) = P4(J,K) / P2
0024                    CALL SNARF(2, T2, T4I,   P2, P4(J,K),  H2, H4I,  CP,  GAM )
0025                    OETA(J,K)  = ( H4I - H2 ) / ( H4 - H2 )
0026                    OETAP(J,K) = ( ALOG(T4I) - T2L )/( ALOG(T4(J,K))- T2L )
0027           100  CONTINUE
              C
              C****** A DO IS USED FOR THE OUTPUT NOW
              C
0028           120  L = 12
0029                WRITE (3,920 )
0030                DO 130 J = 1, JD
0031                  WRITE( 3,916 ) APCP(J), AETA(J)
0032                  L=L+2
0033                  DO 128 K = 1, KD
0034                    WRITE( 3,918 ) CPCP(K), CETA(K), P3(J), T3(J), OPCP(J,K),
                   1          OETA(J,K), OETAP(J,K), P4(J,K),T4(J,K)
0035                    L=L+1
0036                    IF( 66 - L)122, 122, 124
0037           122      L = 20
0038                    WRITE( 3,920 )
0039                    WRITE( 3,918 ) APCP(J), CETA(J)
0040           128    CONTINUE
0041                  IF( 56- L ) 126, 129, 130
0042           126    L = 17
0043                  WRITE( 3,920 )
0044           130    CONTINUE
0045                GO TO 10
              C
0046           902  FORMAT( 2I10 )
0047           904  FORMAT( 7F10.5 )
0048           916  FORMAT(    // T7,*AXIAL COMPRESSOR PERFORMANCE IS *,F6.3,* PRESS*,
                   1     T51,*URE RATIO* /   T40, F5.3, * ADIABATIC EFFICIENCY* /
                   2     T7,*-- CENTRIFUGAL PERFORMANCE ---*--------- OVERALL PERFOR*,
                   3     T62,*MANCE ----------* / T7,*PRESSURE EFFY. P3      T3*,
                   4     T37,*PRESSURE EFFICIENCY  P4       T4* / T8,*RATIO     AD,*,
                   5     T22,*PSIA   DEG.R   * RATIO   AD    POLY  PSIA    DEG.R*/
                   6     T37,*R* )
0049           918  FORMAT( F11.2, F9.3, F6.1, F4.1, '  ', F6.2, F8.3, F6.3, F7.1,
                   1     F8.1 )
0050           920  FORMAT( 1H1 )
0051                END
```

TABLE XV. FIXER AND BLAH INPUT LIST

Card Type	Column	Input Format	Name	Definition
A	1-54	A	TITLE	User's words to define case
	55-56	I	NSPEED	Number of speed lines
	57-64	D	DSPEED	Design speed, RPM
	65-72	D	DFLOW	Design flow, lbs/sec
B	1-8	D	DELEF	Speed line efficiency increment
C	1-8	D	HR1	Inlet hub radius, ft
	9-16	D	TR1	Inlet tip radius, ft
	17-24	D	HRO	Outlet hub radius, ft
	25-32	D	TRO	Outlet tip radius, ft
	Note: C may be submitted blank at present.			
D	1-8	D	F	Flow scale factor
	9-16	D	T1	Inlet total temperature, °R
	17-24	D	P1	Inlet total pressure, psf
E	1-8	I	NPTS	No. of points on next speed line
	9-16	D	ENPC	Percent N_D for next speed line
F	1-8	D	W1	Flow at a point, lb/sec
	9-16	D	PR1	Pressure ratio at a point
	17-24	D	EF1	Adiabatic efficiency at a point
	25-32	D	EN1	Compressor speed at a point, RPM
	33-40	D	W2	Flow at a second point, lb/sec
	41-48	D	PR2	Pressure at a second point
	49-54	D	EF2	Adiabatic efficiency at a second point
	55-64	D	EN2	Compressor speed at a second point, RPM

A FIXER Input Case requires one data set of cards consisting of the following card types in sequence:

A,B,C,D	Beginning of a case
E,F,F,F	First speed line, with enough F cards for NPTS of data
E,F,F,F,F to	Second speed line, with enough F cards for NPTS of data
E,F,F,F,F	Last speed line with enough F cards for NPTS of data
A,B,C,D	Beginning of a new case

A BLAH input case is same as FIXER, but omitting card B.

TABLE XVI. FIXER FORTRAN LISTING

```
FORTRAN IV    MODEL 44  PS       VERSION 3,  LEVEL 2   DATE  69337

              C  PROGRAM FIXER.  THIS PROGRAM USES SUBROUTINE SNARF
              C   TITLE.  USER'S WORDS TO DESCRIBE THE MACHINE.
              C  THIS PROGRAM READS DATA CARDS AND ALSO EFFICIENCY INCREMENTS FOR EACH
              C     SPEED LINE.  IT CORRECTS PRESSURE RATIO FOR THE EFFICIENCY CHANGE
              C     KEEPING THE SAME.  IT THEN PUNCHES NEW CARDS OUT WITH THE
              C     ADJUSTED VALUES IN PLACE OF ORIGINAL VALUES.
              C
              COMMENTS BELOW GIVE DEFINITIONS OF INPUT VARIABLE NAMES.
              C
              C  NSPEED.   THE NUMBER OF SPEED LINES FOR WHICH DATA ARE GIVEN.
              C  DSPEED.   RPM FOR DESIGN SPEED.
              C  DFLOW.    LBS/SEC DESIGN AIRFLOW.
              C  NPTS.     THE NUMBER OF POINTS ON A SPEED LINE FOR WHICH DATA ARE TO
              C              BE GIVEN ON SUBSEQUENT CARDS ( 2 POINTS PER CARD )
              C  HRI-HUB RADIUS AT INLET
              C  TRI-TIP RADIUS AT INLET
              C  HRO-HUB RADIUS AT OUTLET
              C  TRO-TIP RADIUS AT OUTLET
              C  RNPC.     THE SPEED FOR THIS SPEED LINE, PERCENT OF DESIGN
              C  W.        LBS/SEC AIR FLOW
              C  P.        TOTAL PRESSURE RATIO
              C  EF.       ADIABATIC EFFICIENCY, PERCENT
              C  EN.       RPM CORRECTED SHAFT SPEED
              C
 0001               DIMENSION TITLE(27), DFLEF(20)
              C
 0002            10 READ 900, TITLE, NSPEED, DSPEED, DFLOW
 0003               READ 902, ( DFLEF(J), J = 1, NSPEED )
 0004               READ 902, HRI, TRI, HRO, TRO
 0005               READ 902, P, T1, P1
 0006               WRITE( 2,900 ) TITLE, NSPEED, DSPEED, DFLOW
 0007               WRITE( 2,902 ) HRI, TRI, HRO, TRO
 0008               WRITE( 2,902 ) P, T1, P1
 0009               T2 = 518.7
 0010               P2 = 1.0
 0011               DO 50 J = 1, NSPEED
 0012                  READ 903, NPTS, ENPC
 0013                  WRITE( 2,903 ) NPTS, ENPC
 0014                  DO 50 K = 1, NPTS, 2
 0015                    READ 904,W1,PR1,EF1,EN1,W2,PR2,EF2,EN2
 0016                    CALL SNARF( 2, T2,TY, P2,PR1, H2,H3I, CP,GAM )
 0017                    DEM=(H3I-H2)*100./EF1
 0018                    EF1 = EF1 + DFLEF(J)
 0019                    H3I=DEM*EF1/100.+H2
 0020                    CALL SNARF(3,TX,TY,P2,PR1,H2,H3I,CP,GAP)
 0021                    IF( 100. - EF1 ) 25, 25, 26
 0022            25      EF1 = 100.
 0023            26      CONTINUE
 0024                    IF( W2 ) 40, 40, 30

 0025            30      CALL SNARF( 2, T2,TY, P2,PR2, H2,H3I, CP,GAM )
 0026                    DEM=(H3I-H2)*100./EF2
 0027                    EF2 = EF2 + DFLEF(J)
 0028                    H3I=DEM*EF2/100.+H2
 0029                    CALL SNARF(3,TX,TY,P2,PR2,H2,H3I,CP,GAP)
 0030                    IF( 100. - EF2 ) 35, 35, 36
 0031            35      EF2 = 100.
 0032            36      CONTINUE
 0033            40      WRITE( 2,904 ) W1, PR1, EF1, EN1,  W2, PR2, EF2, EN2
 0034            50   CONTINUE
 0035                 GO TO 10
              C
 0036            900  FORMAT     ( 27A2, I2, F8.1, F8.3, F8.3 )
 0037            902  FORMAT     ( 8F8.4 )
 0038            903  FORMAT     ( I8, F8.2 )
 0039            904  FORMAT     ( 2F8.3, F8.2,F8.0,2F8.3,F8.2,F8.1)
 0040                 END
```

TABLE XVII. BLAH SAMPLE OUTPUT

2 STAGE COM.TRANS. (E-1)
50000. RPM IS DESIGN POINT CORRECTED SHAFT SPEED
5.000 LBS/SEC IS DESIGN POINT CORRECTED AIRFLOW

105.0 PERCENT OF DESIGN SPEED DEVELOPS THE FOLLOWING PERFORMANCE

CORRECTED FLOW,LBS/SEC	PRESSURE RATIO	ADIABATIC EFFY PERCENT	CORRECTED SPEED,RPM
5.030	3.012	76.50	52500.
5.030	3.200	78.00	52500.

100.0 PERCENT OF DESIGN SPEED DEVELOPS THE FOLLOWING PERFORMANCE

CORRECTED FLOW,LBS/SEC	PRESSURE RATIO	ADIABATIC EFFY PERCENT	CORRECTED SPEED,RPM
4.940	2.356	66.50	50000.
4.940	2.656	76.00	50000.
4.940	2.883	79.00	50000.
4.940	3.008	80.00	50000.
4.930	3.111	81.50	50000.
4.920	3.215	82.50	50000.
4.870	3.286	83.00	50000.
4.800	3.340	83.50	50000.
4.680	3.364	82.50	50000.

95.0 PERCENT OF DESIGN SPEED DEVELOPS THE FOLLOWING PERFORMANCE

CORRECTED FLOW,LBS/SEC	PRESSURE RATIO	ADIABATIC EFFY PERCENT	CORRECTED SPEED,RPM
4.720	2.524	79.00	47500.
4.700	2.835	84.00	47500.
4.610	2.971	84.50	47500.
4.510	3.045	84.00	47500.
4.310	3.068	82.50	47500.

TABLE XVII - Continued

2 STAGE CON.TRANS. (F1)
50000. RPM IS DESIGN POINT CORRECTED SHAFT SPEED
5.000 LBS/SEC IS DESIGN POINT CORRECTED AIRFLOW SCALE FACTOR IS 1.000

105.0 PERCENT OF DESIGN SPEED DEVELOPS THE FOLLOWING PERFORMANCE

INLET COR FLOW,LBS/SEC	PRESSURE RATIO	ADIABATIC EFFY,PERCENT	POLYTROPIC EFFY	CORRECTED SPEED,RPM	N/SQRT(THETA)	HCD	HCDI	EXIT CORR FLOW,LBS/SEC
5.030	3.012	76.50	79.90	52500.	43130.09	54.61	41.78	2.033
5.030	3.200	79.00	81.35	52500.	42927.32	57.01	44.47	1.927

100.0 PERCENT OF DESIGN SPEED DEVELOPS THE FOLLOWING PERFORMANCE

INLET COR FLOW,LBS/SEC	PRESSURE RATIO	ADIABATIC EFFY,PERCENT	POLYTROPIC EFFY	CORRECTED SPEED,RPM	N/SQRT(THETA)	HCD	HCDI	EXIT CORR FLOW,LBS/SEC
4.960	2.356	66.50	70.32	50000.	42976.60	51.89	34.51	2.694
4.940	2.696	76.00	79.15	50000.	41821.09	53.63	40.74	2.141
4.940	2.883	79.00	81.93	50000.	41590.29	55.63	43.56	2.006
4.940	3.000	80.00	82.90	50000.	41378.44	57.49	45.55	1.944
4.930	3.111	81.50	84.26	50000.	41270.85	58.45	47.44	1.902
4.920	3.215	82.50	85.19	50000.	41131.14	59.71	49.28	1.860
4.870	3.298	83.00	85.65	50000.	41020.79	60.71	50.19	1.835
4.800	3.340	83.50	86.10	50000.	40957.76	61.29	51.18	1.794
4.680	3.364	82.50	85.27	50000.	40825.59	62.47	51.56	1.704

95.0 PERCENT OF DESIGN SPEED DEVELOPS THE FOLLOWING PERFORMANCE

INLET COR FLOW,LBS/SEC	PRESSURE RATIO	ADIABATIC EFFY,PERCENT	POLYTROPIC EFFY	CORRECTED SPEED,RPM	N/SQRT(THETA)	HCD	HCDI	EXIT CORR FLOW,LBS/SEC
4.720	2.524	79.00	81.59	47500.	42405.88	52.82	41.73	2.198
4.730	2.835	84.00	86.20	47500.	39993.33	56.91	47.80	1.970
4.610	2.971	84.50	86.72	47500.	39719.58	59.52	50.30	1.856
4.510	3.045	84.00	86.34	47500.	39529.63	61.46	51.62	1.780
4.310	3.068	82.50	85.08	47500.	39371.23	63.07	52.03	1.695

90.0 PERCENT OF DESIGN SPEED DEVELOPS THE FOLLOWING PERFORMANCE

INLET COR FLOW,LBS/SEC	PRESSURE RATIO	ADIABATIC EFFY,PERCENT	POLYTROPIC EFFY	CORRECTED SPEED,RPM	N/SQRT(THETA)	HCD	HCDI	EXIT CORR FLOW,LBS/SEC
4.420	2.058	70.00	72.32	45000.	39077.16	50.25	35.19	2.473
4.420	2.744	81.50	83.61	45000.	38911.26	51.92	42.12	2.181
4.390	2.891	84.00	87.77	45000.	38576.62	55.58	47.75	1.944
4.270	2.957	86.00	87.95	45000.	38409.19	58.53	50.34	1.860
4.190	2.741	84.50	86.57	45000.	38116.45	60.69	51.28	1.805
4.020	2.763	82.50	84.95	45000.	37937.88	62.79	51.75	1.726

80.0 PERCENT OF DESIGN SPEED DEVELOPS THE FOLLOWING PERFORMANCE

INLET COR FLOW,LBS/SEC	PRESSURE RATIO	ADIABATIC EFFY,PERCENT	POLYTROPIC EFFY	CORRECTED SPEED,RPM	N/SQRT(THETA)	HCD	HCDI	EXIT CORR FLOW,LBS/SEC
3.920	1.722	67.00	69.45	40000.	35774.70	48.71	32.64	2.490

TABLE XVIII. BLAH FORTRAN LISTINGS

```
FORTRAN IV    MODEL 44  PS       VERSION 3,  LEVEL 2    DATE  69337

              C****** PROGRAM COMPRESSOR PERFORMANCE
              C            OF WHICH THE PURPOSE IS TO PUT OVERALL TEST DATA IN A FORM
              C            WHICH IS EASY TO USE IN THE COMPUTER, AND THEN TO USE DATA
              C            AS REQUIREMENTS MAY ARISE.
              C
              COMMENTS BELOW GIVE DEFINITIONS OF INPUT VARIABLE NAMES.
              C
              C  TITLE.  USER'S WORDS TO DESCRIBE THE MACHINE.
              C NSPEED.  THE NUMBER OF SPEED LINES FOR WHICH DATA ARE GIVEN. A ZERO
              C            VALUE MEANS DATA ARE TREATED AS INDIVIDUAL POINTS.
              C DSPEED.  RPM FOR DESIGN SPEED.
              C DFLOW.   LBS/SEC DESIGN AIRFLOW.
              C NPTS.    THE NUMBER OF POINTS ON A SPEED LINE FOR WHICH DATA ARE TO
              C            BE GIVEN ON SUBSEQUENT CARDS ( 2 POINTS PER CARD )
              C HRI-HUB RADIUS AT INLET
              C TRI-TIP RADIUS AT INLET
              C HRO-HUB RADIUS AT OUTLET
              C TRO-TIP RADIUS AT OUTLET
              C ENPC.    THE SPEED FOR THIS SPEED LINE, PERCENT OF DESIGN
              C W.       LBS/SEC AIR FLOW
              C P.       TOTAL PRESSURE RATIO
              C EF.      ADIABATIC EFFICIENCY, PERCENT
              C EN.      RPM CORRECTED SHAFT SPEED
              C
              COMMENTS BELOW DEFINE OUTPUT VARIABLE NAMES.
              C
              C CFM.     CUBIC FEET PER MINUTE AIRFLOW FOR STANDARD AIR
              C EFP      POLYTROPIC EFFICIENCY.
              C
 0001               DIMENSION  CFM(200), EF(200),EFP(200),EN(200),ENPC(200), NPTS(20)
 0002               DIMENSION  P(200), T(200),TITLE(27), W(200)
 0003               COMMON CFM,DFLOW,DSPEED,EF,EFP,EN,ENPC,NPT,NPTS,NSPEED,P,T,TITLE,
                   1W,HRI,TRI,HRO,TRO,TI,PI,F
              C
 0004              10 CALL ERASE
 0005                 CALL INPUT
 0006                 CALL RYTIN
 0007                 CALL BLAH
 0008                 GO TO 10
              C
 0009                 END
```

TABLE XVIII - Continued

```
FORTRAN IV     MODEL 44  PS        VERSION 3,  LEVEL 2    DATE  69337

0001                SUBROUTINE ERASE
                C
0002                DIMENSION A(1017), N(22), B(619)
0003                COMMON A,N, B
                C
0004                DO 2 J=1,1002
0005              2   A(J) = 0
0006                DO 4 J=1,22
0007              4   N(J)=  0
0008                DO 6 J=1,619
0009              6   B(J) = 0
0010                RETURN
                C
0011                END
```

TABLE XVIII - Continued

```
FORTRAN IV    MODEL 44  PS       VERSION 3,  LEVEL 2   DATE  69337

 0001              SUBROUTINE INPUT
                C******  OF WHICH THE FUNCTION IS TO READ THE INPUT DATA
                C
 0002               DIMENSION  CFM(200), EF(200),EFP(200),EN(200),ENPC(200), NPTS(20)
 0003               DIMENSION  P(200), T(200),TITLE(27), W(200)
 0004               COMMON CFM,DFLOW,DSPEED,EF,EFP,EN,ENPC,NPT,NPTS,NSPEED,P,T,TITLE,
                   1W,HRI,TRI,HRC,TRC,T1,P1,F
                C
 0005               READ 900, TITLE, NSPEED, DSPEED, DFLOW
 0006               READ 902, HRI, TRI,HRC,TRC
 0007               READ 902,F,T1,P1
 0008               IF( NSPEED ) 20, 20, 30
 0009            20 READ 901, NPT
 0010               READ 902, ( W(J), P(J), EF(J), EN(J), J = 1, NPT  )
 0011                     GO TO 50
 0012            30 JO = 1
 0013               DO 40 I = 1, NSPEED
 0014                 READ 903, NPTS(I), ENPC(I)
 0015                 NPT = NPTS(I) + JO - 1
 0016                 READ 902, ( W(J), P(J), EF(J), EN(J), J = JO, NPT )
 0017            40   JO = NPT + 1
 0018            50 RETURN
                C
 0019           900 FORMAT(27A2,I2,2F8.4)
 0020           901 FORMAT( I8 )                                              INPUT
 0021           902 FORMAT( 8F8.4 )                                           INPUT
 0022           903 FORMAT( I8, F8.4 )
 0023               END
```

TABLE XVIII - Continued

```
FORTRAN IV    MODEL 44  PS        VERSION 3,  LEVEL 2   DATE  69337

0001                SUBROUTINE RYTIN
                  C******  OF WHICH THE FUNCTION IS TO WRITE THE INPUT DATA
                  C
0002                DIMENSION  CFM(200), EF(200),EFP(200),EN(200),ENPC(200), NPTS(20)
0003                DIMENSION  P(200), T(200),TITLE(27), W(200)
0004                COMMON CFM,DFLOW,DSPEED,EF,EFP,EN,ENPC,NPT,NPTS,NSPEED,P,T,TITLE,
                   1W,HRI,TRI,HRO,TRO,TI,PI,F
                  C
0005                WRITE( 3,900 ) TITLE, DSPEED,DFLOW
0006                IF( NSPEED ) 5, 5, 50
0007              5 JO = 1
0008                NPTO = 50
0009                NPTR = NPT
0010             10 IF(NPTR - NPTO) 15, 20, 20
0011             15 NPTO = NPTR
0012             20 WRITE( 3,901 )
0013                WRITE( 3,902 ) ( W(J), P(J), EF(J), EN(J), J = JO, NPTO )
0014                NPTR = NPTR - NPTO
0015                IF( NPTR ) 85, 85, 10
0016             50 NROWS = 10
0017                JO = 1
0018                DO 80 I = 1, NSPEED
0019                  IF( 57-NROWS- NPTS(I) ) 55, 60, 60
0020             55   WRITE( 3,999 )
0021                  NROWS = 9 + NPTS(I)
0022                        GO TO 70
0023             60   NROWS = 9 + NROWS + NPTS(I)
0024             70   NPTO = JO + NPTS(I) - 1
0025                  WRITE( 3,903 ) ENPC(I)
0026                WRITE( 3,901 )
0027                  WRITE( 3,902 ) ( W(J), P(J), EF(J), EN(J), J = JO,NPTO )
0028             80   JO = 1 + NPTO
0029             85 RETURN
                  C
0030             900 FORMAT( 1H1//,  T6,27A2 / T21, F10.0, T31,' RPM IS DESIGN POINT'
                    1 T52,'CORRECTED SHAFT SPEED' /  T21,F10.3, T32,'LBS/SEC IS DESIGN'RYTIN-UT
                    2 T50,'POINT CORRECTED AIRFLOW'/ )                              RYTIN-UT
0031             901 FORMAT(/ T7,'CORRECTED',T23,'PRESSURE',T36,'ADIABATIC EFFY',     RYTIN
                    1 T54,'CORRECTED'/ T6,'FLOW,LBS/SEC',T24,'RATIO',T39,'PERCENT',  RYTIN
                    2 T54,'SPEED,RPM'/ )                                             RYTIN
0032             902 FORMAT(F15.3,F14.3,F17.2,F17.0 )                               RYTIN
0033             903 FORMAT(/T5,F5.1, T11,'PERCENT OF DESIGN SPEED DEVELOPS THE'     RYTIN
                    1 T49,'FOLLOWING PERFORMANCE')                                   RYTIN
0034             999 FORMAT( 1H1,// )                                              RYTIN-UT
0035                 END
```

TABLE XVIII - Continued

```
FORTRAN IV    MODEL 44  PS       VERSION 3,  LEVEL 2   DATE  69337

0001              SUBROUTINE RLAH
                C******* OF WHICH THE FUNCTION IS TO CALCULATE THERMODYNAMIC PARAMETERS
                C
0002              DIMENSION CFM(200),EFF(200),EFP(200),FN(200),ENPC(200),NPTS(20)
0003              DIMENSION  P(200), T(200),TITLE(27), W(200)
0004              COMMON CFM,DFLOW,DSPEED,EF,EFP,FN,ENPC,NPT,NPTS,NSPEED,P,T,TITLE,
                 1W,HRI,THI,HRO,TRO,T1,P1,F
                C
0005              N=49
0006              NY=0
0007              NDY=0
0008             1 WRITE(3,103)TITLE,DSPEED,DFLOW,F
0009              NAG=1
                C
0010              DO 20 I=1,NSPEED
0011              WRITE(3,104)ENPC(I)
0012              WRITE(3,100)
0013              WRITE(3,101)
0014              NDY=NDY+1
0015              ENPC(I)=ENPC(I)/100.
0016              NAGG=NPTS(I)+NAG-1
                C
0017              DO 10 J=NAG,NAGG
0018              ENN=EN(J)/SQRT(F)
0019              T2=T1
0020              P2=P1
0021              T2L=ALOG(T2)
0022              P3=P1*P(J)
0023              CALL SHARE(2,T2,T3,P2,P3,H2,H3,CPS,GAMMA)
0024              DHI=H3 -H2
0025              T3L=ALOG(T3)
0026              EF=DHI/EFF(J)*(00.
0027              HCO=DH/(ENPC(I))**2
0028              HCOI=DHI/(ENPC(I))**2
0029              H3=H2+DH
0030              CALL SHARE(5,T3,T1,P3,P1,H3,HI,CPS,GAMMA)
0031              T3L=ALOG(T3)
0032              THET3=T3/T2
0033              FN3=ENN/(THET3**.5)
0034              W(J)=W(J)*F
0035              WJ=W(J)*(THET3**.5)/P(J)
0036              EFP(J)=(T3IL-T2L)/(T3L-T2L)*100.
0037              WRITE(3,102)W(J),P(J),EF(J),EFP(J),EAN,FN3,HCO,HCOI,WJ
0038              NY=NY+1
0039              NX=N-NY-6*NDY
0040              IF(NX)5,5,10
0041             5 NY=0
0042              NDY=0
0043              WRITE(3,103)TITLE,DSPEED,DFLOW,F

0044             10 CONTINUE
0045              NAG=NAGG+1
0046             20 CONTINUE
0047              RETURN
                C
0048            100 FORMAT(/T4,'INLET COR',T20,'PRESSURE',T34,'ADIABATIC',T49,'POLYTRO
                   1PIC',T63,'CORRECTED',T77,'N/SQRT(THET3)',T99,'HCC',T112,'HCOI',
                   2T120,'EXIT CORR')
0049            101 FORMAT(T4,'FLOW,LBS/SEC',T20,'RATIO',T33,'EFFY,PERCENT',T63,'SPEED
                   1,RPM',T115,'FLOW,LBS/SEC',T93,'EFFY')
0050            102 FORMAT(F13.3,F12.3,F15.2,F15.2,F15.0,F15.2,F15.2,F15.2,F13.3)
0051            103 FORMAT(1H1//,  T6,27A2 / T21, F10.0, T31,' RPP IS DESIGN POINT'  RYTIN-UT
                   1 T52,'CORRECTED SHAFT SPEED' /  T21,F10.3, T32,'LBS/SEC IS DESIGN'RYTIN-UT
                   2 T50,'POINT CORRECTED AIRFLOW',5X,'SCALE FACTOR IS ',F5.3/)
0052            104 FORMAT(/T5,F5.1, T11,'PERCENT OF DESIGN SPEED DEVELOPS THE'          RYTIN
                   1 T4*,'FOLLOWING PERFORMANCE')                                        RYTIN
0053              END
```

TABLE XVIII - Continued

```
FORTRAN IV    MODEL 44  PS       VERSION 3,  LEVEL 2   DATE  65337

 0001              SUBROUTINE SNAREA(N,T1,T2,P1,P2,H1,H2,CPS,GAMMA)
                  C******OF WHICH THE FUNCTION IS TO INTERPOLATE THERMODYNAMIC PROPERTIES
                  C******FROM TABLES OF DATA. POINT VALUES OR ENDS OF ISENTROPIC PROCESS
                  C****** ARE PRODUCED.
                  C
                  C******FROM TABLES OF DATA
                  C
                  C   N    IS A CONTROL NO. WITH EFFECTS AS DEFINED BELOW
                  C      N=1--GIVEN T1,T2,P1
                  C      N=2--GIVEN P1,P2,T1
                  C      N=3--GIVEN H1,H2,P1
                  C      N=4--GIVEN T1
                  C      N=5--GIVEN H1
                  C      N=6--GIVEN PR1
                  C      FOR N=4,5,&6 P1=PR1 IN THE OUTPUT
                  C    T1  TEMPERATURE AT PROCESS STARTING POINT, DEGREES R
                  C    T2  TEMPERATURE AT PROCESS ENDING POINT, DEGREES R
                  C    P1  PRESSURE AT PROCESS,STARTING POINT, UNITS AS GIVEN
                  C    P2  PRESSURE AT PROCESS ENDING POINT  , UNITS AS GIVEN
                  C    H1  ENTHALPY AT PROCESS,STARTING POINT, BTU/LB
                  C    H2  ENTHALPY AT PROCESS ENDING POINT, BTU/LB
                  C   CPS  SPECIFIC HEAT                                  BTU/LB/DEGREE R
                  C GAMMA RATIO OF SPECIFIC HEATS, CP/CV
                  C   INTERPOLATE(M,A,B,C,D,E,F) DOES INTERPOLATION OF TABLE VALUES
                  C   M IS THE ORDER OF THE INTERPOLATION CURVE
                  C   A IS THE NUMBER OF VLAUES IN TABLE
                  C   B IS THE SET OF INDEPENDANT VARIABLES
                  C   C IS THE SET OF DEPENDANT VARIABLES
                  C   D IS THE VALUE OF THE INDEPENDANT VARIABLE
                  C   E IS THE VALUE OF THE DEPENDANT VARIABLE
                  C
 0002               REAL T(35)/ 500. ,550. ,600. ,650. , 700. ,750. , 800. ,850. ,900.        1
                   1      ,950. , 1000. , 1050. , 1100. , 1150. , 1200. , 1250. , 1300.       2
                   2      ,1350. ,1400. , 1450. ,1500.  ,1550. ,1600. ,1650. , 1700.          3
                   3      ,1750. ,1800. , 1850. ,1900.  ,1950. ,2000. ,2050. , 2100.          4
                   4      ,2150. ,2200.                                                       5
                   1/,  H(35)/ 119.48 ,131.46 ,143.47  ,155.50 ,167.56 ,179.66 ,191.81        6
                   2           ,204.01 ,216.26 ,228.58  ,240.98 ,253.45 ,265.99 ,278.61       7
                   3           ,291.30 ,304.08 ,316.94  ,329.88 ,342.90 ,356.00 ,369.17       8
                   4           ,382.42 ,395.74 ,409.13  ,422.59 ,436.12 ,449.71 ,463.37       9
                   5           ,477.09 ,490.88 ,504.71  ,518.61 ,532.55 ,546.54 ,560.55      10
                   1/, PR(35)/ 1.0590 ,1.4779 ,2.005    ,2.655  ,3.446  ,4.396  ,5.526       11
                   2           ,6.856  ,8.411  ,10.216  ,12.299 ,14.686 ,17.413 ,20.51       12
                   3           ,24.01  ,27.96  ,32.39   ,37.35  ,42.89  ,49.03  ,55.86        13
                   4           ,63.40  ,71.73  ,80.89   ,90.95  ,101.98 ,114.03 ,127.18       14
                   5           ,141.51 ,157.10 ,174.00  ,192.31 ,212.1  ,233.5  ,256.6        15
                   1/, CP(35)/ .2396  ..2399  ..2403   ..2409  ..2416  ..2424  ..2434        16
                   2           ..2446  ..2458  ..2472   ..2486  ..2501  ..2516  ..2532        17
                   3           ..2547  ..2563  ..2579   ..2595  ..2611  ..2628  ..2642        18
```

TABLE XVIII - Continued

```
FORTRAN IV    MODEL 44  PS        VERSION 3,  LEVEL 2    DATE  69337                    PAGE  0002

                    4           ..2656  ..2671  ..2684    ..2698  ..2711  ..2725  ..2738        19
                    5           ..2750  ..2762  ..2773    ..2784  ..2794  ..2804  ..2813        20
                   1/,GAM(35)/ 1.401   ,1.400  ,1.399     ,1.398  ,1.396  ,1.394  ,1.392        21
                    2           ,1.390  ,1.387  ,1.384     ,1.381  ,1.378  ,1.374  ,1.371       22
                    3           ,1.368  ,1.365  ,1.362     ,1.359  ,1.356  ,1.353  ,1.350       23
                    4           ,1.348  ,1.345  ,1.342     ,1.340  ,1.338  ,1.336  ,1.334       24
                    5           ,1.332  ,1.330  ,1.328     ,1.326  ,1.325  ,1.324  ,1.322/       25
              C
0003                 M=4
0004                 M1=35
0005                 IF(N-2)20,30,40
0006              20 CALL INTERP(M,M1,T,PR,T1,PR1)
0007                 CALL INTERP(M,M1,T,H,T1,H1)
0008                 CALL INTERP(M,M1,T,CP,T1,CP1)
0009                 CALL INTERP(M,M1,T,GAM,T1,GAM1)
0010                 CALL INTERP(M,M1,T,PR,T2,PR2)
0011                 CALL INTERP(M,M1,T,H,T2,H2)
0012                 CALL INTERP(M,M1,T,CP,T2,CP2)
0013                 CALL INTERP(M,M1,T,GAM,T2,GAM2)
0014                 P2=PR2*P1/PR1
0015                 GAMMA=(GAM1+GAM2)*.5
0016                 CPS=(CP1+CP2)*.5
0017                 GO TO 1000
0018              30 CALL INTERP(M,M1,T,H,T1,H1)
0019                 CALL INTERP(M,M1,T,CP,T1,CP1)
0020                 CALL INTERP(M,M1,T,GAM,T1,GAM1)
0021                 CALL INTERP(M,M1,T,PR,T1,PR1)
0022                 PR2=PR1*P2/P1
0023                 CALL INTERP(M,M1,PR,T,PR2,T2)
0024                 CALL INTERP(M,M1,PR,H,PR2,H2)
0025                 CALL INTERP(M,M1,PR,CP,PR2,CP2)
0026                 CALL INTERP(M,M1,PR,GAM,PR2,GAM2)
0027                 GAMMA=(GAM1+GAM2)*.5
0028                 CPS=(CP1+CP2)*.5
0029                 GO TO 1000
0030              40 IF(N-4)50,60,70
0031              50 CALL INTERP(M,M1,H,T,H1,T1)
0032                 CALL INTERP(M,M1,H,PR,H1,PR1)
0033                 CALL INTERP(M,M1,H,CP,H1,CP1)
0034                 CALL INTERP(M,M1,H,GAM,H1,GAM1)
0035                 CALL INTERP(M,M1,H,T,H2,T2)
0036                 CALL INTERP(M,M1,H,PR,H2,PR2)
0037                 CALL INTERP(M,M1,H,CP,H2,CP2)
0038                 CALL INTERP(M,M1,H,GAM,H2,GAM2)
0039                 P2=P1*PR2/PR1
0040                 GAMMA=(GAM1+GAM2)*.5
0041                 CPS=(CP1+CP2)*.5
0042                 GO TO 1000
0043              60 CALL INTERP(M,M1,T,H,T1,H1)
```

TABLE XVIII - Continued

```
FORTRAN IV     MODEL 44  PS        VERSION 3,  LEVEL 2    DATE  69337

 0044                CALL INTERP(M,M1,T,CP,T1,CP5)
 0045                CALL INTERP(M,M1,T,GAM,T1,GAMMA)
 0046                CALL INTERP(M,M1,T,PR,T1,PR1)
 0047                P1=PR1
 0048                GO TO 1000
 0049              70 IF(N-5)80,80,90
 0050              80 CALL INTERP(M,M1,H,T,H1,T1)
 0051                 CALL INTERP(M,M1,H,PR,H1,PR1)
 0052                 CALL INTERP(M,M1,H,CP,H1,CP5)
 0053                 CALL INTERP(M,M1,H,GAM,H1,GAMMA)
 0054                 P1=PR1
 0055                 GO TO 1000
 0056              90 PR1=P1
 0057                 CALL INTERP(M,M1,PR,T,PR1,T1)
 0058                 CALL INTERP(M,M1,PR,H,PR1,H1)
 0059                 CALL INTERP(M,M1,PR,CP,PR1,CP5)
 0060                 CALL INTERP(M,M1,PR,GAM,PR1,GAMMA)
 0061           1000 RETURN
                C
 0062            100 FORMAT(5I5)
 0063            101 FORMAT(5F10.4)
 0064            102 FORMAT(T6,'T1=',F6.2,5X,'P1=',F6.2,5X,'H1=',F6.2,5X,'CP1=',F6.4,
                    15X,'GAMMA1=',F5.3/)
 0065            103 FORMAT(T6,'T2=',F6.2,5X,'P2=',F6.2,5X,'H2=',F6.2,5X,'CP2=',F6.2,
                    15X,'GAMMA2=',F5.3/)
 0066            104 FORMAT(T6,'T1=',F6.2,5X,'P1=',F6.2,5X,'H1=',F6.2,5X,'AVERAGE CP='
                    1,F6.4 ,5X,'AVERAGE GAMMA=',F5.3/)
 0067            105 FORMAT(T6,'T1=',F6.2,5X,'P1=',F6.2,5X,'H1=',F6.2)
 0068                 END
```

TABLE XIX. ONE-SPOOL COMPRESSOR MATCH INPUT LIST

Card Type	Column	Input Format	Name	Definition
A	1-72	A	TITLE	User's words to define case
B	1-10	D	XND1	First compressor design speed, RPM
	11-20	D	XND2	Second compressor design speed, RPM
	21-30	D	ENPC1	First compressor percent speed
	31-40	D	BLOOD	Interstage bleed flow rate - lbs/sec
	41-50	D	FLORAT	VBL stator flow change, percent
C	1-10	D	HCO1	First compressor actual enthalpy rise, BTU/lb
	11-20	D	HCOI1	First compressor ideal enthalpy rise, BTU/lb
	21-30	D	W2	First compressor exit corrected flow, lbs/sec
	31-40	D	HCO2	Second compressor actual enthalpy rise, BTU/lb
	41-50	D	HCOI2	Second compressor ideal enthalpy rise, BTU/lb
b	Blank Card			

Each input case requires one data set of cards consisting of the following card types in sequence:

A,	Beginning of a case
B,C,C,C,b,	For first speed line, a C card for each point
B,C,C,C,C,b,	For second speed line, a C card for each point
B,C,C,C,b,	For third speed line, a C card for each point
to	
b	End of case
A	Beginning of a new case

Output of this program includes punched cards which can be used for BLAH input. The cards (see BLAH input description) are:

b
F,F,F,E,
F,F,F,E,
etc.

The E card is out of order and is moved to the front of the group before submitting.

TABLE XX. ONE-SPOOL MATCH SAMPLE OUTPUT

LF + PRATT & WHITNEY C ROTOR CASE13.3

FIRST COMPRESSOR DESIGN SPEED IS 5C7CC.C RPM,SECOND COMPRESSOR DESIGN SPEED IS 432CC.C RPM

FIRST COMPRESSOR PERCENT SPEED IS 100.0

INLET FLOW LBS/SEC	EFF3	P3	T3	W3	INTERSTAGE CORR SPEED	EFF4	P4	T4	EXIT CORR FLOW	INLET CORR SPEED	OVERALL P/P	OVERALL EFFY
3.94	75.1	3.555	851.	1.26	39577.5	82.9	4.630	1383.5	0.35	50700.0	17.5C	75.1
3.97	77.4	3.767	847.	1.24	39687.5	83.7	4.641	1373.4	0.37	5C7CC.C	17.56	76.C
3.99	78.0	3.945	839.	1.23	39854.4	84.0	4.673	1362.4	0.35	5070C.0	16.58	77.0

FIRST COMPRESSOR DESIGN SPEED IS 50700.0 RPM,SECOND COMPRESSOR DESIGN SPEED IS 43200.0 RPM

FIRST COMPRESSOR PERCENT SPEED IS 95.C

INLET FLOW LBS/SEC	EFF3	P3	T3	W3	INTERSTAGE CORR SPEED	EFF4	P4	T4	EXIT CORR FLOW	INLET CORR SPEED	OVERALL P/P	OVERALL EFFY
3.66	79.5	3.858	825.	1.19	38187.4	82.2	4.263	1316.8	0.35	48145.0	16.47	77.6
3.81	79.6	3.755	819.	1.26	38327.9	82.9	4.309	1305.1	0.37	48145.3	16.32	77.8
3.84	77.3	3.621	815.	1.33	38429.0	83.3	4.313	1297.4	0.39	48145.C	15.47	76.9

FIRST COMPRESSOR DESIGN SPEED IS 50700.0 RPM,SECOND COMPRESSOR DESIGN SPEED IS 43200.C RPM

FIRST COMPRESSOR PERCENT SPEED IS 90.C

INLET FLOW LBS/SEC	EFF3	P3	T3	W3	INTERSTAGE CORR SPEED	EFF4	P4	T4	EXIT CORR FLOW	INLET CORR SPEED	OVERALL P/P	OVERALL EFFY
2.92	74.1	3.289	753.	1.10	36909.9	81.8	3.955	1239.5	0.35	45630.0	12.98	75.5
3.23	79.7	3.623	753.	1.16	36909.9	82.5	3.959	1236.5	0.37	45630.C	13.56	77.6
3.42	80.7	3.666	740.	1.22	36583.9	82.8	3.962	1230.C	0.39	45630.0	13.66	78.7

FIRST COMPRESSOR DESIGN SPEED IS 50700.0 RPM,SECOND COMPRESSOR DESIGN SPEED IS 43200.0 RPM

FIRST COMPRESSOR PERCENT SPEED IS 85.C

INLET FLOW LBS/SEC	EFF3	P3	T3	W3	INTERSTAGE CORR SPEED	EFF4	P4	T4	EXIT CORR FLOW	INLET CORR SPEED	OVERALL P/P	OVERALL EFFY
2.15	77.4	2.919	761.	1.01	35576.4	81.2	3.669	1167.2	0.46	43095.0	10.33	76.1
2.56	75.7	2.807	761.	1.07	35576.4	82.0	3.665	1163.9	0.38	43095.C	10.62	75.7
2.75	79.2	2.973	760.	1.12	35603.1	82.7	3.666	1159.3	0.39	43095.C	10.90	77.5

FIRST COMPRESSOR DESIGN SPEED IS 5C7CC.0 RPM,SECOND COMPRESSOR DESIGN SPEED IS 432CC.C RPM

FIRST COMPRESSOR PERCENT SPEED IS 80.C

INLET FLOW LBS/SEC	EFF3	P3	T3	W3	INTERSTAGE CORR SPEED	EFF4	P4	T4	EXIT CORR FLOW	INLET CORR SPEED	OVERALL P/P	OVERALL EFFY
1.96	77.0	2.676	731.	C.96	34176.6	80.8	3.376	1095.5	0.36	4C940.C	8.35	73.4
2.08	79.9	2.819	731.	C.98	34176.6	81.6	3.378	1092.0	0.36	40940.C	8.68	76.7
2.26	78.6	2.901	731.	1.06	34176.6	82.2	3.371	1C89.4	0.38	40940.C	8.70	76.4

FIRST COMPRESSOR DESIGN SPEED IS 50700.0 RPM,SECOND COMPRESSOR DESIGN SPEED IS 43200.0 RPM

FIRST COMPRESSOR PERCENT SPEED IS 75.C

INLET FLOW LBS/SEC	EFF3	P3	T3	W3	INTERSTAGE CORR SPEED	EFF4	P4	T4	EXIT CORR FLOW	INLET CORR SPEED	OVERALL P/P	OVERALL EFFY
1.74	68.C	1.536	677.	0.76	31C60.2	80.3	2.027	968.5	0.31	38690.0	5.68	72.1
1.76	69.1	1.546	677.	0.78	31C60.2	81.1	2.027	96C.8	0.33	38660.C	5.56	73.1
1.82	70.2	1.578	677.	0.82	31C60.2	81.7	2.021	958.0	0.35	38660.0	5.58	74.0

TABLE XXI. ONE-SPOOL MATCH FORTRAN LISTING

```
FORTRAN IV    MODEL 44  PS        VERSION 3, LEVEL 2   DATE  69337

              C**** ONE SPOOL COMPRESSOR MATCHING
              C
              C      XND1 IS FIRST COMPRESSOR DESIGN SPEED
              C      XND2 IS SECOND COMPRESSOR DESIGN SPEED
              C      ENPC1 IS FIRST COMPRESSOR PERCENT SPEED
              C      BLOOD IS INTERSTATE BLEED FLOW RATE LBS/SEC
              C      FLORAT IS VBL STATOR FLOW CHANGE
              C      HCO1 IS FIRST COMPRESSOR ACTUAL ENTHALPY RISE
              C      HCO11 IS FIRST COMPRESSOR IDEAL ENTHALPY RISE
              C      W2 IS FIRST COMPRESSOR EXIT CORRECTED FLOW
              C      HCO2 IS SECOND COMPRESSOR ACTUAL ENTHALPY RISE
              C      HCO12 IS SECOND COMPRESSOR IDEAL ENTHALPY RISE
              C      W1     INLET FLO
              C      EFF1   LP COMPRESSOR STAGE EFFICIENCY
              C      PP1    LP COMPRESSOR STAGE PRESSURE RATIO
              C      T2     LP COMPRESSOR STAGE EXIT TEMPERATURE
              C      W2     LP COMPRESSOR STAGE EXIT CORR. AIRFLOW
              C      XN2 IS INTERSTATE CORR. SPEED
              C      EFF3 IS HP COMPRESSOR EFFICIENCY
              C      PP2   IS HP COMPRESSOR PRESSURE RATIO
              C      T3    IS HP COMPRESSOR TEMPERATURE
              C      W3    IS EXIT CORR. FLOW
              C      XN1   IS INLET CORR. SPEED
              C      PPO   IS OVERALL PRESSURE RATIO
              C      EFFT IS OVERALL EFFICIENCY
              C      PUNCH-CARDS ARE GIVEN FOR INPUT TO PROGRAM PLAN
              C
 0001                 DIMENSION TITLE(18),PU(8)
              C
 0002                 WRITE(3,113)
 0003                 WRITE(2,113)
              C********* K = 0, 1, OR 2. IT IS THE NUMBER OF DATA SETS PUNCHED
              C*********     J IS THE NUMBER OF DATA POINTS ON A SPEED LINE
 0004                 W1=123.56
 0005               1 WRITE(2,113)
 0006                 READ 107,TITLE
 0007                 WRITE(3,102) TITLE
 0008               5 READ 100,XND1,XND2,ENPC1,BLOOD,FLORAT
 0009                 IF(XND1)1,1,7
 0010               7 J=0
 0011                 K=0
 0012                 DO 6 N = 1,8
 0013               6 PU(N) = 0.
 0014                 WRITE(3,103)XND1,XND2
 0015                 WRITE(3,104)ENPC1
 0016                 ENPC1=ENPC1/100.
 0017                 IF(FLORAT)2,3,2
 0018               2 WRITE(3,114) FLORAT
 0019               3 IF(BLOOD)9,9,8
```

TABLE XXI - Continued

```
FORTRAN IV    MODEL 44  PS        VERSION 3,  LEVEL 2   DATE  6 .37

 0020           8  WRITE(3,109)PLOSS
 0021              WRITE(3,105)
 0022              WRITE(3,110)
 0023           9  WRITE(3,106)
 0024              WRITE(3,106)
 0025          10 READ 100,WC01,WC011,W2,WC02,WC12
 0026              IF(WC01)11,11,15
 0027          11 IF(K)14,14,12
 0028          12 WRITE(2,111)(I, PU(N), N= 1, 4 )
 0029              DO 13 N = 1,8
 0030          13 PU(N) = 0.
 0031          14 A= 100.*ENPC1
 0032              WRITE(2,112)( J, A )
 0033              GO TO 5
 0034          15 K=K+1
 0035              J=J+1
 0036              ALEED=PLOSS/W2
 0037              W2=W2*(1.-ALEED)
 0038              DH1=WC01*ENPC1**2
 0039              DH11=WC011*ENPC1**2
           C******** STATEMENTS 17-18 SPECIAL FOR CASE 4,4.VS.  THEY REDUCE P/P TO
           C********     LEVELS OF CONTINENTAL MACHINE.
 0040          17 DH1=DH1*0.56
 0041          18 DH11=DH11*0.56
 0042              DHL1=(DH1-DH11)*(1.0+ABS(FLOAT/100.))**1.2
 0043              IF(FLOAT)20,21,19
 0044          19 DH1 = DH11 + DHL1
 0045              GO TO 21
 0046          20 DH11 = DH1 - DHL1
 0047          21 H2=H1+DH1
 0048              H2I=H1+DH11
 0049              CALL SNARE(3,TX,TY,14.7,P2,H1,H2I,CP,GAMMA)
 0050              P2=P2
 0051              PP1=P2/14.7
 0052              CALL SNARE(3,TI,T2,14.7,PX,H1,H2,CP,GAMMA)
 0053              T2=T2
 0054              XN1=ENPC1*XND1
 0055              THET2=T2/T1
 0056              W1=W2*PP1/(THET2**.5)
 0057              EFF1=DH11/DH1*100.
 0058              XN2=ENPC1*XND1/(THET2**.5)
 0059              DH2=WC02*(XN2/XND2)**2*THET2
 0060              DH2I=WC012*(XN2/XND2)**2*THET2
 0061              H3=H2+DH2
 0062              H3I=H2+DH2I
 0063              CALL SNARE(3,TX,TY,P2,P3,H2,H3I,CP,GAMMA)
 0064              T=P3
 0065              PP2=P3/P2
 0066              PPO=P3/14.7
```

TABLE XXI - Continued

```
FORTRAN IV    MODEL 44  PS       VERSION 3,  LEVEL 2   DATE  69337

0067                CALL  SNARF(3,T2,T3,PZ,P3,H2,H3,CP,GAMMA)
0068                DHT=DH2+DH1
0069                CALL  SNARF(2,T1,TX,14.7,Z,HX,HIT,CP,GAMMA)
0070                DHIT=HIT-H1
0071                EFF3=DH2I/DH2*100.
0072                EFFT=(1.-BLEED)*DHIT/(DH1+(1.-BLEED)*DH2)*100.
0073                W3=W1*(T3/T1)**.5/PPC
0074                XN3=XN1/(T3/T1)**.5
0075                WRITE(3,101)W1,EFF1,PP1,TZ,W2,XN2,EFF3,PP2,T3,W3,XN1,PPO,EFFT
0076                N=4*(K-1)
0077                PU(N+1)= W1
0078                PU(N+2)= PPO
0079                PU(N+3)= EFFT
0080                PU(N+4)= XN1
0081                IF(K-1)10,10,35
0082             35 WRITE(2,111)( PU(N), N=1,8 )
0083                K=0
0084                DO 40 N = 1,8
0085             40 PU(N) = 0.
0086                GO TO 10
                 C
0087            100 FORMAT(7F10.4)
0088            101 FORMAT(2X,F6.2,7X,F5.1,4X,F6.3,3X,F5.0,3X,F6.2,5X,F7.1,5X,F5.1,
                   14X,F6.3,3X,F6.1,4X,F6.2,7X,F7.1,4X,F5.2,3X,F5.1)
0089            102 FORMAT(1H1,18A4//)
0090            103 FORMAT(T2,'FIRST COMPRESSOR DESIGN SPEED IS',F8.1,T43,'RPM,SECOND
                   1COMPRESSOR DESIGN SPEED IS ',F7.1,T91,'RPM'/)
0091            104 FORMAT(T2,'FIRST COMPRESSOR PERCENT SPEED IS ',F5.1/)
0092            105 FORMAT(T2,'INLET FLOW',T17,'EFF3',T27,'P3',T35,'T3',T44,'W3',T51,
                   1'INTERSTAGE',T66,'EFF4'    ,T76,'P4',T85,'T4',T92,'EXIT CORR',
                   2T104,'INLET CORR',T122,'OVERALL')
0093            106 FORMAT(T3,'LBS/SEC',T51,'CORR SPEED',T94,'FLOW',T107,'SPEED',T119,
                   1'P/P    EFFY'/)
0094            107 FORMAT(18A4)
0095            108 FORMAT(1X,F5.2,T8,'POUNDS OF FLOW ARE BLED OFF AT LP EXIT'/)
0096            109 FORMAT(T2,'THE BLEED FLOW IS SUBTRACTED FROM THE LP COMPRESSOR')
0097            110 FORMAT(T2,'IN THE OUTPUT BELOW')
0098            111 FORMAT( 2F8.3, F6.2, F8.0, 2F8.3, F9.2, F8.0 )
0099            112 FORMAT( I8, F8.2 )
0100            113 FORMAT(/)
0101            114 FORMAT( T2,'STATOR BLADE ROW ANGLE ADJUSTMENT MOVES THE',
                   1  ' STALL LINE FLOW BY',F6.1,' PERCENT OF LP FLOW.',/)
0102                END
```

TABLE XXII. TWO-SPOOL COMPRESSOR MATCH INPUT LIST

Card Type	Column	Input Format	Name	Definition
A	1-72	A	TITLE	User's words to define case
B	1-10	D	XND1	First compressor design speed, RPM
	11-20	D	XND2	Second compressor design speed, RPM
	21-30	D	ENPC1	First compressor percent speed
	31-40	D	ENPC2	Second compressor percent speed
C	1-10	D	HCO1	First compressor actual enthalpy rise, BTU/lb
	11-20	D	HCOI1	First compressor ideal enthalpy rise, BTU/lb
	21-30	D	W2	First compressor exit flow rate, lb/sec
	31-40	D	HCO2	Second compressor actual enthalpy rise, BTU/lb
	41-50	D	HCOI2	Second compressor ideal enthalpy rise, BTU/lb
b	Blank Card			

Each input case requires one data set of cards consisting of the following card types in sequence:

A,	Beginning of a case
B,C,C,C,b	For first speed line, a C card for each point
B,C,C,C,b	For second speed line, a C card for each point
B,C,C,C,b	For third speed line, a C card for each point
to	
b	End of case
A	Beginning of a new case

TABLE XXIII. TWO-SPOOL MATCH SAMPLE OUTPUT

T4D STAGE TRANSONIC + PCW 5 ROTOR CASE 11.1 (2 SPOOL,NEW STALL LINE)

H P SPEED PERCENT CORRECT	DESIGN RPM	H P P/P	H P ADIAB EFFY	L P PERCENT SPEED	LP CORR FLOW LBS/SEC	L P P/P	LP ADIAB EFFY	OVERALL P/P	OVERALL ADIAB EFFY	TEMPERATURE AT EXIT OF LP	TEMPERATURE AT EXIT OF HP	L P HCO	L P HCDI	HCO	HCDI
1.05	39000.	6.419	0.82	1.00	4.875	3.262	0.83	20.94	0.787	769.	1395.1	60.40	50.00	95.80	78.20
1.05	39000.	6.441	0.82	1.00	4.930	3.146	0.82	20.26	0.788	762.	1381.2	58.70	48.20	95.50	78.40
1.05	39000.	6.379	0.82	1.00	4.958	3.014	0.81	19.23	0.781	755.	1367.3	57.00	46.10	95.20	77.90
H P SPEED PERCENT CORRECT	DESIGN RPM	H P P/P	H P ADIAB EFFY	L P PERCENT SPEED	LP CORR FLOW LBS/SEC	L P P/P	LP ADIAB EFFY	OVERALL P/P	OVERALL ADIAB EFFY	TEMPERATURE AT EXIT OF LP	TEMPERATURE AT EXIT OF HP	L P HCO	L P HCDI	HCO	HCDI
1.05	39000.	6.412	0.82	0.95	4.566	3.009	0.84	19.30	0.796	746.	1355.3	60.70	51.00	95.80	78.20
1.05	39000.	6.433	0.82	0.95	4.659	2.927	0.84	18.83	0.799	739.	1340.7	58.70	49.50	95.50	78.40
1.05	39000.	6.371	0.82	0.95	4.714	2.819	0.84	17.96	0.797	731.	1324.8	56.50	47.50	95.20	77.90
H P SPEED PERCENT CORRECT	DESIGN RPM	H P P/P	H P ADIAB EFFY	L P PERCENT SPEED	LP CORR FLOW LBS/SEC	L P P/P	LP ADIAB EFFY	OVERALL P/P	OVERALL ADIAB EFFY	TEMPERATURE AT EXIT OF LP	TEMPERATURE AT EXIT OF HP	L P HCO	L P HCDI	HCO	HCDI
1.05	39000.	6.403	0.82	0.90	4.219	2.728	0.86	17.46	0.804	718.	1307.3	56.30	51.00	95.90	78.20
1.05	39000.	6.424	0.82	0.90	4.310	2.658	0.86	17.08	0.808	712.	1295.1	57.50	49.50	95.50	78.40
1.05	39000.	6.363	0.82	0.90	4.405	2.590	0.86	16.48	0.806	707.	1283.5	55.80	48.00	95.20	77.90
H P SPEED PERCENT CORRECT	DESIGN RPM	H P P/P	H P ADIAB EFFY	L P PERCENT SPEED	LP CORR FLOW LBS/SEC	L P P/P	LP ADIAB EFFY	OVERALL P/P	OVERALL ADIAB EFFY	TEMPERATURE AT EXIT OF LP	TEMPERATURE AT EXIT OF HP	L P HCO	L P HCDI	HCO	HCDI
1.05	39000.	6.389	0.82	0.80	3.512	2.196	0.85	14.03	0.803	672.	1226.6	57.50	49.00	95.80	78.20
1.05	39000.	6.411	0.82	0.80	3.637	2.171	0.86	13.92	0.811	667.	1217.0	55.80	48.20	95.50	78.40
1.05	39000.	6.351	0.82	0.80	3.731	2.124	0.86	13.49	0.809	663.	1207.0	54.00	46.70	95.20	77.90
H P SPEED PERCENT CORRECT	DESIGN RPM	H P P/P	H P ADIAB EFFY	L P PERCENT SPEED	LP CORR FLOW LBS/SEC	L P P/P	LP ADIAB EFFY	OVERALL P/P	OVERALL ADIAB EFFY	TEMPERATURE AT EXIT OF LP	TEMPERATURE AT EXIT OF HP	L P HCO	L P HCDI	HCO	HCDI
1.03	39000.	6.041	0.82	0.70	2.886	1.823	0.85	11.01	0.807	633.	1137.3	56.20	47.50	96.20	79.00
1.03	39000.	6.029	0.83	0.70	3.019	1.808	0.86	10.90	0.817	630.	1126.4	54.40	46.80	95.30	78.90
1.03	39000.	5.974	0.83	0.70	3.120	1.781	0.86	10.64	0.818	626.	1117.4	52.70	45.50	94.70	78.40
H P SPEED PERCENT CORRECT	DESIGN RPM	H P P/P	H P ADIAB EFFY	L P PERCENT SPEED	LP CORR FLOW LBS/SEC	L P P/P	LP ADIAB EFFY	OVERALL P/P	OVERALL ADIAB EFFY	TEMPERATURE AT EXIT OF LP	TEMPERATURE AT EXIT OF HP	L P HCO	L P HCDI	HCO	HCDI
0.96	39000.	5.193	0.83	0.60	2.170	1.509	0.77	7.84	0.795	603.	1032.5	56.00	43.10	97.40	80.50
0.96	39000.	5.174	0.83	0.60	2.330	1.528	0.82	7.91	0.816	600.	1027.6	54.10	44.50	96.20	80.30
0.96	39000.	5.117	0.84	0.60	2.462	1.527	0.85	7.81	0.830	597.	1010.4	52.30	44.40	94.40	79.60
H P SPEED PERCENT CORRECT	DESIGN RPM	H P P/P	H P ADIAB EFFY	L P PERCENT SPEED	LP CORR FLOW LBS/SEC	L P P/P	LP ADIAB EFFY	OVERALL P/P	OVERALL ADIAB EFFY	TEMPERATURE AT EXIT OF LP	TEMPERATURE AT EXIT OF HP	L P HCO	L P HCDI	HCO	HCDI
0.89	39000.	4.763	0.82	0.50	1.655	1.322	0.74	5.63	0.793	577.	937.2	55.80	41.30	98.60	81.10
0.89	39000.	4.713	0.83	0.50	1.780	1.338	0.80	5.64	0.814	575.	921.4	54.00	43.20	96.40	80.30
0.89	39000.	4.151	0.84	0.50	1.884	1.343	0.83	5.57	0.826	573.	912.5	52.40	43.70	94.60	79.30

DA2171
/&

TABLE XXIV. TWO-SPOOL MATCH FORTRAN LISTING

```
FORTRAN IV    MODEL 44  PS        VERSION 3,  LEVEL 2    DATE  69337

              C***** TWO SPOOL COMPRESSOR MATCHING PROGRAM
              C**** TWO SPOOL COMPRESSOR MATCHING
              C
              C      XND1 IS FIRST COMPRESSOR DESIGN SPEED
              C      XND2 IS SECOND COMPRESSOR DESIGN SPEED
              C      ENPC1 IS FIST COMPRESSOR PERCENT SPEED
              C      ENPC2 IS SECOND COMPRESSOR PERCENT SPEED
              C      HCO1 IS FIRST COMPRESSOR ACTUAL ENTHALPY RISE
              C      HCOI1 IS FIRST COMPRESSOR IDEAL ENTHALPY RISE
              C      W2    JE FIRST COMPRESSOR EXIT FLOW RATE
              C      HCO2 IS SECOND COMPRESSOR ACTUAL ENTHALPY RISE
              C      HCOI2 IS SECOND COMPRESSOR IDEAL ENTHALPY RISE
              C      ENPC2 IS HP PERCENT CORR. SPEED
              C      XND2 IS HP DESIGN SPEED RPM
              C      PP4   IS HP PRESSURE RATIO
              C      EFF4 IS HP ADIABATIC EFFICIENCY
              C      ENPC1 IS LP PERCENT SPEED
              C      W1 IS LP CORRECTED FLOW LBS/SEC
              C      PP1 IS LP PRESSURE RATIO
              C      EFF1 IS LP ADIABATIC EFFICIENCY
              C      PPO IS OVERALL PRESSURE RATIO
              C      EFFT IS OVERALL ADIABATIC EFFICIENCY
              C      T2 IS LP EXIT TEMPERATURE
              C      T4 IS HP EXIT TEMPERATURE
              C
              C
              C
0001                  DIMENSION TITLE(18)
              C
0002               1  READ 100,TITLE
0003                  WRITE(3,106)TITLE
0004               5  READ 101,XND1,XND2,ENPC1,ENPC2
0005                  IF(XND1)1,1,6
0006               6  WRITE(3,102)
0007                  WRITE(3,103)
0008                  WRITE(3,104)
0009                  ENPC1=ENPC1/100.
0010                  ENPC2=ENPC2/100.
0011              10  READ 101,HCO1,HCOI1,W2,HCO2,HCOI2
0012                  IF(HCO1)5,5,20
0013              20  H1=123.96
0014                  DH1=HCO1*ENPC1**2
0015                  DHI1=HCOI1*ENPC1**2
0016                  H2=H1+DH1
0017                  H2I=H1+DHI1
0018                  CALL SNARF(3,TX,TY,14.7,P2,H1,H2I,CP,GAMMA)
0019                  P2=P2
0020                  PP1=P2/14.7
0021                  CALL SNARF(3,T1,T2,14.7,PX,H1,H2,CP,GAMMA)
```

TABLE XXIV - Continued

```
FORTRAN IV    MODEL 44  PS       VERSION 3,  LEVEL 2   DATE  69337

0022                TZ=T2
0023                XN1=ENPC1*XND1
0024                THET2=T2/T1
0025                W1=W2*PP1/(THET2**.5)
0026                EFF1=DHI1/DH1
0027                XN2=ENPC1*XND1/(THET2**.5)
0028                DH2=HCO2*ENPC2**2*THET2
0029                DHI2=HCOI2*ENPC2**2*THET2
0030                H4=H2+DH2
0031                H4I=H2+DHI2
0032                CALL SNARF(3,TX,TY,PZ,P4,H2,H4I,CP,GAMMA)
0033                Z=P4
0034                PP4=P4/P2
0035                PPO=P4/14.7
0036                CALL SNARF(3,T2,T4,P2,PO,H2,H4,CP,GAMMA)
0037                DHT= DH2+DH1
0038                CALL SNARF(2,T1,TX,14.7,Z,H1,HIT,CP,GAMMA)
0039                DHIT=HIT-H1
0040                EFFT=DHI1/DHT
0041                EFF4=DHI2/DH2
0042                W4=W1*(T4/T1)**.5/PPC
0043                WRITE(3,105)ENPC2,XND2, PP4,EFF4,ENPC1,W1,PP1,EFF1,PPO,EFFT,TZ,T4,
                   1HCO1,HCOI1,HCO2,HCOI2
0044                GO TO 10
                C
0045              100 FORMAT(18A4)
0046              101 FORMAT(7F10.4)
0047              102 FORMAT(T4,'H P SPEED',T22,'H P',T31,'H E',T41,'L P',T48,'LP CORR',
                     1T59,'L P',T67,'LP',T77,'OVERALL',T90,'TEMPERATURE',T108,'L P')
0048              103 FORMAT(T2,'PERCENT  DESIGN',T22,'P/P',T30,'ADIAB',T39,'PERCENT   F
                     1LOW',T59,'P/P    ADIAB    P/P    ADIAB   AT EXIT OF    HCO      HCO
                     2I    HCO    HCOI')
0049              104 FORMAT(T2,'CORRECT   RPM',T30,'EFFY',T40,'SPEED   LBS/SEC',T66,'EF
                     1FY',T82,'EFFY',T90,'LP     HP')
0050              105 FORMAT(1X,F6.2,3X,F6.0,4X,F6.3,3X,F6.2,4X,F6.2,2X,F7.3,3X,F6.3,2X,
                     1F6.2,2X,F6.2,2X,F5.3,1X,F5.0,2X,F6.1,2X,F6.2,2X,F6.2,1X,F6.2,
                     21X,F6.2)
0051              106 FORMAT(1H1,18A4//)
0052                  END
```

Unclassified
Security Classification

DOCUMENT CONTROL DATA - R & D

(Security classification of title, body of abstract and indexing annotation must be entered when the overall report is classified)

1. ORIGINATING ACTIVITY *(Corporate author)*
Curtiss-Wright Corporation
Wood-Ridge, New Jersey

2a. REPORT SECURITY CLASSIFICATION
Unclassified

2b. GROUP

3. REPORT TITLE
SMALL AXIAL-CENTRIFUGAL COMPRESSOR MATCHING STUDY

4. DESCRIPTIVE NOTES *(Type of report and inclusive dates)*
Final Report

5. AUTHOR(S) *(First name, middle initial, last name)*
Laurence E. Brown

6. REPORT DATE	7a. TOTAL NO. OF PAGES	7b. NO. OF REFS
May 1970	221	15

8a. CONTRACT OR GRANT NO.	9a. ORIGINATOR'S REPORT NUMBER(S)
DAAJ02-69-C-0075	USAAVLABS Technical Report 70-20
b. PROJECT NO. Task 1G162203D14413	9b. OTHER REPORT NO(S) *(Any other numbers that may be assigned this report)*
c.	
d.	

10. DISTRIBUTION STATEMENT
This document is subject to special export controls, and each transmittal to foreign governments or foreign nationals may be made only with prior approval of U. S. Army Aviation Materiel Laboratories, Fort Eustis, Virginia 23604.

11. SUPPLEMENTARY NOTES	12. SPONSORING MILITARY ACTIVITY
	U. S. Army Aviation Materiel Laboratories Fort Eustis, Virginia

13. ABSTRACT

The prime objective of this program is to define the preliminary design and matching of an axial-centrifugal compressor for minimum engine specific fuel consumption at 60 percent power and 30 percent power, with secondary importance attached to SFC at 100 percent power.

Analytical procedures were employed to investigate effects of engine cycle parameters, stage-matching characteristics of several axial and centrifugal compressors, variable compressor geometry (two-spools and stator variable setting angles), and power turbine variable area, upon minimum fuel consumption. Design studies were employed in the consideration of shafting and component arrangements. Comparative engine complexity of one-spool and two-spool compressors in front drive engines was evaluated in the selection of an optimum compressor configuration.

The selected compressor preliminary design is based closely on stage pressure ratio levels that have been attained in previous developments; and requirements are an axial compressor with improved efficiency and demonstrated flow variability and a centrifugal compressor with modified configuration for close coupling behind axial stages. The selected compressor can be developed in a three-year program.

DD FORM 1 NOV 68 1473 REPLACES DD FORM 1473, 1 JAN 64, WHICH IS OBSOLETE FOR ARMY USE.

Unclassified
Security Classification

14. KEY WORDS	LINK A		LINK B		LINK C	
	ROLE	WT	ROLE	WT	ROLE	WT
Axial-centrifugal compressor Fuel consumption Turboshaft engines One-spool and two-spool compressor engines						